ABSTRACT

Title of dissertation: ENERGY HARVESTING COMMUNICATION NETWORKS: ONLINE POLICIES, TEMPERATURE CONSIDERATIONS, AND AGE OF INFORMATION

Abdulrahman Baknina, Doctor of Philosophy, 2018

Dissertation directed by: Professor Şennur Ulukuş
Department of Electrical and Computer Engineering

This dissertation focuses on characterizing energy management policies for energy harvesting communication networks in the presence of stochastic energy arrivals and temperature constraints. When the energy arrivals are stochastic and are known only causally at the transmitter, we study two performance metrics: throughput and age of information (AoI). When the energy harvesting system performance is affected by the change of the temperature, we consider the throughput metric.

When the energy arrivals are stochastic, we study the throughput maximization problem for several network settings. We first consider an energy harvesting broadcast channel where a transmitter serves data to two receivers on the downlink. The battery at the transmitter in which the harvested energy is stored is of finite size. We focus on *online* transmission schemes where the transmitter knows the energy arrivals only causally as they happen. We consider the case of general independent and identically distributed (i.i.d.) energy arrivals, and propose a *near-optimal* strategy coined fractional power constant cut-off (FPCC) policy. We

show that the FPCC policy is *near-optimal* in that it yields rates that are within a constant gap from the optimal rate region, for all system parameters.

Next, we study *online* transmission policies for a two-user multiple access channel where both users harvest energy from nature. The energy harvests are i.i.d. over time, but can be arbitrarily correlated between the two users. The transmitters are equipped with arbitrary but finite-sized batteries. We propose a distributed fractional power (DFP) policy, which users implement distributedly with no knowledge of the other user's energy arrival or battery state. We show that the proposed DFP is *near-optimal* as in the broadcast channel case.

Then, we consider *online* power scheduling for energy harvesting channels in which the users incur processing cost per unit time that they are on. The presence of processing costs forces the users to operate in a bursty mode. We consider the single-user and two-way channels. For the single-user case, we consider the case of the general i.i.d. energy arrivals. We propose a *near-optimal* online policy for this case. We then extend our analysis to the case of two-way energy harvesting channels with processing costs; in this case, the users incur processing costs for being on for transmitting or receiving data. Our proposed policy is distributed, which users can apply independently with no need for cooperation or coordination between them.

Next, we consider a single-user channel in which the transmitter is equipped with finite-sized data and energy buffers. The transmitter receives energy and data packets randomly and intermittently over time and stores them in the finite-sized buffers. The arrival amounts are known only causally as they happen. We focus on the special case when the energy and data arrivals are fully-correlated. We

propose a structured policy and bound its performance by a multiplicative gap from the optimal. We then show that this policy *is optimal* when the energy arrivals dominate the data arrivals, and is *near-optimal* when the data arrivals dominate the energy arrivals.

Then, we consider another performance metric which captures the freshness of data, i.e., AoI. For this metric, we first consider an energy harvesting transmitter sending status updates to a receiver over an erasure channel. The energy arrivals and the channel erasures are i.i.d. and Bernoulli distributed in each slot. In order to combat the effects of the erasures in the channel and the uncertainty in the energy arrivals, we use channel coding to encode the status update symbols. We consider two types of channel coding: maximum distance separable (MDS) codes and rateless erasure codes. For each of these models, we study two achievable schemes: best-effort and save-and-transmit. We analyze the average AoI under each of these policies. We show that rateless coding with save-and-transmit outperforms all other schemes.

Next, we consider a scenario where the transmitter harvests i.i.d. Bernoulli energy arrivals and status updates carry information about an independent message. The transmitter encodes this message into the timings of the status updates. The receiver needs to extract this encoded information, as well as update the status of the observed phenomenon. The timings of the status updates, therefore, determine both the AoI and the message rate (rate). We study the trade-off between the achievable message rate and the achievable average AoI. We propose several achievable schemes and compare their rate-AoI performances.

Then, with the motivation to understand the effects of temperature sensitivity on wireless data transmission performance for energy harvesting communication networks, we study several temperature models. We assume non-causal knowledge of the energy arrivals. First, we consider throughput maximization in a single-user energy harvesting communication system under continuous time energy and temperature constraints. We model three main temperature related physical defects in wireless sensors mathematically, and investigate their impact on throughput maximization. Specifically, we consider temperature dependent energy leakage, effects of processing circuit power on temperature, and temperature increases due to the energy harvesting process itself. In each case, we determine the optimum power schedule.

Next, different from the previous work, we consider a discrete time system where transmission power is kept constant in each slot. We consider two models that capture different effects of temperature. In the first model, the temperature is constrained to be below a critical temperature at all time instants; we coin this model as *explicit temperature constrained model*. We investigate throughput optimal power allocation for multiple energy arrivals under general, as well as temperature and energy limited regimes. In the second model, we consider the effect of the temperature on the channel quality via its influence on additive noise power; we coin this model as *implicit temperature constrained model*. In this model, the change in the variance of the additive noise due to previous transmissions is non-negligible. In particular, transmitted signals contribute as interference for all subsequent slots and thus affect the signal to interference plus noise ratio (SINR). In this case, we

investigate throughput optimal power allocation under general, as well as low and high SINR regimes. Finally, we consider the case in which implicit and explicit temperature constraints are simultaneously active.

Finally, we extend the discrete time explicit temperature constraint model to a multi-user setting. We consider a two-user energy harvesting multiple access channel where the temperatures of the nodes are affected by the electromagnetic waves due to data transmission. We study the optimal power allocations when the temperatures of the nodes are subject to peak temperature constraints, where each node has a different peak temperature requirement and the nodes have different temperature parameters. We study the optimal power allocation in this case and derive sufficient conditions under which the rate region collapses to a single pentagon.

Energy Harvesting Communication Networks: Online Policies, Temperature Considerations, and Age of Information

by

Abdulrahman Baknina

Dissertation submitted to the Faculty of the Graduate School of the
University of Maryland, College Park in partial fulfillment
of the requirements for the degree of
Doctor of Philosophy
2018

Advisory Committee:
Professor Şennur Ulukuş, Chair/Advisor
Professor Richard La
Professor Gang Qu
Professor Nuno Martins
Professor Amr Baz

Dedication

To my family.

Acknowledgments

First and foremost, all praises and gratitude are due to God, Allah. Allah the All-Mighty has blessed me throughout my life. He provided me with all the strength and patience needed to finish this endeavor.

I would like to thank my adviser, Professor Şennur Ulukuş. She was very dedicated and supportive throughout my journey. Not only did I learn from her how to develop new interesting and meaningful ideas and analyze them, but also how to present these ideas elegantly. I would like thank her for giving me such a great opportunity and for everything; I indeed learned from her a lot.

I would like to thank my committee members Professors Richard La, Gang Qu, Nuno Martins, and Amr Baz, for their valuable time and their useful feedback. I also want to thank Professor Gilmer Blankenship who gave me the opportunity to co-teach with him the undergraduate digital signal processing class; I really learned a lot from him personally and technically.

I am thankful to all the professors I engaged with, either through courses or personally, over the past five years at University of Maryland. In particular I would like to thank Professor Andre Tits, Adrian Papamarcou, Armand Makowski, Behtash Babadi and Leonid Koralov.

I am thankful to all my colleagues at the University of Maryland. I would like to thank Karim Banawan and Yi-Peng Wei who accompanied me throughout my journey at the CSPL lab; we really had great time together. I am especially thankful to Karim Banawan for accompanying me in the educational process for the

last ten years. I would also like to thank Ahmed Arafa for being there whenever I needed him, technically and personally. We had a lot of technical discussions which resulted in several published papers. I would also like to thank all CSPL my lab mates: Jianwei Xie, Omur Ozel, Berk Gurakan, Pritam Mukherjee, Praneeth Boda, Ajaykrishnan Nageswaran, Baturalp Buyukates, Melih Bastopcu, Brian Kim and Bibhusa Rawal. Special thanks to Omur Ozel whom I had many fruitful discussions with; these discussions resulted in several joint works which are part of this thesis.

I am grateful to my family who supported me throughout this journey. My parents were always there for me when I needed their guidance and support. Their prayers for me played an essential role throughout my life. Without them and their prayers, it would have been very hard to accomplish much of this work. I also like to thank my brother and sisters for their continuous encouragements and support.

I am grateful to my wife, Amira. She has been very supportive throughout my journey. During this journey, she took care of many responsibilities to make life easier for me. She gave me strength and support at hard times. She scarifies many things to make sure we, as a family, complete this journey successfully. I am thankful for my kids, Mai and Omar, whom I relied on their smile to change my mood and get support at hard times.

I would like to thank my second family, the Tauba community. From the moment I arrived to Maryland, I received great support from them. They were always there for me when I needed them. I cannot imagine how my journey would have been without such a great community.

Finally, I would like to thank the staff of the ECE department at the University

of Maryland who strive to make the process smooth for the students. I would like specifically to thank Melanie Prange; she was very supportive and helpful. She helped me in countless number of ways, even before I joined the University of Maryland. I also would like to thank Bill Churma and Emily Irwin, whom I enjoyed working with to organize many workshops.

Table of Contents

List of Figures

CHAPTER 1

Introduction

1.1 Overview

The focus of this dissertation is to study power allocation policies for energy harvesting communication networks in different settings. When the energy arrivals are stochastic and known only casually, we consider two performance metrics: throughput and age of the information (AoI). Then, when the energy arrivals are known non-causally, we study the effect of temperature on the throughput of the network.

Energy harvesting communication has been the subject of intense research recently. Most of the research focused on power scheduling for the throughput metric either in offline or online settings. *Offline* power scheduling, where all energy arrivals are known non-causally ahead of time, has been studied in many different settings, e.g., [1–30]. References [1–4] consider the single-user setting, where [1] develops a geometric approach for the case of an infinite-sized battery, [2] generalizes it to the case of a finite-sized battery, and [3] develops a directional water-filling algorithm for the case with fading. References [5–16] consider the offline scheduling problem in multi-user systems, in particular, [5–7] consider the broadcast channel, [8,9] consider

the multiple access channel, [10] considers the interference channel, [11–13] consider the two-hop relay channel, [14, 15] consider the two-hop relay channel with two parallel relays, i.e., the diamond channel, and [16] considers the bi-directional relay channel, i.e., the multiple access channel with user cooperation [31]. More general settings with battery imperfections are considered in [17, 18], effects of processing costs are incorporated in [19–21] leading to bursty communication as in glue pouring [32]. Receiver side energy harvesting is considered in [22–27] where the receivers incur energy costs for decoding incoming data. Energy cooperation and sharing is incorporated into offline power scheduling in [28, 29]. The effect of temperature on the power allocation is studied in [30].

In contrast, *online* power scheduling, where energy harvests are known only casually, has been considered in fewer works and mostly for single-user systems so far [3, 4, 33–50]. In this case, there is a difficulty that arises due to the uncertainty about the future energy arrivals and the finiteness of the battery size. When the future energy arrivals are not known: if the energy is used too slowly, the resulting rate will be smaller and sufficient space will not be open for future energy arrivals into the battery resulting in wasting of energy; on the other hand, if the energy is used too fast, from the concavity of the rate-power relationship, the resulting rate will again be smaller and energy outages will occur due to frequent empty battery. In most cases, the online problem formulation results in algorithms relying mainly on dynamic programming and Markov decision process techniques [33–38]. References [3, 39, 40] propose several sub-optimal schemes which do not rely on dynamic programming, [41] studies competitive ratios of online strategies, [42] uses an adap-

tive stochastic control approach, [43] uses a Lyapunov optimization technique, [44] uses a linear programming approach, and [45] considers a multiple access channel setting with a storage dam model. As dynamic programming needs the knowledge of the underlying distribution, [46] uses a learning-theoretic approach to remove this assumption.

More recently, another performance metric, the AoI, has been introduced. The AoI measures the freshness of the data at the receiver. Status updates and AoI metric is studied in many different settings, for example, see [51–63]. References [51–55] study minimizing the AoI with a queuing theoretic approach; penalty functions and non-linear costs are studied in [56,57]; the optimality of last-come-first-serve for multi-hop settings is shown in [58]; and erasure channels are considered in [59, 60]. The online energy harvesting case is studied in [61–63]. The optimality of threshold policies for the case of unit batteries is shown in [63] and extended to larger sized batteries in [64,65]. Energy harvesting single-user and multi-hop settings with offline energy arrival knowledge are studied in [66, 67].

We first study the setting in which the energy arrivals are known only casually at the transmitter. For this setting, we study two performance metrics: throughout and AoI. For the throughput problem, we study the optimal and near-optimal power scheduling policies for single-user and multi-user network settings. For the multi-user settings, we consider the broadcast and multiple access channels. For the single-user setting, we consider the case when the system has an additional data arrival constraint. When the transmitter and the receiver have imperfections, we study both the single-user channel and the two-way channel. In all of these settings,

we generalize the framework developed in [48, 49].

Then we study the AoI metric. We first consider the single-user setting in which the transmitter sends status updates to the receiver through an erasure channel. To tackle the energy outage and channel erasures, we propose several joint coding and power allocation policies and study their resulting AoI. We then study an AoI setting in which the packets sent to the receiver carry two pieces of information. The content of the packet contains the status update while the timing of the packet contains a message which is independent of the status update. We study the trade-off between the achievable AoI and the achievable message rate.

Finally, we relax the causal knowledge of the energy arrivals and consider the case when the energy arrivals are known non-causally. For this case, we consider the throughput metric and study the effects of temperature on offline power management policies. Temperature dynamics in such systems are typically determined by the temperature of the surrounding environment, transmit power for data transmission, and circuit power associated with processing. In energy harvesting wireless sensors, an additional cause of temperature increase is the energy harvesting process itself. The increase in temperature can have several undesired outcomes. In particular, it can cause damage to the device [68] or to its surrounding environment [69]. In this case, a hard peak temperature constraint could be more suitable. Another effect of temperature increase is the energy leakage or the energy lost without utilization. Typically, the energy leakage in sensors is temperature dependent [70]. Temperature increase can also change the communication rate by affecting the channel quality; this is because the thermal noise variance is proportional to the system temperature.

1.2 Outline

We first study energy harvesting systems when the energy arrivals are known only causally; we study the throughput metric in Chapters 2 through 6 and we study the AoI metric in Chapters 6 and 7. Then, with non-causal energy arrival knowledge, we study the effect of temperature on the network throughput in Chapters 8 through 10.

In Chapter 2, we consider an energy harvesting broadcast channel and develop *online* power scheduling algorithms for this channel model. This work is most closely related to [5,7] and [48,49]. References [5,7] consider the energy harvesting broadcast channel and develop optimal *offline* power scheduling schemes for infinite-sized and finite-sized batteries, respectively. They show that the optimum *total* transmit power is equal to the optimum single-user power, which is constant between energy arrivals [1]. In addition, they show that there exists a *cut-off* power level: the stronger user is served with the cut-off power when possible, and the weaker user is served only with the remaining part of the power after the cut-off power is used for the stronger user; if the total power is less than the cut-off power, only the stronger user is served. On the other hand, reference [49] consider the single-user energy harvesting channel and develop online power scheduling algorithms. They show that near-optimal transmit power decreases over time. Our work may be viewed as extending the offline broadcast setting of [5, 7] to the case of online broadcast setting; or it may be viewed as extending the online single-user setting of [48, 49] to the case of online broadcast setting.

Initially, we consider a special energy arrival process which is Bernoulli that either brings no energy or fills the battery completely. In this case, we solve for the *exactly optimum* online power scheduling strategy. We show that the optimal total transmit power between the energy arrivals is decreasing in time, and there exists a cut-off level below which all power is allocated to serve the stronger user, and only the power above which is allocated to serve the weaker user. Unlike [5, 7], the optimum total transmit power is not equal to the optimum single-user power, as the optimum single-user power is not universal as in [1] since it depends on the receiver noise variance in this case. We determine the optimum online strategy to achieve any point on the boundary of the broadcast channel capacity region. In certain parts of the region, only a single user may be served, depending on the user priorities; in other parts, both users will be served. We show that, when both users are served, the stronger user is served for a duration no less than the weaker user is served; that is, the weaker user may be served for a portion of the stronger user's serving duration, however the opposite may not occur. We show that between the energy arrivals, whenever the stronger user's power allocation is decreasing, the weaker user's power allocation is zero; and whenever the stronger user's power allocation is equal to the cut-off power, the weaker user's power allocation is decreasing.

Next, inspired by the optimum solution for Bernoulli arrivals, we propose a sub-optimal strategy that is valid for all i.i.d. energy arrivals: fractional power constant cut-off (FPCC) policy. In FPCC, the transmitter uses a universal but sub-optimal fractional power policy, however, this power is allocated optimally to users based on a cut-off power. We develop a lower bound for the performance of

the FPCC policy, and a universal upper bound for the capacity region of the energy harvesting broadcast channel which depends only on the average recharge rate. We show that the FPCC scheme is *near-optimal* in that it yields rates that are within a constant gap from the developed upper bound, and thus, from the actual capacity region, for all system parameters.

Next, in Chapter 3, we consider an energy harvesting multiple access channel and develop *online* power scheduling algorithms for this channel model. This work is most closely related with [8] and [49]. Reference [8] develops optimum power allocation schemes for the energy harvesting multiple access channel in the offline setting using generalized directional water-filling techniques. Reference [49], as mentioned, develop a unique approach to the online power allocation problem in the single-user setting.

In this work, we first consider the case of fully-correlated Bernoulli energy arrivals. In this case, the Bernoulli arrivals at the two users are synchronized. For this case, we obtain the jointly *optimum* online power schedules for the users. We show that the optimum transmission powers of both users decrease exponentially in time. We show that the capacity region, which is in general a union of pentagons over power allocation policies, is a single pentagon for synchronized Bernoulli energy arrivals. We show that at the corner points of the pentagon where one of the users gets the single-user rate, the user getting the single-user rate transmits for a shorter (or equal) duration than the other user.

Motivated by the fractional structure of the optimal policies for fully-correlated Bernoulli arrivals and the single pentagon structure of the capacity region, we pro-

pose a sub-optimal policy, which is fixed but distributed between the users, coined *distributed fractional power* (DFP) policy. The DFP is *universal* in that, it does not depend on the statistics of the energy arrival processes; it depends only on the average recharge rate and the size of the battery at each user. Users implement this algorithm distributedly with no knowledge of the other user's energy arrival or battery state. We obtain a lower bound on the performance of the the proposed DFP for the case of fully-correlated (synchronous) Bernoulli arrivals.

Next, we study arbitrarily correlated Bernoulli energy arrivals, in which case, the Bernoulli arrivals at the users are not synchronized. We show that under the DFP policy, the performance of the energy arrivals coming from a fully-correlated Bernoulli energy arrivals forms a lower bound on the performance of arbitrarily correlated Bernoulli energy arrivals with the same mean. Finally, we show that the performance with Bernoulli energy arrivals forms a lower bound for the performance with any other energy arrivals with the same mean. Then, we derive a *universal* upper bound that is valid for all online policies. This upper bound is valid for general energy arrivals, and is universal in that it depends only on the average recharge rates at the users. We show that the derived upper and lower bounds are within a constant gap of each other, and hence, the proposed DFP policy achieves rates that are within a constant gap from the optimal online capacity region for the multiple access channel under equal normalized recharge rates.

In Chapter 4, we extend the fractional policy approach for the single-user and two-way channels with processing costs. For the single-user case, this may be viewed as an extension of the online setting in [49] to incorporate processing costs at the

transmitter, or equivalently, as an extension of the offline setting in [19, 20] which consider processing costs to an online setting. In addition, we further extend our setting from consideration of a single-user channel to the case of two-way channels.

For the single-user case, we first consider the case of i.i.d. Bernoulli energy arrivals, where the energy arrival amount is either zero or equals the size of the battery, i.e., either no energy arrives or the energy arrival fills the battery resetting the system. For this case, we determine the exactly optimal online transmission policy. We show that the optimum transmit power decreases exponentially between energy arrivals. Due to the presence of processing costs, there may exist bursts in the transmission, i.e., slots may not be fully utilized. We show that the bursty transmission can only occur in the last slot. We also show that the total transmission duration decreases with the processing cost. Next, we consider the case of general i.i.d. energy arrivals, and propose a sub-optimal policy. We develop multiplicative and additive lower bounds on the performance of the proposed policy, and a universal upper bound for the performance of any online policy with processing costs. We show that the developed lower and upper bounds are within a constant gap for all energy arrivals and battery sizes; hence, the proposed sub-optimal policy performs within a constant gap from the optimal policy.

We then consider the two-way channel with fully-correlated energy arrivals. This may happen in practice if the users harvest energy from a common source, which may occur, for instance, if the users are within a close proximity of each other and are exposed to the same energy harvesting source. We note that even though the energy arrivals are fully-correlated, the energy intakes of the users are different

due to their different battery sizes. As in the single-user case, we first consider i.i.d. Bernoulli arrivals where each energy arrival amount is either zero or larger than the sizes of both batteries so it fills both batteries simultaneously resetting the system. We show that the optimum powers of the users decrease over time, and the on-off times of the users are fully synchronized. We show that a burst may occur only in the last slot. Next, we consider the case of general i.i.d. energy arrivals. For this case, we propose a distributed sub-optimal policy for power and burst duration selection. The policy is fully distributed and can be applied by each user independently without a need for cooperation or coordination. We develop multiplicative and additive lower bounds on the performance of the proposed policy. We show that the proposed sub-optimal policy is near-optimal in that it performs within a constant gap of the optimal policy for all energy arrival processes and sizes of the batteries at the users.

In Chapter 5, we consider the single-user setting with both data and energy arrival constraints. We consider the case when the data and energy arrivals are fully-correlated. This setting may practically arise when energy and information are simultaneously transferred as in simultaneous wireless energy and information transfer [71]. We propose a structured near-optimal solution for the online problem. We also show, for some special cases, that the proposed policy is exactly optimal. This setting is closely related to [72] in that it extends the presented model to the online setting as developed in [49]. We first study the case of synchronized Bernoulli arrivals, where both data and energy arrivals are either zero or they fill up their corresponding queues simultaneously. We characterize the exactly optimal

solution for this case. Then, for the case of fully-correlated general arrivals with the same arrival means as the Bernoulli arrivals, we propose a structured policy. We show that this policy is optimal when the energy arrivals dominate, and it is within a constant additive gap when the data arrivals dominate. In addition, we derive a multiplicative gap result for the performance of the proposed policy in all cases.

In Chapter 6, we consider an energy harvesting communication system with the objective of minimizing the average AoI at the receiver. This setting is closely related to [60], in which coded status updates are proposed in order to overcome channel errors. We consider a single-user channel, where the transmitter is energy harvesting and further transmission errors may occur due to energy outages. We consider two different types of channel codes to encode the status updates. First, we consider maximum distance separable (MDS) codes. With MDS coding, the transmitter encodes the k status update symbols into n symbols. The receiver receives the update successfully if it receives any k of these n encoded symbols. Next, we consider rateless codes, for example, fountain codes. In this case, the transmitter encodes the k update symbols into as many symbols as needed until k of these symbols are received successfully. For each of these models, we consider two different policies: best-effort and save-and-transmit. Best-effort and save-and-transmit schemes were originally considered in [73], in the context of achieving the capacity of the energy harvesting AWGN channel. In the best-effort scheme, in each slot, the transmitted symbol may suffer from two errors: channel erasure and energy outage. In the save-and-transmit scheme, the transmitter remains silent at the beginning to save energy and to reduce the errors due to energy outage.

For all these cases, we derive the average AoI. Through numerical results, we show that as the average recharge rate decreases, MDS coding with save-and-transmit outperforms all the best-effort schemes. The gain becomes significant for low values of average energy arrivals. We observe that rateless coding with save-and-transmit outperforms all other policies.

In Chapter 7, different from the existing literature, we consider the scenario where the timings of the status updates also carry an independent message. In order to obtain a tractable formulation, we consider an abstraction where the physical channel is noiseless and the transmitter has a battery of unit size. This work is closely related to the models presented in [74] and [75]. Intuitively, as will be clarified shortly, there is a trade-off between the AoI and the rate of the message. Our goal in this chapter is to characterize this trade-off.

For this scenario, under causal (i.e., online) knowledge of energy arrivals, [75] has determined that, in order to minimize the long-term average AoI, the transmitter needs to apply a *threshold based* policy: There exists a fixed and deterministic threshold τ_0 such that if an energy arrives sooner than τ_0 seconds since the last update, the transmitter waits until τ_0 and sends the update packet; on the other hand, if it has been more than τ_0 seconds since the last update, the transmitter sends an update packet right away when an energy arrives.

On the other hand, again for this scenario, [74] has considered the information-theoretic capacity of this energy harvesting channel. The main information-theoretic challenge arises due to having a state-dependent channel (where the state is the energy availability), time-correlation introduced in the state due to the existence

of a battery at the transmitter where energy can be saved and used later, and the unavailability of the state information at the receiver. Reference [74] converts the problem from regular channel uses to a timing channel and obtains the capacity in terms of some auxiliary random variables using a bits through queues approach as in [76].

Sending information necessarily requires the transmitter to send out a packet after a random amount of time following an energy arrival in [74], whereas minimizing AoI requires the transmitter to apply a deterministic threshold based policy in [75]. Note that in [75], the transmitter sends a packet either at a deterministic time τ_0 after an energy arrival, or right at the time of an energy arrival, thus, it cannot send any rate with the packet timings even though it minimizes the AoI. This is the main source of the tension between AoI minimization and information rate maximization.

In this work, we first present a general trade-off region between the achievable AoI and the achievable information rate. We then consider the class of renewal policies in which the system action depends only on the most recent transmission. Within this class of policies, we first propose policies that determine the next transmission instant as a function of the time difference between the most recent energy arrival and the most recent status update. We then consider simpler policies which we call *separable* policies. These policies separate the update decision and information transmission in an additive manner: When an energy arrives, the transmitter decides when to update, neglecting the information transmission; once the transmitter decides to send an update, it then encodes the message on top of that update

timing. For all the policies, we derive the average achievable AoI and the achievable rate. We then compare the trade-off regions of these policies. We observe numerically that the first class of policies achieve better trade-off regions. We also observe that as the value of the average energy arrival increases, policies perform similarly.

In Chapter 8, we consider the throughput maximization problem for energy harvesting transmitters under temperature constraints in an offline setting. In order to address temperature sensitivity of such systems, we consider problem formulations that capture temperature related physical defects in energy harvesting communications. In particular, we investigate the impact of these physical defects on the optimal throughput for energy harvesting communications. We first address the temperature dependent energy leakage. Energy leakage is inevitable in wireless sensors due to power dissipated in the electronics circuitry of the system. It is well-known that the energy leakage increases with temperature. We adopt a linear leakage model as in [70, 77, 78] and investigate the optimal transmit power policy.

Next, we consider the problem of processing cost. Processing cost has been studied earlier in energy harvesting communications [19, 20]. In view of [20, 32], it is well-known that the processing cost forces the optimal transmission to be bursty. In the absence of temperature constraints, the silent and active periods affect the throughput only through their lengths. However, with temperature constraints, their sequence has to be properly designed in addition to their lengths. We address this problem by allowing the transmitter to divide the transmission duration into two consecutive transmission and silence periods, and identify the optimal policy in this case. Then, we study the effects of the heat caused by the energy harvesting

process itself. While harvesting more energy improves the throughput, it also increases the temperature. In this case, the transmitter has to determine the transmit power level as well as the amount of harvested energy (i.e., energy intake). Under a linear relation between temperature increase and harvested energy, we investigate the jointly optimal energy harvesting and transmit power policy.

In Chapter 9, we consider the scheduling problem under energy harvesting and temperature constraints in discrete time. Our interest in discrete time solution stems from the fact that circuits typically run on digital clocks and decisions on the transmission strategy are taken at discrete time intervals. In the first model we consider here, which we coin as the *explicit temperature constrained model*, we consider an explicit peak temperature constraint as in [30] and obtain a discrete time version of the problem considered in [30]. In this temperature constrained problem, increasing the transmission power increases the throughput and the temperature. Due to the fixed temperature budget, higher temperature levels mean smaller admissible transmission power levels for future slots. When the temperature constraint is not binding, the problem reduces to the single-user energy harvesting channel studied in [1], where the optimal power sequence is monotone increasing. When the energy constraint is not binding, we show that the optimal power sequence is monotone decreasing, and the resulting temperature is monotone increasing.

In the second model we consider here, which we coin as the *implicit temperature constrained model*, the temperature is not explicitly constrained, however, the temperature affects the additive noise power and hence the channel quality. This problem arises when the dynamic range of the temperature is large and affects the

noise added at the receiver circuitry in the spirit of [79]. Our focus here is to investigate this problem in a scheduling-theoretic setting. In this case, the transmit powers used in earlier time slots affect the thermal noise in the form of inter symbol interference, and hence, the channel becomes a *use dependent* or *action dependent* channel, see [80–82]. Our work represents, to the best of our knowledge, the first instance of this implicit temperature constrained problem in the context of energy harvesting communications.

In the implicit temperature constrained model, transmissions in the previous slots interfere with the current transmission due to temperature dependent noise and the causality of the temperature filter. This filter is the discrete time version of the continuous time first order filter that defines the temperature dynamics. For the general signal to interference plus noise ratio (SINR), we observe that the problem is non-convex and is a signomial problem for which we obtain a local optimal solution using the single condensation method in [83]. We then propose a heuristic algorithm which improves upon the local optimal solution and may achieve the global optimal solution. Then, we consider the extreme settings of low and high SINR regimes. We show that in the low SINR regime, saving energy till the last slot and transmitting only in the last slot is optimal. For the high SINR regime, we observe that the problem is a *geometric program* and we explore specific structural results in this setting. Expanding upon the equivalence of this problem to its convex counterpart via a one-to-one transformation, we show that the KKT conditions in the original problem have a unique solution. Then, we obtain an algorithm to solve the KKT conditions in the original problem. We show convergence of this algorithm to the

unique solution of the KKT conditions. We then show that for this unique solution, the power sequence is monotone increasing; hence, proving the monotone increasing property of the optimal power sequence.

Then, we consider the case when implicit and explicit temperature constraints are simultaneously active. In general, we observe that the problem is non-convex and the same signomial programming approach as in the implicit temperature constrained case is applicable. In the high SINR regime, the problem is a geometric program and we show in the temperature limited case that the optimal power sequence is monotone decreasing under certain conditions. We illustrate our findings in various numerical results.

In Chapter 10, we extend the explicit temperature constraint model studied in Chapter 9 to a multi-user setting. We study the optimal offline power allocation for the two-user multiple access channel model. We first show that the capacity region for the energy harvesting multiple access channel with peak temperature constraints is a convex region, and hence, the region can be fully characterized by studying its tangent lines. For the single energy arrival, we show that the optimal achievable rate region is a single pentagon which is constructed by the intersection of two pentagons which result from the energy and temperature constraints. We show that for the multiple energy arrivals that the optimal power allocations can be obtained by generalized water-filling. We then study the special case when the energy is abundant and the only binding constraint is the peak temperature constraint at the nodes. In this case, we provide an explicit structure for the optimal power allocations; we show that at any point in the optimal rate region at least one of

the powers is non-increasing. We also show that the sum of the powers is also non-decreasing in most of the optimal rate region. Then, we derive sufficient conditions under which the optimal rate region of the multiple access channel reduces to a single pentagon.

In Chapter 11, we provide conclusions to this dissertation.

CHAPTER 2

Optimal and Near-Optimal Online Strategies for Energy Harvesting Broadcast Channels

2.1 Introduction

We consider an energy harvesting broadcast channel, Fig. 2.1, in which a transmitter which harvests energy from nature at random times and amounts, serves data to two receivers on the downlink. The transmitter has two buffers, one for the incoming data and one for the harvested energy. The data buffer is infinitely backlogged. The energy buffer (battery), which is of finite size B, is recharged randomly by the energy harvesting process throughout the course of communication. We consider the *online* setting where the transmitter gets to know the energy arrivals (harvests) only causally as they happen. The transmitter needs to determine a *transmission policy*, which chooses the total transmit power and also the amount of power allocated to serve each user's data, as a function of the available energy in the battery.

2.2 System Model

We consider a two-user energy harvesting broadcast channel, see Fig. 2.1. The transmitter has a battery of size B. The time is slotted. At each time slot i, E_i units of energy enters the battery (is harvested), where E_i is an i.i.d. random process. We denote the amount of energy in the battery at time i as b_i. We follow a transmit-first strategy, where in each slot data is transmitted first and then energy is harvested. The battery energy level evolves as:

$$b_i = \min\{B, b_{i-1} - P_{i-1} + E_i\} \tag{2.1}$$

where P_{i-1} is the energy of the symbol transmitted in slot $i-1$, and it is limited by the amount of energy available in the battery in that slot, i.e., $P_{i-1} \leq b_{i-1}$.

The underlying physical layer is a Gaussian broadcast channel, where the received signal at receiver k is $Y_k = X + N_k$, for $k = 1, 2$. Here, X is the transmitted signal and N_k are the Gaussian receiver noises with variances σ_k^2. Without loss of generality, let $\sigma_1^2 < \sigma_2^2$. The Gaussian broadcast channel is degraded. In this case, it is degraded in favor of the first user, i.e., the first user is the stronger user and the second user is the weaker user. The capacity region of the Gaussian broadcast channel in slot i is [84] (see e.g., [5–7]):

$$r_{1i} \leq \frac{1}{2} \log\left(1 + \frac{\alpha_i P_i}{\sigma_1^2}\right) \tag{2.2}$$

$$r_{2i} \leq \frac{1}{2} \log\left(1 + \frac{(1-\alpha_i) P_i}{\alpha_i P_i + \sigma_2^2}\right) \tag{2.3}$$

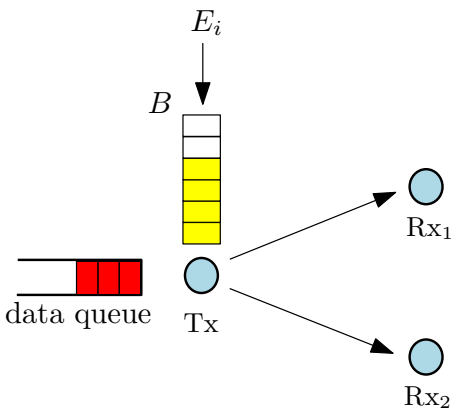

Figure 2.1: System model: an energy harvesting broadcast channel.

The boundary of the capacity region is traced by sweeping α_i in $[0, 1]$. On the boundary, X is Gaussian with power P_i, where $\alpha_i P_i$ portion of this power is allocated to serve the data of the stronger user, and $(1-\alpha_i)P_i$ is allocated to serve the data of the weaker user. The stronger user experiences no interference as it can decode and subtract the weaker user's signal (see (2.2)), while the weaker user experiences the power allocated for the stronger user as interference (see (2.3)). On the boundary of the capacity region where (2.2) and (2.3) are satisfied with equality, we can write P_i in terms of the rates r_{1i} and r_{2i} as:

$$P_i = \sigma_1^2 e^{2(r_{1i}+r_{2i})} + (\sigma_2^2 - \sigma_1^2)e^{2r_{2i}} - \sigma_2^2 \triangleq g(r_{1i}, r_{2i}) \tag{2.4}$$

Therefore, $g(r_{1i}, r_{2i})$ is the minimum total power needed to provide users with rates r_{1i} and r_{2i}.

Our goal in this chapter is to characterize the optimal long-term throughput region of the system. We characterize this region by characterizing its tangent lines. Therefore, characterizing this region is equivalent to determining long-term weighted

average throughput:

$$\Phi = \max_{P \in \hat{\mathcal{F}}} \lim_{n \to \infty} \mathbb{E}\left[\frac{1}{n}\sum_{i=1}^{n} \max_{\alpha_i \in [0,1]} (\mu_1 r_{1i} + \mu_2 r_{2i})\right] \tag{2.5}$$

for all $\mu_1, \mu_2 \in [0,1]$, where $\hat{\mathcal{F}}^n$ denotes the feasible region for transmit powers subject to causal energy knowledge. From (2.1), the current battery state b_i depends on the previous slot through the action, P_{i-1}, and battery state, b_{i-1}, along with the current energy arrival E_i. The stage reward is $\max_{\alpha_i \in [0,1]}(\mu_1 r_{1i} + \mu_2 r_{2i})$ and the admissible policies at each stage, P_i, are the values in $[0, b_i]$ which depend only on the current battery state. Hence, it follows that the optimal policy exists and is Markovian see e.g., [85, Theorem 6.4] and [86, Theorem 4.4.2], respectively. The optimal Markov policy can then be found using dynamic programming by solving Bellman's equations [87, Chapter 4]. Hence, (2.5) can be expressed as:

$$\Phi = \lim_{n \to \infty} \mathbb{E}\left[\frac{1}{n}\sum_{i=1}^{n} (\mu_1 r_{1i}^* + \mu_2 r_{2i}^*)\right] \tag{2.6}$$

where r_{1i} and r_{2i} are replaced by r_{1i}^* and r_{2i}^*, respectively, due to the existence of the optimal Markovian policy.

While we will eventually consider an arbitrary i.i.d. energy arrival process E_i, initially, we will consider a special i.i.d. energy arrival process which is Bernoulli with a particular support set, in particular, $E_i = 0$ with probability $1 - p$, and $E_i = B$ with probability p. That is, the energy arrival process is such that, either no energy arrives, or when energy arrives, it fills the battery completely. This process will

enable *renewals* when energy arrives. We will start with this special energy arrival process in Section 2.3 and consider the general arrivals in Section 2.4.

2.3 Optimal Strategy: Case of Bernoulli Arrivals

Since broadcast rate region is convex, we characterize it by determining its tangent lines. Thus, we consider all weighted sum rates of the form $\mu_1 r_1 + \mu_2 r_2$, where μ_1, μ_2 are both in $[0, 1]$, and are referred to as the *priorities* of the users. The average weighted sum rate is:

$$\lim_{n\to\infty} \mathbb{E}\left[\frac{1}{n}\sum_{i=1}^{n}(\mu_1 r_{1i}^* + \mu_2 r_{2i}^*)\right] \tag{2.7}$$

A non-zero energy arrival resets the system and forms a *renewal*. Then, from [88, Theorem 3.6.1] (see also [89]):

$$\lim_{n\to\infty} \mathbb{E}\left[\frac{1}{n}\sum_{i=1}^{n}(\mu_1 r_{1i}^* + \mu_2 r_{2i}^*)\right] = \frac{1}{\mathbb{E}[L]}\mathbb{E}\left[\sum_{i=1}^{L}(\mu_1 r_{1i}^* + \mu_2 r_{2i}^*)\right] \tag{2.8}$$

$$= p\sum_{k=1}^{\infty} p(1-p)^{k-1}\sum_{i=1}^{k}(\mu_1 r_{1i}^* + \mu_2 r_{2i}^*) \tag{2.9}$$

$$= \sum_{i=1}^{\infty}\sum_{k=i}^{\infty} p^2(1-p)^{k-1}(\mu_1 r_{1i}^* + \mu_2 r_{2i}^*) \tag{2.10}$$

$$= \sum_{i=1}^{\infty} p(1-p)^{i-1}(\mu_1 r_{1i}^* + \mu_2 r_{2i}^*) \tag{2.11}$$

where L is the inter-arrival time, which is geometric with p. We used $\mathbb{P}[L = k] = p(1-p)^{k-1}$, and $\mathbb{E}[L] = 1/p$ in (2.8)-(2.11). Hence, the rate and therefore power

allocation problem becomes:

$$\begin{aligned} \max_{\{r_{1i},r_{2i}\}} \quad & \sum_{i=1}^{\infty} p(1-p)^{i-1}(\mu_1 r_{1i} + \mu_2 r_{2i}) \\ \text{s.t.} \quad & \sum_{i=1}^{\infty} g(r_{1i}, r_{2i}) \leq B \\ & r_{1i}, r_{2i} \geq 0, \quad \forall i \end{aligned} \tag{2.12}$$

which is an optimization problem only in terms of the rates. In essence, this optimization problem aims to maximize the expected (weighted sum) transmitted rate before the next energy arrival. Therefore, the power allocation policy obtained as the solution of (2.12) corresponds to the optimum power allocation policy between two energy arrivals.

Here, μ_1 and μ_2 determine the point on the boundary of the capacity region, and also the power (and rate) schedule that achieves it. First, we will consider the case where one of the μ_i is zero (without loss of generality $\mu_2 = 0$). This will achieve the intercept of the boundary of the capacity region with one of the axes. This will also reduce our multi-user broadcast setting into the single-user setting of [48, 49]. We present this setting in the next sub-section for completeness and also to emphasize some of the properties of the solution. We will consider the general case where μ_1 and μ_2 are non-zero in the subsequent sub-section.

2.3.1 $\mu_1 > 0$, $\mu_2 = 0$

In this case, the problem in (2.12) specializes to:

$$\begin{aligned} \max_{\{r_{1i}\}} \quad & \sum_{i=1}^{\infty} p(1-p)^{i-1} r_{1i} \\ \text{s.t.} \quad & \sum_{i=1}^{\infty} \sigma_1^2 e^{2r_{1i}} - \sigma_1^2 \leq B \\ & r_{1i} \geq 0, \quad \forall i \end{aligned} \tag{2.13}$$

This problem is convex and is solved in [48, 49]. The Lagrangian is:

$$\mathcal{L} = -\sum_{i=1}^{\infty} p(1-p)^{i-1} r_{1i} + \lambda \left(\sum_{i=1}^{\infty} \sigma_1^2 e^{2r_{1i}} - \sigma_1^2 - B \right) - \sum_{i=1}^{\infty} \nu_i r_{1i} \tag{2.14}$$

where λ, $\nu_i \geq 0$, $\forall i$. The necessary and sufficient KKT optimality conditions are:

$$-p(1-p)^{i-1} + \lambda \sigma_1^2 e^{2r_{1i}} - \nu_i = 0, \quad \forall i \tag{2.15}$$

Here, and also in all the subsequent KKT conditions, we absorb constants into Lagrange multipliers. For instance, in (2.15) a factor of 2 in the second term is absorbed into the Lagrange multiplier λ, i.e., we implicitly define a new Lagrange multiplier which is equal to 2λ. Note that this does not affect the optimum solution or the analysis of the problem. When $r_{1i} > 0$, from complementary slackness $\nu_i = 0$,

and we have:

$$e^{2r_{1i}} = \frac{p(1-p)^{i-1}}{\lambda\sigma_1^2} \tag{2.16}$$

Accordingly, from $r_{1i} = \frac{1}{2}\log\left(1 + \frac{P_i}{\sigma_1^2}\right)$, when $P_i > 0$, we have:

$$P_i = \frac{p(1-p)^{i-1}}{\lambda} - \sigma_1^2 \tag{2.17}$$

We first note from (2.16)-(2.17) that the optimum rate and power decrease in time; they decrease strictly when $p \in (0, 1)$. Therefore, there exists a time i at which power P_i hits zero. Let us denote the last instance when $P_i > 0$ as $\tilde{N}$. Therefore, $\tilde{N}$ is the smallest integer such that,

$$p(1-p)^{\tilde{N}} < \lambda\sigma_1^2 \tag{2.18}$$

In addition, all power must be consumed, i.e., $\lambda > 0$, as otherwise, we can increase one of the powers and improve the objective function. Thus,

$$\sum_{i=1}^{\tilde{N}} \left(\frac{p(1-p)^{i-1}}{\lambda} - \sigma_1^2\right) = B \tag{2.19}$$

From (2.19), we have,

$$\lambda = \frac{1 - (1-p)^{\tilde{N}}}{B + \tilde{N}\sigma_1^2} \tag{2.20}$$

Inserting (2.20) into (2.18), we find the optimum $\tilde{N}$ as the smallest integer satisfying,

$$\left[p\left(\frac{B}{\sigma_1^2}+\tilde{N}\right)+1\right](1-p)^{\tilde{N}}<1 \tag{2.21}$$

We note from (2.21) that $\tilde{N}$, and therefore, the optimum power depends on the noise variance σ_1^2. Next, we show that, if the noise variance is larger, then the transmission duration is shorter. To that end, by rearranging (2.21), we obtain,

$$\frac{B}{\sigma_1^2}<\frac{1-(1-p)^{\tilde{N}}}{p(1-p)^{\tilde{N}}}-\tilde{N} \tag{2.22}$$

Let us denote the right hand side of (2.22) as $f(i)\triangleq\frac{1-(1-p)^i}{p(1-p)^i}-i$. Then, $f(i)$ increases in i since,

$$f(i+1)-f(i)=\frac{1}{(1-p)^{i+1}}-1\geq 0 \tag{2.23}$$

Therefore, as σ_1^2 increases, the left hand side of (2.22) decreases, and thus, the smallest value of $\tilde{N}$ for which (2.22) is satisfied decreases.

We summarize the important properties of the optimum single-user transmission policy compactly in the following lemma, whose proof is developed above in this sub-section.

Lemma 2.1 *The optimal single-user online power allocation policy for i.i.d. Bernoulli energy arrivals: 1) decreases in time; 2) depends on the noise variance, i.e., is not universal; and 3) the transmission duration $\tilde{N}$ decreases as the noise variance in-*

creases.

2.3.2 $\mu_1, \mu_2 > 0$

First, we note that, from the degradedness of the channel, if $\mu_1 \geq \mu_2$ then $r_{1i} > 0$ and $r_{2i} = 0$. Hence, we go back to the single-user power allocation as in the previous sub-section when $\mu_1 \geq \mu_2$. Therefore, the only remaining case to solve for is the case when $\mu_1 < \mu_2$.

The Lagrangian for the problem in (2.12) is:

$$\begin{aligned}\mathcal{L} = &- \sum_{i=1}^{\infty} p(1-p)^{i-1}(\mu_1 r_{1i} + \mu_2 r_{2i}) \\ &+ \lambda \left(\sum_{i=1}^{\infty} \sigma_1^2 e^{2(r_{1i}+r_{2i})} + (\sigma_2^2 - \sigma_1^2)e^{2r_{2i}} - \sigma_2^2 - B \right) \\ &- \sum_{i=1}^{\infty} \nu_{1i} r_{1i} - \sum_{i=1}^{\infty} \nu_{2i} r_{2i} \end{aligned} \tag{2.24}$$

The necessary and sufficient KKT optimality conditions $\forall i$ are:

$$-\mu_1 p(1-p)^{i-1} + \lambda \sigma_1^2 e^{2(r_{1i}+r_{2i})} - \nu_{1i} = 0 \tag{2.25}$$

$$-\mu_2 p(1-p)^{i-1} + \lambda \left(\sigma_1^2 e^{2(r_{1i}+r_{2i})} + (\sigma_2^2 - \sigma_1^2)e^{2r_{2i}} \right) - \nu_{2i} = 0 \tag{2.26}$$

Starting from (2.26) and using (2.4), we have

$$g(r_{1i}, r_{2i}) = \frac{\mu_2 p(1-p)^{i-1} + \nu_{2i}}{\lambda} - \sigma_2^2 \tag{2.27}$$

$$\geq \sigma_1^2 e^{2(r_{1i}+r_{2i})} - \sigma_1^2 \tag{2.28}$$

$$= \frac{\mu_1 p(1-p)^{i-1} + \nu_{1i}}{\lambda} - \sigma_1^2 \tag{2.29}$$

$$\geq \frac{\mu_1 p(1-p)^{i-1}}{\lambda} - \sigma_1^2 \tag{2.30}$$

where the inequality in (2.28) is satisfied with equality when $r_{2i} = 0$, (2.29) follows from (2.25), and the inequality in (2.30) is satisfied with equality when $r_{1i} > 0$. Therefore, when $r_{2i} > 0$, we have

$$g(r_{1i}, r_{2i}) = \frac{\mu_2 p(1-p)^{i-1}}{\lambda} - \sigma_2^2 > \frac{\mu_1 p(1-p)^{i-1}}{\lambda} - \sigma_1^2 \tag{2.31}$$

While, when $r_{2i} = 0$ (which also implies that $r_{1i} > 0$), we have

$$g(r_{1i}, r_{2i}) = \frac{\mu_1 p(1-p)^{i-1}}{\lambda} - \sigma_1^2 > \frac{\mu_2 p(1-p)^{i-1}}{\lambda} - \sigma_2^2 \tag{2.32}$$

Therefore, we have

$$g(r_{1i}, r_{2i}) = \max\{u_i, v_i\} \tag{2.33}$$

where

$$u_i = \frac{\mu_2 p(1-p)^{i-1}}{\lambda} - \sigma_2^2 \tag{2.34}$$

$$v_i = \frac{\mu_1 p(1-p)^{i-1}}{\lambda} - \sigma_1^2 \tag{2.35}$$

Hence, (2.33)-(2.35) give the general form of the optimum $g(r_{1i}, r_{2i})$, which is the optimum total transmit power, P_i^*, in the broadcast channel.

Next, we solve for the components of the optimum total transmit power allocated to serving the two users' data, i.e., we solve for α_i, or in other words, for P_{1i} and P_{2i}, where $P_{1i} = \alpha_i P_i$ and $P_{2i} = (1-\alpha_i)P_i$, or equivalently the optimal rates r_{1i} and r_{2i}. To that end, let us assume that we have solved for the ith slot total transmit power allocation P_i^* for all i already. Then, within the ith slot, the optimization problem is:

$$\begin{aligned} \max_{\{r_{1i}, r_{2i}\}} \quad & p(1-p)^{i-1}(\mu_1 r_{1i} + \mu_2 r_{2i}) \\ \text{s.t.} \quad & g(r_{1i}, r_{2i}) \leq P_i^* \\ & r_{1i}, r_{2i} \geq 0 \end{aligned} \tag{2.36}$$

If $\mu_1 \geq \mu_2$, then from the degradedness of the channel, all the total power will be allocated to the message of user 1, i.e., $P_{1i} = P_i^*$. For $\mu_1 < \mu_2$, using the KKT optimality conditions for (2.36), we obtain the following structure for the optimum solution:

$$P_c = \left(\frac{\mu_1 \sigma_2^2 - \mu_2 \sigma_1^2}{\mu_2 - \mu_1} \right)^+ \tag{2.37}$$

$$P_{1i} = \min\{P_c, P_i^*\} \tag{2.38}$$

$$P_{2i} = P_i^* - P_{1i} \tag{2.39}$$

We provide the details of the derivation of (2.37)-(2.39) in the Appendix. In (2.37)-(2.39), P_c is the *cut-off* power level, which determines the maximum possible power to allocate to the message of user 1. We already know from the discussion before

(2.37) that if $\mu_1 \geq \mu_2$, then all the total power will be allocated to the message of user 1, i.e., $P_{1i} = P_i^*$ and $P_{2i} = 0$. From (2.37)-(2.39), we see that, if $\mu_2 \geq \frac{\sigma_2^2}{\sigma_1^2}\mu_1$, then $P_c = 0$, and hence, no power will be allocated to the message of user 1, and all the power will be allocated for the message of user 2, i.e., $P_{1i} = 0$ and $P_{2i} = P_i^*$. For all the other cases, i.e., when $\mu_1 < \mu_2 < \frac{\sigma_2^2}{\sigma_1^2}\mu_1$, P_c is positive and user 1 will be allocated the minimum of P_c and the total available power P_i^*, and user 2 will be allocated the remaining power.

From the development in this sub-section, we conclude the following observations: First, the optimum total transmit power, P_i^*, which is given by (2.33)-(2.35) is decreasing in time, as both u_i in (2.34) and v_i in (2.35) are decreasing, and $g(r_{1i}, r_{2i})$ in (2.33) is the maximum of two decreasing sequences, which is decreasing. Second, the power allocated to the stronger user's message, P_{1i}, is either equal to P_c if $P_i^* \geq P_c$ and therefore is constant, or is equal to P_i^* if $P_i^* < P_c$ and therefore is decreasing. Thus, the power allocated to the stronger user's message is decreasing. Third, the power allocated to the weaker user's message, P_{2i}, is either decreasing or equal to zero; it is decreasing when $P_{1i} = P_c$ and is equal to zero when $P_{1i} = P_i^*$. Note that, when the stronger user's power allocation is strictly decreasing, i.e., when $P_{1i} = P_i^*$, this happens towards the end of the transmission, and during this time the weaker user's power allocation is zero. This means that there exist numbers $\tilde{M}$ and $\tilde{N}$ with $\tilde{M} < \tilde{N}$ such that powers allocated to both users are positive for slots $i = 1, \ldots, \tilde{M}$ and the power allocated only for the stronger user is positive for slots $i = \tilde{M} + 1, \ldots, \tilde{N}$. This optimal policy is illustrated in Fig. 2.2.

We summarize the important properties of the optimum broadcast transmis-

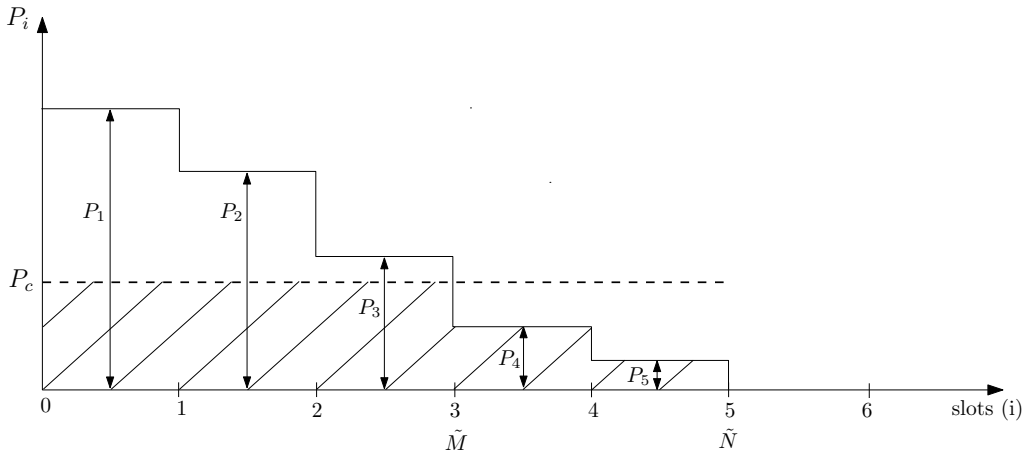

Figure 2.2: Structure of the optimal policy. The shaded part is the portion of the power dedicated to user 1 (stronger user), and the unshaded part is dedicated for user 2 (weaker user). In this example, $\tilde{M} = 3$ and $\tilde{N} = 5$.

sion policy compactly in the following lemma, whose proof is developed above in this sub-section.

Lemma 2.2 *The optimal online power allocation policy for the broadcast channel with i.i.d. Bernoulli energy arrivals is as follows: 1) the total transmit power decreases in time; 2) the individual powers allocated to both users' messages decrease in time; 3) the stronger user's power allocation is positive for a duration longer than the duration for which the weaker user's power allocation is positive.*

We now give the explicit solution for the optimum broadcast channel power schedule. When $\mu_1 > \mu_2$ or $\mu_2 \geq \frac{\sigma_2^2}{\sigma_1^2}\mu_1$, the problem reduces to a single-user problem, and the method in the previous sub-section can be used. When $\mu_1 < \mu_2 \leq \mu_1\frac{\sigma_2^2}{\sigma_1^2}$, both users are served according to the properties of the optimum solution described above. Hence, we need to solve for $\tilde{M}$ and $\tilde{N}$. For slots $i = 1, \ldots, \tilde{M}$, both users are served, and hence from (2.31), we have $g(r_{1i}, r_{2i}) = u_i$, for $i = 1, \ldots, \tilde{M}$. For slots $i = \tilde{M}+1, \ldots, \tilde{N}$, only the stronger user is served, and hence from (2.32), we have

$g(r_{1i}, r_{2i}) = v_i$. In addition, the total power constraint needs to be satisfied with equality and hence, λ should be chosen such that,

$$\sum_{i=1}^{\tilde{M}} u_i + \sum_{i=\tilde{M}+1}^{\tilde{N}} v_i = B \tag{2.40}$$

Using (2.34)-(2.35), we solve (2.40) for λ and obtain

$$\lambda = \frac{\mu_2 - (\mu_2 - \mu_1)(1-p)^{\tilde{M}} - \mu_1(1-p)^{\tilde{N}}}{B + \tilde{N}\sigma_1^2 + \tilde{M}(\sigma_2^2 - \sigma_1^2)} \tag{2.41}$$

Therefore, if the values of $\tilde{M}$ and $\tilde{N}$ are known, λ can be obtained from (2.41). The problem then becomes to find the values of $\tilde{M}$ and $\tilde{N}$; in fact, the problem is to solve for $\tilde{M}$, $\tilde{N}$ and λ jointly. The optimal $\tilde{M} \leq \tilde{N}$ are the smallest integers such that the following conditions are satisfied

$$\mu_1 p(1-p)^{\tilde{N}} < \sigma_1^2 \lambda \tag{2.42}$$

$$\frac{\mu_2 p(1-p)^{\tilde{M}}}{\lambda} - \sigma_2^2 < P_c \tag{2.43}$$

where λ is given by (2.41). The first condition is similar to the single-user condition in (2.18) which ensures that there is no further slot that can be utilized after slot $\tilde{N}$, i.e., the power drops below zero after slot $\tilde{N}$. The second condition is to obtain the slot number $\tilde{M}$ after which the power drops below P_c, hence the weaker user is no longer served. The solution to (2.41)-(2.43) is unique since it is the smallest pair of numbers satisfying these conditions. An example case where $\tilde{M}$, $\tilde{N}$ and P_c are

marked is shown in Fig. 2.2.

2.4 Near Optimal Strategies: General Energy Arrivals

In this section, we consider the case of general i.i.d. energy arrivals which are not necessarily Bernoulli. Let E_i be an arbitrary i.i.d. energy arrival process with average recharge rate $\mathbb{E}[E_i] = \mu$. In this case, finding the *exactly optimal* transmission scheme analytically seems intractable, as there is no *renewal* property as in Bernoulli arrivals. Nevertheless, we will determine a *nearly optimal* transmission scheme. Towards that end, we first propose a sub-optimal online scheme which depends only on the average recharge rate μ and the variances of the receiver noises, σ_1^2, σ_2^2 in the next sub-section. We then develop a lower bound on the performance of this policy for the case of Bernoulli arrivals. Next, we show that, under this scheme, the performance of Bernoulli energy arrivals provides a lower bound for the performance of any general i.i.d. energy arrival process. Finally, we develop a universal upper bound which depends only on the average recharge rate and receiver noise variances (does not depend on the specific statistics of the energy arrival process), and show that the proposed sub-optimal online scheme is within a constant gap from the upper bound, and therefore, from the optimum online scheme.

2.4.1 Sub-Optimal Scheme: Fractional Power Constant Cut-Off (FPCC) Policy

We first define the policy for Bernoulli energy arrivals, and then generalize it to general energy arrivals. We note that for Bernoulli energy arrivals, the optimal total transmit power allocated decreases exponentially over time, see (2.33)-(2.35); and the total transmit power is divided among users according to a cut-off property, see (2.37)-(2.39). As in [48, 49], this motivates us to construct a fractional power policy over time. Consider that in a Bernoulli arrival case, we had an energy arrival and the battery became full. Then, in the next slot we allocate a p fraction of the available energy for transmission, i.e., Bp. This reduces the available energy in the battery to $B(1-p)$. In the next slot, we allocate a p fraction of the available energy for transmission, i.e., $Bp(1-p)$, and so on so forth. This gives a total power allocation policy which is $P_i = Bp(1-p)^{i-1}$ in slot i, which is different from the optimum described in (2.33)-(2.35), but preserves the *fractional* structure. Next, we follow the exact optimum partition of this sub-optimal total transmit power in all slots among the two users as in (2.37)-(2.39). That is, we allocate $P_{1i} = \min\{P_c, Bp(1-p)^{i-1}\}$ for user 1, and $P_{2i} = Bp(1-p)^{i-1} - P_{1i}$ for user 2. Note that, this results in a *universal* allocation of total transmit power, which does not depend on priorities μ_1, μ_2 (unlike the optimum (2.33)-(2.35)), while the allocation of individual powers is optimum as in (2.37)-(2.39) and depends on μ_1, μ_2.

For general energy arrivals, we allocate a fraction $q = \mu/B$ of the available energy in the battery for transmission, i.e., if the energy available in the battery in

slot i is b_i, we choose the total transmit power in that slot as $P_i = qb_i$. Then, we partition the total transmit power between the two users as in the optimum scheme in (2.37)-(2.39), i.e., we allocate $P_{1i} = \min\{P_c, qb_i\}$ for user 1, and $P_{2i} = qb_i - P_{1i}$ for user 2.

2.4.2 A Lower Bound on the Proposed Online Policy

We first develop a lower bound for the proposed FPCC policy for the case of Bernoulli arrivals. The power allocated to the stronger user is $P_{1i} = \min\{P_c, Bp(1-p)^{i-1}\}$. Let us define a deterministic integer i^* as

$$i^* \triangleq \max\{i \in \mathbb{N} : P_c \leq Bp(1-p)^{i-1}\} \tag{2.44}$$

If $P_c \leq pB$, then, i^* represents the last slot until which the stronger user's power share is P_c; after i^*, the stronger user gets the entire power. We further define a random variable K as

$$K \triangleq \min\{i^*, L\} \tag{2.45}$$

where L is a geometric random variable with parameter p as used in (2.8)-(2.11). First, we give a lower bound for $\frac{\mathbb{E}[K]}{\mathbb{E}[L]}$ in the following lemma.

Lemma 2.3 *The quantity* $\frac{\mathbb{E}[K]}{\mathbb{E}[L]}$ *is lower bounded by* $\left(1 - \frac{P_c}{pB}\right)$.

Proof: Note that K takes values in $[1, i^*]$ with pmf $\mathbb{P}[K = k] = p(1-p)^{k-1}$ for

$k = 1, \ldots, i^* - 1$, and $\mathbb{P}[K = i^*] = (1-p)^{i^*-1}$. This follows since whenever $k < i^*$, we have $\mathbb{P}[K = k] = \mathbb{P}[L = k]$, which is the pmf of L which is geometric with parameter p; and, $K = i^*$ when $L \geq i^*$. Then,

$$\mathbb{E}[K] = \sum_{i=1}^{i^*-1} ip(1-p)^{i-1} + i^*(1-p)^{i^*-1} \tag{2.46}$$

$$= \frac{1}{p}\left(1 - (1-p)^{i^*}\right) \tag{2.47}$$

Then, noting $\mathbb{E}[L] = 1/p$, we have

$$\frac{\mathbb{E}[K]}{\mathbb{E}[L]} = 1 - (1-p)^{i^*} \geq \left(1 - \frac{P_c}{pB}\right) \tag{2.48}$$

where the inequality follows because by the definition in (2.44) i^* satisfies $P_c > Bp(1-p)^{i^*}$. ■

Next, in the following lemma, we derive a lower bound for the rate region achievable with the FPCC policy for all i.i.d. Bernoulli energy arrivals.

Lemma 2.4 *The achievable rate region with the FPCC policy for any i.i.d. Bernoulli energy arrival process is lower bounded as follows,*

$$r_1 \geq \frac{1}{2}\log\left(1 + \frac{\alpha\mu}{\sigma_1^2}\right) - 0.72 \tag{2.49}$$

$$r_2 \geq \frac{1}{2}\log\left(1 + \frac{(1-\alpha)\mu}{\alpha\mu + \sigma_2^2}\right) - 0.99 \tag{2.50}$$

for some $\alpha \in [0,1]$, where $\mu = \mathbb{E}[E_i]$ is the average recharge rate.

Proof: When $\mu_1 \geq \mu_2$, the entire power is allocated to the message of the first user, and when $\mu_2 \geq \mu_1 \frac{\sigma_2^2}{\sigma_1^2}$, the entire power is allocated to the message of the second user. In these two cases, the system reduces to a single-user system [49]. These conditions are valid for both the optimum power allocation and the sub-optimum power allocation of FPCC. In addition, specific to FPCC, due to the sub-optimal fractional power allocation, from $P_{1i} = \min\{P_c, Bp(1-p)^{i-1}\}$, if $P_c > Bp$, then $P_c > Bp(1-p)^{i-1}$ for all i, and the stronger user gets all the power all the time, and the system again reduces to a single-user system [49]. Using (2.37), this last case happens when $\mu_1 \geq \frac{\sigma_1^2+Bp}{\sigma_2^2+Bp}\mu_2$. Therefore, in the following, we only consider the remaining case, which is $\frac{\sigma_2^2+Bp}{\sigma_1^2+Bp}\mu_1 < \mu_2 < \frac{\sigma_2^2}{\sigma_1^2}\mu_1$. In this case, $0 < P_c < Bp$, and $i^* \geq 1$.

First, we consider the first user's rate,

$$r_1 = \frac{1}{\mathbb{E}[L]}\mathbb{E}\left[\sum_{i=1}^{K}\frac{1}{2}\log\left(1+\frac{P_c}{\sigma_1^2}\right)+\sum_{i=K+1}^{L}\frac{1}{2}\log\left(1+\frac{Bp(1-p)^{i-1}}{\sigma_1^2}\right)\right] \tag{2.51}$$

$$\geq \frac{1}{\mathbb{E}[L]}\mathbb{E}\left[\sum_{i=1}^{K}\frac{1}{2}\log\left(1+\frac{P_c}{\sigma_1^2}\right)+\sum_{i=K+1}^{L}\left(\frac{1}{2}\log\left(1+\frac{Bp}{\sigma_1^2}\right)+\frac{i-1}{2}\log(1-p)\right)\right] \tag{2.52}$$

$$\geq \frac{1}{\mathbb{E}[L]}\mathbb{E}\left[\sum_{i=1}^{K}\frac{1}{2}\log\left(1+\frac{P_c}{\sigma_1^2}\right)+\sum_{i=K+1}^{L}\frac{1}{2}\log\left(1+\frac{Bp}{\sigma_1^2}\right)+\sum_{i=1}^{L}\frac{i-1}{2}\log(1-p)\right] \tag{2.53}$$

$$\geq \frac{1}{\mathbb{E}[L]}\mathbb{E}\left[\sum_{i=1}^{K}\frac{1}{2}\log\left(1+\frac{P_c}{\sigma_1^2}\right)+\sum_{i=K+1}^{L}\frac{1}{2}\log\left(1+\frac{P_c}{\sigma_1^2}\right)+\sum_{i=1}^{L}\frac{i-1}{2}\log(1-p)\right] \tag{2.54}$$

$$= \frac{1}{\mathbb{E}[L]}\mathbb{E}\left[\sum_{i=1}^{L}\frac{1}{2}\log\left(1+\frac{P_c}{\sigma_1^2}\right)+\sum_{i=1}^{L}\frac{i-1}{2}\log(1-p)\right] \tag{2.55}$$

$$=\frac{1}{2}\log\left(1+\frac{P_c}{\sigma_1^2}\right)+\frac{1}{\mathbb{E}[L]}\mathbb{E}\left[\frac{L(L-1)}{4}\log(1-p)\right] \tag{2.56}$$

$$\geq\frac{1}{2}\log\left(1+\frac{P_c}{\sigma_1^2}\right)-0.72 \tag{2.57}$$

where (2.52) follows because $\log(a+x)$ is monotone in x, (2.53) follows since $\log(1-p)$ is negative, (2.54) follows since $P_c \leq Bp$, and (2.57) follows by bounding the last term numerically as in [49].

Next, we consider the second user's rate,

$$r_2 =\frac{1}{\mathbb{E}[L]}\mathbb{E}\left[\sum_{i=1}^{K}\frac{1}{2}\log\left(1+\frac{Bp(1-p)^{i-1}-P_c}{P_c+\sigma_2^2}\right)\right] \tag{2.58}$$

$$=\frac{1}{\mathbb{E}[L]}\mathbb{E}\left[\sum_{i=1}^{K}\frac{1}{2}\log\left(\frac{Bp(1-p)^{i-1}+\sigma_2^2}{P_c+\sigma_2^2}\right)\right] \tag{2.59}$$

$$\geq\frac{1}{\mathbb{E}[L]}\mathbb{E}\left[\sum_{i=1}^{K}\frac{1}{2}\log\left(\frac{(1-p)^{i-1}\left(Bp+\sigma_2^2\right)}{P_c+\sigma_2^2}\right)\right] \tag{2.60}$$

$$=\frac{1}{\mathbb{E}[L]}\mathbb{E}\left[\sum_{i=1}^{K}\frac{1}{2}\log\left(\frac{Bp+\sigma_2^2}{P_c+\sigma_2^2}\right)\right]+\frac{1}{\mathbb{E}[L]}\mathbb{E}\left[\sum_{i=1}^{K}\frac{i-1}{2}\log(1-p)\right] \tag{2.61}$$

$$\geq\frac{1}{\mathbb{E}[L]}\mathbb{E}\left[\sum_{i=1}^{K}\frac{1}{2}\log\left(\frac{Bp+\sigma_2^2}{P_c+\sigma_2^2}\right)\right]+\frac{1}{\mathbb{E}[L]}\mathbb{E}\left[\sum_{i=1}^{L}\frac{i-1}{2}\log(1-p)\right] \tag{2.62}$$

$$=\frac{1}{\mathbb{E}[L]}\mathbb{E}\left[\sum_{i=1}^{K}\frac{1}{2}\log\left(\frac{Bp+\sigma_2^2}{P_c+\sigma_2^2}\right)\right]+\frac{1}{\mathbb{E}[L]}\mathbb{E}\left[\frac{L(L-1)}{4}\log(1-p)\right] \tag{2.63}$$

$$\geq\frac{1}{\mathbb{E}[L]}\mathbb{E}\left[\sum_{i=1}^{K}\frac{1}{2}\log\left(\frac{Bp+\sigma_2^2}{P_c+\sigma_2^2}\right)\right]-0.72 \tag{2.64}$$

$$=\frac{\mathbb{E}[K]}{\mathbb{E}[L]}\frac{1}{2}\log\left(\frac{Bp+\sigma_2^2}{P_c+\sigma_2^2}\right)-0.72 \tag{2.65}$$

$$\geq\left(1-\frac{P_c}{pB}\right)\frac{1}{2}\log\left(1+\frac{Bp-P_c}{P_c+\sigma_2^2}\right)-0.72 \tag{2.66}$$

where (2.60) follows because $\log(a+x)$ is monotone in x, (2.62) follows since $\log(1-p)$

is negative, (2.64) follows by bounding the last term numerically as in [49], and (2.66) follows from Lemma 2.3.

Since $P_c < Bp$, by substituting $P_c = \alpha pB$ with some $\alpha \in [0,1]$, and denoting $\mu = Bp$, from (2.57) and (2.66), we obtain the simultaneous lower bounds for the two rates,

$$r_1 \geq \frac{1}{2}\log\left(1+\frac{\alpha\mu}{\sigma_1^2}\right) - 0.72 \tag{2.67}$$

$$r_2 \geq \frac{(1-\alpha)}{2}\log\left(1+\frac{(1-\alpha)\mu}{\alpha\mu+\sigma_2^2}\right) - 0.72 \tag{2.68}$$

Next, we develop a further lower bound for the rate of user 2 as,

$$r_2 \geq \frac{1}{2}\log\left(1+\frac{(1-\alpha)\mu}{\alpha\mu+\sigma_2^2}\right) - \frac{\alpha}{2}\log\left(1+\frac{(1-\alpha)\mu}{\alpha\mu+\sigma_2^2}\right) - 0.72 \tag{2.69}$$

$$\geq \frac{1}{2}\log\left(1+\frac{(1-\alpha)\mu}{\alpha\mu+\sigma_2^2}\right) - \frac{\alpha}{2}\log\left(\frac{1}{\alpha}\right) - 0.72 \tag{2.70}$$

$$\geq \frac{1}{2}\log\left(1+\frac{(1-\alpha)\mu}{\alpha\mu+\sigma_2^2}\right) - 0.99 \tag{2.71}$$

where (2.70) follows since the second term increases in μ, hence, a lower bound is obtained by letting $\mu \to \infty$, and (2.71) follows by upper bounding the term $\frac{\alpha}{2}\log_2\left(\frac{1}{\alpha}\right)$ numerically to 0.265. This, combined with the 0.72 bound, gives a constant bound of 0.99. ■

The next step in lower bounding the achievable rates for general i.i.d. arrivals is to show that the Bernoulli energy arrivals give the lowest rate over all i.i.d. energy arrivals with the same mean. This was proved for the single-user case in [49]. We invoke this result in [49] together with a concavity result from [7] to prove the

following lemma.

Lemma 2.5 *For the FPCC policy, any i.i.d. energy arrival process yields an achievable rate region no smaller than that of the Bernoulli energy arrivals with the same mean.*

Proof: For the FPCC policy, the achievable weighted sum rate, $\mathcal{J}(g^n, E, x, \mu_1, \mu_2)$, under any energy arrival process E, initial battery state x, transmission policy $g^n = \{qb_i\}_{i=1}^n$, and for a given μ_1, μ_2 is given by,

$$\mathcal{J}(g^n, E, x, \mu_1, \mu_2) = \frac{1}{n}\mathbb{E}\left[\sum_{i=1}^{n} f(qb_i, \mu_1, \mu_2)\middle| b_1 = x\right] \tag{2.72}$$

where $f(g_i, \mu_1, \mu_2) \triangleq \max_{\alpha_i} \mu_1 r_1(\alpha_i, g_i) + \mu_2 r_2(\alpha_i, g_i)$, b_i is the battery state in slot i, and q is the fraction of power transmitted. It was shown in [7, Lemma 2], that after optimizing α_i, the function which is only in terms of the total power, $f(g_i, \mu_1, \mu_2)$ is strictly concave in the transmit power g_i. Hence, we can apply [49, Lemma 2], and following similar steps to [49, Proposition 4], we conclude that the rate region for Bernoulli arrivals provides a lower bound for all other i.i.d. energy arrivals. ■

Finally, we give a universal lower bound for the proposed FPCC policy under any i.i.d. energy arrival process in the following theorem. The lower bound depends only on the average recharge rate, but not on the statistics, of the energy harvesting process.

Theorem 2.1 *The achievable rate region with the FPCC policy for any arbitrary*

i.i.d. energy arrival process is lower bounded as follows,

$$r_1 \geq \frac{1}{2}\log\left(1+\frac{\alpha\mu}{\sigma_1^2}\right) - 0.72 \tag{2.73}$$

$$r_2 \geq \frac{1}{2}\log\left(1+\frac{(1-\alpha)\mu}{\alpha\mu+\sigma_2^2}\right) - 0.99 \tag{2.74}$$

for some $\alpha \in [0,1]$, where $\mu = \mathbb{E}[E_i]$ is the average recharge rate.

The proof of Theorem 2.1 follows from combining Lemma 2.4 and Lemma 2.5.

2.4.3 An Upper Bound for Online Policies

Here, we develop an upper bound for the performance of all online scheduling algorithms only in terms of the average recharge rate.

Theorem 2.2 *The optimal online achievable rate region is upper bounded as follows,*

$$r_1 \leq \frac{1}{2}\log\left(1+\frac{\alpha\mu}{\sigma_1^2}\right) \tag{2.75}$$

$$r_2 \leq \frac{1}{2}\log\left(1+\frac{(1-\alpha)\mu}{\alpha\mu+\sigma_2^2}\right) \tag{2.76}$$

for some $\alpha \in [0,1]$, where $\mu = \mathbb{E}[E_i]$ is the average recharge rate.

Proof: First, we note that the achievable rate region for the optimum online algorithm is upper bounded by the achievable rate region with the optimum offline algorithm, where all of the energy arrival information is known ahead of time. In addition, the achievable rate region with finite-sized battery is upper bounded by

the achievable rate region with an unlimited-sized battery. For the offline problem, eliminating the *no-energy-overflow* constraints due to the finite battery size, the feasible set for the total transmit power control policy g^n is

$$\mathcal{F}^n \triangleq \left\{ \{g_i\}_{i=1}^n : \frac{1}{m}\sum_{i=1}^{m} g_i \leq \frac{1}{m}\left(\sum_{i=1}^{m} E_i + B\right), \forall m = 1, \ldots, n \right\} \tag{2.77}$$

where we have added B to the right hand side of (2.77) to allow for the optimistic scenario that the system has started with a full battery at the beginning (while the upper bound does not depend on the initial battery state). Then the offline weighted sum rate with weights μ_1, μ_2 is,

$$R_{off} \triangleq \lim_{n\to\infty} \max_{\{g_i\}_{i=1}^n \in \mathcal{F}^n} \frac{1}{n}\sum_{i=1}^{n} f(g_i, \mu_1, \mu_2) \tag{2.78}$$

where $f(g_i, \mu_1, \mu_2)$ is the maximized weighted sum rate only in terms of the total transmit power g_i in slot i, after maximization with respect to partitioning of the power to users, i.e., $f(g_i, \mu_1, \mu_2) \triangleq \max_{\alpha_i} \mu_1 r_1(\alpha_i, g_i) + \mu_2 r_2(\alpha_i, g_i)$. We further upper bound this rate as,

$$R_{off} \leq \lim_{n\to\infty} \max_{\{g_i\}_{i=1}^n \in \mathcal{F}^n} f\left(\frac{1}{n}\sum_{i=1}^{n} g_i, \mu_1, \mu_2\right) \tag{2.79}$$

$$\leq f(\mu, \mu_1, \mu_2) \tag{2.80}$$

where the first inequality follows due to the concavity of $f(g_i, \mu_1, \mu_2)$ in g_i [7, Lemma 2]. The second inequality follows by relaxing the feasible set in (2.77) by

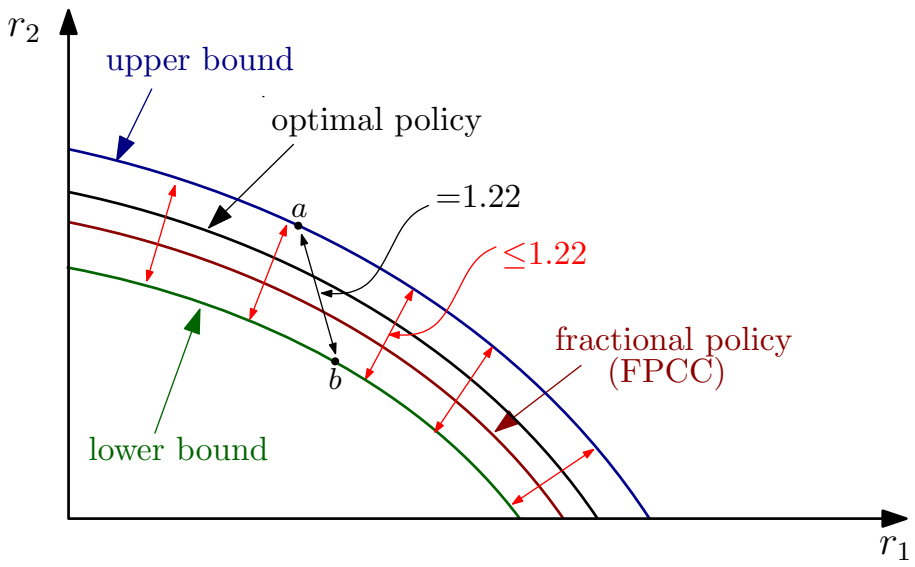

Figure 2.3: Illustration of the bounds on the optimal online policy and the proposed online policy FPCC. The distance between the upper and lower bound is less than 1.22. a and b are two points on the upper and lower bounds, respectively, with the same α.

removing all but the last constraint when $m = n$: $\frac{1}{n}\sum_{i=1}^{n} g_i \leq \frac{1}{n}(\sum_{i=1}^{n} E_i + B)$, and by noting that from strong law of large numbers $\frac{1}{n}\sum_{i=1}^{n} E_i \to \mu$ almost surely, and the remaining $\frac{1}{n}B$ terms goes to zero as n tends to infinity. Since, this is valid for all μ_1, μ_2, then $f(\mu, \mu_1, \mu_2)$ traces the boundary of the capacity region of the broadcast channel with average power constraint μ. ■

The Euclidean distance between any two points with the same α on the upper and lower bounds is equal to $\sqrt{0.72^2 + 0.99^2} = 1.22$. Since the distance between the two points with the same α can be no less than the distance between the two bounds, the distance between the two bounds is less than or equal to 1.22. Hence, combining Theorem 2.1 and Theorem 2.2, we conclude that the proposed online FPCC policy yields rates which are within a constant gap from the universal upper bound, and therefore, from the optimum online policy, for all system parameters.

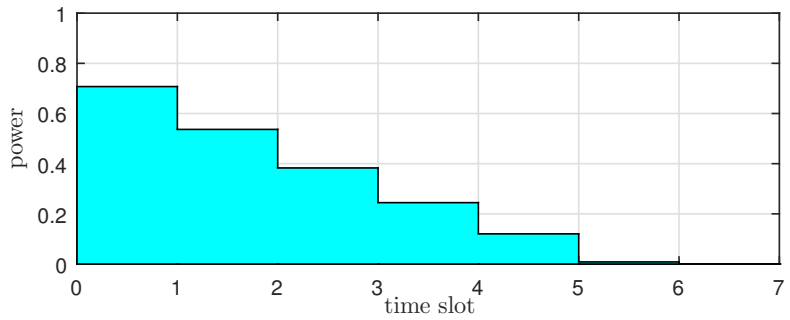

Figure 2.4: Optimum single-user power allocation for i.i.d. Bernoulli arrivals. Here, the receiver noise variance is $\sigma_1^2 = 1$.

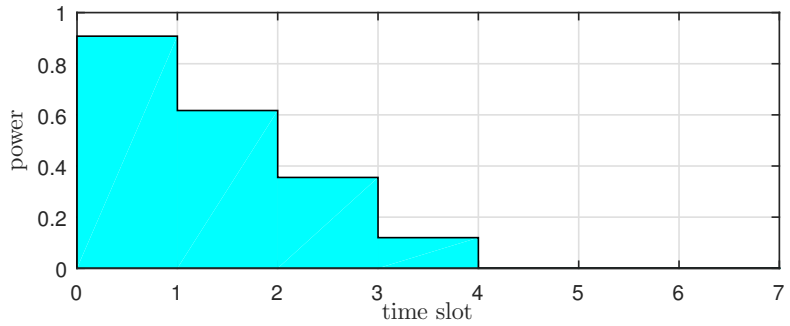

Figure 2.5: Optimum single-user power allocation for i.i.d. Bernoulli arrivals. Here, the receiver noise variance is $\sigma_1^2 = 2$.

We show the relations developed in Fig. 2.3.

2.5 Numerical Results

In this section, we illustrate the results obtained in this chapter using several numerical examples.

We first show the effect of receiver noise variance on the optimal online power allocation for the single-user case with i.i.d. Bernoulli arrivals. We let $B = 2$ and $p = 0.1$. The problem is stated in (2.13). We first solve it for $\sigma_1^2 = 1$ and plot the optimum power allocation in Fig. 2.4, and then solve it for $\sigma_1^2 = 2$ and plot the optimum power allocation in Fig. 2.5. We observe from Figs. 2.4 and 2.5, that 1)

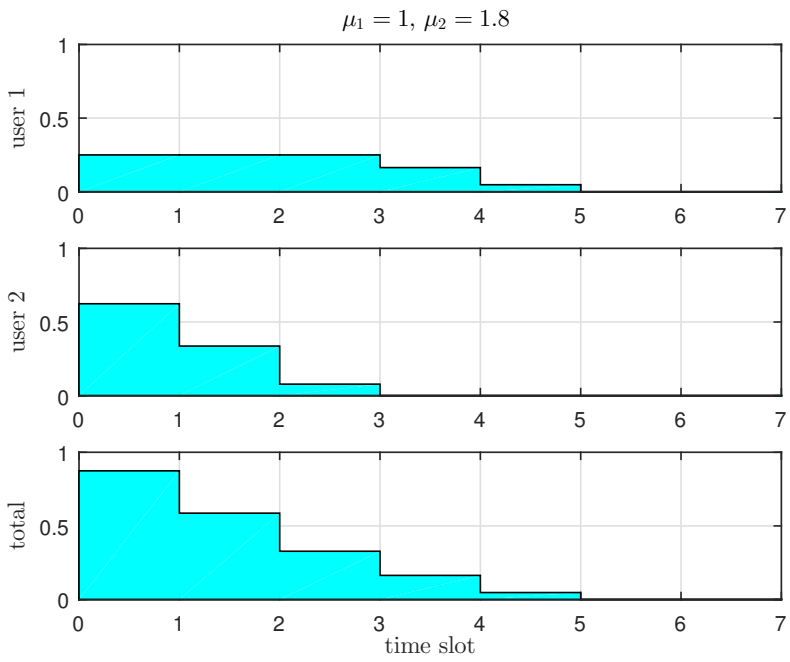

Figure 2.6: Optimal online power allocation for the broadcast channel with i.i.d. Bernoulli arrivals. Here, $\mu_1 < \mu_2 \leq \mu_1 \frac{\sigma_2^2}{\sigma_1^2}$, both user rates are positive: $\mu_1 = 1$, $\mu_2 = 1.8$.

the optimum power decreases over time, 2) depends on the noise variance, and 3) the transmission duration decreases as the noise variance increases: when $\sigma_1^2 = 1$, the total power is transmitted in $\tilde{N} = 6$ slots, while when $\sigma_1^2 = 2$, the total power is transmitted in $\tilde{N} = 4$ slots. That is, the power allocation shrinks towards the earlier slots as the noise variance increases. This also shows that the single-user solution is not universal as it depends on the receiver noise variance; this is unlike the case for the offline problem [1], where the solution is the same for all receiver noise variances, in fact, it is the same for all concave functions.

Next, we consider the broadcast channel with i.i.d. Bernoulli arrivals, and find the optimum power allocations: the optimum total power allocation P_i and its optimum distribution to users P_{1i} and P_{2i}. In this broadcast channel, we let $\sigma_1^2 = 1$

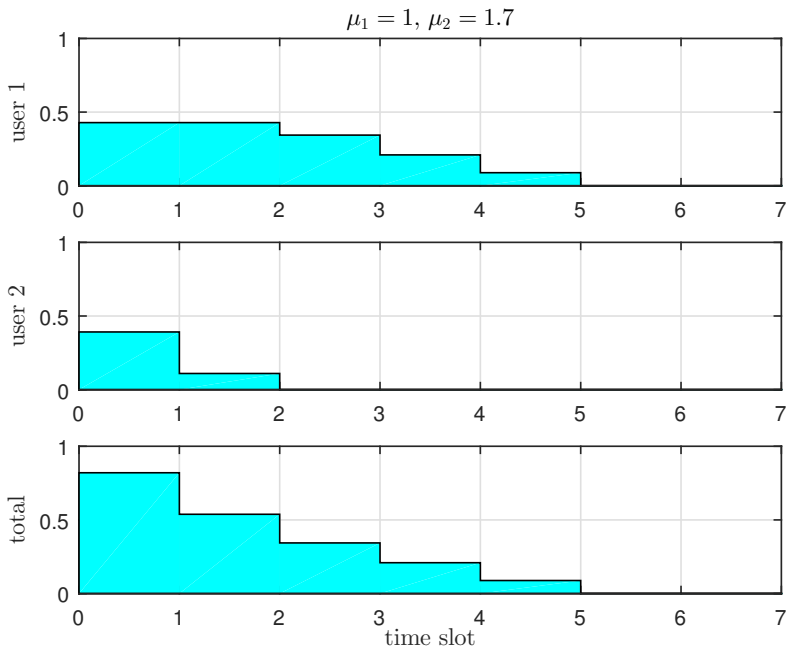

Figure 2.7: Optimal online power allocation for the broadcast channel with i.i.d. Bernoulli arrivals. Here, $\mu_1 < \mu_2 \leq \mu_1 \frac{\sigma_2^2}{\sigma_1^2}$, both user rates are positive: $\mu_1 = 1$, $\mu_2 = 1.7$.

and $\sigma_2^2 = 2$, and $B = 2$ and $p = 0.1$. In Figs. 2.6 and 2.7, we plot the optimum power allocations for two different points on the boundary of the capacity region corresponding to two different μ_1, μ_2 pairs. In both figures, μ_1, μ_2 are such that $\mu_1 < \mu_2 < \frac{\sigma_2^2}{\sigma_1^2}$ so that both users are allocated power and both users achieve non-zero rates. In Fig. 2.6, $\mu_1 = 1$, $\mu_2 = 1.8$ and Fig. 2.7, $\mu_1 = 1$, $\mu_2 = 1.7$; that is, in Fig. 2.7 the second user's priority is decreased. The problem is stated in (2.12). We solve it using the optimum total transmit power in (2.33)-(2.35) together with λ in (2.41), and the optimum power shares of the users in (2.37)-(2.39) and the transmission durations of the users $\tilde{M}$ and $\tilde{N}$ in (2.42)-(2.43). As proved in Lemma 2.2, we observe from Figs. 2.6 and 2.7, that 1) the optimum total transmit power decreases over time, 2) the individual powers allocated to users decrease over time as well,

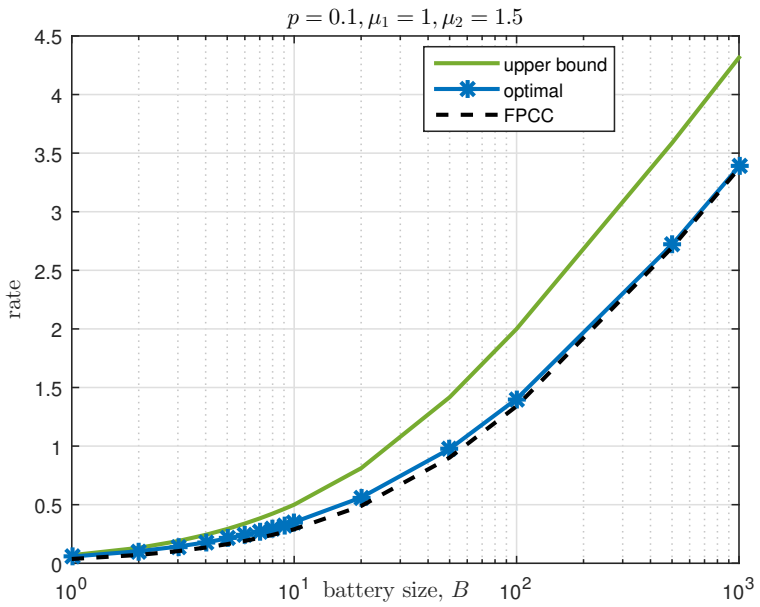

Figure 2.8: Achievable weighted sum rate for the optimum online and sub-optimum FPCC together with the upper bound as a function of the battery size B for a fixed energy arrival probability p for i.i.d. Bernoulli arrivals.

3) the stronger (first) user's power allocation is positive for a longer duration than that for the weaker (second) user. We also note that when the first user's power is constant (slots 1, 2, 3 in Fig. 2.6 and slots 1, 2 in Fig. 2.7), the second user's power is decreasing; and when the first user's power is decreasing (slots 4, 5 in Fig. 2.6 and slots 3, 4, 5 in Fig. 2.7), the second user's power is zero. We note that in Fig. 2.6, $\tilde{M} = 3$ and $\tilde{N} = 5$, and Fig. 2.7, $\tilde{M} = 2$ and $\tilde{N} = 5$. We note that as μ_2 decreases from the setting of Fig. 2.6 to the setting of Fig. 2.7, the second user's power allocation decreases.

Next, we consider the achievable rates as a function of the battery size B and energy arrival probability p for the case of i.i.d. Bernoulli arrivals. We consider a fixed set of weights: $\mu_1 = 1$ and $\mu_2 = 1.5$. In Fig. 2.8, we plot the achievable weighted sum rate with the optimal online solution and the sub-optimal FPCC

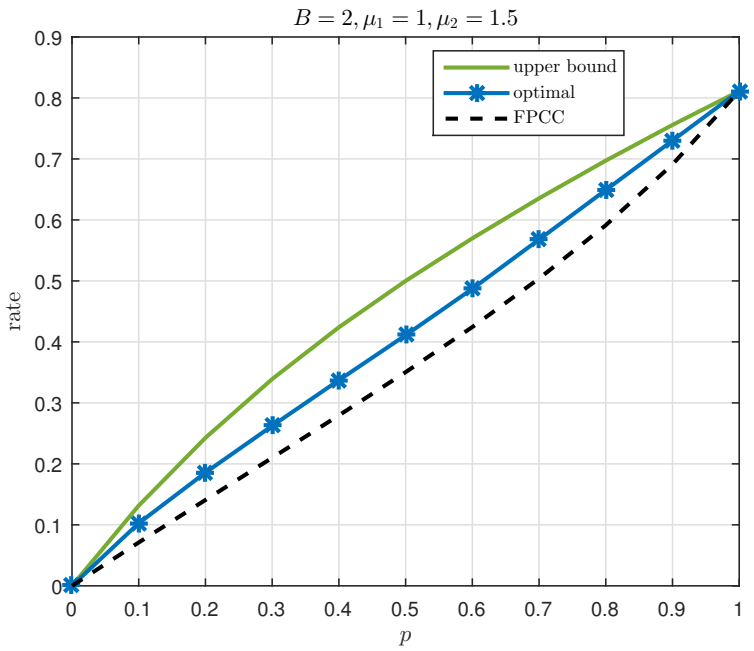

Figure 2.9: Achievable weighted sum rate for the optimum online and sub-optimum FPCC together with the upper bound as a function of the energy arrival probability p for a fixed battery size B for i.i.d. Bernoulli arrivals.

scheme together with the upper bound as a function of the battery size B for a fixed energy arrival probability of $p = 0.1$. We observe that FPCC performs close to the optimal online. In Fig. 2.9, we plot the achievable rates as a function of the energy arrival probability p for a fixed battery size $B = 2$. We again observe FPCC perform close to the optimal online.

In Fig. 2.10, we plot the entire achievable and upper bound regions for the broadcast channel with i.i.d. Bernoulli energy arrivals $B = 5$, $p = 0.5$, and $\sigma_1^2 = 1$, $\sigma_2^2 = 5$. The arrows denote the movement of achievable rate pairs from the optimal policy to the sub-optimum FPCC. In particular, the optimal policy curve is traced with changing μ_1, μ_2, equivalently by changing P_c. The arrows point to the achievable rates when the optimal total transmit power is replaced with the

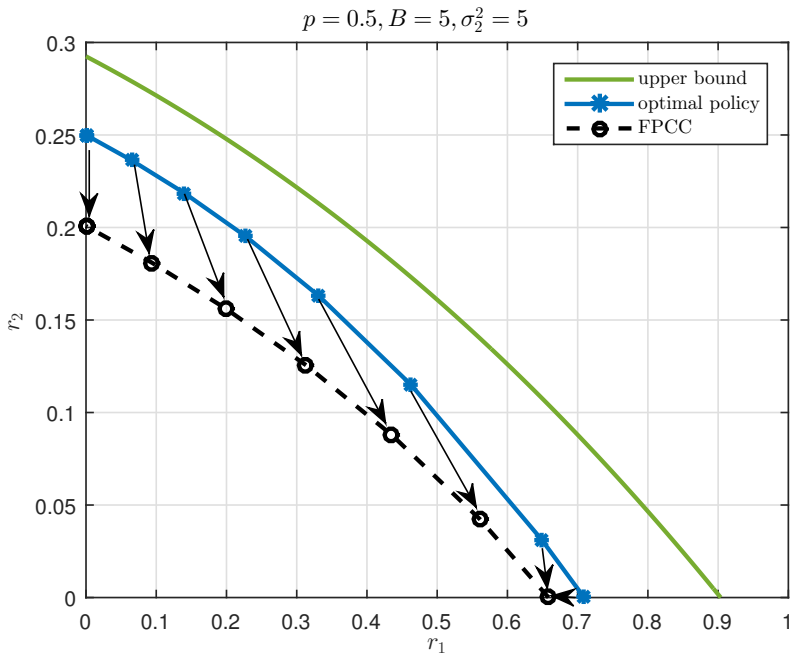

Figure 2.10: Rate regions with the optimum online and sub-optimum FPCC together with the upper bound for i.i.d. Bernoulli arrivals.

fractional power policy for the same cut-off power P_c.

Finally, we consider an example of general i.i.d. energy arrivals by considering a (continuous) uniform probability distribution for the energy arrivals in $[0, B]$. Therefore, the average recharge rate is $\mu = B/2$. In Fig. 2.11, we plot the rate regions with sub-optimum FPCC and the optimum policy which is found by using dynamic programming for this uniform energy arrivals. We also show the achievable rate region with a corresponding Bernoulli arrivals; for this case energies arrive in amounts 0 and B with probabilities $p = 0.5$ and $1-p = 0.5$. As proved in Lemma 2.5, the case of Bernoulli arrivals with the same average recharge rate yields a smaller achievable rate region with the FPCC scheme.

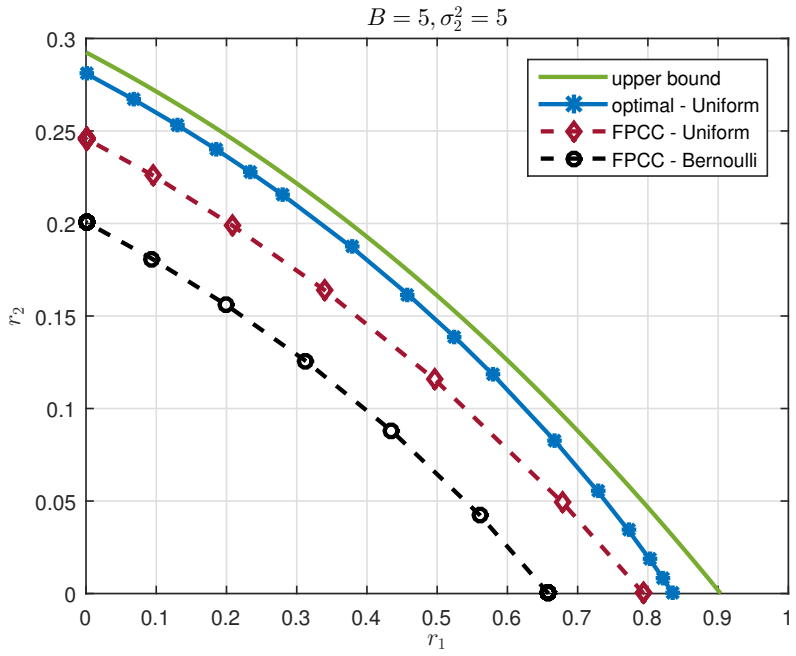

Figure 2.11: Achievable rate regions for the sub-optimum FPCC for i.i.d. uniform arrivals together with i.i.d. Bernoulli arrivals with the same average recharge rate. In addition, the optimum achievable rate region for i.i.d. uniform found by dynamic programming, and the upper bound.

2.6 Conclusion

In this chapter, we studied the optimal online transmission policies for the broadcast channel with an energy harvesting transmitter. We noted that, unlike the offline setting, the online optimal policy depends on the noise variance even in the single-user case. For Bernoulli arrivals, we showed that the optimal online total transmit power decreases in time. Depending on the priorities of the users, and hence the operating point on the boundary of the rate region, only one of the users may be served, in which case the problem reduces to a single-user problem. When both users are served simultaneously, then the weaker user may be served for only a subset of the duration that the stronger user is served. Depending on the user priorities,

the stronger user is either not allocated any power throughout the transmission duration or it is allocated power for the entire duration. We showed that, as in the offline problem, there exists a cut-off power which is dedicated for the stronger user; the cut-off level depends on the operating point on the rate region. We showed that whenever the stronger user's allocated power is decreasing, the weaker user's allocated power is zero; and whenever the stronger user's allocated power is constant, the weaker user's allocated power is decreasing. Next, we considered the general i.i.d. energy arrivals. We proposed a sub-optimum online algorithm, FPCC, where the total transmit power follows a fractional allocation, and the individual user powers are cut-off based. The proposed scheme does not depend on the energy arrival distribution. We obtained bounds on the performance of the FPCC policy for any general i.i.d. energy arrivals, and showed that it is within a constant gap from the developed upper bound, therefore, from the optimum online policy.

2.7 Appendix: Solution of problem (2.36)

We can equivalently write problem (2.36) as:

$$\max_{\alpha\in[0,1]} \ \frac{\mu_1}{2}\log\left(1+\frac{\alpha P_i^*}{\sigma_1^2}\right)+\frac{\mu_2}{2}\log\left(1+\frac{(1-\alpha)P_i^*}{\alpha P_i^*+\sigma_2^2}\right) \tag{2.81}$$

where $P_{1i}=\alpha P_i^*$ and $P_{2i}=(1-\alpha)P_i^*$. Problem (2.81) can be further rewritten as:

$$\max_{\alpha\in[0,1]} \ \left[\frac{\mu_1}{2}\log\left(1+\frac{\alpha P_i^*}{\sigma_1^2}\right)-\frac{\mu_2}{2}\log\left(\alpha P_i^*+\sigma_2^2\right)+\frac{\mu_2}{2}\log\left(P_i^*+\sigma_2^2\right)\right] \tag{2.82}$$

Differentiating the objective function of (2.82) with respect α and equating to zero we have:

$$\alpha P_i^* = \frac{\mu_1\sigma_2^2 - \mu_2\sigma_1^2}{\mu_2 - \mu_1} \tag{2.83}$$

We further need to impose the constraint $\alpha \in [0, 1]$, i.e., we need to have $0 \leq \alpha P_i^* \leq P_i^*$. This gives:

$$\alpha P_i^* = \min\left\{P_i^*, \left(\frac{\mu_1\sigma_2^2 - \mu_2\sigma_1^2}{\mu_2 - \mu_1}\right)^+\right\} \tag{2.84}$$

Denoting $P_c = \left(\frac{\mu_1\sigma_2^2 - \mu_2\sigma_1^2}{\mu_2 - \mu_1}\right)^+$ gives the expressions in (2.37)-(2.39).

CHAPTER 3

Energy Harvesting Multiple Access Channels: Optimal and Near-Optimal Online Policies

3.1 Introduction

We consider a two-user energy harvesting multiple access channel, Fig. 3.1, where each user harvests energy from nature into its (arbitrary) finite-sized battery. The energy harvests at the transmitters are i.i.d. in time but can be arbitrarily correlated between the users at any instant. The average recharge rates can be different, but we assume that average recharge rate per unit battery for both users is equal. We consider the *online* setting where the energy arrivals are known only causally at the transmitters. The users have no prior knowledge about the joint probability distribution of the energy harvesting processes. We study the *online* power scheduling problem where the users need to determine their transmit power levels based only on the energy arrival information so far. Our goal is to determine optimal and near-optimal online power allocation policies that achieve or approach the boundary of the capacity region.

3.2 System Model

We consider a two-user energy harvesting multiple access channel. User k has a battery of size B_k, see Fig. 3.1. There are two energy harvesting sources which deliver $E_{ki} = e_{ki}$ amount of energy to the kth user in slot i; e_{ki} is a realization of the random variable E_{ki}. We assume that the slot duration is equal to unity. We assume without loss of generality that $E_{ki} \leq B_k$ almost surely. The energy harvests are i.i.d. in time but can be arbitrarily correlated between the users. The battery state of user k at time i, b_{ki}, evolves as $b_{k(i+1)} = \min\{B_k, b_{ki} - P_{ki} + e_{ki}\}$. Here, P_{ki} is the transmit power of user k at time i, which is limited as $P_{ki} \leq b_{ki}$.

The physical layer is a Gaussian multiple access channel with noise variance at the receiver equal to σ^2. The single slot capacity region, $\mathcal{C}(P_{1i}, P_{2i})$, of this channel in slot i is [84] (also see e.g., [8]):

$$r_{1i} \leq \frac{1}{2} \log \left(1 + \frac{P_{1i}}{\sigma^2}\right) \tag{3.1}$$

$$r_{2i} \leq \frac{1}{2} \log \left(1 + \frac{P_{2i}}{\sigma^2}\right) \tag{3.2}$$

$$r_{1i} + r_{2i} \leq \frac{1}{2} \log \left(1 + \frac{P_{1i} + P_{2i}}{\sigma^2}\right) \tag{3.3}$$

The formulation here assumes that the slots are long enough that the coding is done within the course of each slot. This results in being able to achieve the capacity region in (3.1)-(3.3) in each slot i; see for example, [1–22, 27–30, 47–50, 84, 90–100].

The above single slot capacity region is a pentagon. The overall capacity region is a union of all possible pentagons corresponding to all feasible power al-

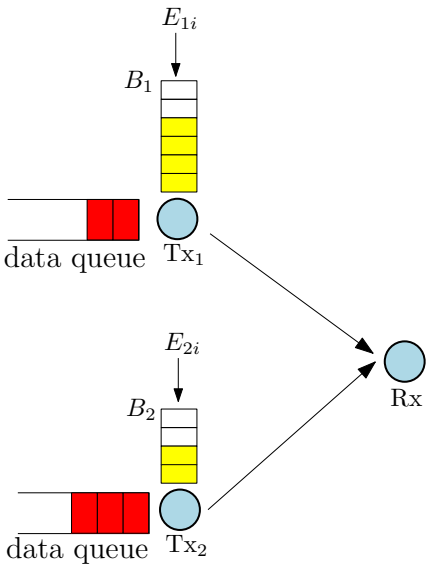

Figure 3.1: System model: an energy harvesting multiple access channel model.

locations over time, and thus, may no longer be a pentagon [8](see also [101]), as shown in Fig. 3.2. For a feasible policy at user k for n slots, we define a set of power allocations as: $P_k^n = [P_{k1}, \ldots, P_{kn}]$ where P_{ki} is a function of $(e_{ki}, e_{kj}, P_{kj}, b_{kj}, j \in \{1, \ldots, i-1\}, k \in \{1, 2\})$. Then, the n slot average achievable rate region under this policy is defined as:

$$r_1 \leq \mathbb{E}\left[\frac{1}{n}\sum_{i=1}^{n}\frac{1}{2}\log\left(1+\frac{P_{1i}}{\sigma^2}\right)\right] \tag{3.4}$$

$$r_2 \leq \mathbb{E}\left[\frac{1}{n}\sum_{i=1}^{n}\frac{1}{2}\log\left(1+\frac{P_{2i}}{\sigma^2}\right)\right] \tag{3.5}$$

$$r_1 + r_2 \leq \mathbb{E}\left[\frac{1}{n}\sum_{i=1}^{n}\frac{1}{2}\log\left(1+\frac{P_{1i}+P_{2i}}{\sigma^2}\right)\right] \tag{3.6}$$

where the expectation is over the joint distribution of the energy arrivals. The long-term average capacity region is equal to the union of all such pentagons over all feasible policies as n tends to infinity. This is a convex region, see [8, Lemma 3].

We aim to characterize the long-term average rate region under online knowl-

edge of the harvested energies. We first characterize the set of all feasible policies subject to causal knowledge of energy arrivals, denoted as $\hat{\mathcal{F}}$:

$$\hat{\mathcal{F}} = \{\forall i \in \{1,2,3,\ldots\}, \forall k \in \{1,2\},$$
$$P_{ki}(e_{ki}, e_{kj}, P_{kj}, b_{kj}, j \in \{1,\ldots,i-1\}, k \in \{1,2\}) | P_{ki} \leq b_{ki}\} \tag{3.7}$$

This defines the set of all admissible power policies. The power in each slot is constrained by the energy available in the battery and can be a function of all the previous power allocations, battery states, energy arrivals and the current energy arrival.

Since the long-term average rate region is convex, it can be characterized by its tangent lines; see [8, 101]. Therefore, the problem of characterizing the long-term average capacity region, which is the largest long-term average rate region, is equivalent to solving the following problem for all $\mu_1, \mu_2 \in [0,1]$,

$$\Phi = \sup_{P \in \hat{\mathcal{F}}} \lim_{n\to\infty} \mathbb{E}\left[\frac{1}{n}\sum_{i=1}^{n}(\mu_1 r_{1i} + \mu_2 r_{2i})\right] \tag{3.8}$$

where the rates (r_{1i}, r_{2i}) belongs to the capacity region in slot i, i.e., satisfies (3.1)-(3.3). The expectation is with respect to the joint distribution of the energy arrivals. The stage reward in (3.8) is $(\mu_1 r_{1i} + \mu_2 r_{2i})$ and the admissible policies at each stage, $P_{1i} \times P_{2i}$, are the values in $[0, b_{1i}] \times [0, b_{2i}]$ which depend only on the current battery states b_{1i} and b_{2i}. Hence, an optimal policy exists and is Markovian, see e.g., [85, Theorem 6.4] and [86, Theorem 4.4.2]. We denote the rates achieved by an

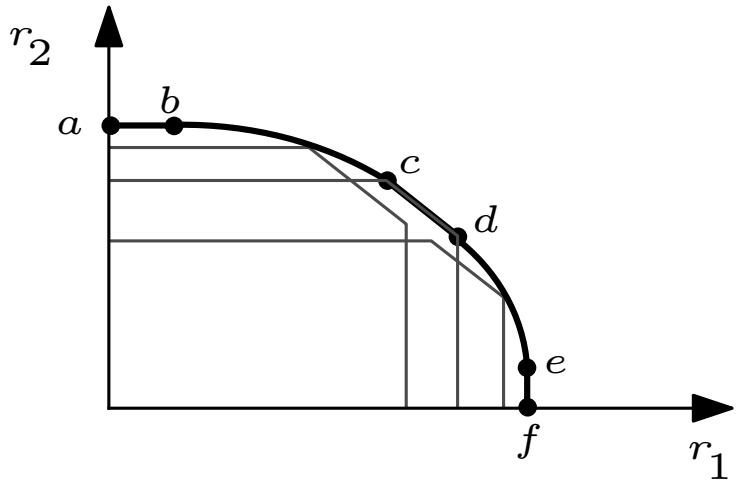

Figure 3.2: Capacity region of a multiple access channel. Points a, f characterize the single-user rates, points c, d characterize the sum-rate and points b, e characterize the maximum rates achieved while the other user is operating with its single-user rate.

optimal Markovian policy for user j in slot i by r_{ji}^* and hence (3.8) can be rewritten as:

$$\Phi = \lim_{n\to\infty} \mathbb{E}\left[\frac{1}{n}\sum_{i=1}^{n}(\mu_1 r_{1i}^* + \mu_2 r_{2i}^*)\right] \tag{3.9}$$

The optimal Markovian policy can be found via dynamic programming by solving Bellman's equations [87, Chapter 4], however, this will give little intuition or information about the structure of the solution. Instead, in the following, we develop a fixed and structured solution that will be exactly optimum for certain special energy arrivals and near-optimal for general energy arrivals.

We first study the special case of the fully-correlated (i.e., synchronized) Bernoulli energy arrivals with a particular support set in Section 3.3, and determine the *exactly optimum* power allocation policies for this case. In this case, either no energy arrives, or when it arrives, it arrives simultaneously to both users, and

it fills their respective batteries completely. That is, either $E_{1i} = E_{2i} = 0$ with probability $1-p$, or energies arrive in the amounts of $E_{1i} = B_1$ and $E_{2i} = B_2$ with probability p. Intuitively, we also coin this case as the *common energy source* case, see Fig. 3.3; see also [99]. In the common energy arrival analogy, there is a common energy source, where either $E_i \triangleq E_{1i} = E_{2i} = 0$ with probability $1-p$, or a common energy arrives in the amount of $E_i = B$ with probability p, where $B \geq \max\{B_1, B_2\}$. Such an energy arrival process implies that, when energy arrives, the batteries of both users fill completely. This constitutes a *renewal* for the system, and we can evaluate the optimal expected throughput analytically. In Section 3.4, we propose a distributed *near-optimal* power allocation policy and lower bound its performance under synchronous Bernoulli energy arrivals. By *near-optimal* policy, we mean a policy which yields rates that are within a constant gap from the optimal policy for all system parameters. In Section 3.5, we show that under the near-optimal policy proposed in Section 3.4, the performance of asynchronous Bernoulli energy arrivals is lower bounded by the performance of synchronous Bernoulli energy arrivals with the same mean. We also show that the performance of the asynchronous Bernoulli energy arrivals forms a lower bound on the performance of all general energy arrivals.

3.3 Optimal Strategy: Case of Synchronous Bernoulli Energy Arrivals

For the synchronous case, see Fig. 3.3, the expectation in (3.8) is over a single random variable (the common energy arrival). Whenever a positive energy arrives,

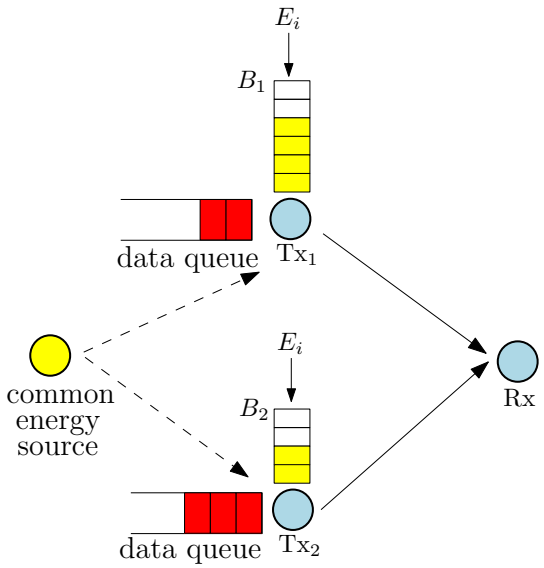

Figure 3.3: System model: a synchronous energy harvesting multiple access channel model.

the battery states at both users are reset to the full battery state, i.e., we have $\mathbb{P}[E_{1i} = 0, E_{2i} = 0] = 1 - p$ and $\mathbb{P}[E_{1i} = B_1, E_{2i} = B_2] = p$. Hence, whenever an energy arrives a *renewal* occurs. From [88, Theorem 3.6.1], the long-term weighted average throughput is:

$$\lim_{n\to\infty} \mathbb{E}\left[\frac{1}{n}\sum_{i=1}^{n}(\mu_1 r_{1i}^* + \mu_2 r_{2i}^*)\right] = \frac{1}{\mathbb{E}[L]}\mathbb{E}\left[\sum_{i=1}^{L}(\mu_1 r_{1i}^* + \mu_2 r_{2i}^*)\right] \tag{3.10}$$

$$= p\sum_{k=1}^{\infty} p(1-p)^{k-1}\sum_{i=1}^{k}(\mu_1 r_{1i}^* + \mu_2 r_{2i}^*) \tag{3.11}$$

$$= \sum_{i=1}^{\infty}\sum_{k=i}^{\infty} p^2(1-p)^{k-1}(\mu_1 r_{1i}^* + \mu_2 r_{2i}^*) \tag{3.12}$$

$$= \sum_{i=1}^{\infty} p(1-p)^{i-1}(\mu_1 r_{1i}^* + \mu_2 r_{2i}^*) \tag{3.13}$$

where L is the inter-energy arrival time which is geometric with parameter p, i.e., $\mathbb{E}[L] = \frac{1}{p}$.

Therefore, continuing from (3.13), we focus on the optimization problem:

$$\begin{aligned} \max_{\{P_{1i},P_{2i},r_{1i},r_{2i}\}} \quad & \sum_{i=1}^{\infty} p(1-p)^{i-1}\left(\mu_1 r_{1i}+\mu_2 r_{2i}\right) \\ \text{s.t.} \quad & (r_{1i},r_{2i}) \in \mathcal{C}(P_{1i},P_{2i}), \quad \forall i \\ & \sum_{i=1}^{\infty} P_{1i} \le B_1 \\ & \sum_{i=1}^{\infty} P_{2i} \le B_2, \;\; P_{1i},P_{2i} \ge 0, \quad \forall i \end{aligned} \tag{3.14}$$

This problem, in effect, maximizes the expected weighted sum rate until the next energy arrival, given that an energy arrival has just occurred. Point a in Fig. 3.2 represents the single-user rate for user 2, corresponding to $\mu_1 = 0$, and can be obtained as in [48, 49]. Point b represents the largest rate user 1 gets when user 2 maintains its single-user rate; this point can be obtained by fixing the second user's rate at its single-user rate and maximizing the first user's rate. The line between points c and d represents the sum-rate line where the sum of the two users' rates is constant; these points are obtained by setting $\mu_1 = \mu_2$. The curved part of the long-term average capacity region between b and c is obtained by tracing μ_1, μ_2 over $\mu_1 < \mu_2$.

We first consider point a. At this point, $P_{1i} = 0$, and user 2 transmits with its optimum single-user rate [48, 49]:

$$P_{2i}^{*} = \frac{p(1-p)^{i-1}}{\lambda_2} - \sigma^2, \qquad i = 1, \ldots, \tilde{N}_2 \tag{3.15}$$

where the optimum power decreases in time and $\tilde{N}_2$ is the last slot where the power is positive; λ_2 in (3.15) is found by satisfying the total power constraint with equality.

Next, we consider point b. At this point, we maximize the first user's rate, after fixing the power allocation of the second user to its optimal single-user power allocation P_{2i}^*:

$$\begin{aligned} \max_{\{P_{1i}, r_{1i}\}} \quad & \sum_{i=1}^{\infty} p(1-p)^{i-1} r_{1i} \\ \text{s.t.} \quad & (r_{1i}, \mathcal{C}(P_{2i}^*)) \in \mathcal{C}(P_{1i}, P_{2i}^*) \\ & \sum_{i=1}^{\infty} P_{1i} \leq B_1, \ P_{1i} \geq 0, \quad \forall i \end{aligned} \tag{3.16}$$

where $C(P_{2i}^*) = \frac{1}{2}\log(1 + P_{2i}^*)$ denotes the single-user capacity of user 2 with power P_{2i}^*; see point b in Fig. 3.2, see also [8, 101].

The Lagrangian of this problem is:

$$\mathcal{L} = -\sum_{i=1}^{\infty} p(1-p)^{i-1} \log\left(1 + \frac{P_{1i}}{P_{2i}^* + \sigma^2}\right) + \lambda_1 \left(\sum_{i=1}^{\infty} P_{1i} - B_1\right) - \sum_{i=1}^{\infty} \nu_{1i} P_{1i} \tag{3.17}$$

The KKT optimality conditions are:

$$P_{1i} = \frac{p(1-p)^{i-1}}{\lambda_1 - \nu_{1i}} - \sigma^2 - P_{2i}^* \tag{3.18}$$

along with complementary slackness and $\lambda_1, \nu_{1i} \geq 0$.

We prove that at point b user 1 transmits for a duration no shorter than user 2, before proceeding to determine P_{1i}^*.

Lemma 3.1 *With synchronized i.i.d. Bernoulli energy arrivals, at point b, where user 2 gets its single-user capacity, user 1 transmits for a duration no shorter than user 2.*

Proof: At point b in Fig. 3.2, the rate of user 2 is given by $\sum_{i=1}^{\infty} p(1-p)^{i-1} \log\left(1+\frac{P_{2i}}{\sigma^2}\right)$ and the optimal power allocation for user 2 is given by (3.15). The rate of user 1 at point b in Fig. 3.2 is given by $\sum_{i=1}^{\infty} p(1-p)^{i-1} \log\left(1+\frac{P_{1i}}{P_{2i}^*+\sigma^2}\right)$. The coefficient $p(1-p)^{i-1}$ in front of the ith term in this expression is decreasing in i. However, the interference term in the denominator, P_{2i}^*, is decreasing as well in i; see from (3.15). Therefore, for any power P_1 to be assigned to the first user: from the coefficient perspective, we should put this power at earlier i as the coefficient is higher there, however, from an interference perspective, we should put this power at later i as the interference is lower there. That is, there is a tension here between the pre-log coefficient and the interference in the denominator.

The rate achieved by user 1 will depend on the value of the interference caused by user 2. If user 1 transmits at slots $i = \{1, \ldots, \tilde{N}_2\}$, then from (3.15), by inserting P_{2i}^* into its rate expression, user 1 will achieve a rate equal to $p(1-p)^{i-1} \log\left(1+\frac{P_{1i}}{p(1-p)^{i-1}/\lambda_2}\right)$. On the other hand, if user 1 transmits at slots $i = \{\tilde{N}_2+1, \ldots\}$, it will achieve a rate equal to $p(1-p)^{i-1} \log\left(1+\frac{P_{1i}}{\sigma^2}\right)$; this follows as $P_{2i}^* = 0$ for slots $i = \{\tilde{N}_2+1, \ldots\}$.

We first consider the slots $i = \{1, \ldots, \tilde{N}_2\}$. We will show that if user 1 transmits in slots $i = \{1, \ldots, \tilde{N}_2\}$, it has to begin transmission at slot $i = 1$, i.e., it is sub-optimal for user 1 to have zero power in slot $i = 1$ while it puts a non-zero power

at any of the slots $i = \{2, \ldots, \tilde{N}_2\}$. To see this, note that, the rate achieved in these slots can be written in the form $x \log\left(1 + \frac{P_1\lambda_2}{x}\right)$, where we denoted $p(1-p)^{i-1}$ as x. The function $x \log\left(1 + \frac{P_1\lambda_2}{x}\right)$ is increasing in x. Thus, if we have a single energy P_1 to put into this objective function, we will put it when x is larger, i.e., when i is smaller. This necessitates for user 1 to start as early as possible, i.e., at $i = 1$, instead of any other slot in $i = \{2, \ldots, \tilde{N}_2\}$.

We next consider the slots $i = \{\tilde{N}_2 + 1, \ldots\}$. We will show that if user 1 transmits in slots $i = \{\tilde{N}_2 + 1, \ldots\}$, it has to begin transmission at slot $i = \tilde{N}_2 + 1$, i.e., it is sub-optimal for user 1 to have zero power in slot $i = \tilde{N}_2 + 1$ while it puts a non-zero power at any of the slots $i = \{\tilde{N}_2 + 2, \ldots\}$. The objective function for $i > \tilde{N}_2$, is also decreasing in i and hence if we have a single energy P_1 to put into this objective function, we will put it in earlier slots, i.e., at $i = \tilde{N}_2 + 1$, instead of any other slot in $i = \{\tilde{N}_2 + 2, \ldots\}$.

We then consider slots $i = \tilde{N}_2$ and $\tilde{N}_2 + 1$. We will show that it is sub-optimal for user 1 to have zero power in slot $i = \tilde{N}_2$ while it puts non-zero power in slot $i = \tilde{N}_2 + 1$; hence, user 1 has to start its transmission at slot 1. To prove this, we show that the objective function also decreases from slot $\tilde{N}_2$ to slot $\tilde{N}_2 + 1$ as follows:

$$\begin{aligned} p(1-p)^{\tilde{N}_2-1} \log\left(1 + \frac{P_1}{p(1-p)^{\tilde{N}_2-1}/\lambda_2}\right) &> p(1-p)^{\tilde{N}_2} \log\left(1 + \frac{P_1}{p(1-p)^{\tilde{N}_2}/\lambda_2}\right) \\ &> p(1-p)^{\tilde{N}_2} \log\left(1 + \frac{P_1}{\sigma^2}\right) \end{aligned}$$

where the last inequality follows since we have $\frac{p(1-p)^{\tilde{N}_2}}{\lambda_2} \leq \sigma^2$, as otherwise, P_{2i}^* would

have been strictly greater than zero for $i = \tilde{N}_2 + 1$ as well from (3.15). Hence, user 1 starts its transmission in slot 1 and always utilizes earlier slots with the non-zero transmit power.

Then, the rest of the proof follows by contradiction. Assume user 1 has a transmission duration $\tilde{N}_1 < \tilde{N}_2$. Then,

$$\sum_{i=1}^{\tilde{N}_1} \left(\frac{1}{\lambda_1} - \frac{1}{\lambda_2} \right) p(1-p)^{i-1} = B_1 \tag{3.19}$$

Thus, we have $\frac{1}{\lambda_1} - \frac{1}{\lambda_2} > 0$. Next, by assumption, we have $P_{1i} = 0, P_{2i} > 0$ in slot $\tilde{N}_2$. Then, from (3.18), we have

$$P_{1\tilde{N}_2} = p(1-p)^{\tilde{N}_2 - 1} \left(\frac{1}{\lambda_1 - \nu_{1\tilde{N}_2}} - \frac{1}{\lambda_2} \right) = 0 \tag{3.20}$$

However, since we have $\nu_{1\tilde{N}_2} \geq 0$ and $p(1-p)^{\tilde{N}_2 - 1} > 0$,

$$0 = \left(\frac{1}{\lambda_1 - \nu_{1\tilde{N}_2}} - \frac{1}{\lambda_2} \right) \geq \left(\frac{1}{\lambda_1} - \frac{1}{\lambda_2} \right) > 0 \tag{3.21}$$

which is a contradiction. Thus, $\tilde{N}_1 \geq \tilde{N}_2$. ■

Hence, at point b, user 1 transmits for a duration $\tilde{N}_1$ where $\tilde{N}_1 \geq \tilde{N}_2$. At this point, user 2 transmits with its single-user power allocation until $\tilde{N}_2$. Then, for user 1,

$$\sum_{i=1}^{\tilde{N}_2} \left(\frac{1}{\lambda_1} - \frac{1}{\lambda_2} \right) p(1-p)^{i-1} + \sum_{i=\tilde{N}_2+1}^{\tilde{N}_1} \left(\frac{p(1-p)^{i-1}}{\lambda_1} - \sigma^2 \right) = B_1 \tag{3.22}$$

where λ_2 and $\tilde{N}_2$ are obtained from the second user's single-user power allocation, while λ_1 and $\tilde{N}_1$ are obtained from solving (3.22) and ensuring that the Lagrange multiplier λ_1 is non-negative, i.e., $\tilde{N}_1$ is the largest integer satisfying,

$$p(1-p)^{\tilde{N}_1-1} \geq \lambda_1 \sigma^2 \tag{3.23}$$

and $\lambda_2 > \lambda_1$, simultaneously. Solving (3.22) for λ_1 we have

$$\lambda_1 = \frac{1-(1-p)^{\tilde{N}_1}}{B_1 + (\tilde{N}_1 - \tilde{N}_2)\sigma^2 + \frac{1}{\lambda_2}(1-(1-p)^{\tilde{N}_2})} \tag{3.24}$$

Therefore, $\tilde{N}_1$ is the largest integer that satisfies (3.23) when λ_1 in (3.24) is inserted into (3.23).

We also note that, at point b, both users' powers are decreasing in time. It is clear that the second user's power is decreasing, as it follows the single-user allocation in (3.15). For user 1, it is clear from (3.22) that the power is decreasing for the first $\tilde{N}_2$ slots, and again decreasing from slot $\tilde{N}_2 + 1$ onwards. Thus, it remains to check the transition from slot $\tilde{N}_2$ to slot $\tilde{N}_2 + 1$. We have,

$$P_{1\tilde{N}_2} = \left(\frac{1}{\lambda_1} - \frac{1}{\lambda_2}\right) p(1-p)^{\tilde{N}_2-1} \tag{3.25}$$

$$\geq \left(\frac{1}{\lambda_1} - \frac{1}{\lambda_2}\right) p(1-p)^{\tilde{N}_2} \tag{3.26}$$

$$\geq \frac{1}{\lambda_1} p(1-p)^{\tilde{N}_2} - \sigma^2 \tag{3.27}$$

$$= P_{1(\tilde{N}_2+1)} \tag{3.28}$$

where (3.26) follows since $(1-p) \leq 1$ and (3.28) follows since the second user's transmission ends at $\tilde{N}_2$, hence $\frac{p(1-p)^{\tilde{N}_2}}{\lambda_2} < \sigma^2$. Thus, the first user's power is also decreasing throughout its transmission. This concludes the characterization of the optimal policies achieving point b.

Next, we consider sum capacity achieving points between point c and point d. For the sum rate, problem (3.14) reduces to:

$$\begin{aligned} \max_{\{P_{1i},P_{2i}\}} \quad & \frac{1}{2}\sum_{i=1}^{\infty} p(1-p)^{i-1} \log\left(1+\frac{P_{1i}+P_{2i}}{\sigma^2}\right) \\ \text{s.t.} \quad & \sum_{i=1}^{\infty} P_{1i} \leq B_1 \\ & \sum_{i=1}^{\infty} P_{2i} \leq B_2, \ P_{1i}, P_{2i} \geq 0, \quad \forall i \end{aligned} \tag{3.29}$$

Consider the *relaxed* problem with a total power constraint:

$$\begin{aligned} \max_{\{P_{1i},P_{2i}\}} \quad & \frac{1}{2}\sum_{i=1}^{\infty} p(1-p)^{i-1} \log\left(1+\frac{P_{1i}+P_{2i}}{\sigma^2}\right) \\ \text{s.t.} \quad & \sum_{i=1}^{\infty} P_{1i}+P_{2i} \leq B_1+B_2, \ P_{1i}, P_{2i} \geq 0, \quad \forall i \end{aligned} \tag{3.30}$$

First, we remark that problems in (3.29) and (3.30) are equivalent: This follows since, any optimal solution of (3.29) is also feasible in (3.30) with the same optimum value; and, any optimal solution for (3.30), $P_{1i}^* + P_{2i}^*$, can be made feasible in (3.29) by defining $P_{1i} = (P_{1i}^* + P_{2i}^*)\frac{B_1}{B_1+B_2}$ and $P_{2i} = (P_{1i}^* + P_{2i}^*)\frac{B_2}{B_1+B_2}$, with the same optimum value. The equivalence here is in the sense of [102].

Using this equivalence, we can find the sum-rate optimal policies by first solv-

ing a single-user problem with a battery size $B_s = B_1 + B_2$, and then dividing the total power to users in a feasible way. The feasible policy is not unique, and each feasible policy results in a different point on the c-d line.

Next, we characterize the two extreme points of this line: c and d. From the single-user analysis in [48, 49], it follows that the transmission duration $\tilde{N}$ is an increasing function of the battery size, i.e., the larger the battery, the longer the transmission duration will be, see also [98, Lemma 1]. Hence, in the optimal solution for (3.30), $P_{1i}^* + P_{2i}^*$ is positive for a duration $\tilde{N}_s$ which is no less than the durations for the single-user solutions of the users.

We now show that the extreme achievable sum rate optimal point c is actually the point b, i.e., the long-term average capacity region for the case of synchronized Bernoulli arrivals is a single pentagon. We will show this by showing that, given the optimum total power allocation policy in (3.30), a feasible distribution can be found such that the single-user capacity for either of the users (we will show for user 2) is achieved. We denote the optimal Lagrange multiplier and the transmission duration for problem (3.30) by λ_s and $\tilde{N}_s$, respectively. Similarly, we have λ_2 and $\tilde{N}_2$ for the second user single-user power allocation. It is sufficient to show that $\lambda_s \leq \lambda_2$, since it will imply:

$$\left(\frac{p(1-p)^{i-1}}{\lambda_s} - \sigma^2\right) - \left(\frac{p(1-p)^{i-1}}{\lambda_2} - \sigma^2\right) \geq 0 \tag{3.31}$$

Recall that we have $\tilde{N}_s \geq \tilde{N}_2$. First, if $\tilde{N}_s = \tilde{N}_2$, then we have

$$\sum_{i=1}^{\tilde{N}_2} \left(\frac{p(1-p)^{i-1}}{\lambda_2} - \sigma^2 \right) = B_2 \leq B_1 + B_2 = \sum_{i=1}^{\tilde{N}_s} \left(\frac{p(1-p)^{i-1}}{\lambda_s} - \sigma^2 \right) \tag{3.32}$$

which can happen if and only if $\lambda_s \leq \lambda_2$. Next, if $\tilde{N}_s > \tilde{N}_2$, i.e., $\tilde{N}_s - 1 \geq \tilde{N}_2$, then we have,

$$\lambda_s \sigma^2 \leq p(1-p)^{\tilde{N}_s - 1} \leq p(1-p)^{\tilde{N}_2} < \lambda_2 \sigma^2 \tag{3.33}$$

implying $\lambda_s < \lambda_2$. In (3.33) the middle inequality follows from the monotonicity, and the outer inequalities follow since $\lambda_s, \lambda_2, \tilde{N}_s, \tilde{N}_2$ satisfy their optimality conditions. Hence, we have proved the following result.

Lemma 3.2 *With synchronized i.i.d. Bernoulli energy arrivals, the online long-term average capacity region of the multiple access channel is a single pentagon.*

3.4 Near-Optimal Strategy: Case of Synchronous General Energy Arrivals

In this section, we consider the general but synchronized i.i.d. energy arrivals, i.e., energy arrivals which are fully-correlated but not necessarily Bernoulli distributed. This can be represented by an arbitrary i.i.d. random variable $\beta_i \in [0, 1]$ and then we have $E_{1i} = \beta_i B_1$, and $E_{2i} = \beta_i B_2$. Hence, there is only one source of randomness, which is the random variable β_i. We propose a sub-optimal online policy for this

case, and develop a lower bound on its performance. Let the average recharge rate at user k be $\bar{P}_k$, where $\bar{P}_k = \lim_{n\to\infty} \frac{1}{n} \sum_{i=1}^{n} E_{ki} = \mathbb{E}[E_{ki}]$.

3.4.1 Distributed Fractional Power (DFP) Policy

We first define the proposed sub-optimal online policy, which we coin as distributed fractional power (DFP) policy, for Bernoulli arrivals and then generalize it to arbitrary arrivals. The optimal powers achieving any point on the capacity of the multiple access channel are exponentially decreasing, hence as in [48,49], this motivates us for a fractional structure for the sub-optimal policy. Moreover, the long-term average capacity region for Bernoulli arrivals is a single pentagon, this motivates that the policy need not depend on μ_1, μ_2. For Bernoulli arrivals, each transmitter transmits a fraction p of its available energy. The first user transmits with power $B_1 p(1-p)^{i-1}$ and the second user transmits with power $B_2 p(1-p)^{i-1}$ in slot i. In general, user k transmits with a fraction of $q_k \triangleq \frac{\bar{P}_k}{B_k}$ of its available energy in its battery, i.e., $P_{ki} = q_k b_{ki}$.

3.4.2 A Lower Bound on the Proposed Online Policy

Theorem 3.1 *Under the proposed DFP policy, the achievable long-term average rate region with i.i.d. synchronous Bernoulli energy arrivals is lower bounded as,*

$$r_1 \geq \frac{1}{2} \log\left(1 + \frac{\bar{P}_1}{\sigma^2}\right) - 0.72 \tag{3.34}$$

$$r_2 \geq \frac{1}{2} \log\left(1 + \frac{\bar{P}_2}{\sigma^2}\right) - 0.72 \tag{3.35}$$

$$r_1 + r_2 \geq \frac{1}{2}\log\left(1 + \frac{\bar{P}_1 + \bar{P}_2}{\sigma^2}\right) - 0.72 \tag{3.36}$$

Proof: It is clear that the achievable long-term average rate region with the proposed DFP is a pentagon, as it is a single policy which does not depend on μ_1, μ_2. Hence, the whole long-term average region is completely characterized by four points, which are shown by a, b, c, d in Fig. 3.4. Therefore, to lower bound this region it suffices to lower bound the points a, b, c and d. Points a and d are the single-user rates which can be lower bounded as in [49] to obtain $r_1 \geq \frac{1}{2}\log\left(1 + \frac{\bar{P}_1}{\sigma^2}\right) - 0.72$ and $r_2 \geq \frac{1}{2}\log\left(1 + \frac{\bar{P}_2}{\sigma^2}\right) - 0.72$, which are (3.34) and (3.35), respectively. These identify points a', d'. Then, we lower bound the achievable sum rate by noting for the proposed policy: $P_{1i} + P_{2i} = (B_1 + B_2)p(1-p)^{i-1}$. Hence, again using [49], we have (3.36). This identifies points b', c'. ■

Since the long-term average rate region with the DFP policy is a pentagon even for general energy arrivals, to show that Bernoulli arrivals give a lower bound for all other energy arrivals, it suffices to show it only for the single-user and sum rates. These follow directly for the single-user rates from [49, Proposition 4]. It also follows for the sum rate, since the expectation is taken over a single random variable which is the fully-correlated energy arrival process. Hence, [49, Lemma 2] can still be applied and the proof follows similar to the proof of [49, Proposition 4].

Theorem 3.2 *With the DFP policy, any arbitrary i.i.d. synchronous energy arrival process yields an achievable long-term average rate region no smaller than the long-term average rate region an i.i.d. synchronous Bernoulli energy arrival process with*

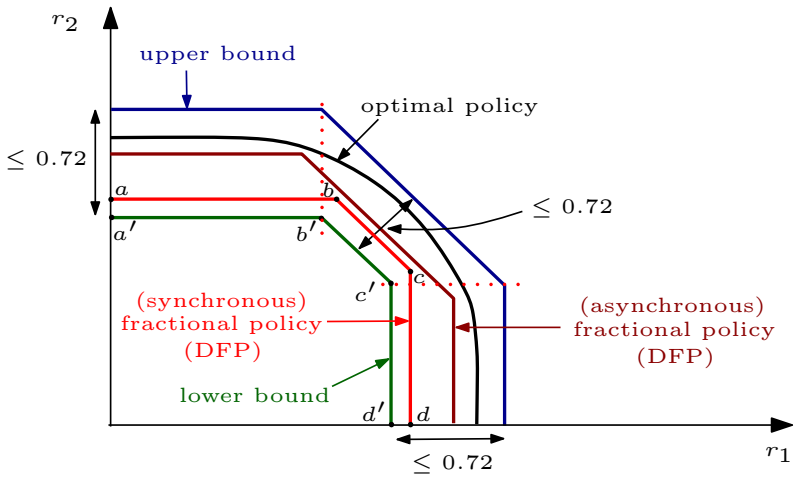

Figure 3.4: Relationships between the bounds. We compare: universal lower bound, DFP policy for fully-correlated energy arrivals, DFP policy for arbitrary-correlated energy arrivals, optimal policy and a universal upper bound.

the same recharge rate yields.

3.5 General Energy Arrivals

In this section, we study the case of general i.i.d. energy arrivals. We first study the relation between synchronous and asynchronous Bernoulli energy arrivals. We show that under the DFP policy and i.i.d. Bernoulli energy arrivals, the performance of synchronous Bernoulli energy arrivals forms a lower bound for the performance of all asynchronous Bernoulli energy arrivals with the same mean. We then show that under the DFP policy and i.i.d. energy arrivals, the performance of asynchronous Bernoulli energy arrivals forms a lower bound for the performance of all general energy arrivals with the same mean. Finally, we develop a universal upper bound for all online policies. We show that the gap between the developed upper bound and the performance of the DFP under i.i.d. synchronous Bernoulli energy arrivals is finite for all system parameters. This implies that the performance of the DFP policy

for any general energy arrival process is within a constant gap from the performance of the optimal online policy for energy arrivals which have equal recharge rate per unit battery.

3.5.1 Relation Between Synchronous and Asynchronous Bernoulli Energy Arrivals

Consider a synchronous Bernoulli energy arrival process where $\mathbb{P}[E_{1i} = 0, E_{2i} = 0] = 1 - p$ and $\mathbb{P}[E_{1i} = B_1, E_{2i} = B_2] = p$; we denote the expectation over this distribution by $\mathbb{E}_{sync}[\cdot]$. Now, consider any arbitrary asynchronous Bernoulli energy arrival process where $\mathbb{P}[E_{1i} = 0, E_{2i} = 0] = p_{00}$, $\mathbb{P}[E_{1i} = 0, E_{2i} = B_2] = p_{01}$, $\mathbb{P}[E_{1i} = B_1, E_{2i} = 0] = p_{10}$ and $\mathbb{P}[E_{1i} = B_1, E_{2i} = B_2] = p_{11}$; we denote the expectation over this distribution by $\mathbb{E}_{async}[\cdot]$. For a fair comparison, we require that the marginal distributions of the users in the synchronous and asynchronous cases are the same. In fact, for Bernoulli arrivals, requiring the marginals to be the same is equivalent to requiring the average recharge rates to be the same. Under this condition, we need $p_{00} + p_{01} = p_{00} + p_{10} = 1 - p$ and $p_{11} + p_{01} = p_{11} + p_{10} = p$. This implies that $p_{01} = p_{10}$, i.e., the joint distribution is symmetric.

We will now show that, under the DFP policy, the achievable long-term average rate region with synchronous Bernoulli arrivals is smaller than the achievable long-term average rate region with asynchronous Bernoulli arrivals for all permissible probability distributions. We first note that both achievable long-term average regions are pentagons, therefore, we only need to investigate individual rates and

the sum rates. We also note that the individual rates are identical in synchronous and asynchronous cases, as the marginal distributions are identical. Therefore, we only need to investigate the sum rates in both cases.

We will need the following lemma for this investigation. This lemma states that, due to the concavity of logarithm, extreme values for transmit power give lower objective functions (rates) than all other intermediate values. Intuitively, in the synchronous case, the battery levels of the two users are either high or low simultaneously, implying simultaneous high or low transmit powers, therefore, high or low sum powers inside the logarithm. On the other hand, in the asynchronous case, the users will have mixed battery states (one battery level high, other battery level low), implying that users' transmit powers will be disparate and balance each other out. This, in effect, will average out the power components inside the logarithm of the sum rate, and will yield larger sum rates for the asynchronous case.

Lemma 3.3 *For any four non-negative numbers x, y, w, z, with $w \leq (x, y) \leq z$ and $x + y = w + z$, the following inequality holds,*

$$\log(x) + \log(y) \geq \log(w) + \log(z) \tag{3.37}$$

Proof: Since we have $w \leq (x, y) \leq z$, we can write x as a convex combination of w, z, i.e., for some $\alpha \in [0, 1]$

$$x = \alpha w + (1 - \alpha) z \tag{3.38}$$

Then, inserting this in $x + y = w + z$, we have

$$y = (1 - \alpha)w + \alpha z \tag{3.39}$$

From the concavity of the log function, we have

$$\log(x) + \log(y) = \log(\alpha w + (1 - \alpha)z) + \log((1 - \alpha)w + \alpha z) \tag{3.40}$$

$$\geq \alpha \log(w) + (1 - \alpha) \log(z) + (1 - \alpha) \log(w) + \alpha \log(z) \tag{3.41}$$

$$= \log(w) + \log(z) \tag{3.42}$$

completing the proof.

Alternatively, we note that the relationship between the vectors $[x, y]$ and $[w, z]$ is exactly that of majorization [103], i.e., the vector $[x, y]$ is majorized by the vector $[w, z]$. That is, the components of $[x, y]$ are more nearly equal than the components of $[w, z]$. As the function $\Theta(x, y) = \log(x) + \log(y)$ is Schur-concave, from [103, Proposition C.1], we have $\Theta(x, y) \geq \Theta(w, z)$, i.e., more nearly equal components through a concave function yield larger values. ■

We now show in the following theorem that the performance of DFP with asynchronous Bernoulli energy arrivals is lower bounded by the performance of DFP with synchronous Bernoulli energy arrivals (with the same individual recharge rates). This theorem implies that extreme correlation between energy arrivals at the users affects the achievable rates negatively.

Theorem 3.3 *With the DFP policy, any arbitrarily correlated (i.e., asynchronous)*

i.i.d. Bernoulli energy arrival process yields an achievable long-term average rate region no smaller than the long-term average rate region a fully-correlated (i.e., synchronous) i.i.d. Bernoulli energy arrival process yields.

We provide the proof of Theorem 3.3 in the Appendix.

3.5.2 Non-Bernoulli Energy Arrivals

We now relate the performance of asynchronous i.i.d. Bernoulli energy arrivals and any general i.i.d. energy arrivals with the same mean. The energy arrivals belong to any arbitrary distribution, i.e., $E_{1i} \in [0, B_1]$ and $E_{2i} \in [0, B_2]$ with arbitrary correlation between them. We first state the following lemma which is an extension of [49, Lemma 2] to the case of two random variables. This lemma compares the expected value of a concave function over Bernoulli and non-Bernoulli random variables. While we state the lemma for jointly concave functions, in fact, individual concavity of the function with respect to each variable is sufficient for the proof. In our case, the function is the sum rate which is jointly concave with respect to both user powers.

Lemma 3.4 *Let $f(x, y)$ be a jointly concave function in x, y on $[0, B_1] \times [0, B_2]$. Let X, Y be random variables arbitrarily distributed on $[0, B_1] \times [0, B_2]$. Let $(\hat{X}, \hat{Y})$ be Bernoulli random variables distributed on the same support set with the probability mass function $p_{11} = \frac{\mathbb{E}[XY]}{B_1 B_2}$, $p_{10} = \frac{\mathbb{E}[X]}{B_1} - \frac{\mathbb{E}[XY]}{B_1 B_2}$, $p_{01} = \frac{\mathbb{E}[Y]}{B_2} - \frac{\mathbb{E}[XY]}{B_1 B_2}$, and $p_{00} =$*

$1 - \frac{\mathbb{E}[X]}{B_1} - \frac{\mathbb{E}[Y]}{B_2} + \frac{\mathbb{E}[XY]}{B_1 B_2}$. *Then,*

$$\mathbb{E}[f(\hat{X}, \hat{Y})] \leq \mathbb{E}[f(X, Y)] \tag{3.43}$$

Proof: Applying the concavity of $f(x, y)$ first with respect to x and then with respect to y,

$$\begin{aligned} f(x,y) \geq & \frac{x}{B_1} f(B_1, y) + \frac{B_1 - x}{B_1} f(0, y) && (3.44) \\ \geq & \frac{B_2 - y}{B_2} \frac{x}{B_1} f(B_1, 0) + \frac{y}{B_2} \frac{x}{B_1} f(B_1, B_2) \\ & + \frac{B_2 - y}{B_2} \frac{B_1 - x}{B_1} f(0, 0) + \frac{y}{B_2} \frac{B_1 - x}{B_1} f(0, B_2) && (3.45) \end{aligned}$$

Then, setting $x = X, y = Y$, taking the expectation of both sides, and applying the relationship between the probability mass function of the Bernoulli random variable and the expectations as described above, gives the desired result. ■

The following theorem relates the performance of the DFP policy under Bernoulli and general energy arrivals. The proof follows similar to [49, Proposition 4] using Lemma 3.4 above.

Theorem 3.4 *With the DFP policy, any general i.i.d. energy arrival process yields an achievable long-term average rate region no smaller than the long-term average rate region a corresponding arbitrary (i.e., asynchronous) i.i.d. Bernoulli energy arrival process with the same recharge rate yields.*

3.5.3 An Upper Bound for Online Policies

We now develop an upper bound which is valid for all online policies. This upper bound is universal in that it does not depend on the joint distribution of the energy arrival processes. It is valid for all energy arrival processes, and depends only on the average recharge rates of the energy arrival processes.

Theorem 3.5 *The online long-term average capacity region for the multiple access channel is upper bounded as,*

$$r_1 \leq \frac{1}{2}\log\left(1+\frac{\bar{P}_1}{\sigma^2}\right) \tag{3.46}$$

$$r_2 \leq \frac{1}{2}\log\left(1+\frac{\bar{P}_2}{\sigma^2}\right) \tag{3.47}$$

$$r_1+r_2 \leq \frac{1}{2}\log\left(1+\frac{\bar{P}_1+\bar{P}_2}{\sigma^2}\right) \tag{3.48}$$

where $\bar{P}_k$ is the average recharge rate of user k.

Proof: The achievable long-term average rate region for any online policy is upper bounded by the achievable long-term average rate region with the optimum offline policy, where all of the energy arrival information is known non-causally ahead of time. In addition, the achievable long-term average rate region with finite-sized battery is upper bounded by the achievable long-term average rate region with an unlimited-sized battery. For the offline problem, eliminating the *no-energy-overflow* constraints due to the finite battery size, the feasible set for the transmit power

policy for user k, denoted as g_k^n, becomes

$$\mathcal{F}_k^n \triangleq \left\{ \{g_{ki}\}_{i=1}^n : \frac{1}{m}\sum_{i=1}^{m} g_{ki} \leq \frac{1}{m}\left(\sum_{i=1}^{m} E_{ki} + B_k\right), \quad m = 1, \ldots, n \right\}, \quad k = 1, 2 \tag{3.49}$$

where we have added B_k to the right hand side of (3.49) to allow for the case when the system has started with a full battery at the beginning of the communication session. We assume without loss of generality that $E_{ki} \leq B_k$. Next, we define a larger feasible set as,

$$\mathcal{G}^n \triangleq \left\{ \{g_{1i}\}_{i=1}^n, \{g_{2i}\}_{i=1}^n : \frac{1}{n}\sum_{i=1}^{n} g_{1i} + g_{2i} \leq \frac{1}{n}\left(\sum_{i=1}^{n} E_{1i} + B_1 + \sum_{i=1}^{n} E_{2i} + B_2\right) \right\} \tag{3.50}$$

which is formed by considering only one of the constraints for $m = n$ instead of all of the constraints $m = 1, \ldots, n$ in the set $\mathcal{F}_k^n$, and by adding up the inequalities. Then, the offline sum rate is upper bounded as,

$$\begin{aligned}
R_{off} &\triangleq \lim_{n\to\infty} \max_{\{g_{ki}\}_{i=1}^n \in \mathcal{F}_k^n} \frac{1}{n}\sum_{i=1}^{n} \frac{1}{2}\log\left(1 + \frac{g_{1i} + g_{2i}}{\sigma^2}\right) && (3.51)\\
&\leq \lim_{n\to\infty} \max_{\{g_{ki}\}_{i=1}^n \in \mathcal{G}^n} \frac{1}{n}\sum_{i=1}^{n} \frac{1}{2}\log\left(1 + \frac{g_{1i} + g_{2i}}{\sigma^2}\right) && (3.52)\\
&\leq \lim_{n\to\infty} \max_{\{g_{ki}\}_{i=1}^n \in \mathcal{G}^n} \frac{1}{2}\log\left(1 + \frac{\frac{1}{n}\left(\sum_{i=1}^{n} g_{1i} + g_{2i}\right)}{\sigma^2}\right) && (3.53)\\
&\leq \lim_{n\to\infty} \frac{1}{2}\log\left(1 + \frac{\frac{1}{n}\left(\sum_{i=1}^{n} E_{1i} + B_1 + \sum_{i=1}^{n} E_{2i} + B_2\right)}{\sigma^2}\right) && (3.54)\\
&= \frac{1}{2}\log\left(1 + \frac{\bar{P}_1 + \bar{P}_2}{\sigma^2}\right) && (3.55)
\end{aligned}$$

where (3.52) follows because $\mathcal{G}^n$ is a larger feasible set, (3.53) follows from the concavity of the log function, (3.54) follows by applying the inequality in $\mathcal{G}^n$, and (3.55) follows by the strong law of large numbers and since the remaining $\frac{1}{n}B_k$ terms go to zero as n tends to infinity. This proves (3.48). The proofs for (3.46) and (3.47) follow similarly. ■

Finally, comparing the lower bound in Theorem 3.1 and the upper bound in Theorem 3.5, we note that the distance in all directions is bounded by a finite number (0.72 in this case) which is independent of all system parameters. We recall that: 1) the lower bound in Theorem 3.1 is valid for all synchronous Bernoulli arrivals; 2) by Theorem 3.2, the rates of any general synchronous energy arrivals are no smaller than the rates of synchronous Bernoulli arrivals; 3) by Theorem 3.3, the rates of any arbitrary (asynchronous) Bernoulli arrivals are no smaller than the rates of a corresponding synchronous Bernoulli arrivals; and 4) by Theorem 3.4, the rates of any arbitrary energy arrivals are no smaller than a corresponding arbitrary (asynchronous) Bernoulli arrivals.

To complete the argument, and put everything together, we note the following subtlety: Starting from any arbitrary energy arrival processes, the Bernoulli energy arrivals obtained in Theorem 3.4 (see the construction of the joint probability mass function in Lemma 3.4) is not in general such that $p_{01} = p_{10}$, which is required by Theorem 3.3. Note that, we have $p_{01} = p_{10}$, if the average recharge rates per unit battery are equal, i.e., $\frac{\bar{P}_1}{B_1} = \frac{\bar{P}_2}{B_2}$. This ensures $\frac{\mathbb{E}[X]}{B_1} = \frac{\mathbb{E}[Y]}{B_2}$ in Lemma 3.4, and therefore, ensures $p_{01} = p_{10}$. We refer to this condition as either *equal normalized recharge rates,* or alternatively as *equal recharge rates per unit battery.* Our final

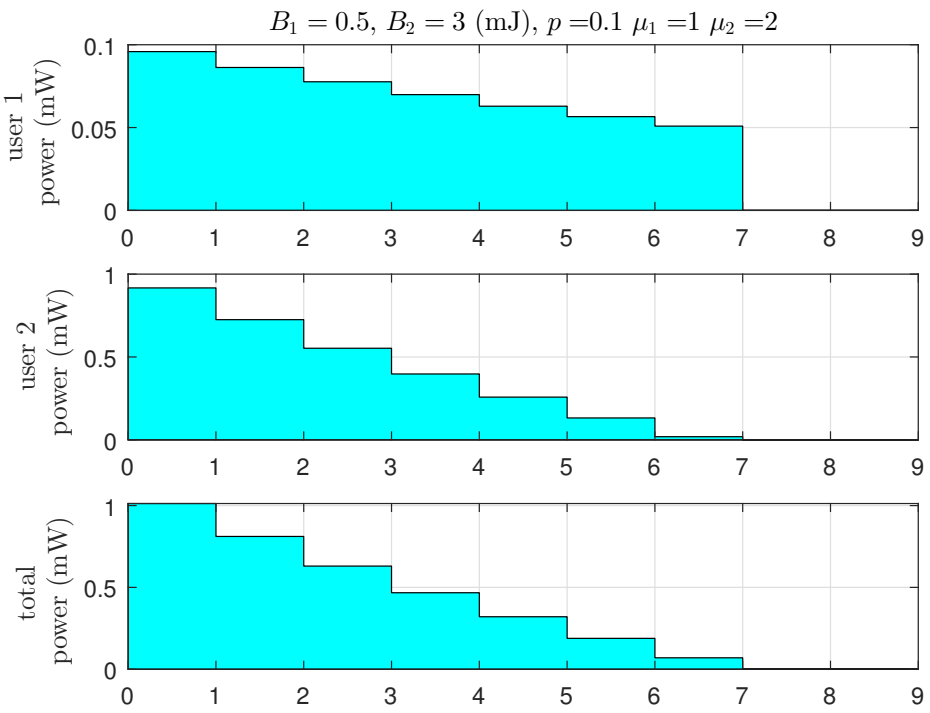

Figure 3.5: Optimal powers for Bernoulli arrivals (fully-correlated arrivals).

result therefore is that, under *equal recharge rates per unit battery*, the proposed DFP policy is near-optimal as it yields rates that are within a constant gap from the optimal online policy for all system parameters.

We note though that this restriction is not too strict as it does not necessarily imply a complete symmetry in the system with $B_1 = B_2$ and $\bar{P}_1 = \bar{P}_2$. For instance, all uniform distributed energy arrival processes with realizations in $[0, B_k]$ satisfy this condition. This restriction allows us to make a direct comparison between synchronous and asynchronous Bernoulli energy arrivals as in Theorem 3.3, and gives more intuition. We note that the same lower bound follows without this condition as in [100] without making any comparisons with fully-synchronized energy arrivals.

We show the relationships between the bounds derived in this chapter in

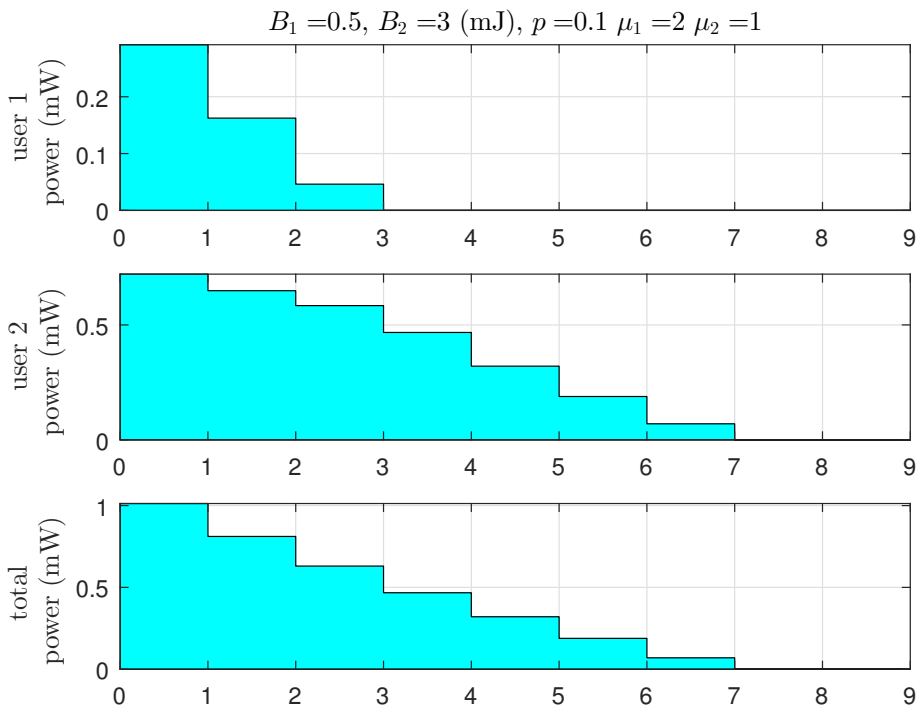

Figure 3.6: Optimal powers for Bernoulli arrivals (fully-correlated arrivals).

Fig. 3.4.

3.6 Numerical Examples

In this section, we illustrate the results obtained through several numerical examples. We set $\sigma^2 = 1$ mW (milli-Watt). We first consider the case of fully-correlated (synchronized) i.i.d. Bernoulli energy arrivals. For the corner point where user 2 operates at its single-user capacity, i.e., when $\mu_2 > \mu_1$, we plot the optimal power allocations in Fig. 3.5, for $p = 0.1, B_1 = 0.5$ mJ (milli-Joule) and $B_2 = 3$ mJ. As we proved, user 1 transmits for a longer duration than user 2, and user 2 follows its single-user power allocation. Note that this occurs even though the battery at user 1 is much smaller than the battery at user 2. Similarly, when $\mu_1 > \mu_2$, Fig. 3.6 shows

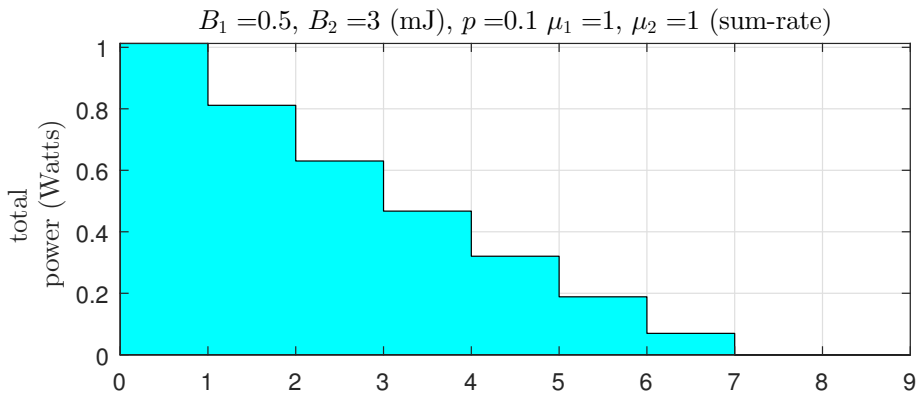

Figure 3.7: Optimal powers for Bernoulli arrivals (fully-correlated arrivals).

that user 1 operates at its single-user rate and user 2 transmits for a longer duration. We then plot the total power achieving the optimal long-term average sum-rate in Fig. 3.7. As we proved, the total power is higher than the optimal single-user power allocations of the users in every slot.

Next, we show the performance of the proposed DFP policy versus the optimal online policy and the upper bound in Fig. 3.8 for fully-correlated Bernoulli arrivals. We study the sum-rate point at which we have $\mu_1 = \mu_2$. We observe that DFP performs close to the optimal. We also study the performance of the greedy policy in which the transmitter transmits whenever there is energy in the battery. We notice that the performance of the greedy policy is poor. The reason for this poor performance is that under Bernoulli arrivals, the transmitters transmits with probability p a rate of $\frac{1}{2}\log(1+B_1+B_2)$ and remains silent with probability $1-p$, thus, the long-term average throughput is equal to $p\frac{1}{2}\log(1+B_1+B_2)$ and for low values of p this rate is far from optimal.

In Fig. 3.9, we study the performance of the DFP policy for the fully-correlated

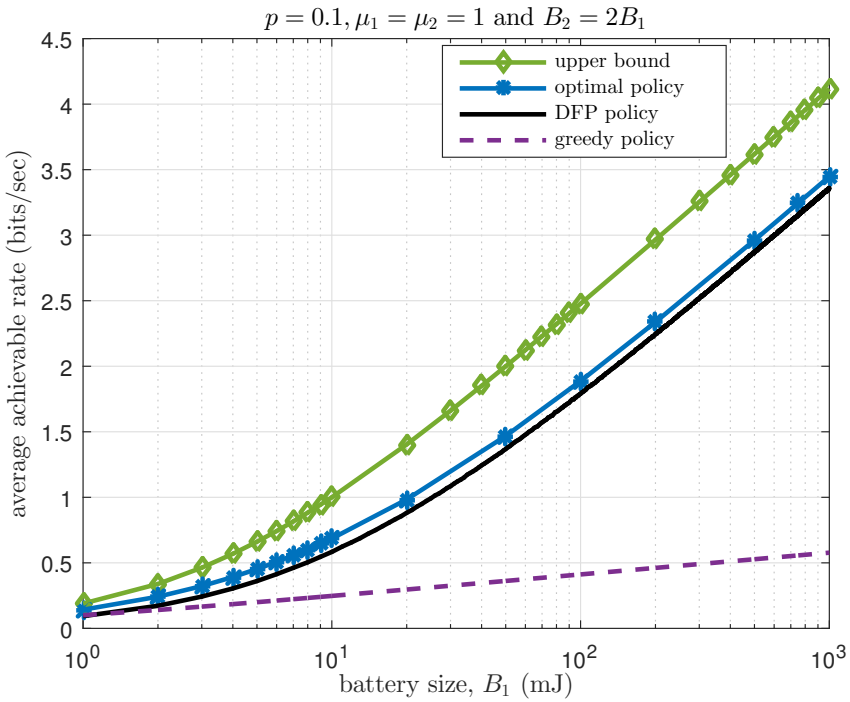

Figure 3.8: Sum rate: optimal policy, DFP policy, greedy policy and upper bound (fully-correlated Bernoulli arrivals).

Bernoulli energy arrivals under fixed average recharge rate. We fix the average recharge rate to $\bar{P}_1 = 1$mJ and $\bar{P}_2 = 2$mJ. The performance of the DFP policy is close to the performance of the optimal policy. The performance of both the optimal and the DFP policies decrease with the battery size. This is because the average recharge rate for the Bernoulli arrivals is equal to $\bar{P}_k = B_k p$, thus, for a fixed average recharge rate, as the value of the battery increases the value of p decreases. The smaller the value of p the less frequent the energy will arrive and this will degrade the performance.

In Fig. 3.10, we compare the performance of the DFP policy for fully-correlated and independent Bernoulli energy arrivals. As proved, the achievable performance of fully-correlated energy arrivals serves as a lower bound for the performance of

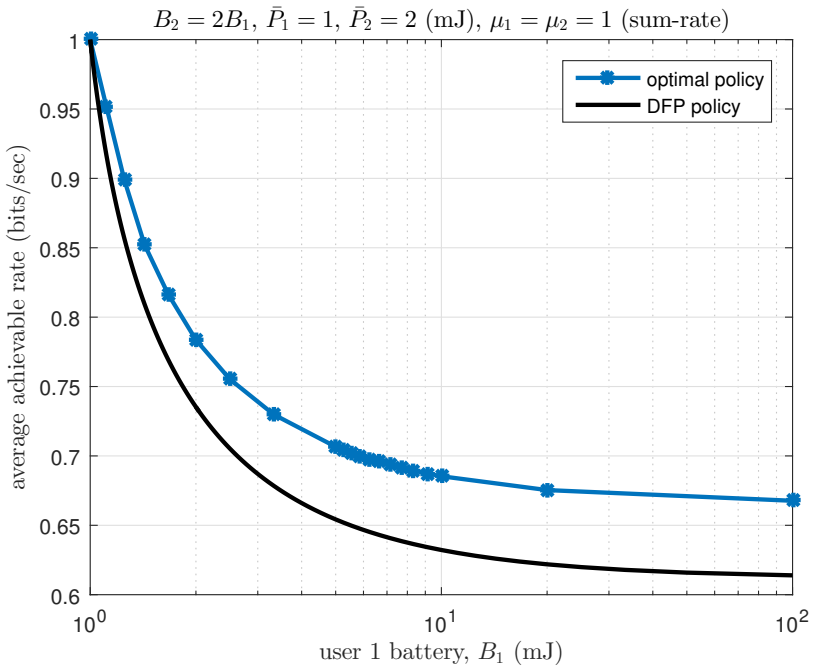

Figure 3.9: Sum rate: optimal policy and DFP policy (fully-correlated Bernoulli arrivals) for fixed average recharge rate.

asynchronous (in this case completely independent) energy arrivals. In Fig. 3.11, we compare the achievable rates of the DFP policy for fully-correlated and independent (asynchronous) uniformly-distributed (i.e., not Bernoulli) energy arrivals with the support of $[0, B_k]$ at user k. We note that fully-correlated energy arrivals yield lower sum rates. However, the gap between the two is less than the gap between the performances of the fully-correlated and independent Bernoulli energy arrivals in Fig. 3.10. In Fig. 3.12, we show the long-term average rate regions obtained by the DFP policy for fully-correlated and independent energy arrivals for Bernoulli and uniform-distributed energy arrivals. We observe that in both cases, independent arrivals yield larger rates, and also uniform arrivals yield larger rates than Bernoulli arrivals.

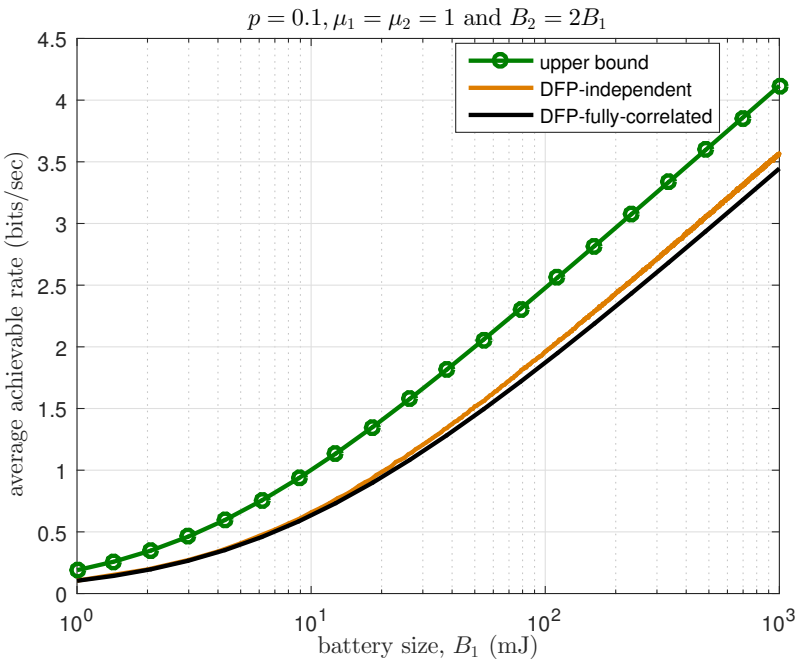

Figure 3.10: Sum rate: Upper bound and DFP policy (fully-correlated and independent Bernoulli arrivals).

3.7 Conclusion

In this chapter, we studied the optimal and near-optimal online power control policies which achieve the largest long-term average rate region for a two-user multiple access channel under equal average recharge rate per unit battery. We first considered the synchronous i.i.d. Bernoulli energy arrivals and obtained the exactly optimum policy. For this case, we showed that the long-term average rate region is a single pentagon and the optimal power allocation achieving the boundary of this region is decreasing between energy arrivals. The fractional form of the optimal policy and the single pentagon structure of the rate region motivated the proposed distributed fractional power (DFP) policy. We showed that under the DFP policy and for Bernoulli energy arrivals, synchronous arrivals yield a smaller rate re-

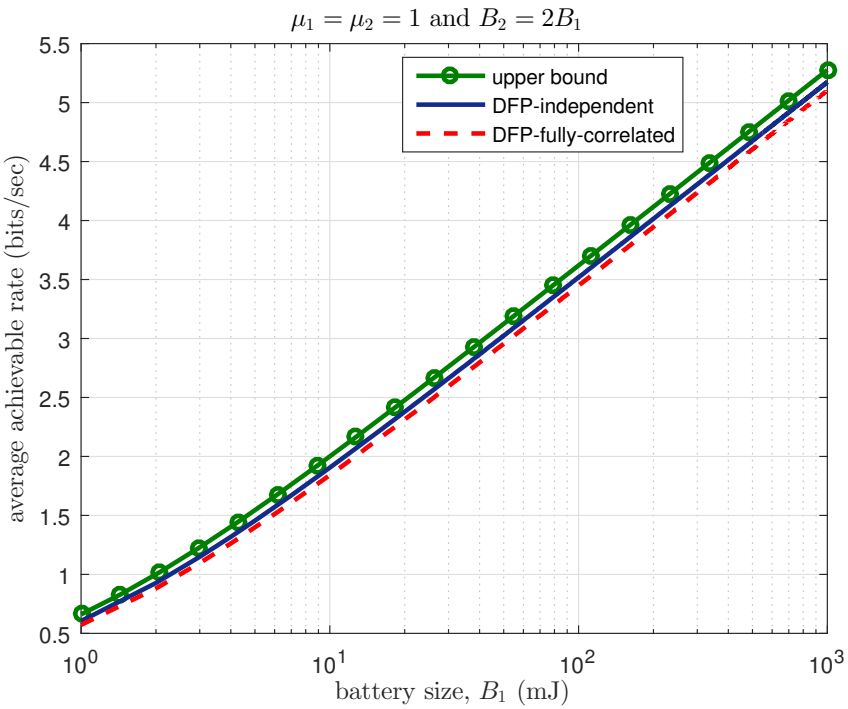

Figure 3.11: Sum rate: Upper bound and DFP policy (fully-correlated and independent uniform arrivals).

gion than the asynchronous arrivals. Then, we showed that under the DFP policy, Bernoulli energy arrivals yield a smaller rate region than general energy arrivals. We developed a lower bound for the synchronous Bernoulli energy arrivals and a universal upper bound for all energy arrivals and all online policies. We showed that the developed lower and upper bounds are within a constant gap of each other, and hence, the optimal online policy is within a constant gap to the proposed DFP policy for equal normalized average recharge rates.

3.8 Appendix: Proof of Theorem 3

As discussed at the beginning of this sub-section, we consider a synchronous Bernoulli energy arrival process with parameter p, and an asynchronous Bernoulli energy ar-

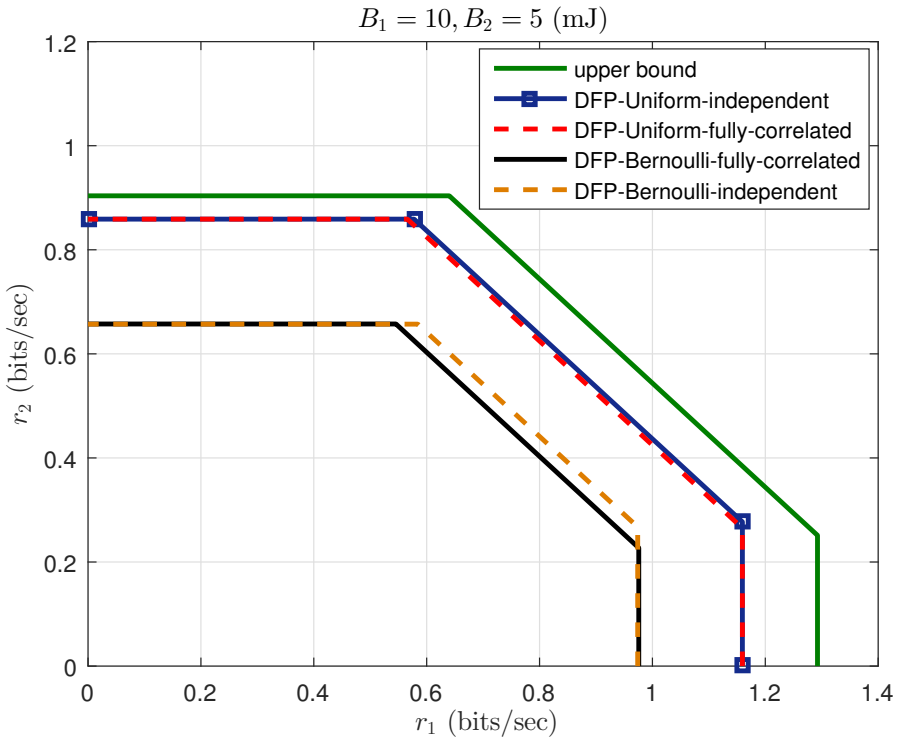

Figure 3.12: Achievable rate regions (fully-correlated and independent arrivals for uniform and Bernoulli).

rival process with parameters p_{00}, p_{01}, p_{10} and p_{11} with $p_{01} = p_{10}$. As also discussed, it suffices to consider only the sum rate, i.e., we need to show,

$$\lim_{n\to\infty}\frac{1}{n}\mathbb{E}_{sync}\left[\sum_{i=1}^{n}\frac{1}{2}\log\left(1+pb_{1i}+pb_{2i}\right)\middle| x_1, x_2\right] \leq \lim_{n\to\infty}\frac{1}{n}\mathbb{E}_{async}\left[\sum_{i=1}^{n}\frac{1}{2}\log\left(1+pb_{1i}+pb_{2i}\right)\middle| x_1, x_2\right] \tag{3.56}$$

where pb_{1i} and pb_{2i} inside the logarithms show that p fraction of the available energy b_{1i} and b_{2i} are being used for transmission, and x_k is the initial battery state at the kth user in slot 1. To prove (3.56), it suffices to prove it for each individual slot,

i.e.,

$$\mathbb{E}_{sync}\left[\log\left(1+pb_{1i}+pb_{2i}\right)\middle|x_1,x_2\right]\leq\mathbb{E}_{async}\left[\log\left(1+pb_{1i}+pb_{2i}\right)\middle|x_1,x_2\right],\quad\forall i \tag{3.57}$$

To give intuition, we first prove the inequality for a few indices. First note that when $i=1$, both sides of (3.57) are identical and equal to $\log\left(1+px_1+px_2\right)$, and therefore, the inequality in (3.57) holds as an equality.

For $i=2$, we evaluate the expectations by considering the possibilities of an energy arrival and no arrival in slot 1, for the synchronous case as,

$$\begin{aligned}&\mathbb{E}_{sync}\left[\log\left(1+pb_{12}+pb_{22}\right)\middle|x_1,x_2\right]\\&=p\log\left(1+pB_1+pB_2\right)+(1-p)\log\left(1+p(1-p)x_1+p(1-p)x_2\right)\end{aligned} \tag{3.58}$$

and for the asynchronous case as,

$$\begin{aligned}&\mathbb{E}_{async}\left[\log\left(1+pb_{12}+pb_{22}\right)\middle|x_1,x_2\right]\\&=p_{11}\log\left(1+pB_1+pB_2\right)+p_{10}\log\left(1+pB_1+p(1-p)x_2\right)\\&\quad+p_{01}\log\left(1+p(1-p)x_1+pB_2\right)+p_{00}\log\left(1+p(1-p)x_1+p(1-p)x_2\right)\end{aligned} \tag{3.59}$$

$$\begin{aligned}&\geq p_{11}\log\left(1+pB_1+pB_2\right)+p_{10}\log\left(1+p(1-p)x_1+p(1-p)x_2\right)\\&\quad+p_{01}\log\left(1+pB_1+pB_2\right)+p_{00}\log\left(1+p(1-p)x_1+p(1-p)x_2\right)\end{aligned} \tag{3.60}$$

$$=p\log\left(1+pB_1+pB_2\right)+(1-p)\log\left(1+p(1-p)x_1+p(1-p)x_2\right) \tag{3.61}$$

$$=\mathbb{E}_{sync}\left[\log\left(1+pb_{12}+pb_{22}\right)\middle|x_1,x_2\right] \tag{3.62}$$

where the inequality in (3.60) follows from Lemma 3.3 and the fact that $p_{01}=p_{10}$; (3.61) follows because $p_{11}+p_{01}=p$ and $p_{00}+p_{10}=1-p$; and (3.62) follows from (3.58).

For $i=3$, we evaluate the expectations by considering the possibilities of energy arrivals and no arrivals in slots 1 and 2, for the synchronous case as,

$$\begin{aligned}&\mathbb{E}_{sync}\left[\log\left(1+pb_{13}+pb_{23}\right)\middle|x_1,x_2\right]\\&=p\log\left(1+pB_1+pB_2\right)+p(1-p)\log\left(1+p(1-p)B_1+p(1-p)B_2\right)\\&\quad+(1-p)^2\log\left(1+p(1-p)^2x_1+p(1-p)^2x_2\right)\end{aligned} \tag{3.63}$$

and for the asynchronous case as,

$$\begin{aligned}&\mathbb{E}_{async}\left[\log\left(1+pb_{13}+pb_{23}\right)\middle|x_1,x_2\right]\\&=p_{11}\log\left(1+pB_1+pB_2\right)+p_{10}(1-p)\log\left(1+pB_1+p(1-p)^2x_2\right)\\&\quad+p_{01}(1-p)\log\left(1+p(1-p)^2x_1+pB_2\right)\\&\quad+p_{00}^2\log\left(1+p(1-p)^2x_1+p(1-p)^2x_2\right)\\&\quad+p_{01}p_{00}\log\left(1+p(1-p)^2x_1+p(1-p)B_2\right)\\&\quad+p_{10}p_{00}\log\left(1+p(1-p)B_1+p(1-p)^2x_2\right)\end{aligned}$$

$$
\begin{aligned}
&+ p_{11}p_{00}\log\left(1+p(1-p)B_1+p(1-p)B_2\right)\\
&+ p_{01}p\log\left(1+p(1-p)B_1+pB_2\right)\\
&+ p_{10}p\log\left(1+pB_1+p(1-p)B_2\right) \qquad (3.64)\\
\geq& p_{11}\log\left(1+pB_1+pB_2\right)+p_{10}(1-p)\log\left(1+pB_1+pB_2\right)\\
&+ p_{01}(1-p)\log\left(1+p(1-p)^2x_1+p(1-p)^2x_2\right)\\
&+ p_{00}^2\log\left(1+p(1-p)^2x_1+p(1-p)^2x_2\right)\\
&+ p_{01}p_{00}\log\left(1+p(1-p)^2x_1+p(1-p)^2x_2\right)\\
&+ p_{10}p_{00}\log\left(1+p(1-p)B_1+p(1-p)B_2\right)\\
&+ p_{11}p_{00}\log\left(1+p(1-p)B_1+p(1-p)B_2\right)\\
&+ p_{01}p\log\left(1+p(1-p)B_1+p(1-p)B_2\right)\\
&+ p_{10}p\log\left(1+pB_1+pB_2\right) \qquad (3.65)\\
=& p\log\left(1+pB_1+pB_2\right)+p(1-p)\log\left(1+p(1-p)B_1+p(1-p)B_2\right)\\
&+ (1-p)^2\log\left(1+p(1-p)^2x_1+p(1-p)^2x_2\right) \qquad (3.66)\\
=& \mathbb{E}_{sync}\left[\log\left(1+pb_{13}+pb_{23}\right)\middle| x_1,x_2\right] \qquad (3.67)
\end{aligned}
$$

where (3.65) follows from Lemma 3.3 and the fact that $p_{01}=p_{10}$; (3.66) follows from adding up similar terms; and (3.67) follows from (3.63).

We now proceed to the proof of the general case where $i=k$. For this case, the sum rate for the synchronous case is,

$$
\mathbb{E}_{sync}\left[\log\left(1+pb_{1k}+pb_{2k}\right)\middle| x_1,x_2\right]
$$

$$
\begin{aligned}
&= (1-p)^{k-1} \log\left(1 + p(1-p)^{k-1}x_1 + p(1-p)^{k-1}x_2\right) \\
&\quad + \sum_{j=0}^{k-2} p(1-p)^j \log\left(1 + p(1-p)^j B_1 + p(1-p)^j B_2\right) \qquad (3.68)
\end{aligned}
$$

and for the asynchronous case is,

$$
\begin{aligned}
&\mathbb{E}_{async}\left[\log\left(1 + pb_{1k} + pb_{2k}\right) \middle| x_1, x_2 \right] \\
&\quad = p_{00}^{k-1} \log\left(1 + p(1-p)^{k-1}x_1 + p(1-p)^{k-1}x_2\right) \\
&\qquad + \sum_{j=0}^{k-2} p_{01} p_{00}^j (1-p)^{k-2-j} \log\left(1 + p(1-p)^{k-1}x_1 + p(1-p)^j B_2\right) \\
&\qquad + \sum_{j=0}^{k-2} p_{10} p_{00}^j (1-p)^{k-2-j} \log\left(1 + p(1-p)^j B_1 + p(1-p)^{k-1}x_2\right) \\
&\qquad + \sum_{j=0}^{k-3} p_{01} p_{00}^j p(1-p)^{k-3-j} \log\left(1 + p(1-p)^{k-2} B_1 + p(1-p)^j B_2\right) \\
&\qquad + \sum_{j=0}^{k-3} p_{10} p_{00}^j p(1-p)^{k-3-j} \log\left(1 + p(1-p)^j B_1 + p(1-p)^{k-2} B_2\right) \\
&\qquad + \sum_{j=0}^{k-4} p_{01} p_{00}^j p(1-p)^{k-4-j} \log\left(1 + p(1-p)^{k-3} B_1 + p(1-p)^j B_2\right) \\
&\qquad + \sum_{j=0}^{k-4} p_{10} p_{00}^j p(1-p)^{k-4-j} \log\left(1 + p(1-p)^j B_1 + p(1-p)^{k-3} B_2\right) \\
&\qquad \vdots \\
&\qquad + \sum_{j=0}^{1} p_{01} p_{00}^j p(1-p)^{1-j} \log\left(1 + p(1-p)^2 B_1 + p(1-p)^j B_2\right) \\
&\qquad + \sum_{j=0}^{1} p_{10} p_{00}^j p(1-p)^{1-j} \log\left(1 + p(1-p)^j B_1 + p(1-p)^2 B_2\right) \\
&\qquad + p_{01} p \log\left(1 + p(1-p)B_1 + pB_2\right) + p_{10} p \log\left(1 + pB_1 + p(1-p)B_2\right) \\
&\qquad + \sum_{j=0}^{k-2} p_{11} p_{00}^j \log\left(1 + p(1-p)^j B_1 + p(1-p)^j B_2\right) \qquad (3.69)
\end{aligned}
$$

The proof for the general case follows similarly by applying Lemma 3.3 between all two consecutive terms except for the first and the last, and then, by adding up similar terms.

CHAPTER 4

Online Scheduling for Energy Harvesting Channels with Processing Costs

4.1 Introduction

We consider two settings in which the receiving terminals incur processing costs to receive information. We first consider a single-user energy harvesting channel, see Fig. 4.1, where the transmitter incurs a processing cost per unit time that it is on. The processing cost is the power consumed by the transmitter to be on and transmitting. This cost forces the transmitter to transmit in bursts instead of transmitting continually. The transmitter has a finite-sized battery, which is recharged by an exogenous i.i.d. energy harvesting process. We consider the problem of *online* scheduling, where the transmitter knows the energy arrivals only causally, and needs to determine a power allocation and burst length policy with only a causal knowledge of the energy arrivals. We then extend our analysis to the case of a two-way energy harvesting channel, Fig. 4.2, where users harvest energy from a fully correlated energy source. The users have finite but arbitrary-sized batteries to save unused energy for future use. Each user is subject to an arbitrary processing cost

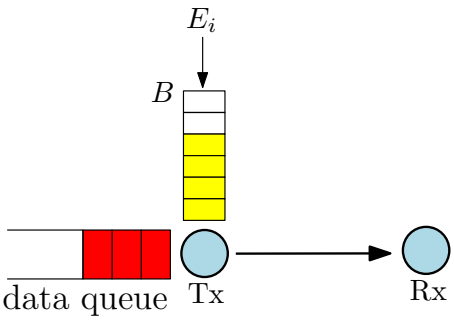

Figure 4.1: Single-user energy harvesting channel.

which accounts for power used per unit time by the user for being on to transmit or receive data. The processing costs force users to operate in bursty modes, where they do not utilize the entire duration available for communication. The users need to determine their power allocation and burst length policies based only on causal knowledge of energy arrivals.

4.2 Single-User Channel

We first consider a single-user energy harvesting channel, see Fig. 4.1. The transmitter has a battery of size B. Time is slotted. The amount of energy in the battery, b_i, evolves as:

$$b_{i+1} = \min\{B, b_i - \theta_i (P_i + \epsilon) + E_{i+1}\} \tag{4.1}$$

where E_i is the energy harvested in slot i, ϵ is the processing cost (power) per unit time, and θ_i is the duration in slot i that the transmitter is on and transmitting. In (4.1), $\theta_i P_i$ is the energy spent for transmission, and $\theta_i \epsilon$ is the energy spent for being on.

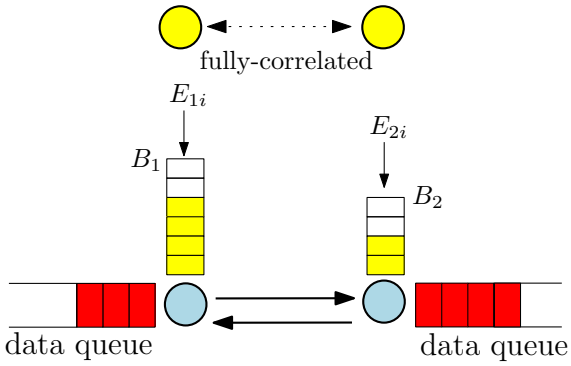

Figure 4.2: Two-way energy harvesting channel with fully-correlated energy arrivals.

The physical layer is Gaussian with rate transmitted in slot i [84],

$$r_i = \frac{\theta_i}{2} \log\left(1 + P_i\right) \tag{4.2}$$

where P_i is the allocated power and θ_i is the transmission duration in slot i. These two variables satisfy $\theta_i(P_i + \epsilon) \leq b_i$, which means that the total energy used is less than the energy available in the battery in this slot.

We first consider the case where E_i are i.i.d. Bernoulli random variables with a particular support: $\mathbb{P}[E_i = B] = p$ and $\mathbb{P}[E_i = 0] = 1 - p$, that is, when energy arrives it fills the battery completely. For this case, we determine the optimal online policy in the next sub-section. We then consider the general i.i.d. energy arrivals and propose a near-optimal policy in the following sub-section, and prove optimality guarantees on it.

4.2.1 Optimal Strategy: Case of Bernoulli Arrivals

Due to the special i.i.d. Bernoulli energy arrival structure, when an energy arrives, it fills the battery, and resets the system. This constitutes a *renewal*. Then, from [88,

Theorem 3.6.1] (see also [48–50, 97–100]), the long-term average rate can be found as:

$$\lim_{n\to\infty} \mathbb{E}\left[\frac{1}{n}\sum_{i=1}^{n} r_i\right] = \frac{1}{\mathbb{E}[L]}\mathbb{E}\left[\sum_{i=1}^{L} r_i\right] \tag{4.3}$$

$$= p\sum_{k=1}^{\infty} p(1-p)^{k-1}\sum_{i=1}^{k} r_i \tag{4.4}$$

$$= \sum_{i=1}^{\infty}\sum_{k=i}^{\infty} p^2(1-p)^{k-1} r_i \tag{4.5}$$

$$= \sum_{i=1}^{\infty} p(1-p)^{i-1} r_i \tag{4.6}$$

where L is the inter-arrival time between energy harvests, which is geometric with parameter p, and $\mathbb{E}[L] = 1/p$. Note that, via renewal reward theory, (4.3) reduces the infinite horizon problem into a finite horizon problem; instead of calculating the average reward over time, it is calculated over a single renewal event. The renewal event here is an energy arrival. Then, (4.4) follows by substituting a geometric distribution with parameter p for random variable L, (4.5) follows by interchanging the order of summations, and (4.6) follows by evaluating the inner sum.

Inserting (4.2) in (4.6), the online power allocation problem is:

$$\begin{aligned} \max_{\{P_i,\theta_i\}} \quad & \sum_{i=1}^{\infty} p(1-p)^{i-1}\frac{\theta_i}{2}\log\left(1+P_i\right) \\ \text{s.t.} \quad & \sum_{i=1}^{\infty}\theta_i(P_i+\epsilon) \le B \\ & 0 \le \theta_i \le 1, \quad P_i \ge 0, \quad \forall i \end{aligned} \tag{4.7}$$

This optimization problem can be viewed as maximizing the *expected* transmitted rate before the next energy arrival.

The problem in (4.7) is non-convex. We transform it to an equivalent convex problem by defining new variables $\bar{P}_i = P_i\theta_i$,

$$\begin{aligned} \max_{\{\bar{P}_i,\theta_i\}} \quad & \sum_{i=1}^{\infty} p(1-p)^{i-1}\frac{\theta_i}{2}\log\left(1+\frac{\bar{P}_i}{\theta_i}\right) \\ \text{s.t.} \quad & \sum_{i=1}^{\infty}\bar{P}_i + \theta_i\epsilon \le B \\ & 0 \le \theta_i \le 1, \quad \bar{P}_i \ge 0, \quad \forall i \end{aligned} \tag{4.8}$$

Here, $\bar{P}_i$ can be interpreted as the transmit energy allocated to the ith slot, and θ_i is the duration during which this energy is transmitted. The optimum online scheduling problem is to find the sequence of $\{\bar{P}_i, \theta_i\}_{i=1}^{\infty}$.

The Lagrangian for the problem in (4.8) is:

$$\begin{aligned} \mathcal{L} = & -\sum_{i=1}^{\infty} p(1-p)^{i-1}\frac{\theta_i}{2}\log\left(1+\frac{\bar{P}_i}{\theta_i}\right) - \sum_{i=1}^{\infty}\gamma_i\bar{P}_i \\ & + \lambda\left(\sum_{i=1}^{\infty}\bar{P}_i + \theta_i\epsilon - B\right) - \sum_{i=1}^{\infty}\mu_i\theta_i - \sum_{i=1}^{\infty}\nu_i(1-\theta_i) \end{aligned} \tag{4.9}$$

where $\lambda, \gamma_i, \mu_i, \nu_i$ are non-negative Lagrange multipliers.

First, we note that, in the optimum solution of (4.7), $P_i = 0$ if and only if $\theta_i = 0$. This follows because, when P_i or θ_i is zero, the objective function is zero, and choosing the other variable non-zero wastes resources. While by definition $\bar{P}_i = 0$ when either $P_i = 0$ or $\theta_i = 0$, from the preceding argument, in the optimum

solution of (4.8), $\bar{P}_i = 0$ if and only if $P_i = 0$ and $\theta_i = 0$. Since the problem in (4.8) is convex, the optimal solution is found by the KKT optimality conditions. Taking the derivative of (4.9) with respect to $\bar{P}_i$, equating it to zero, and using the corresponding complementary slackness condition:

$$\frac{\bar{P}_i}{\theta_i} = \frac{p(1-p)^{i-1}}{\lambda} - 1 \tag{4.10}$$

for slots where $\theta_i > 0$. When $\theta_i = 0$, from the preceding discussion $\bar{P}_i = 0$. Noting that $P_i = \frac{\bar{P}_i}{\theta_i}$, from (4.10), we conclude that the optimal power is decreasing over time. Therefore, there exists a time slot when it hits zero. Hence, we define $\tilde{N}$ for which we have $\bar{P}_i, P_i, \theta_i > 0, \forall i \in \{1, \ldots, \tilde{N}\}$, and $\bar{P}_i = P_i = \theta_i = 0, \forall i \in \{\tilde{N}+1, \ldots\}$. Note that the transmission duration of the single-user problem with no processing costs in [49] (let us denote it as $\tilde{N}_{npc}$) forms an upper bound for the transmission duration here, i.e., $\tilde{N} \leq \tilde{N}_{npc}$. This is because, any processing costs use up energy for being on and reduce the effective battery size, and the transmission duration is an increasing function of the battery size [97].

Next, taking the derivative of (4.9) with respect to θ_i, we have

$$-p(1-p)^{i-1} \log\left(1 + \frac{\bar{P}_i}{\theta_i}\right) + \frac{\bar{P}_i}{\theta_i} \frac{p(1-p)^{i-1}}{1 + \frac{\bar{P}_i}{\theta_i}} + \lambda\epsilon - \mu_i + \nu_i = 0 \tag{4.11}$$

The optimal θ_i can be 0, 1, or $0 < \theta_i < 1$. When $0 < \theta_i < 1$, we have bursty transmission. In this case, from complementary slackness, we have $\mu_i = \nu_i = 0$.

Then, from (4.10)-(4.11),

$$p(1-p)^{i-1}\left(\log\left(\frac{p(1-p)^{i-1}}{\lambda}\right)-1\right)=\lambda(\epsilon-1) \tag{4.12}$$

Hence, (4.12) should be satisfied in any slot i where $0<\theta_i<1$, i.e., where there is burstiness. Next, we note that, since the left hand side of (4.12) is monotonically decreasing in i, (4.12) can be satisfied in at most one slot. Moreover, this slot can only be the last slot. This follows from the presence of factor $p(1-p)^{i-1}$ in front of the log in (4.8). Hence, it is always better to fill-up (i.e., $\theta_i=1$) earlier slots first; fractional θ_i should come later.

Next, we discuss how to solve for the optimum online policy. We just showed above that for all slots we have $\theta_i=1$, except for possibly the last slot where $\theta_{\tilde{N}}\leq 1$. From the total energy constraint and (4.10), we have:

$$\sum_{i=1}^{\tilde{N}-1}\left(\frac{p(1-p)^{i-1}}{\lambda}-1+\epsilon\right)+\theta_{\tilde{N}}\left(\frac{p(1-p)^{\tilde{N}-1}}{\lambda}-1+\epsilon\right)=B \tag{4.13}$$

In addition, for $i\in\{1,\ldots,\tilde{N}\}$, we need to satisfy:

$$p(1-p)^{i-1}\geq\lambda \tag{4.14}$$

$$p(1-p)^{i-1}\left(1-\log\left(\frac{p(1-p)^{i-1}}{\lambda}\right)\right)+\lambda(\epsilon-1)\leq 0 \tag{4.15}$$

where (4.14) ensures the non-negativity of power in (4.10), and (4.15) ensures the existence of non-negative Lagrange multipliers $\{\nu_i\}$ satisfying (4.11). Hence, we need

to find the optimal $\tilde{N}, \lambda, \theta_{\tilde{N}}$ that satisfy (4.12), (4.13), (4.14) and (4.15). Towards this end, we consider the following approach: We first fix $\tilde{N}$ to be the single-user transmission duration with no processing costs in [49], i.e., $\tilde{N} = \tilde{N}_{npc}$, and solve for λ in (4.12) with $i = \tilde{N}$. Then, we check whether (4.14) and (4.15) are satisfied. If they are, then, we solve for $\theta_{\tilde{N}}$ from (4.13). If there does not exist a solution, then we reduce $\tilde{N}$ and repeat until we reach $\tilde{N} = 1$. If we do not have a solution when we reach $\tilde{N} = 1$, then this means that (4.12) cannot be satisfied, and we must have $\theta_{\tilde{N}} = 1$. In this case, (4.13) becomes:

$$\sum_{i=1}^{\tilde{N}} \left(\frac{p(1-p)^{i-1}}{\lambda} - 1 + \epsilon \right) = B \tag{4.16}$$

For this case, we solve (4.16) along with (4.14)-(4.15) for the largest $\tilde{N}$ and the corresponding λ.

4.2.2 Near-Optimal Strategy: General Arrivals

Now, we consider a general i.i.d. energy arrival process E_i with recharge rate $\mathbb{E}[E_i] = \mu$. In this case, we no longer have a *renewal* structure, and finding the *exactly optimal* online policy is analytically intractable. Instead, we propose a sub-optimal online policy and prove that it performs close to optimal.

4.2.2.1 Sub-Optimal Policy

We first define the proposed sub-optimal online policy for Bernoulli energy arrivals and then extend it to general energy arrivals. We note from (4.10) that, for Bernoulli

energy arrivals, the optimal total transmit power allocated decreases exponentially over time. As in [48–50, 97–100], this motivates us to construct a fractional power policy over time, in particular, we use a total allocated energy of $Bp(1-p)^{i-1}$ in slot i. That is, we allocate a fixed p fraction of available energy in the battery to use in slot i. We then decide on the duration of the burst θ_i by solving a single-slot problem as:

$$\begin{aligned} \max_{\bar{P}_i, \theta_i} \quad & \frac{\theta_i}{2} \log\left(1 + \frac{\bar{P}_i}{\theta_i}\right) \\ \text{s.t.} \quad & \bar{P}_i + \theta_i \epsilon \leq Bp(1-p)^{i-1} \\ & 0 \leq \theta_i \leq 1, \quad \bar{P}_i \geq 0 \end{aligned} \tag{4.17}$$

In the optimal policy, the first constraint is satisfied with equality, hence $\bar{P}_i = Bp(1-p)^{i-1} - \theta_i \epsilon$, and the problem can be written only in terms of θ_i as:

$$\max_{\theta_i \in [0,1]} \quad \frac{\theta_i}{2} \log\left(1 + \frac{Bp(1-p)^{i-1}}{\theta_i} - \epsilon\right) \tag{4.18}$$

For general energy arrivals, we allocate a fraction $q = \mu/B$ of the available energy in the battery for slot i, i.e., qb_i. Then, solve for the optimum burst θ_i in each slot as in (4.18):

$$\max_{\theta_i \in [0,1]} \quad \frac{\theta_i}{2} \log\left(1 + \frac{qb_i}{\theta_i} - \epsilon\right) \tag{4.19}$$

4.2.2.2 A Lower Bound on the Proposed Online Policy

In Lemma 4.1 and Lemma 4.2 below, we develop multiplicative and additive lower bounds for the performance of the proposed sub-optimal algorithm for Bernoulli arrivals. In the following, we denote the solution of maximization problems in (4.18) and (4.19) for available power P as $\theta^*(P,\epsilon)$, i.e., the solution of (4.18) is $\theta^*(Bp(1-p)^{i-1},\epsilon)$ and the solution of (4.19) is $\theta^*(qb_i,\epsilon)$.

Lemma 4.1 *The achievable rate with the proposed sub-optimal policy for any i.i.d. Bernoulli energy arrival process with average recharge rate of $\mu = \mathbb{E}[E_i]$ is lower bounded as,*

$$r \geq \frac{1}{2-\frac{\mu}{B}} \max_{\theta\in[0,1]} \frac{\theta}{2} \log\left(1+\frac{\mu}{\theta}-\epsilon\right) \tag{4.20}$$

$$\geq \frac{1}{2} \max_{\theta\in[0,1]} \frac{\theta}{2} \log\left(1+\frac{\mu}{\theta}-\epsilon\right) \tag{4.21}$$

We provide the proof of Lemma 4.1 in Appendix 4.6.1. The multiplicative bound in Lemma 4.1 performs well when the achievable rates are small, whereas the additive bound in Lemma 4.2 performs well when the achievable rates are large. We provide the proof of Lemma 4.2 in Appendix 4.6.2.

Lemma 4.2 *The achievable rate with the proposed sub-optimal policy for any i.i.d. Bernoulli energy arrival process with average recharge rate of $\mu = \mathbb{E}[E_i]$ is lower*

bounded as,

$$r \geq \max_{\theta \in [0,1]} \frac{\theta}{2} \log\left(1 + \frac{\mu}{\theta} - \epsilon\right) - 0.72 - \frac{1}{2}\log^{+}(\epsilon) \tag{4.22}$$

where $\log^{+}(x) = \max\{\log(x), 0\}$.

We next show that i.i.d. Bernoulli energy arrivals yield the lowest rate over all i.i.d. energy arrivals with the same mean. The proof follows by the approach in [49, Proposition 4] as,

$$f(x) = \max_{\theta_i \in [0,1]} \frac{\theta_i}{2} \log\left(1 + \frac{qx}{\theta_i} - \epsilon\right) \tag{4.23}$$

is concave in x. The concavity of $f(x)$ follows since it is equivalent to the maximization of $\frac{\theta_i}{2}\log\left(1 + \frac{\bar{P}_i}{\theta_i}\right)$ over the feasible set $\bar{P}_i + \theta_i\epsilon \leq qx$, $0 \leq \theta_i \leq 1$, $\bar{P}_i \geq 0$. The objective of this equivalent problem is jointly concave in $\theta_i, \bar{P}_i$, and the constraint set is affine in x, θ_i and $\bar{P}_i$. Then, it follows that $f(x)$ is concave in x; see also [102, Section 3.2.5].

Lemma 4.3 *The rate of the proposed sub-optimal policy with any i.i.d. energy arrival process is no smaller than that with an i.i.d. Bernoulli energy arrival process of the same mean.*

Combining Lemmas 4.1, 4.2, and 4.3, we have the following general theorem for arbitrary i.i.d. energy arrival processes.

Theorem 4.1 *The achievable rate with the proposed sub-optimal policy for any ar-*

bitrary i.i.d. energy arrival process with average recharge rate $\mu = \mathbb{E}[E_i]$ is lower bounded as in (4.20) and (4.22).

4.2.2.3 An Upper Bound for Online Policies

In Theorem 4.2 below, we develop a universal upper bound for the performance of any online policy in terms of $\mathbb{E}[E_i] = \mu$.

Theorem 4.2 *For a recharge rate of $\mathbb{E}[E_i] = \mu$, the achievable rate of any online algorithm is upper bounded as,*

$$r \leq \max_{\theta \in [0,1]} \frac{\theta}{2} \log\left(1 + \frac{\mu}{\theta} - \epsilon\right) \tag{4.24}$$

Proof: We consider the rate of the optimum offline algorithm which upper bounds the rates achievable by any online algorithm. We consider the following larger than actual feasible region for the offline policy by neglecting the no-energy-overflow constraints due to the finite-sized battery [2, 3]:

$$\mathcal{F}^n \triangleq \left\{ \{\bar{P}_i, \theta_i\}_{i=1}^n : \frac{1}{m}\sum_{i=1}^{m} \bar{P}_i + \theta_i \epsilon \leq \frac{1}{m}\sum_{i=1}^{m} E_i, \ \forall m \right\} \tag{4.25}$$

Then, we consider the further larger feasible set by keeping only the bound for $m = n$, and starting with a full battery B,

$$\mathcal{G}^n \triangleq \left\{ \{\bar{P}_i, \theta_i\}_{i=1}^n : \frac{1}{n}\sum_{i=1}^{n} \bar{P}_i + \theta_i \epsilon \leq \frac{1}{n}\left(\sum_{i=1}^{n} E_i + B\right) \right\} \tag{4.26}$$

Then, we have:

$$r \leq \lim_{n\to\infty} \max_{\{\bar{P}_i,\theta_i\}_{i=1}^n \in \mathcal{G}^n} \frac{1}{n}\sum_{i=1}^{n} \frac{\theta_i}{2} \log\left(1+\frac{\bar{P}_i}{\theta_i}\right) \tag{4.27}$$

Since the energies E_i are i.i.d., from strong law of large numbers, for all $\delta > 0$, there exists an integer N such that, for all $n \geq N$, we have $\frac{1}{n}\left(\sum_{i=1}^{n} E_i + B\right) \leq \mu + \delta$. Hence, for large enough n, i.e., $n \geq N$, we have $\mathcal{G}^n$ to be

$$\mathcal{G}^n \triangleq \left\{ \{\bar{P}_i,\theta_i\}_{i=1}^n : \frac{1}{n}\sum_{i=1}^{n} \bar{P}_i + \theta_i\epsilon \leq \mu + \delta \right\} \tag{4.28}$$

Then, from the joint concavity of the objective function, it is maximized when all $\theta_i = \theta$ and all $\bar{P}_i = \bar{P}$. Hence, we have $\bar{P} + \theta\epsilon \leq \mu + \delta$. Since this is valid for all $\delta > 0$, we take its limit to zero, which gives the desired result in (4.24). ■

4.2.2.4 Putting the Bounds Together

The additive lower bound in Theorem 4.1 (i.e., (4.22)) together with the general upper bound in Theorem 4.2 (i.e., (4.24)) imply that there is a constant gap between the bounds. Both the proposed sub-optimal policy and the optimal policy live between these bounds which are separated by a finite gap. Hence, the proposed online policy performs within a constant gap of the optimal online policy for all system parameters.

4.3 Two-Way Channel

We next consider a two-way energy harvesting channel with a common energy harvesting source, see Fig. 4.2. Transmitter j has a battery of finite size B_j. The energy available in the jth user battery in slot i, b_{ji}, evolves as:

$$b_{j(i+1)} = \min\{B_j, b_{ji} - \theta_{ji}P_{ji} - \max\{\theta_{1i}, \theta_{2i}\}\epsilon_j + E_{j(i+1)}\} \tag{4.29}$$

where P_{ji} is the power transmitted by user j in slot i, E_{ji} is the energy harvested at the jth user in slot i, ϵ_j is the processing cost incurred per unit time for being on[1], and θ_{ji} is the duration for which user j is on, either transmitting or receiving, in slot i.

The physical layer is Gaussian with sum rate in slot i [84],

$$r_{1i} + r_{2i} = \frac{\theta_{1i}}{2}\log\left(1 + P_{1i}\right) + \frac{\theta_{2i}}{2}\log\left(1 + P_{2i}\right) \tag{4.30}$$

where r_{ji} is the rate of user j in slot i. The power and burst of user j, θ_{ji}, P_{ji}, are constrained by the current battery state as $\theta_{ji}P_{ji} + \max\{\theta_{1i}, \theta_{2i}\}\epsilon_j \leq b_{ji}$. The objective of the online scheduling is to obtain the optimal policy which consists of $\{\theta_{1i}, \theta_{2i}, P_{1i}, P_{2i}\}$ to maximize the expected rate. In (4.30), the $\frac{1}{2}$ factors in front of logs are due to Shannon capacity formula (see e.g., [84, Eqn. (9.17)]), not due to time-sharing. There is no time-sharing; the system is full-duplex, and hence, the

[1]In this chapter, we assume that the cost of being on while transmitting is the same as cost of being on while receiving. A more general model could be to consider different energy costs for being on for transmission and reception.

sum of two single-user rates is achievable (see e.g., [84, Section 15.1.6]).

In the following, we first consider the case where the energy arrivals, $E_{1i} = E_{2i} = E_i$, are i.i.d. Bernoulli random variables with support $\{0, B\}$, and with $\mathbb{P}[E_{1i} = E_{2i} = B] = p$, where $B \geq \max\{B_1, B_2\}$, i.e., when an energy comes it fills both batteries completely. For this case, we determine the optimal online policy. Subsequently, we consider the case of general i.i.d. energy arrivals, and propose a distributed near-optimal policy.

4.3.1 Optimal Strategy: Case of Bernoulli Arrivals

With Bernoulli energy arrivals, each energy arrival resets the system state; energy arrivals form a *renewal process*. From [88, Theorem 3.6.1], the long-term average throughput is,

$$\lim_{n\to\infty} \mathbb{E}\left[\frac{1}{n}\sum_{i=1}^{n}(r_{1i}+r_{2i})\right] = \frac{1}{\mathbb{E}[L]}\mathbb{E}\left[\sum_{i=1}^{L}(r_{1i}+r_{2i})\right] \tag{4.31}$$

$$= p\sum_{k=1}^{\infty} p(1-p)^{k-1}\sum_{i=1}^{k}(r_{1i}+r_{2i}) \tag{4.32}$$

$$= \sum_{i=1}^{\infty}\sum_{k=i}^{\infty} p^2(1-p)^{k-1}(r_{1i}+r_{2i}) \tag{4.33}$$

$$= \sum_{i=1}^{\infty} p(1-p)^{i-1}(r_{1i}+r_{2i}) \tag{4.34}$$

where L is the geometric inter-arrival time with $\mathbb{E}[L] = 1/p$.

Hence, the online power allocation problem becomes:

$$\max_{\{P_{ji}\},\{\theta_{ji}\}} \quad \sum_{i=1}^{\infty} p(1-p)^{i-1}\left(r_{1i}+r_{2i}\right)$$

$$\begin{aligned}
\text{s.t.} \quad & \sum_{i=1}^{\infty}(\theta_{1i}P_{1i} + \max\{\theta_{1i},\theta_{2i}\}\epsilon_1) \leq B_1 \\
& \sum_{i=1}^{\infty}(\theta_{2i}P_{2i} + \max\{\theta_{1i},\theta_{2i}\}\epsilon_2) \leq B_2 \\
& P_{1i}, P_{2i} \geq 0, \quad 0 \leq \theta_{1i}, \theta_{2i} \leq 1, \quad \forall i
\end{aligned} \tag{4.35}$$

This optimization problem can be viewed as maximizing the *expected* transmitted sum rate before the next energy arrival.

Problem (4.35) is non-convex. We transform it to an equivalent convex problem by defining new variables $\bar{P}_{ji} = \theta_{ji}P_{ji}$,

$$\begin{aligned}
\max \quad & \sum_{i=1}^{\infty} p(1-p)^{i-1}\left(\frac{\theta_{1i}}{2}\log\left(1+\frac{\bar{P}_{1i}}{\theta_{1i}}\right)+\frac{\theta_{2i}}{2}\log\left(1+\frac{\bar{P}_{2i}}{\theta_{1i}}\right)\right) \\
\text{s.t.} \quad & \sum_{i=1}^{\infty}(\bar{P}_{1i} + \max\{\theta_{1i},\theta_{2i}\}\epsilon_1) \leq B_1 \\
& \sum_{i=1}^{\infty}(\bar{P}_{2i} + \max\{\theta_{1i},\theta_{2i}\}\epsilon_2) \leq B_2 \\
& \bar{P}_{1i}, \bar{P}_{2i} \geq 0, \quad 0 \leq \theta_{1i}, \theta_{2i} \leq 1, \quad \forall i
\end{aligned} \tag{4.36}$$

where the maximization is over $\{\bar{P}_{ji}\}, \{\theta_{ji}\}$.

Before proceeding with finding the optimal policy, we state two important observations: First, both users should consume all of their energies in their batteries. If a user does not consume all of its energy, then we can increase its power until all of its energy is used, increasing the objective function. Second, the two users' transmissions should be fully synchronized, i.e.., $\theta_{1i} = \theta_{2i}$, for all i. If for a slot i users are not synchronized, say e.g., $\theta_{1i} < \theta_{2i}$, then we can always increase θ_{1i} to be

equal to θ_{2i} without violating the constraints of the problem, while increasing the objective function. Hence, hereafter, we will assume that $\theta_{1i} = \theta_{2i} = \theta_i$ for all i, so that $\max\{\theta_{1i}, \theta_{2i}\} = \theta_i$. In this case, the Lagrangian for (4.36) is:

$$\begin{aligned}\mathcal{L} =& -\sum_{i=1}^{\infty} p(1-p)^{i-1}\left(\frac{\theta_i}{2}\log\left(1+\frac{\bar{P}_{1i}}{\theta_i}\right)+\frac{\theta_i}{2}\log\left(1+\frac{\bar{P}_{2i}}{\theta_i}\right)\right)\\ &+\lambda_1\left(\sum_{i=1}^{\infty}(\bar{P}_{1i}+\theta_i\epsilon_1)-B_1\right)-\sum_{i=1}^{\infty}\nu_{1i}P_{1i}\\ &+\lambda_2\left(\sum_{i=1}^{\infty}(\bar{P}_{2i}+\theta_i\epsilon_2)-B_2\right)-\sum_{i=1}^{\infty}\nu_{2i}P_{2i}\\ &-\sum_{i=1}^{\infty}\mu_i^l\theta_i-\sum_{i=1}^{\infty}\mu_i^u(1-\theta_i)\end{aligned} \tag{4.37}$$

From the KKTs, the optimal powers for the slots with $\theta_i > 0$:

$$\frac{\bar{P}_{1i}}{\theta_i} = \left(\frac{p(1-p)^{i-1}}{\lambda_1}-1\right)^+, \quad \frac{\bar{P}_{2i}}{\theta_i} = \left(\frac{p(1-p)^{i-1}}{\lambda_2}-1\right)^+ \tag{4.38}$$

For the slots with $\theta_i = 0$, both powers are zero, i.e., $\bar{P}_{1i} = \bar{P}_{2i} = 0$, as otherwise, any assigned positive power is wasted, since the objective function is zero when $\theta_i = 0$.

From (4.38), we observe that for slots with $\theta_i > 0$, the powers P_{1i} and P_{2i} are monotonically decreasing in time. In addition, due to the decreasing $p(1-p)^{i-1}$ factors before the log, we can divide the slots into $\{1, \ldots, \tilde{N}\}$ where $\theta_i > 0$, and $\{\tilde{N}+1, \ldots\}$ where $\theta_i = 0$. Furthermore, the transmission duration $\tilde{N}$ is bounded above by the maximum of the user transmission durations without any processing costs (define them as $\tilde{N}_{npc1}$ and $\tilde{N}_{npc2}$), i.e., $\tilde{N} \leq \max\{\tilde{N}_{npc1}, \tilde{N}_{npc2}\}$. This follows as the processing costs reduce the energy available in the battery dedicated for

transmission, and hence reduce the effective battery size at both users; it is shown in [97] that the transmission duration is monotone increasing in the battery size.

Similarly, from the optimality conditions, the bursts satisfy:

$$\sum_{j=1}^{2} \log\left(1+\frac{\bar{P}_{ji}}{\theta_i}\right) - \frac{\frac{\bar{P}_{ji}}{\theta_i}}{1+\frac{\bar{P}_{ji}}{\theta_i}} = \frac{\sum_{j=1}^{2} \lambda_j \epsilon_j + \mu_i^u - \mu_i^l}{p(1-p)^{i-1}} \tag{4.39}$$

substituting (4.38), we obtain,

$$\sum_{j=1}^{2} \log\left(\frac{p(1-p)^{i-1}}{\lambda_j}\right) = \frac{\sum_{j=1}^{2} \lambda_j (\epsilon_j - 1) + \mu_i^u - \mu_i^l}{p(1-p)^{i-1}} + 2 \tag{4.40}$$

From complementary slackness, if $\theta_i \in (0,1)$, then we have $\mu_i^u = \mu_i^l = 0$. Thus, in this case, (4.40) becomes:

$$\sum_{j=1}^{2} \left(\log\left(\frac{p(1-p)^{i-1}}{\lambda_j}\right) - 1\right) = \frac{\sum_{j=1}^{2} \lambda_j \left(\epsilon_j - 1\right)}{p(1-p)^{i-1}} \tag{4.41}$$

The left and right hand sides of (4.41) are monotone decreasing and increasing, respectively. Hence, (4.41) can be satisfied at most for one time index, thus the bursty transmission can occur at most in one slot. Due to decreasing $p(1-p)^{i-1}$ multiplying the rate, this bursty transmission can occur only in the last slot.

From the above, the optimal solution is characterized by $\lambda_1, \lambda_2, \tilde{N}, \theta_{\tilde{N}}$. Next, we solve for them. For the complete solution we need to solve (4.40) along with the

total power constraints, which using (4.38) become:

$$\sum_{i=1}^{\tilde{N}-1}\left[\frac{p(1-p)^{i-1}}{\lambda_1}-1+\epsilon_1\right]+\theta_{\tilde{N}}\left[\frac{p(1-p)^{\tilde{N}-1}}{\lambda_1}-1+\epsilon_1\right]=B_1 \tag{4.42}$$

$$\sum_{i=1}^{\tilde{N}-1}\left[\frac{p(1-p)^{i-1}}{\lambda_2}-1+\epsilon_2\right]+\theta_{\tilde{N}}\left[\frac{p(1-p)^{\tilde{N}-1}}{\lambda_2}-1+\epsilon_2\right]=B_2 \tag{4.43}$$

Solving (4.42) and (4.43) for $\theta_{\tilde{N}}$ we have:

$$\theta_{\tilde{N}} = \frac{B_1 - \sum_{i=1}^{\tilde{N}-1}\left(\frac{p(1-p)^{i-1}}{\lambda_1} - 1 + \epsilon_1\right)}{\frac{p(1-p)^{\tilde{N}-1}}{\lambda_1} - 1 + \epsilon_1} \tag{4.44}$$

$$= \frac{B_2 - \sum_{i=1}^{\tilde{N}-1}\left(\frac{p(1-p)^{i-1}}{\lambda_2} - 1 + \epsilon_2\right)}{\frac{p(1-p)^{\tilde{N}-1}}{\lambda_2} - 1 + \epsilon_2} \tag{4.45}$$

We note that (4.44) and (4.45) are strictly increasing in λ_1 and λ_2 when the numerators and denominators are non-negative. Hence, for each fixed λ_1 which makes $\theta_{\tilde{N}} \in (0,1)$ there corresponds a unique λ_2 which makes (4.44) and (4.45) equal. This in effect makes it easy to search over the pairs $\{\lambda_1, \lambda_2\}$ which equate (4.44) and (4.45), using a one dimensional search on either λ_1 or λ_2. We also need to satisfy for $i \in \{1, \ldots, \tilde{N}\}$:

$$\lambda_1 \leq p(1-p)^{i-1} \tag{4.46}$$

$$\lambda_2 \leq p(1-p)^{i-1} \tag{4.47}$$

$$0 \leq \sum_{j=1}^{2}\left(\log\left(\frac{p(1-p)^{i-1}}{\lambda_j}\right)-1\right)+\frac{\sum_{j=1}^{2}\lambda_j\,(1-\epsilon_j)}{p(1-p)^{i-1}} \tag{4.48}$$

where (4.46) and (4.47) ensure the non-negativity of the power, and (4.48) guaran-

tees the existence of a non-negative Lagrange multiplier μ_i^u satisfying (4.40).

Towards this end, next, we present a method to obtain the optimal solution. We first initialize $\tilde{N} = \max\{\tilde{N}_{npc1}, \tilde{N}_{npc2}\}$, where $\tilde{N}_{npcj}$ can be found by solving a single-user problem with no processing costs for user j as in [49]. From this, we obtain $\{\lambda_1, \lambda_2\}$ pairs which equate equations (4.44) and (4.45) and make $\theta_{\tilde{N}} \in (0, 1)$. Then, we check if any of the obtained pairs satisfies (4.41), (4.46), (4.47) and (4.48). If yes, then this is the optimal solution. Otherwise, we decrease $\tilde{N}$ by one and repeat this again. If we reach $\tilde{N} = 1$ and no solution is found, then, this implies that $\theta_{\tilde{N}} = 1$. Hence, we solve similarly for the largest integer $\tilde{N}$ and that corresponding λ_1, λ_2 that satisfy:

$$\sum_{i=1}^{\tilde{N}} \left(\frac{p(1-p)^{i-1}}{\lambda_1} - 1 + \epsilon_1 \right) = B_1 \tag{4.49}$$

$$\sum_{i=1}^{\tilde{N}} \left(\frac{p(1-p)^{i-1}}{\lambda_2} - 1 + \epsilon_2 \right) = B_2 \tag{4.50}$$

along with the conditions (4.46), (4.47) and (4.48).

4.3.2 Near-Optimal Strategy: General Arrivals

Now, we consider an arbitrary i.i.d. energy arrival process E_i with average admitted recharge rate $\mu_j = \mathbb{E}[\max\{B_j, E_i\}]$ at user j. Although finding the *exactly optimal* policy in this case may not be tractable, we propose a *distributed* sub-optimal policy which we show is near-optimal.

4.3.2.1 Sub-Optimal Policy

We first present our proposed sub-optimal policy for the Bernoulli case and then extend it to the case of general energy arrivals. For Bernoulli energy arrivals, motivated by (4.38), we assign exponentially decaying total power for each user. In each slot, the users allocate a fraction p of the available energy in the battery, and then optimize the transmit power and burst duration. Hence, in slot i, the energy allocated for transmission by user j is $B_j p(1-p)^{i-1}$. Then, the users solve the following single-slot optimization problem:

$$\begin{aligned} \max_{\bar{P}_{ji},\theta_i} \quad & \frac{\theta_i}{2}\log\left(1+\frac{\bar{P}_{1i}}{\theta_i}\right)+\frac{\theta_i}{2}\log\left(1+\frac{\bar{P}_{2i}}{\theta_i}\right) \\ \text{s.t.} \quad & \bar{P}_{1i}+\theta_i\epsilon_1 \le B_1 p(1-p)^{i-1} \\ & \bar{P}_{2i}+\theta_i\epsilon_2 \le B_2 p(1-p)^{i-1} \\ & \bar{P}_{1i},\bar{P}_{2i}\ge 0, \quad 0\le\theta_i\le 1 \end{aligned} \tag{4.51}$$

Since, the first two constraints will be satisfied with equality we have $\bar{P}_{ji} = B_j p(1-p)^{i-1} - \theta_i\epsilon_j$, which reduces (4.51) to:

$$\max_{\theta_i\in[0,1]} \frac{\theta_i}{2}\log\left(1+\frac{B_1 p(1-p)^{i-1}}{\theta_i}-\epsilon_1\right)+\frac{\theta_i}{2}\log\left(1+\frac{B_2 p(1-p)^{i-1}}{\theta_i}-\epsilon_2\right) \tag{4.52}$$

Similarly, for the case of general energy arrivals, we allocate a fraction $q_j = \frac{\mu_j}{B_j}$ of the battery energy, i.e., $q_j b_{ji}$, and solve:

$$\max_{\theta_i \in [0,1]} \frac{\theta_i}{2} \log\left(1+\frac{q_1 b_{1i}}{\theta_i}-\epsilon_1\right)+\frac{\theta_i}{2}\log\left(1+\frac{q_2 b_{2i}}{\theta_i}-\epsilon_2\right) \tag{4.53}$$

Problems (4.52) and (4.53) can be solved by both users independently, because both users know the energy arrival E_i, and they are consuming the power in a deterministic fractional way, hence, both users can track the state of both batteries.

4.3.2.2 An Upper Bound for Online Policies

In the following theorem, we develop an upper bound for all online policies in terms of the average admitted energy.

Theorem 4.3 *For an average admitted energy μ_j at user j, the achievable rate for any online policy is upper bounded by:*

$$r_{ub} = \max_{\theta \in [0,1]} \frac{\theta}{2}\left(\log\left(1+\frac{\mu_1}{\theta}-\epsilon_1\right)+\log\left(1+\frac{\mu_2}{\theta}-\epsilon_2\right)\right) \tag{4.54}$$

Proof: We denote the admitted energy arrivals as $\tilde{E}_{ji} = \min\{B_j, E_{ji}\}$. We use the offline achievable rate as an upper bound for the online achievable rate. We consider the following set which is larger than the feasible set of the offline case:

$$\mathcal{F}^n \triangleq \left\{ \{\bar{P}_{1i}, \bar{P}_{2i}, \theta_i\}_{i=1}^n : \frac{1}{m}\sum_{i=1}^m \bar{P}_{1i}+\theta_i\epsilon_1 \leq \frac{1}{m}\left(\sum_{i=1}^m \tilde{E}_{1i}\right),\right.$$

$$\frac{1}{m}\sum_{i=1}^{m}\bar{P}_{2i}+\theta_i\epsilon_2 \leq \frac{1}{m}\left(\sum_{i=1}^{m}\tilde{E}_{2i}\right), \forall m=1,\ldots,n\Bigg\} \tag{4.55}$$

which neglects the overflow constraints due to the finite battery [2, 3]. We then consider a bigger feasible set by considering the constraints only when $m = n$ to get:

$$\mathcal{G}^n \triangleq \Bigg\{\{\bar{P}_{1i},\bar{P}_{2i},\theta_i\}_{i=1}^n : \frac{1}{n}\sum_{i=1}^{n}\bar{P}_{1i}+\theta_i\epsilon_1 \leq \frac{1}{n}\left(\sum_{i=1}^{n}\tilde{E}_{1i}\right), \\ \frac{1}{n}\sum_{i=1}^{n}\bar{P}_{2i}+\theta_i\epsilon_2 \leq \frac{1}{n}\left(\sum_{i=1}^{n}\tilde{E}_{2i}\right)\Bigg\} \tag{4.56}$$

Hence, the online achievable rate is upper bounded by:

$$\lim_{n\to\infty}\max_{\mathcal{G}^n}\frac{1}{n}\sum_{i=1}^{n}\frac{\theta_i}{2}\left(\log\left(1+\frac{\bar{P}_{1i}}{\theta_i}\right)+\log\left(1+\frac{\bar{P}_{2i}}{\theta_i}\right)\right) \tag{4.57}$$

Since the energies $\tilde{E}_{1i}, \tilde{E}_{2i}$ are i.i.d., from strong law of large numbers, for all $\delta > 0$ there exists an integer N such that for all $n \geq N$, we have $\frac{1}{n}\sum_{i=1}^{n}\tilde{E}_{1i} \leq \mu_1+\delta$ and $\frac{1}{n}\sum_{i=1}^{n}\tilde{E}_{2i} \leq \mu_2+\delta$. For large enough n, i.e., $n \geq N$, the constraints in (4.56) will be:

$$\frac{1}{n}\sum_{i=1}^{n}\bar{P}_{1i}+\theta_i\epsilon_1 \leq \mu_1+\delta, \quad \frac{1}{n}\sum_{i=1}^{n}\bar{P}_{2i}+\theta_i\epsilon_2 \leq \mu_2+\delta \tag{4.58}$$

Then, from the joint concavity of the objective function, it is maximizes when all $\theta_i = \theta$ and $\bar{P}_{ji} = \bar{P}_j$. Since this is valid for all $\delta > 0$, we can the take δ to zero, which gives (4.54). ■

4.3.2.3 A Lower Bound on the Proposed Online Policy

In this section, we derive multiplicative and additive bounds for the performance of the proposed sub-optimal policy. In what follows, we denote the solution of the problems in (4.52) and (4.53) for available powers P_1, P_2 as $\theta^*(P_1, P_2)$, i.e., the solutions of (4.52) and (4.53) are denoted as $\theta^*(B_1 p(1-p)^{i-1}, B_2 p(1-p)^{i-1})$ and $\theta^*(q_1 b_{1i}, q_2 b_{2i})$, respectively.

Lemma 4.4 *The achievable rate with the proposed fractional policy for any i.i.d. Bernoulli energy arrival process with average admitted energy μ_j at user j is lower bounded as:*

$$r \geq \frac{1}{2} r_{ub} \tag{4.59}$$

We provide the proof of Lemma 4.4 in Appendix 4.6.3.

Lemma 4.5 *The achievable rate under the proposed fractional policy for any i.i.d. Bernoulli energy arrival process with average admitted energy μ_j at user j is lower bounded as:*

$$r \geq r_{ub} - 1.44 - \frac{1}{2}\log^+(\epsilon_1) - \frac{1}{2}\log^+(\epsilon_2) \tag{4.60}$$

where $\log^+(x) = \max\{0, \log(x)\}$.

We provide the proof of Lemma 4.5 in Appendix 4.6.4.

We next show that i.i.d. Bernoulli energy arrivals give the lowest rate over

all i.i.d. energy arrivals with the same mean. The proof follows by the approach in [49, Proposition 4] as

$$f(x_1, x_2) \triangleq \max_{\theta_i \in [0,1]} \frac{\theta_i}{2} \left(\log \left(1 + \frac{q_1 x_1}{\theta_i} - \epsilon_1 \right) + \log \left(1 + \frac{q_2 x_2}{\theta_i} - \epsilon_2 \right) \right) \tag{4.61}$$

is jointly concave in x_1, x_2. The concavity of $f(x_1, x_2)$ follows since it is equivalent to maximizing $\frac{\theta_i}{2} \log \left(1 + \frac{\bar{P}_{1i}}{\theta_i} \right) + \frac{\theta_i}{2} \log \left(1 + \frac{\bar{P}_{2i}}{\theta_i} \right)$ over the feasible set $\bar{P}_{1i} + \theta_i \epsilon_1 \leq q_1 x_1$, $\bar{P}_{2i} + \theta_i \epsilon_2 \leq q_2 x_2$, $0 \leq \theta_i \leq 1$, $\bar{P}_{1i}, \bar{P}_{2i} \geq 0$. The objective function here is jointly concave $\theta_i, \bar{P}_{1i}, \bar{P}_{2i}$ and the constraint set is affine in $x_1, x_2, \theta_i, \bar{P}_{1i}, \bar{P}_{2i}$. Then, it follows that $f(x_1, x_2)$ is concave in x_1, x_2; [102, Section 3.2.5]. In addition, [49, Lemma 2] can be used as we have a single random variable representing the common energy arrival.

Lemma 4.6 *For the proposed fractional policy, any i.i.d. energy arrival process yields an achievable sum rate no less than that of the Bernoulli energy arrivals with the same mean.*

Combining Lemmas 4.4, 4.5, and 4.6, we have the following general theorem for arbitrary i.i.d. energy arrival processes.

Theorem 4.4 *The achievable sum rate with the proposed sub-optimal policy for any arbitrary i.i.d. energy arrival process with average admitted energy of μ_j at user j and with $\frac{\mu_1}{B_1} = \frac{\mu_2}{B_2}$ is lower bounded by (4.59) and (4.60).*

4.3.2.4 Putting the Bounds Together

The additive lower bound in Theorem 4.4 (i.e., (4.60)) together with the general upper bound in Theorem 4.3 (i.e., (4.54)) imply that there is a constant gap between the bounds. Both the proposed sub-optimal policy and the optimal policy live between these bounds which are separated by a finite gap. Hence, the proposed online policy performs within a constant gap of the optimal online policy for all system parameters.

4.4 Numerical Results

In this section, we illustrate our results using several numerical examples. We begin with the single-user setting. We first show the optimal policy for Bernoulli energy arrivals. We fix the battery size to $B = 2$ and the probability of energy arrival to $p = 0.1$. We show the optimal policy in Fig. 4.3 for ϵ values of 0.1 and 1.5. As the processing cost increases, the transmission time decreases. When $\epsilon = 0.1$, the optimal power is decreasing and is non-zero for a total duration of 2.6 slots. However, when the processing cost is 1.5, the transmission duration decreases to 0.55 slots. Next, in Fig. 4.4, for the case of Bernoulli energy arrivals, we show the optimal policy versus the proposed sub-optimal policy. Here, we have $B = 3$, $p = 0.3$, $\epsilon = 0.1$. In the sub-optimal policy the energy is spread over more (infinite) slots.

In Figs. 4.5 and 4.6, we show the performance of the proposed sub-optimal policy and the optimal policy in terms of the expected rate versus the battery size.

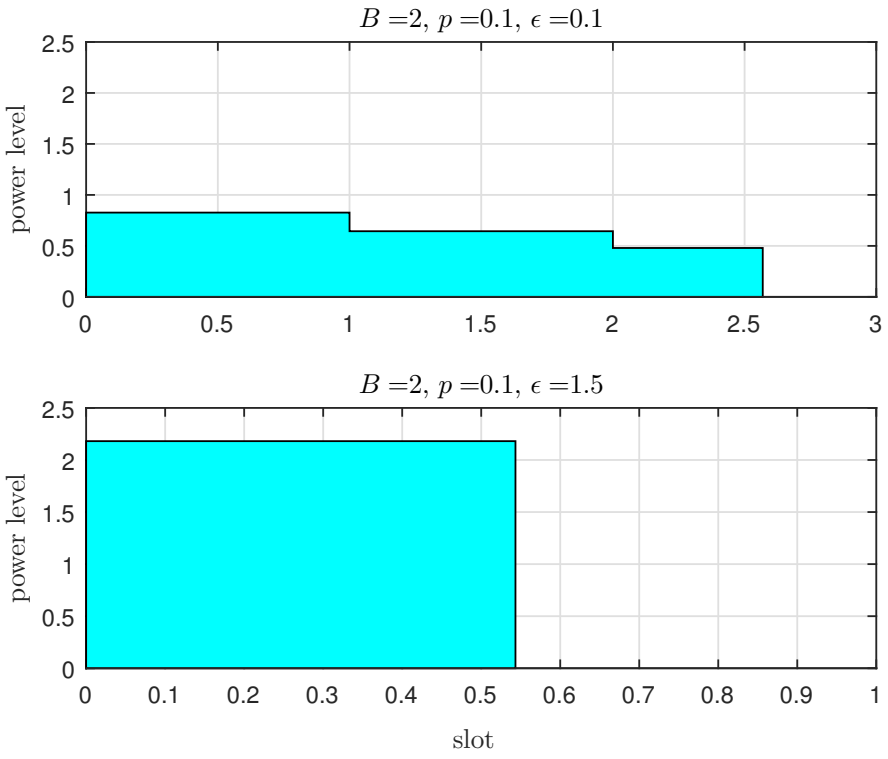

Figure 4.3: Optimum online power allocation for i.i.d. Bernoulli arrivals.

We fix $p = 0.1$ and show the performance for processing costs of $\epsilon = 1$ and $\epsilon = 10$ in Figs. 4.5 and 4.6. We note that, for the case of Bernoulli arrivals, the performance of the proposed sub-optimal policy is quite close to the performance of the optimal policy, in fact, much closer than the derived theoretical bounds show. In Figs. 4.5 and 4.6, we further plot two other sub-optimal schemes. The first scheme uses the same total fractional power as our proposed policy but fixes $\theta_i = 1$ for all i (i.e., neglects the processing cost effect) and transmits whenever it is feasible to transmit. The second scheme also uses the same total fractional power as our proposed policy but uses a fractional decreasing burstiness as $\theta_i = (1-p)^{i-1}\theta^*$. We observe that both of these policies perform worse than our proposed policy. We observe that the policy with $\theta = 1$ performs close to the optimal when the value of processing cost

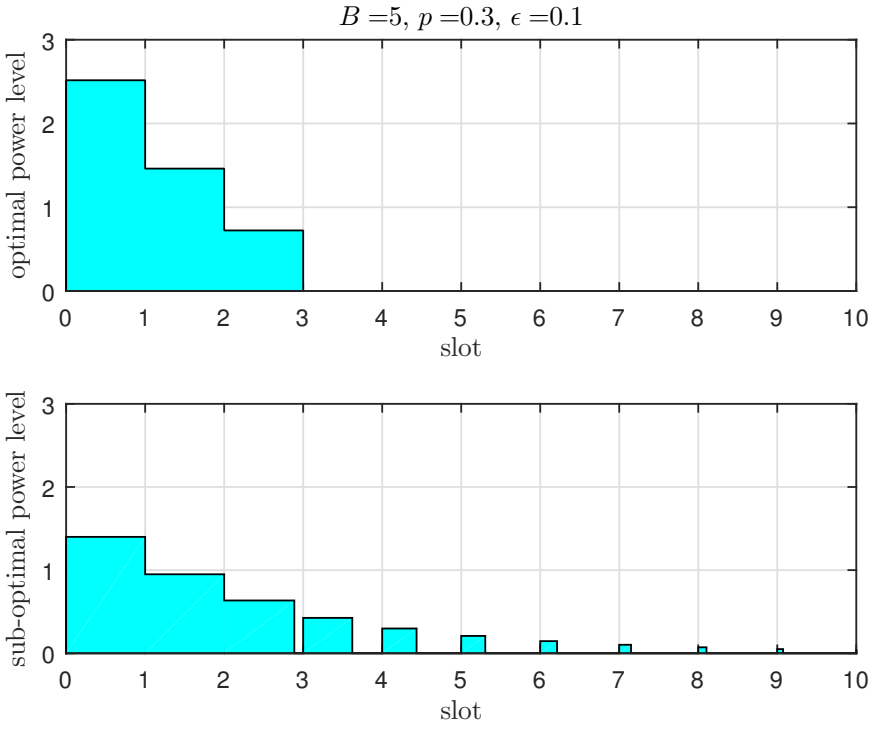

Figure 4.4: Optimum online power allocation versus sub-optimal power allocation for i.i.d. Bernoulli arrivals.

is negligible with respect to the battery size, i.e., for large battery sizes. However, for small battery sizes, e.g., B in $[1, 10]$ when $\epsilon = 1$ and B in $[1, 100]$ when $\epsilon = 10$, this algorithm performs poorly.

In Figs. 4.5 and 4.6, we also plot the performance of the proposed sub-optimal policy when the energy arrivals come from a continuous uniform distribution (non-Bernoulli) with the same mean as the Bernoulli energy arrivals. As expected, the rate is higher for the case of general energy arrivals compared to Bernoulli energy arrivals with the same mean. Finally, we show the performance of our scheme versus the processing cost in Fig. 4.7. The gap between the optimal and the sub-optimal decreases for high processing costs.

Next, we consider the two-way channel. We first show the optimal versus

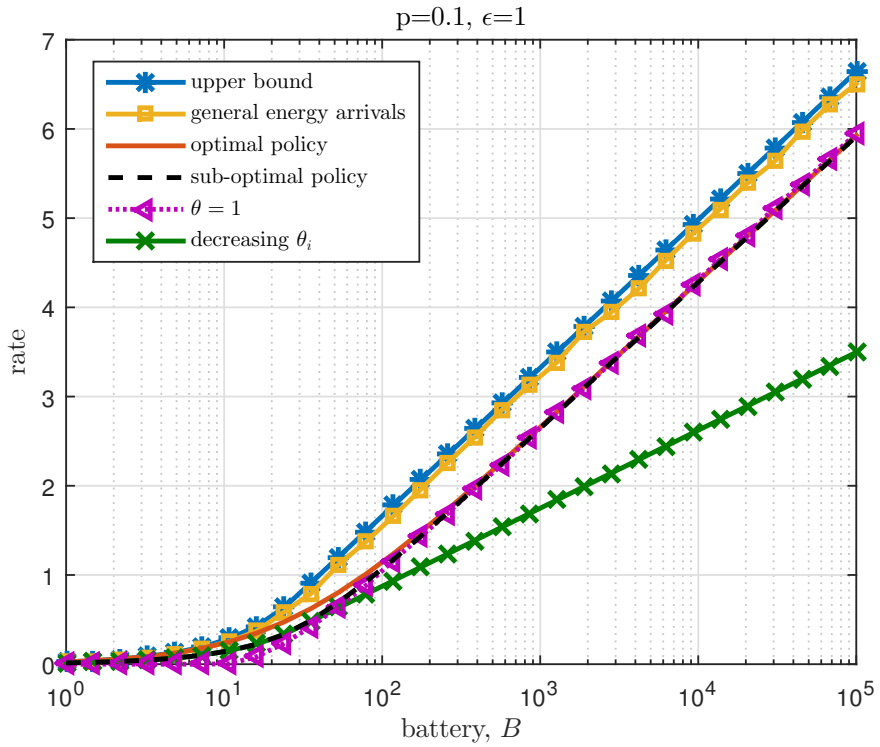

Figure 4.5: Optimum online policy versus proposed sub-optimum online policy.

proposed sub-optimal power allocation for Bernoulli arrivals in Fig. 4.8. As we showed, in the optimal power allocation, bursty transmission takes place only in the last slot. We then compare the performance of the proposed sub-optimal scheme and the optimal policy in Fig. 4.9. The performance of our proposed policy is close to the optimal. We also show the performance of the sub-optimal policy on a general energy arrival with a continuous uniform distribution with the same mean as Bernoulli. In Fig. 4.9 we also show the performance of the fractional θ_i scheme which is used in the proof of Lemma 4.4, and a scheme which always uses $\theta_i = 1$ whenever feasible, i.e., neglects the processing costs. Both perform worse than our proposed policy. Finally, we show the performance of our scheme versus the processing cost in Fig. 4.10. We observe that for high processing costs the performance gap is small.

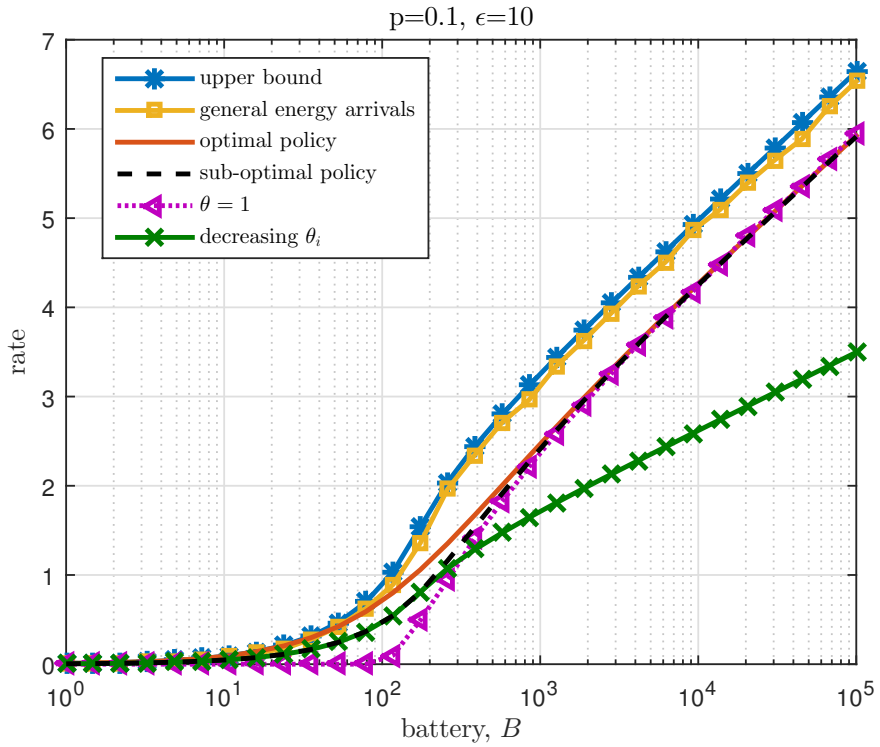

Figure 4.6: Optimum online policy versus proposed sub-optimum online policy.

4.5 Conclusion

In this chapter, we considered energy harvesting channels where users incur processing costs (power spent to run the circuitry) for being *on* to transmit or receive data, in addition to the power spent for communication. Such processing costs may result in *bursty* transmissions, where users may not be on all the time. In such channels, the users need to determine the optimal burst duration (duration to be on) and the optimal transmit power. In this chapter, we considered the design of *online* power control algorithms which use only the causal knowledge of energy arrivals. First, we studied the single-user channel. In this channel, we characterized the optimal online policy for the case of Bernoulli energy arrivals. We showed that the optimal power

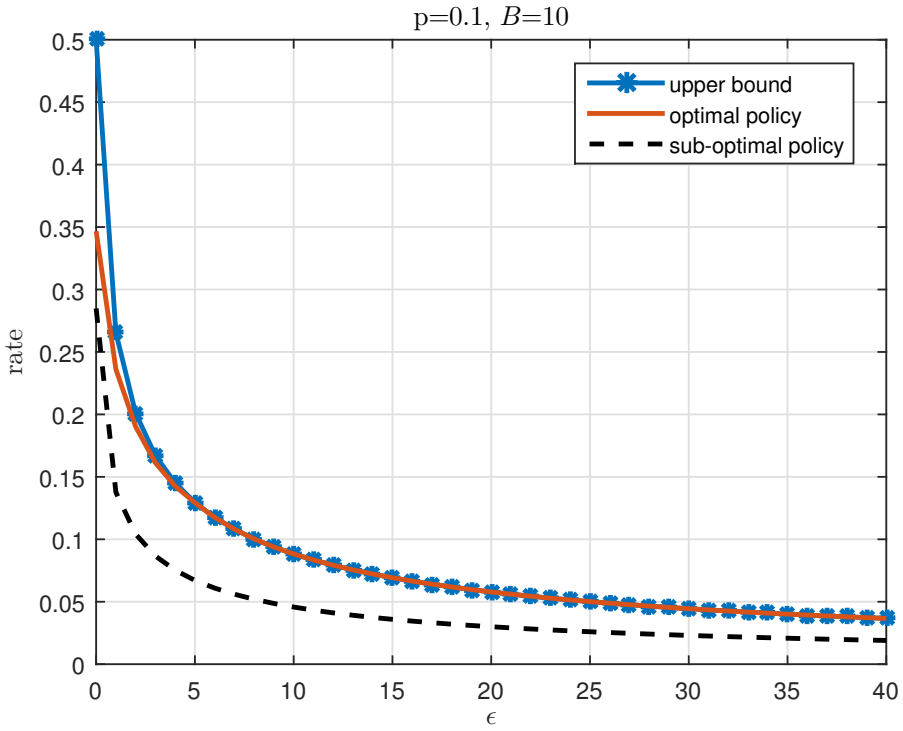

Figure 4.7: Performance versus processing cost for i.i.d. Bernoulli arrivals.

policy is decreasing and can be bursty (i.e., the user may not utilize the entire slot). However, the bursty transmission can occur only in the last slot of transmission. We then considered the case of general energy arrivals. For this case, we proposed a sub-optimal online power control scheme, and proved that it performs within a constant gap of the optimal. The sub-optimal policy allocates powers fractionally over time and solves a single-slot optimization problem to determine the burst duration in each slot. We then extended our analysis to the two-way channel model. We considered the special case of fully-correlated energy arrivals at the users. In this channel, we first characterized the optimal policy for the case of Bernoulli energy arrivals. We showed that the powers of both users decrease and the transmission of both users need to be synchronized, i.e., both users turn on or off simultane-

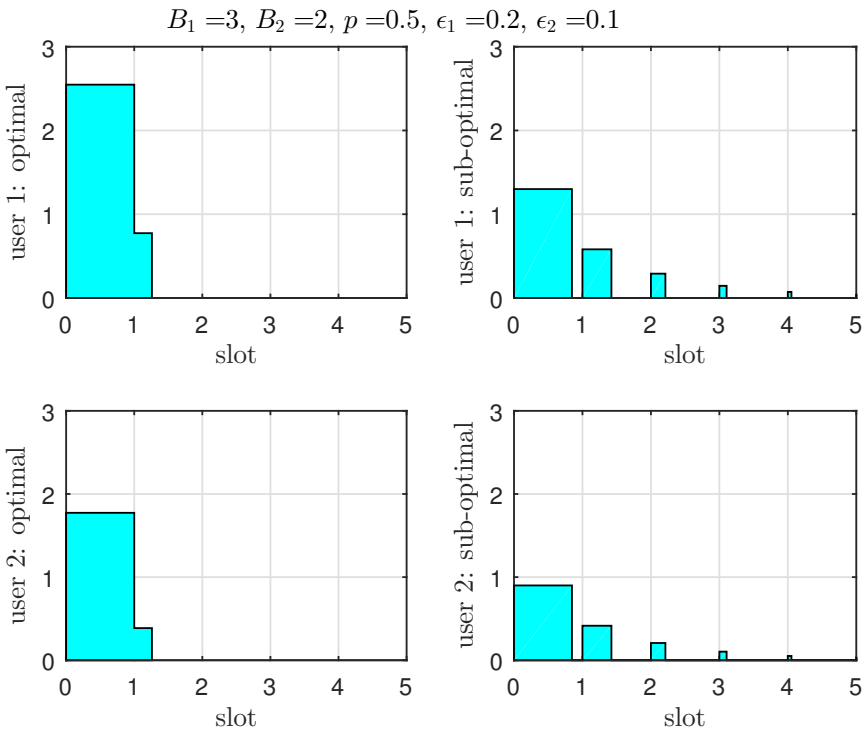

Figure 4.8: The optimal and sub-optimal power allocations for Bernoulli.

ously. We then proposed a sub-optimal distributed policy for the case of general fully-correlated energy arrivals. The proposed policy allocates powers fractionally in a distributed manner, and each user solves a single-slot problem distributedly. We proved that the proposed distributed scheme performs within a constant gap of the optimal.

In the two-way channel, we assumed that the energy cost for being on is the same for transmitting and receiving data. As a future work, different energy costs for transmission and reception can be considered. In addition, we assumed that the energy arrivals at the two users are fully-correlated. Arbitrarily correlated energy arrivals at the users can be considered in future work. Further research directions are to consider energy cooperation between the users in an online setting, and finite-

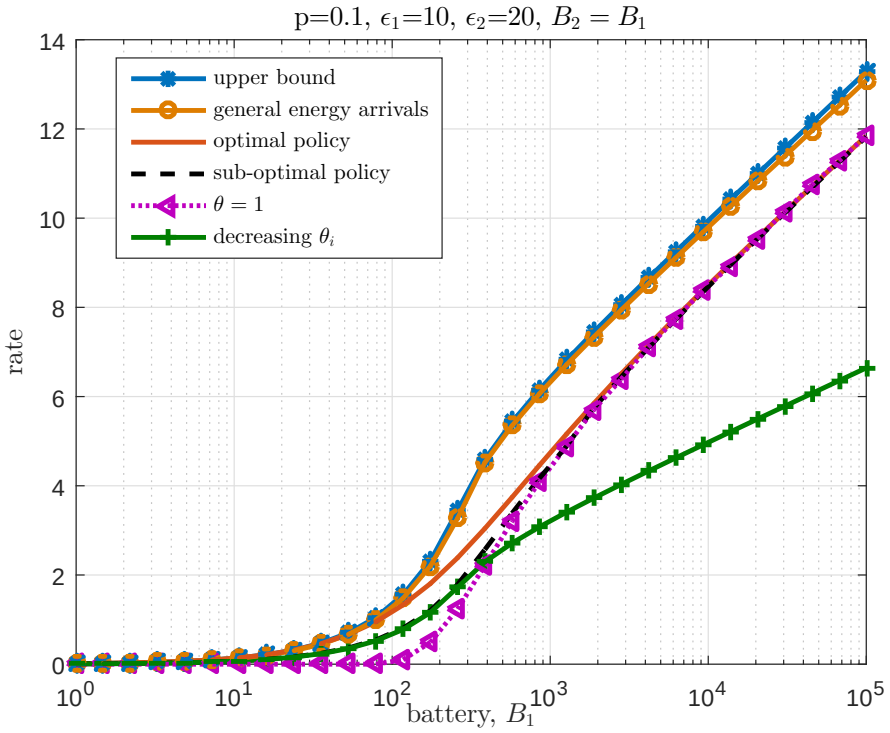

Figure 4.9: Performance of Bernoulli and general energy arrivals.

sized data buffers at both users.

4.6 Appendix

4.6.1 Proof of Lemma 4.1

We lower bound the performance as follows. The first lower bounding step in (4.63) is obtained by choosing all θ_i as $\theta_i = (1-p)^{i-1}\theta^*$, where θ^* denotes $\theta^*(Bp, \epsilon)$ in short:

$$r = \frac{1}{\mathbb{E}[L]} \mathbb{E}\left[\sum_{i=1}^{L} \max_{\theta_i \in [0,1]} \frac{\theta_i}{2} \log\left(1 + \frac{Bp(1-p)^{i-1}}{\theta_i} - \epsilon\right)\right] \tag{4.62}$$

$$\geq \frac{1}{\mathbb{E}[L]} \mathbb{E}\left[\sum_{i=1}^{L} \frac{\theta^*(1-p)^{i-1}}{2} \log\left(1 + \frac{Bp}{\theta^*} - \epsilon\right)\right] \tag{4.63}$$

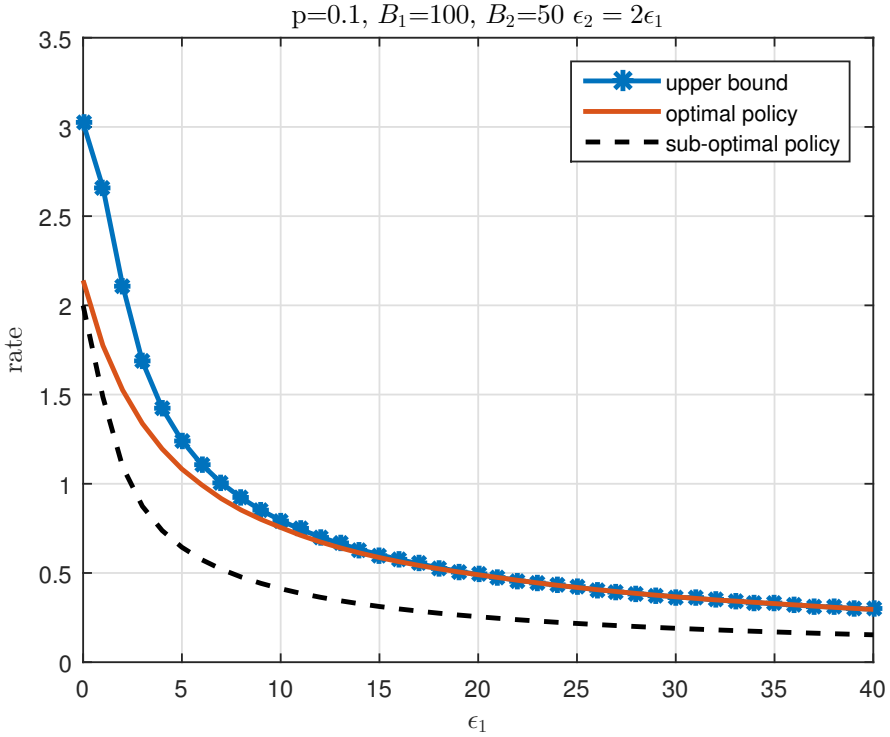

Figure 4.10: Performance of Bernoulli energy arrivals versus the processing cost.

$$= \frac{\theta^*}{2} \log\left(1 + \frac{Bp}{\theta^*} - \epsilon\right) \frac{1}{\mathbb{E}[L]} \mathbb{E}\left[\sum_{i=1}^{L} (1-p)^{i-1}\right] \tag{4.64}$$

$$= \frac{\theta^*}{2} \log\left(1 + \frac{Bp}{\theta^*} - \epsilon\right) p \left[\sum_{L=1}^{\infty} p(1-p)^{L-1} \sum_{i=1}^{L} (1-p)^{i-1}\right] \tag{4.65}$$

$$= \frac{\theta^*}{2} \log\left(1 + \frac{Bp}{\theta^*} - \epsilon\right) \left[\sum_{L=1}^{\infty} p^2 (1-p)^{L-1} \frac{1-(1-p)^L}{p}\right] \tag{4.66}$$

$$= \frac{\theta^*}{2} \log\left(1 + \frac{Bp}{\theta^*} - \epsilon\right) \left[\sum_{L=1}^{\infty} p(1-p)^{L-1} \left(1-(1-p)^L\right)\right] \tag{4.67}$$

$$= \frac{\theta^*}{2} \log\left(1 + \frac{Bp}{\theta^*} - \epsilon\right) \left[\sum_{L=1}^{\infty} p\left((1-p)^{L-1} - (1-p)^{2L-1}\right)\right] \tag{4.68}$$

$$= \frac{\theta^*}{2} \log\left(1 + \frac{Bp}{\theta^*} - \epsilon\right) \left[p\left(\frac{1}{p} - \frac{(1-p)}{2p-p^2}\right)\right] \tag{4.69}$$

$$= \frac{\theta^*}{2} \log\left(1 + \frac{Bp}{\theta^*} - \epsilon\right) \left(\frac{1}{2-p}\right) \tag{4.70}$$

$$= \frac{1}{2 - \frac{\mu}{B}} \max_{\theta \in [0,1]} \frac{\theta}{2} \log\left(1 + \frac{\mu}{\theta} - \epsilon\right) \tag{4.71}$$

which is (4.20). Here, (4.71) follows since $\mathbb{E}[E_i] = \mu = Bp$ and $\theta^* = \theta^*(Bp, \epsilon) = \theta^*(\mu, \epsilon)$. Finally, (4.21) follows as $\frac{\mu}{B} \geq 0$.

4.6.2 Proof of Lemma 4.2

We first prove for the case $\epsilon < 1$. The first lower bounding step in (4.73) is obtained by choosing all θ_i as $\theta_i = \theta^*$, where θ^* denotes $\theta^*(Bp, \epsilon)$ in short:

$$
\begin{aligned}
r =& \frac{1}{\mathbb{E}[L]} \mathbb{E}\left[\sum_{i=1}^{L} \max_{\theta_i \in [0,1]} \frac{\theta_i}{2} \log\left(1 + \frac{Bp(1-p)^{i-1}}{\theta_i} - \epsilon\right)\right] && (4.72)\\
\geq& \frac{1}{\mathbb{E}[L]} \mathbb{E}\left[\sum_{i=1}^{L} \frac{\theta^*}{2} \log\left(1 + \frac{Bp(1-p)^{i-1}}{\theta^*} - \epsilon\right)\right] && (4.73)\\
=& \frac{\theta^*}{2} \frac{1}{\mathbb{E}[L]} \mathbb{E}\left[\sum_{i=1}^{L} \log\left((1-\epsilon)\left(1 + \frac{Bp(1-p)^{i-1}}{(1-\epsilon)\theta^*}\right)\right)\right] && (4.74)\\
=& \frac{\theta^*}{2} \frac{1}{\mathbb{E}[L]} \mathbb{E}\left[\sum_{i=1}^{L} \log(1-\epsilon) + \log\left(1 + \frac{Bp(1-p)^{i-1}}{(1-\epsilon)\theta^*}\right)\right] && (4.75)\\
\geq& \frac{\theta^*}{2} \frac{1}{\mathbb{E}[L]} \mathbb{E}\left[\sum_{i=1}^{L} \log(1-\epsilon) + \log\left(1 + \frac{Bp}{(1-\epsilon)\theta^*}\right) + \log\left((1-p)^{i-1}\right)\right] && (4.76)\\
\geq& \frac{\theta^*}{2} \frac{1}{\mathbb{E}[L]} \mathbb{E}\left[\sum_{i=1}^{L} \log(1-\epsilon) + \log\left(1 + \frac{Bp}{(1-\epsilon)\theta^*}\right)\right] - 0.72 && (4.77)\\
=& \frac{\theta^*}{2} \log\left(1 + \frac{Bp}{\theta^*} - \epsilon\right) - 0.72 && (4.78)
\end{aligned}
$$

which is (4.22), since $\mathbb{E}[E_i] = \mu = Bp$, $\theta^* = \theta^*(Bp, \epsilon)$, and $\log^+(\epsilon) = 0$ in this case.

Next, we prove for the case $\epsilon \geq 1$:

$$
\begin{aligned}
r =& \frac{1}{\mathbb{E}[L]} \mathbb{E}\left[\sum_{i=1}^{L} \max_{\theta_i \in [0,1]} \frac{\theta_i}{2} \log\left(1 + \frac{Bp(1-p)^{i-1}}{\theta_i} - \epsilon\right)\right] && (4.79)\\
\geq& \frac{1}{\mathbb{E}[L]} \mathbb{E}\left[\sum_{i=1}^{L} \max_{\theta_i \in [0,1]} \frac{\theta_i}{2} \log\left(1 + \frac{\frac{Bp(1-p)^{i-1}}{\theta_i} - \epsilon}{\epsilon}\right)\right] && (4.80)
\end{aligned}
$$

$$=\frac{1}{\mathbb{E}[L]}\mathbb{E}\left[\sum_{i=1}^{L}\max_{\theta_i\in[0,1]}\frac{\theta_i}{2}\log\left(1+\frac{Bp(1-p)^{i-1}}{\theta_i\epsilon}-1\right)\right] \tag{4.81}$$

$$\geq\frac{1}{\mathbb{E}[L]}\mathbb{E}\left[\sum_{i=1}^{L}\max_{\theta_i\in[0,1]}\frac{\theta_i}{2}\log\left(\frac{Bp}{\theta_i}\right)\right]-\frac{1}{\mathbb{E}[L]}\mathbb{E}\left[\sum_{i=1}^{L}\max_{\theta_i\in[0,1]}\frac{\theta_i}{2}\log\left(\epsilon\right)\right]$$
$$-\frac{1}{\mathbb{E}[L]}\mathbb{E}\left[\sum_{i=1}^{L}\max_{\theta_i\in[0,1]}\frac{\theta_i}{2}\log\left(\frac{1}{(1-p)^{i-1}}\right)\right] \tag{4.82}$$

$$=\frac{1}{\mathbb{E}[L]}\mathbb{E}\left[\sum_{i=1}^{L}\max_{\theta_i\in[0,1]}\frac{\theta_i}{2}\log\left(\frac{Bp}{\theta_i}\right)\right]-\frac{1}{\mathbb{E}[L]}\mathbb{E}\left[\sum_{i=1}^{L}\frac{1}{2}\log\left(\epsilon\right)\right]$$
$$-\frac{1}{\mathbb{E}[L]}\mathbb{E}\left[\sum_{i=1}^{L}\frac{1}{2}\log\left((1-p)^{i-1}\right)\right] \tag{4.83}$$

$$=\max_{\theta\in[0,1]}\frac{\theta}{2}\log\left(\frac{Bp}{\theta}\right)-\frac{1}{2}\log\left(\epsilon\right)-0.72 \tag{4.84}$$

$$\geq\max_{\theta\in[0,1]}\frac{\theta}{2}\log\left(1+\frac{Bp}{\theta}-\epsilon\right)-\frac{1}{2}\log\left(\epsilon\right)-0.72 \tag{4.85}$$

which is (4.22), since $\log^+(\epsilon)=\log(\epsilon)$ in this case. Here, (4.80) follows since at the maximum $\frac{Bp(1-p)^{i-1}}{\theta_i}-\epsilon$ is non-negative and $\epsilon\geq 1$, (4.82) follows since for any three positive functions $a(x),b(x),c(x)$, we have: $\max_x[a(x)-b(x)-c(x)]\geq\max_x a(x)-\max_x b(x)-\max_x c(x)$, and (4.85) follows since we added a negative term $(1-\epsilon)$ inside the log.

4.6.3 Proof of Lemma 4.4

The first step, (4.87), for the lower bound follows by using a sub-optimal decreasing burst as $\theta_i=\theta^*(1-p)^{i-1}$, where θ^* is a short notation for $\theta^*(B_1p,B_2p)$:

$$r=\frac{1}{\mathbb{E}[L]}\mathbb{E}\left[\sum_{i=1}^{L}\max_{\theta_i\in[0,1]}\frac{\theta_i}{2}\left(\log\left(1+\frac{B_1p(1-p)^{i-1}}{\theta_i}-\epsilon_1\right)+\log\left(1+\frac{B_2p(1-p)^{i-1}}{\theta_i}-\epsilon_2\right)\right)\right] \tag{4.86}$$

$$\geq \frac{1}{\mathbb{E}[L]}\mathbb{E}\left[\sum_{i=1}^{L}(1-p)^{i-1}r_{ub}\right] \tag{4.87}$$

$$= r_{ub}\frac{1}{\mathbb{E}[L]}\mathbb{E}\left[\sum_{i=1}^{L}(1-p)^{i-1}\right] \tag{4.88}$$

$$= r_{ub}\frac{1}{\mathbb{E}[L]}\left[\sum_{L=1}^{\infty}p(1-p)^{L-1}\sum_{i=1}^{L}(1-p)^{i-1}\right] \tag{4.89}$$

$$= r_{ub}\left[\sum_{L=1}^{\infty}p^2(1-p)^{L-1}\frac{1-(1-p)^L}{p}\right] \tag{4.90}$$

$$= r_{ub}\left[p\left(\frac{1}{p}-\frac{(1-p)}{2p-p^2}\right)\right] \tag{4.91}$$

$$= r_{ub}\left(\frac{1}{2-p}\right) \tag{4.92}$$

$$\geq \frac{1}{2}r_{ub} \tag{4.93}$$

where (4.93) follows since $p \geq 0$.

4.6.4 Proof of Lemma 4.5

The proof technique we use for the case $\epsilon_j \leq 1$ is different than $\epsilon_j > 1$. In what follows, we assume that $\epsilon_1 > 1$ while $\epsilon_2 \leq 1$, however, all other combinations follow similarly. We bound the performance of (4.86) as follows:

$$r \geq \frac{1}{\mathbb{E}[L]}\mathbb{E}\left[\sum_{i=1}^{L}\max_{\theta_i\in[0,1]}\frac{\theta_i}{2}\left(\log\left(1+\frac{\frac{B_1p(1-p)^{i-1}}{\theta_i}-\epsilon_1}{\epsilon_1}\right)+\log\left(1+\frac{B_2p(1-p)^{i-1}}{\theta_i}-\epsilon_2\right)\right)\right] \tag{4.94}$$

$$= \frac{1}{\mathbb{E}[L]}\mathbb{E}\left[\sum_{i=1}^{L}\max_{\theta_i\in[0,1]}\frac{\theta_i}{2}\left(\log\left(1+\frac{B_1p(1-p)^{i-1}}{\epsilon_1\theta_i}-1\right)+\log\left(1+\frac{B_2p(1-p)^{i-1}}{\theta_i}-\epsilon_2\right)\right)\right] \tag{4.95}$$

$$\geq \frac{1}{\mathbb{E}[L]}\mathbb{E}\left[\sum_{i=1}^{L}\max_{\theta_i\in[0,1]}\frac{\theta_i}{2}\left(\log\left(\frac{B_1 p}{\theta_i}\right)+\log\left(1+\frac{B_2 p(1-p)^{i-1}}{\theta_i}-\epsilon_2\right)\right)\right]$$
$$-\frac{1}{\mathbb{E}[L]}\mathbb{E}\left[\sum_{i=1}^{L}\max_{\theta_i\in[0,1]}\frac{\theta_i}{2}\log(\epsilon_1)\right]-\frac{1}{\mathbb{E}[L]}\mathbb{E}\left[\sum_{i=1}^{L}\max_{\theta_i\in[0,1]}\frac{\theta_i}{2}\log\left(\frac{1}{(1-p)^{i-1}}\right)\right] \quad (4.96)$$
$$\geq \frac{1}{\mathbb{E}[L]}\mathbb{E}\left[\sum_{i=1}^{L}\max_{\theta_i\in[0,1]}\frac{\theta_i}{2}\left(\log\left(\frac{B_1 p}{\theta_i}\right)+\log\left(1+\frac{B_2 p(1-p)^{i-1}}{\theta_i}-\epsilon_2\right)\right)\right]$$
$$-\frac{1}{2}\log(\epsilon_1)-0.72 \quad (4.97)$$
$$\geq \frac{1}{\mathbb{E}[L]}\mathbb{E}\left[\sum_{i=1}^{L}\max_{\theta_i\in[0,1]}\frac{\theta_i}{2}\left(\log\left(1+\frac{B_1 p}{\theta_i}-\epsilon_1\right)+\log\left(1+\frac{B_2 p(1-p)^{i-1}}{\theta_i}-\epsilon_2\right)\right)\right]$$
$$-\frac{1}{2}\log(\epsilon_1)-0.72 \quad (4.98)$$
$$\geq \frac{1}{\mathbb{E}[L]}\mathbb{E}\left[\sum_{i=1}^{L}\frac{\theta^*}{2}\left(\log\left(1+\frac{B_1 p}{\theta^*}-\epsilon_1\right)+\log\left(1+\frac{B_2 p(1-p)^{i-1}}{\theta^*}-\epsilon_2\right)\right)\right]$$
$$-\frac{1}{2}\log(\epsilon_1)-0.72 \quad (4.99)$$
$$= \frac{\theta^*}{2}\log\left(1+\frac{B_1 p}{\theta^*}-\epsilon_1\right)-\frac{1}{2}\log(\epsilon_1)-0.72$$
$$+\frac{1}{\mathbb{E}[L]}\mathbb{E}\left[\sum_{i=1}^{L}\frac{\theta^*}{2}\log\left((1-p)^{i-1}\left(\frac{1-\epsilon_2}{(1-p)^{i-1}}+\frac{B_2 p}{\theta^*}\right)\right)\right] \quad (4.100)$$
$$\geq \frac{\theta^*}{2}\log\left(1+\frac{B_1 p}{\theta^*}-\epsilon_1\right)-\frac{1}{2}\log(\epsilon_1)-0.72$$
$$+\frac{1}{\mathbb{E}[L]}\mathbb{E}\left[\sum_{i=1}^{L}\frac{\theta^*}{2}\log\left((1-p)^{i-1}\left(1-\epsilon_2+\frac{B_2 p}{\theta^*}\right)\right)\right] \quad (4.101)$$
$$\geq \frac{\theta^*}{2}\log\left(1+\frac{B_1 p}{\theta^*}-\epsilon_1\right)-\frac{1}{2}\log(\epsilon_1)-1.44+\frac{\theta^*}{2}\log\left(1+\frac{B_2 p}{\theta^*}-\epsilon_2\right) \quad (4.102)$$

where (4.94) follows as the maximum $\frac{B_1 p(1-p)^{i-1}}{\theta_i}-\epsilon_1$ is non-negative, and $\epsilon_1 > 1$, (4.96) follows since for any three positive functions $a(x), b(x), c(x)$ we have: $\max_x[a(x)-b(x)-c(x)] \geq \max_x a(x) - \max_x b(x) - \max_x c(x)$, (4.97) follows by bounding the last term numerically by 0.72, (4.98) follows since we added $1-\epsilon_1$ which is negative, (4.102) follows again by numerically bounding $\frac{1}{\mathbb{E}[L]}\mathbb{E}\left[\sum_{i=1}^{L}\frac{1}{2}\log\left(\frac{1}{(1-p)^{i-1}}\right)\right]$

by 0.72. The θ^* used here is a shorthand for $\theta^*(B_1 p, B_2 p)$.

CHAPTER 5

Single-User Channel with Data and Energy Arrivals: Online Policies

5.1 Introduction

We consider an energy harvesting single-user system where the transmitter receives energy and data packets randomly and intermittently over time, and stores them in finite-sized queues, see Fig. 5.1. We study the *online* power scheduling problem for this system, where both energy and data arrivals are known only causally at the transmitter. We focus on the case when the energy and data arrivals are fully-correlated. We characterize the optimal policy in the special case of Bernoulli arrivals. We then propose a structured policy for general arrivals. The proposed policy takes into account the available energy and data at each instant. We show that the performance of this policy is near-optimal for general arrivals.

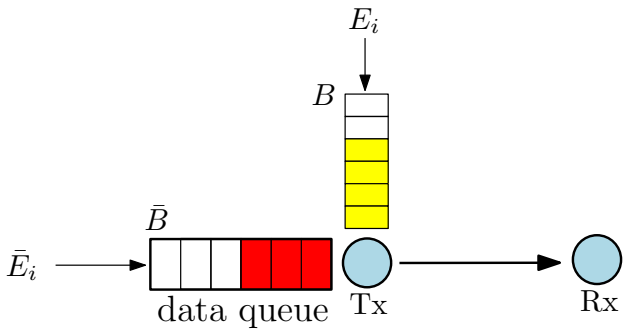

Figure 5.1: An energy harvesting single-user transmitter with finite-sized energy and data buffers.

5.2 System Model

The physical layer is a Gaussian single-user channel with noise variance at the receiver equal to unity. The capacity of this channel in slot i is,

$$r_i = \frac{1}{2}\log\left(1 + P_i\right) \tag{5.1}$$

where P_i is the transmit power in slot i. The transmitter is equipped with finite-sized data and energy buffers, with sizes $\bar{B}$ and B, respectively. The battery state b_i evolves as,

$$b_{i+1} = \min\left\{B, b_i - P_i + E_{i+1}\right\} \tag{5.2}$$

The data queue state, denoted as $\bar{b}_i$, evolves as,

$$\bar{b}_{i+1} = \min\left\{\bar{B}, \bar{b}_i - \frac{1}{2}\log\left(1 + P_i\right) + \bar{E}_{i+1}\right\} \tag{5.3}$$

The transmit power, P_i, is constrained by,

$$P_i \leq \min\left\{b_i, 2^{2\bar{b}_i} - 1\right\} \tag{5.4}$$

This constraint ensures that the transmission power does not exceed the energy available in the battery and does not attempt to send more data than remaining in the queue.

The objective then is to maximize the long term-average throughput subject to data and energy constraints,

$$\Phi = \lim_{n\to\infty} \max_{P^n \in \mathcal{F}^n} \mathbb{E}\left[\frac{1}{n}\sum_{i=1}^{n} \frac{1}{2}\log(1+P_i)\right] \tag{5.5}$$

where $\mathcal{F}^n$ is the set of all feasible online policies for n time slots. The aim now is to characterize the optimal power allocation. Under the existence of the optimal Markov policy, the optimal power allocation will be function of the current energy and battery states. We fully characterize the powers in the case of Bernoulli arrivals. For general arrivals, we propose a structured policy and we determine the cases in which it is optimal or near optimal.

5.3 Optimal Strategy: Bernoulli Arrivals

In this section, we characterize the optimal policy for Bernoulli arrivals. We consider the case when data and energy arrivals are fully-correlated; whenever the energy queue is filled, the data queue is filled also and there is no intermediate values for

the energy or data arrivals. In other words, we have $E_i = \alpha \bar{E}_i$, and $\mathbb{P}[E_i = \alpha \bar{E}_i = B] = 1 - \mathbb{P}[E_i = \alpha \bar{E}_i = 0] = p$. From [88, Theorem 3.6.1], and similar to [49,98,99], we characterize the optimal powers by solving a modified offline problem with a single arrival. For the case of data and energy arrivals, we obtain the optimal powers by solving,

$$\begin{aligned} \max_{\{P_i\}} \quad & \sum_{i=1}^{\infty} p(1-p)^{i-1} \frac{1}{2} \log\left(1 + P_i\right) \\ \text{s.t.} \quad & \sum_{i=1}^{\infty} P_i \leq B, \quad \sum_{i=1}^{\infty} \frac{1}{2} \log(1 + P_i) \leq \bar{B} \end{aligned} \tag{5.6}$$

This is a non-convex problem due to the last constraint which is a non-convex constraint. We transform this problem to an equivalent convex problem by expressing the problem in terms of rates, i.e., we apply the transformation $r_i = \frac{1}{2} \log\left(1 + P_i\right)$. The equivalent problem is,

$$\begin{aligned} \max_{\{r_i\}} \quad & \sum_{i=1}^{\infty} p(1-p)^{i-1} r_i \\ \text{s.t.} \quad & \sum_{i=1}^{\infty} 2^{2r_i} - 1 \leq B, \quad \sum_{i=1}^{\infty} r_i \leq \bar{B} \end{aligned} \tag{5.7}$$

This is a convex optimization problem in r_i which we can solve using the KKTs which are necessary and sufficient. The Lagrangian of this problem is,

$$\mathcal{L} = -\sum_{i=1}^{\infty} p(1-p)^{i-1} r_i + \lambda \left(\sum_{i=1}^{\infty} 2^{2r_i} - 1 - B \right) + \mu \left(\sum_{i=1}^{\infty} r_i - \bar{B} \right) \tag{5.8}$$

We differentiate with respect to r_i and equate to zero to get,

$$r_i = \frac{1}{2}\log\left(\frac{p(1-p)^{i-1}}{\lambda} - \frac{\mu}{\lambda}\right), \quad i = 1, \ldots, \tilde{N} \tag{5.9}$$

It is clear that the transmit power decreases in time. The rates should be non-negative. Thus, we need $\frac{p(1-p)^{i-1}}{\lambda} - \frac{\mu}{\lambda} \geq 1$ to be satisfied for $i = 1, \ldots, \tilde{N}$. Hence, it suffices just to ensure that it is satisfied in the last slot, i.e.,

$$p(1-p)^{\tilde{N}-1} \geq \lambda + \mu \tag{5.10}$$

We can then identify the optimal λ, μ and $\tilde{N}$ by solving (5.10) along with the total energy and data constraints. This can be done using simple one-dimensional line search.

5.4 Near-Optimal Strategy: General Arrivals

In this section, we propose a structured online policy as in [49], [98–100, 104, 105]. We first note that the optimal power allocation in (5.9) follows a fractional policy. The power allocation is controlled by the available data through the Lagrange multiplier μ. Hence, we propose the following fractional policy which is bounded by the available data in the queue,

$$P_i = \min\left\{pb_i, 2^{\bar{2b}_i} - 1\right\} \tag{5.11}$$

The policy mimics the optimal policy in (5.9) in that it is fractional when the amount of fractional power is less than the amount needed to transmit the remaining data, or else it is limited by the remaining data. To describe the policy for the Bernoulli energy arrivals, we first define i^* as follows,

$$i^* = \max\left\{i : Bp(1-p)^{i-1} \leq 2^{2\left[\bar{B}-\sum_{k=1}^{i-1}\frac{1}{2}\log\left(1+Bp(1-p)^{k-1}\right)\right]} - 1\right\} \tag{5.12}$$

This represents the last index at which the policy transmits with a fractional decreasing power. In slot i^*+1, if no new arrival occurs, the transmitter transmits all the remaining data in its buffer. Hence, the allocated power is as follows,

$$P_i = Bp(1-p)^{i-1}, \qquad i = 1, \ldots, i^* \tag{5.13}$$

$$P_i = 2^{2\left[\bar{B}-\sum_{k=1}^{i-1}\frac{1}{2}\log(1+Bp(1-p)^{k-1})\right]} - 1, \qquad i = i^*+1 \tag{5.14}$$

$$P_i = 0, \qquad i > i^*+1 \tag{5.15}$$

Note that i^* is a deterministic number which depends only on the system parameters $B, \bar{B}, p$. We define the following random variable, which will be useful later in the analysis,

$$K = \min\{L, i^*\} \tag{5.16}$$

where L is the time between the Bernoulli arrivals, which is geometrically distributed with parameter p.

In what follows, we begin by deriving a universal upper bound for all online policies with general arrivals. We then study the performance of the policy proposed in (5.11) under Bernoulli energy arrivals. We first derive a multiplicative lower bound. Then, we study the case when this policy is optimal and the case when it is within a constant additive gap. We then show that the performance of the proposed policy is the worst under Bernoulli arrivals with the same arrival rate, hence, all the lower bounds derived for Bernoulli arrivals are also valid for general arrivals.

5.4.1 Upper Bound

In the following lemma, we present a universal upper bound which depends only on the average arrival rates.

Lemma 5.1 *For an average energy arrival rate of μ_e and an average data arrival rate of μ_d, the throughput of any online policy is upper bounded as,*

$$r_{on} \leq \min \left\{ \frac{1}{2} \log \left(1 + \mu_e\right), \mu_d \right\} \tag{5.17}$$

The proof of Lemma 5.1 follows from the single-user offline upper bound with no data arrival constraints [49] in addition to the data arrival constraint: the transmitter cannot transmit more data on average than the average data arrival. Hence, the upper bound on the rate is the minimum of these two upper bounds.

5.4.2 Multiplicative Gap

We now analyze the performance of the proposed policy. We first derive a multiplicative gap for Bernoulli arrivals.

Lemma 5.2 *The performance of the fractional policy is lower bounded by,*

$$r_{on} \geq \max\{p, c\} \min\left\{\frac{1}{2}\log\left(1+pB\right), \bar{B}p\right\} \tag{5.18}$$

where c is defined as,

$$c = \frac{1+\max\left\{2^{2\left[\bar{B}-\sum_{k=1}^{\infty}\frac{1}{2}\log(1+Bp(1-p)^{k-1})\right]}-1,0\right\}}{2-p} - \frac{\max\left\{2^{2\left[\bar{B}-\frac{1}{2}\log(1+Bp)\right]}-1,0\right\}}{Bp} \tag{5.19}$$

Proof: We derive two lower bounds and then take the maximum of both. For the case when $i^*=0$, we show later that the policy is optimal. Hence, the multiplicative lower bound is still valid. Thus, we now consider, without loss of generality, the case when $i^* \geq 1$. We first begin with the one with p multiplicative gap in (5.18). For this case, we have,

$$\begin{aligned} r_{on} =& \sum_{i=1}^{i^*} \frac{1}{2}p(1-p)^{i-1}\log\left(1+Bp(1-p)^{i-1}\right) \\ &+ p(1-p)^{i^*}\left[\bar{B}-\sum_{k=1}^{i^*}\frac{1}{2}\log\left(1+Bp(1-p)^{k-1}\right)\right] \qquad (5.20) \\ \geq& \sum_{i=1}^{i^*} \frac{1}{2}p(1-p)^{i-1}\log\left(1+Bp(1-p)^{i-1}\right) \qquad (5.21) \end{aligned}$$

$$\geq \sum_{i=1}^{i^*} \frac{1}{2} p(1-p)^{2(i-1)} \log\left(1+Bp\right) \tag{5.22}$$

$$= \left(\frac{1-(1-p)^{2i^*}}{2-p}\right) \frac{1}{2} \log\left(1+Bp\right) \tag{5.23}$$

$$\geq \left(\frac{1-(1-p)^{2}}{2-p}\right) \frac{1}{2} \log\left(1+Bp\right) \tag{5.24}$$

$$= p\frac{1}{2} \log\left(1+Bp\right) \tag{5.25}$$

$$\geq p \min\left\{\frac{1}{2} \log\left(1+Bp\right), \bar{B}p\right\} \tag{5.26}$$

where (5.21) follows from the positivity of $\bar{B} - \sum_{k=1}^{i^*} \frac{1}{2} \log\left(1+Bp(1-p)^{k-1}\right)$, (5.22) follows from the monotonicity of the logarithm, and (5.24) follows by setting $i^* = 1$. This proves the first lower bound.

We then derive the other lower bound with c multiplicative gap in (5.18). We first derive an upper bound on $(1-p)^{i^*}$,

$$Bp(1-p)^{i^*} \leq Bp(1-p)^{i^*-1} \tag{5.27}$$

$$\leq 2^{2\left[\bar{B} - \sum_{k=1}^{i^*-1} \frac{1}{2} \log(1+Bp(1-p)^{k-1})\right]} - 1 \tag{5.28}$$

$$\leq 2^{2\left[\bar{B} - \frac{1}{2} \log(1+Bp)\right]} - 1 \tag{5.29}$$

where (5.27) follows from monotonicity, (5.28) follows from the definition of i^*, and (5.29) follows by considering only the first term in the summation. Hence, we have,

$$(1-p)^{i^*} \leq \frac{2^{2\left[\bar{B} - \frac{1}{2} \log(1+Bp)\right]} - 1}{Bp} \tag{5.30}$$

We also derive a lower bound on $(1-p)^{i^*}$,

$$Bp(1-p)^{i^*} > 2^{2\left[\bar{B}-\sum_{k=1}^{i^*}\frac{1}{2}\log(1+Bp(1-p)^{k-1})\right]}-1 \tag{5.31}$$

$$> 2^{2\left[\bar{B}-\sum_{k=1}^{\infty}\frac{1}{2}\log(1+Bp(1-p)^{k-1})\right]}-1 \tag{5.32}$$

Hence, we have,

$$(1-p)^{i^*} > \frac{2^{2\left[\bar{B}-\sum_{k=1}^{\infty}\frac{1}{2}\log(1+Bp(1-p)^{k-1})\right]}-1}{Bp} \tag{5.33}$$

We now derive the c multiplicative lower bound in (5.18),

$$\begin{aligned}
r_{on} =& \sum_{i=1}^{i^*}\frac{1}{2}p(1-p)^{i-1}\log\left(1+Bp(1-p)^{i-1}\right) \\
&+ p(1-p)^{i^*}\left[\bar{B}-\sum_{k=1}^{i^*}\frac{1}{2}\log\left(1+Bp(1-p)^{k-1}\right)\right] && (5.34)\\
=& \sum_{i=1}^{i^*}\frac{1}{2}\left(p(1-p)^{i-1}-p(1-p)^{i^*}\right)\log\left(1+Bp(1-p)^{i-1}\right)+p(1-p)^{i^*}\bar{B} && (5.35)\\
\geq& \sum_{i=1}^{i^*}\frac{1}{2}\left(p(1-p)^{i-1}-p(1-p)^{i^*}\right)(1-p)^{i-1}\log\left(1+Bp\right)+p(1-p)^{i^*}\bar{B} && (5.36)\\
=& \sum_{i=1}^{i^*}\frac{1}{2}\left(p(1-p)^{2(i-1)}-p(1-p)^{i^*+i-1}\right)\log\left(1+Bp\right)+p(1-p)^{i^*}\bar{B} && (5.37)\\
=& w\left(1-(1-p)^{i^*}\right)\frac{1}{2}\log\left(1+Bp\right)+p(1-p)^{i^*}\bar{B} && (5.38)
\end{aligned}$$

where w is defined as follows:

$$w \triangleq \sum_{i=1}^{i^*}\frac{\left(p(1-p)^{2(i-1)}-p(1-p)^{i^*+i-1}\right)}{\left(1-(1-p)^{i^*}\right)} \tag{5.39}$$

$$= \frac{\frac{1-(1-p)^{2i^*}}{2-p} - (1-p)^{i^*}\left(1-(1-p)^{i^*}\right)}{(1-(1-p)^{i^*})} \tag{5.40}$$

$$= \frac{1+(1-p)^{i^*}}{2-p} - (1-p)^{i^*} \tag{5.41}$$

It is clear that $0 \leq w \leq 1$. Hence, continuing from (5.38),

$$r_{on} \geq w\left(1-(1-p)^{i^*}\right)\frac{1}{2}\log\left(1+Bp\right) + wp(1-p)^{i^*}\bar{B} \tag{5.42}$$

$$\geq w \min\left\{\frac{1}{2}\log\left(1+Bp\right), \bar{B}p\right\} \tag{5.43}$$

where (5.43) follows since for any x, y and $\theta \in [0,1]$,

$$\theta x + (1-\theta)y \geq \min\{x, y\} \tag{5.44}$$

It now remains to lower bound w which follows directly from (5.30) and (5.33). ■

5.4.3 Optimal Case: Energy Dominant Case

We study here the case when the proposed policy is optimal, which we state in the following lemma.

Lemma 5.3 *The policy proposed in (5.11) is optimal when*

$$Bp \geq 2^{2\bar{B}} - 1 \tag{5.45}$$

Proof: When we have $Bp \geq 2^{2\bar{B}} - 1$, then

$$P_1 = 2^{2\bar{B}} - 1, \;\; P_i = 0 \;\; \forall i > 1 \tag{5.46}$$

Then evaluating the achievable rate explicitly gives,

$$r_{on} = p\bar{B} \geq \min \left\{ \frac{1}{2} \log \left(1 + pB\right), p\bar{B} \right\} \tag{5.47}$$

which is exactly equal to the upper bound. Hence, the gap is equal to zero in this case and this policy is optimal. ■

We call this the energy dominant case because the average energy arrival rate, Bp, is larger than the energy needed to transmit a full data buffer, i.e., $Bp \geq 2^{2\bar{B}} - 1$.

5.4.4 Constant Additive Gap: Data Dominant Case

We now study the case when the proposed policy yields performance within a constant additive gap of the optimal.

Lemma 5.4 *When* $\frac{1}{2} \log \left(1 + Bp\right) + \frac{Bp}{2} \leq \bar{B}p$, *the performance of the fractional policy is lower bounded by,*

$$r_{on} \geq \min \left\{ \frac{1}{2} \log \left(1 + pB\right), \bar{B}p \right\} - 0.72 \tag{5.48}$$

Proof: The throughput under the sub-optimal policy,

$$
\begin{aligned}
r_{on} \geq & \frac{1}{\mathbb{E}[L]}\mathbb{E}\left[\sum_{i=1}^{K}\frac{1}{2}\log\left(1+Bp(1-p)^{i-1}\right)\right] \\
& +\mathbb{E}\left[\frac{\mathbb{1}[L>i^*]}{\mathbb{E}[L]}\left[\bar{B}-\sum_{k=1}^{i^*}\frac{1}{2}\log\left(1+Bp(1-p)^{k-1}\right)\right]\right] && (5.49)\\
= & \frac{1}{\mathbb{E}[L]}\mathbb{E}\left[\sum_{i=1}^{K}\frac{1}{2}\log\left(1+Bp(1-p)^{i-1}\right)\right] \\
& +\frac{\mathbb{P}[L>i^*]}{\mathbb{E}[L]}\left[\bar{B}-\sum_{k=1}^{i^*}\frac{1}{2}\log\left(1+Bp(1-p)^{k-1}\right)\right] && (5.50)\\
\geq & \frac{\mathbb{E}[K]}{\mathbb{E}[L]}\frac{1}{2}\log\left(1+Bp\right)-0.72 \\
& +\frac{\mathbb{P}[L>i^*]}{\mathbb{E}[L]}\left[\bar{B}-\sum_{k=1}^{i^*}\frac{1}{2}\log\left(1+Bp(1-p)^{k-1}\right)\right] && (5.51)\\
= & (1-(1-p)^{i^*})\frac{1}{2}\log\left(1+Bp\right)-0.72 \\
& +p(1-p)^{i^*}\left[\bar{B}-\sum_{k=1}^{i^*}\frac{1}{2}\log\left(1+Bp(1-p)^{k-1}\right)\right] && (5.52)\\
= & (1-(1-p)^{i^*})\frac{1}{2}\log\left(1+Bp\right)-0.72+p(1-p)^{i^*}\bar{B} \\
& -p(1-p)^{i^*}\sum_{k=1}^{i^*}\frac{1}{2}\log\left(1+Bp(1-p)^{k-1}\right) && (5.53)\\
\geq & (1-(1-p)^{i^*})\frac{1}{2}\log\left(1+Bp\right)-0.72+p(1-p)^{i^*}\bar{B} \\
& -p(1-p)^{i^*}\sum_{k=1}^{i^*}\frac{1}{2}Bp(1-p)^{k-1} && (5.54)\\
\geq & (1-(1-p)^{i^*})\frac{1}{2}\log\left(1+Bp\right)-0.72+p(1-p)^{i^*}\bar{B}-p(1-p)^{i^*}\frac{B}{2} && (5.55)\\
= & (1-(1-p)^{i^*})\frac{1}{2}\log\left(1+Bp\right)-0.72+p(1-p)^{i^*}\left(\bar{B}-\frac{B}{2}\right) && (5.56)\\
\geq & \min\left\{\frac{1}{2}\log\left(1+Bp\right), p\left(\bar{B}-\frac{B}{2}\right)\right\}-0.72 && (5.57)\\
= & \frac{1}{2}\log\left(1+Bp\right)-0.72 && (5.58)
\end{aligned}
$$

$$\geq \min\left\{\frac{1}{2}\log\left(1+Bp\right), pB\right\} - 0.72 \tag{5.59}$$

where (5.52) follows as in the proof of [98, Lemma 3] and (5.58) follows if $\frac{1}{2}\log\left(1+Bp\right) \leq p\left(\bar{B}-\frac{B}{2}\right)$. ■

We call this the data dominant case because the average data arrival rate, $\bar{B}p$, is larger than the amount of data that can be transmitted by the average energy arrival in addition to half the average energy arrival rate, i.e., $\frac{1}{2}\log\left(1+Bp\right)+\frac{Bp}{2} \leq \bar{B}p$.

5.4.5 General Energy Arrivals

For the general arrival case we have the following lemma.

Lemma 5.5 *The performance of the proposed policy under Bernoulli arrivals forms a lower bound on the performance of the proposed policy under general fully-correlated arrival distributions with the same arrival mean.*

Since the minimum of concave functions is concave, the objective function with (5.11) is concave and the proof of Lemma 5.5 follows similar to [49].

From Lemma 5.5, we conclude that all the derived bounds for the fully-correlated Bernoulli arrivals are also valid for the fully-correlated general arrivals with the same arrival rates. Hence, the policy is optimal when the energy is more dominant, in particular, when $Bp \geq 2^{2\bar{B}}-1$, and is within a constant 0.72 gap when the data is more dominant, in particular, when $\frac{1}{2}\log\left(1+Bp\right)+\frac{Bp}{2} \leq \bar{B}p$.

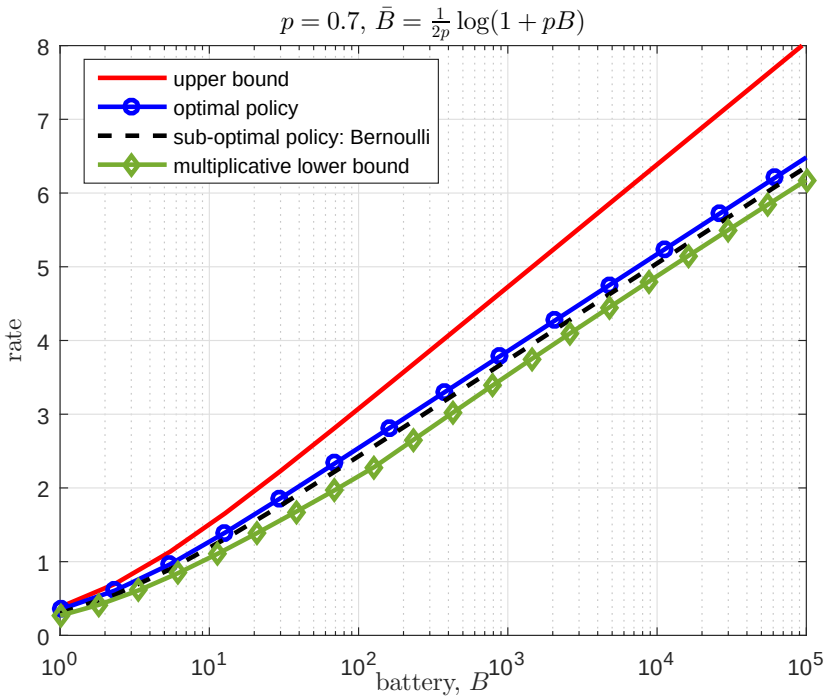

Figure 5.2: Illustration of upper bound, optimal policy and the sub-optimal policy. Bernoulli arrivals.

5.5 Numerical Examples

In this section, we illustrate our results using simple numerical examples. We first show the case when $\bar{B} = \frac{1}{2p}\log(1+Bp)$ in Fig. 5.2. In this case, we show that the proposed policy performs close to the optimal policy. In addition, the multiplicative lower bound closely lower bounds the performance of the proposed policy. We then show in Fig. 5.3 that when $\bar{B} = \frac{1}{2}\log(1+Bp)$, the optimal policy and the proposed policies for uniform arrivals are the same.

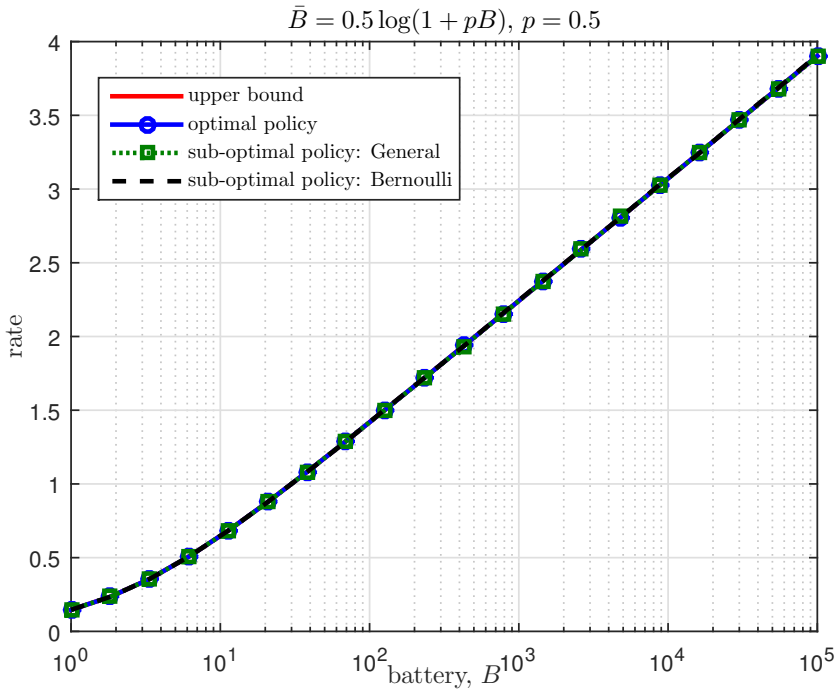

Figure 5.3: Illustration of upper bound, optimal policy and the sub-optimal policy. General arrivals: uniform.

5.6 Conclusion

In this chapter, we considered a single-user energy harvesting setting in which the transmitter gets data and energy arrivals throughout the course of communication. The transmitter knows the data and the energy arrivals only causally, i.e., after they arrive. We restricted our attention to the case of fully-correlated data and energy arrivals which may occur in practice as in the case of simultaneous data and energy transfer. We proposed a structured near-optimal policy which adapts to the available data and energy in the buffers. We showed that this policy is within a multiplicative gap to the optimal. We further showed that this policy is optimal when the average energy arrival is higher than the energy required to send a full data buffer and it is within a constant additive gap to the optimal when the average

data arrivals is higher than a threshold.

CHAPTER 6

Coded Status Updates in an Energy Harvesting Erasure Channel

6.1 Introduction

We consider an energy harvesting single-user system, where the communication channel between the transmitter and the receiver is an erasure channel. The transmitter collects measurements of a certain phenomenon and sends updates on this phenomenon to the receiver; these updates are referred to as *status updates*. The purpose of sending status updates is to minimize the age of information (AoI) at the receiver. We consider two different types of channel codes to encode the status updates. First, we consider maximum distance separable (MDS) codes. With MDS coding, the transmitter encodes the k status update symbols into n symbols. The receiver receives the update successfully if it receives any k of these n encoded symbols. Next, we consider rateless codes, for example, fountain codes. In this case, the transmitter encodes the k update symbols into as many symbols as needed until k of these symbols are received successfully. For each of these models, we consider two different policies: best-effort and save-and-transmit.

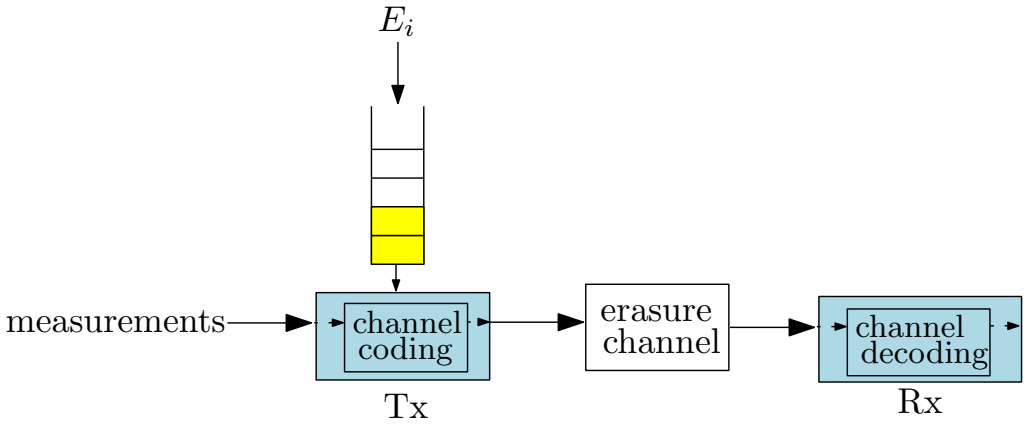

Figure 6.1: An energy harvesting transmitter with an infinite battery. The transmitter collects measurements and sends updates to the receiver over an erasure channel.

6.2 System Model

We consider a single-user channel with a transmitter which has an infinite-sized battery, see Fig. 6.1. The energy arrivals are Bernoulli and i.i.d.: in slot i, a unit energy arrives with probability p or no energy arrives with probability $1-p$, i.e., $\mathbb{P}[E_i = 1] = 1 - \mathbb{P}[E_i = 0] = p$. The transmitter obtains the measurements (status updates), which are packets of length k, which should be sent to the receiver in a way to minimize the average AoI at the receiver.

The total AoI up to time T is,

$$\Delta_T = \int_0^T (t - u(t))\, dt \tag{6.1}$$

where $u(t)$ is the time stamp of the latest received status update packet and $\Delta(t) = t - u(t)$ is the instantaneous AoI.

An example evolution of the AoI is shown in Fig. 6.2. The average long-term

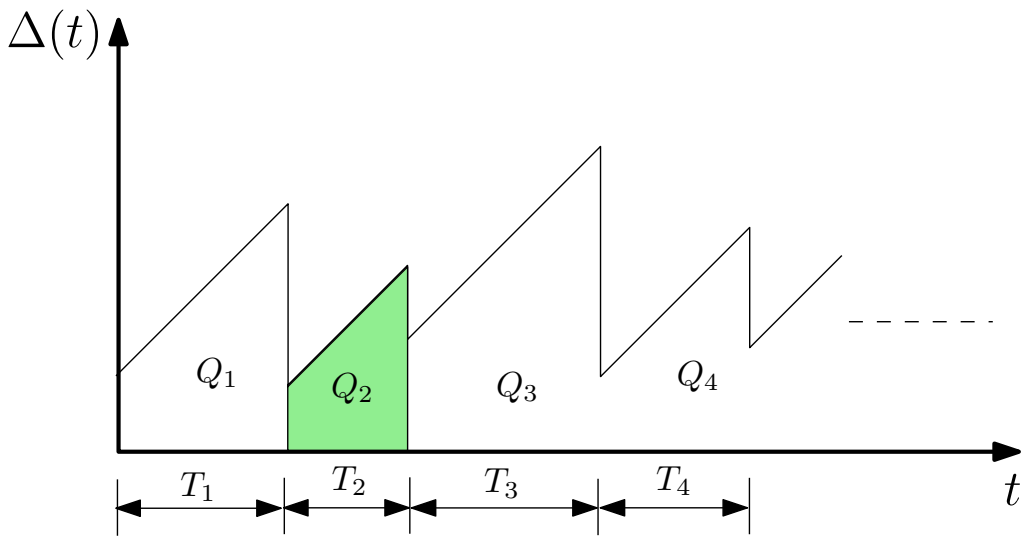

Figure 6.2: An example for the evolution of the age of information.

AoI in this case is calculated as,

$$\Delta = \lim_{T\to\infty} \frac{\Delta_T}{T} = \lim_{i\to\infty} \frac{\sum_{j=1}^{i} Q_j}{\sum_{j=1}^{i} T_j} \tag{6.2}$$

In all the subsequent analysis we will assume renewal policies, i.e., where Q_j and T_j are i.i.d. The AoI then reduces to,

$$\Delta = \lim_{i\to\infty} \frac{\frac{1}{i}\sum_{j=1}^{i} Q_j}{\frac{1}{i}\sum_{j=1}^{i} T_j} = \frac{\mathbb{E}[Q]}{\mathbb{E}[T]} \tag{6.3}$$

where we dropped the subscript j as Q_j and T_j are i.i.d.

The channel between the transmitter and the receiver is an i.i.d. erasure channel. The probability of symbol erasure (loss) in each slot is δ. In order to combat the channel erasures and the energy outages, the transmitter encodes the status updates before sending them through the channel.

We consider two types of channel codes: MDS and rateless codes. We first

consider MDS channel codes. For this case we have an (n, k) channel coding scheme, where k is the length of an uncoded status update and n is the length of an encoded codeword which is sent through the channel with $n \geq k$. When the transmitter is done with sending the n symbols, it generates a new update and begins sending it. This is irrespective of the success of the transmission of these n symbols. The optimal value of n depends on k, δ, and p. For MDS channel coding, we study two achievable schemes. We first study a save-and-transmit scheme in which the transmitter saves energy from the incoming energy arrivals until it has at least n units of energy in its battery. This in effect makes sure that errors which can occur during the codeword transmission are only due to the erasures in the channel. To ensure that the synchronization is maintained between the transmitter and the receiver, the transmitter remains in the saving phase for a number of slots which is multiple of n. We then study a best-effort scheme, in which the transmitter attempts transmission in each slot. In this case, the error in each symbol can be either due to an energy outage or a channel erasure or both.

We next study the case of rateless coding in which the transmitter keeps sending the update until k symbols are successfully received. For this case, we also study two schemes: best-effort and save-and-transmit. In the best-effort scheme, once the update is successfully received, the transmitter generates a new update and begins transmitting it immediately. In the save-and-transmit scheme, once the update is successfully received, the transmitter waits some time in order to save some energy in the battery to prevent future energy outages. The transmitter saves for m slots, where the optimal m should be obtained as a function of the system

parameters δ, k, and p.

6.3 AoI Under MDS Channel Coding

6.3.1 Save-and-Transmit Policy

In the save-and-transmit policy, before the transmitter attempts to transmit the coded update, the transmitter remains silent for an integer multiple of n slots until the battery has energy at least equal to n. The duration the transmitter remains silent for the jth time while transmitting the ith update is a random variable denoted by $Z_{ij} \in \{n, 2n, 3n, \ldots\}$ which depends on the energy arrival distribution. The random variable Z_{ij} can be expressed as:

$$Z_{ij} = \left\lceil \frac{W_i}{n} \right\rceil n \tag{6.4}$$

where W_i is the random variable which denotes the number of slots needed to save n units of energy and $\lceil x \rceil$ denotes the smallest integer greater than or equal to x. Since the energy arrivals follow an i.i.d. Bernoulli distribution, W_i will follow a negative binomial distribution as follows:

$$P_{W_i}(w) = \binom{w-1}{n-1} p^n (1-p)^{w-n}, \quad w = n, n+1, \ldots \tag{6.5}$$

The distribution of Z_{ij} can be obtained using (6.5) as follows:

$$P_{Z_{ij}}(z) = \sum_{w=z-n+1}^{z} P_{W_i}(w), \quad z = n, 2n, \ldots \tag{6.6}$$

After the saving phase, the transmission resumes for n slots. After the transmitter is done transmitting the n coded symbols, the transmitter again goes to the saving phase until it recharges its battery to at least n. The transmitter alternates between saving and transmission phases.

The update is successful if at least k symbols are received without being erased; there will be no energy outage due to the saving phase. Hence, the probability of having a success in a n slot of duration is,

$$\epsilon_{k,n}(\delta) = \sum_{x=k}^{n} \binom{x-1}{k-1} (1-\delta)^k \delta^{x-k} \tag{6.7}$$

Thus, in the n consecutive slots the transmission is successful with probability $\epsilon_{k,n}(\delta)$. Now, the update will be successful in the Vth transmission, where V is a geometrically distributed random variable with a the following pmf,

$$P_{V^{(n)}}(v) = \epsilon_{k,n}(\delta)(1-\epsilon_{k,n}(\delta))^{v-1}, \quad v = 1, 2, \ldots \tag{6.8}$$

Hence, we may need to repeat the save-and-transmit phases for V times before we have a successful status update.

We now characterize the random variable which identifies the instant at which the update will be successful within the n consecutive slots. We denote this random

variable by $\tilde{X}_i$ which has a conditional pmf $P_{X_i|X_i\leq n}(x)$ where

$$P_{X_i}(x) = \binom{x-1}{k-1}(1-\delta)^k\delta^{x-k}, \quad x = k, k+1, \ldots \tag{6.9}$$

Hence, $\tilde{X}_i$ is distributed as:

$$P_{\tilde{X}_i}(x) = \frac{\binom{x-1}{k-1}(1-\delta)^k\delta^{x-k}}{\epsilon_{k,n}(\delta)}, \quad x = k, k+1, \ldots, n \tag{6.10}$$

An example which illustrates the AoI evolution is shown in Fig. 6.3. In this figure, the transmitter at first waits $3n$ slots in order to recharge the battery to at least the level n. It then attempts to transmit. The transmission in this case is not successful due to the channel erasures so the transmitter again waits for n slots in order to charge the battery. The transmission then proceeds again in the next slot. The transmission is then successful and the receiver received the update after $\tilde{X}_i$ transmissions, where $k \leq \tilde{X}_i \leq n$.

We now consider a renewal policy which serves as an upper bound for the save-and-transmit policy described above. We assume that at the end of the update period, the transmitter depletes all its battery. Thus, the transmitter renews its state at the end of each successful update and always begins with a depleted battery. In this case, the AoI can be written as:

$$\Delta_{MDS-ST} = \frac{\mathbb{E}[Q_i]}{\mathbb{E}[T_i]} \tag{6.11}$$

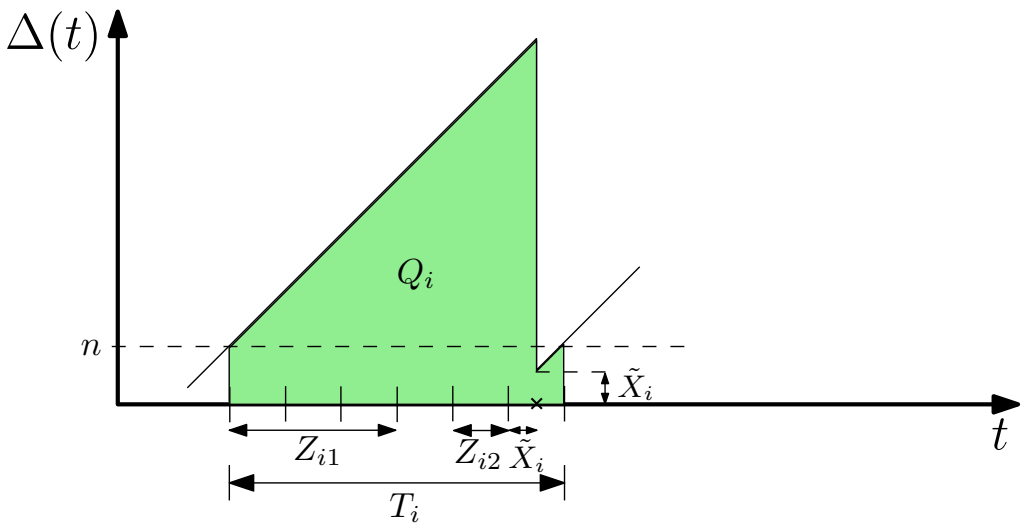

Figure 6.3: An example for the evolution of the age of information under the save-and-transmit scheme for the MDS channel coding case.

Next, we evaluate $\mathbb{E}[Q_i]$ and $\mathbb{E}[T_i]$. We first obtain Q_i as,

$$\begin{aligned} Q_i =& n\left[n\left(V_i-1\right)+\tilde{X}_i+\sum_{j=1}^{V_i} Z_{ij}\right] \\ &+\frac{1}{2}\left[n\left(V_i-1\right)+\tilde{X}_i+\sum_{j=1}^{V_i} Z_{ij}\right]^2+\frac{n^2}{2}-\frac{\tilde{X}_i^2}{2} \qquad (6.12) \\ =& n^2\frac{V_i^2}{2}+nV_i\tilde{X}_i+n\sum_{j=1}^{V_i} Z_{ij} \\ &+\left[n\left(V_i-1\right)+\tilde{X}_i\right]\sum_{j=1}^{V_i} Z_{ij}+\frac{1}{2}\left(\sum_{j=1}^{V_i} Z_{ij}\right)^2 \qquad (6.13) \end{aligned}$$

We then obtain T_i as,

$$T_i = nV_i+\sum_{j=1}^{V_i} Z_{ij} \qquad (6.14)$$

Now, it remains to calculate the expectation of Q_i and T_i. We first calculate

the first and second moments of $\sum_{j=1}^{V_i} Z_{ij}$, using [106, Theorem 6.13], as follows:

$$\mathbb{E}\left[\sum_{j=1}^{V_i} Z_{ij}\right] = \frac{\mathbb{E}[Z]}{\epsilon_{k,n}(\delta)} \tag{6.15}$$

Similarly, we have:

$$\mathbb{E}\left[\left(\sum_{j=1}^{V_i} Z_{ij}\right)^2\right] = \frac{\mathbb{E}[Z^2]}{\epsilon_{k,n}(\delta)} + \frac{2-2\epsilon_{k,n}(\delta)}{\epsilon_{k,n}^2(\delta)}\mathbb{E}[Z]^2 \tag{6.16}$$

We then combine all these to obtain:

$$\mathbb{E}[T_i] = \frac{n}{\epsilon_{k,n}(\delta)} + \frac{\mathbb{E}[Z]}{\epsilon_{k,n}(\delta)} \tag{6.17}$$

and

$$\begin{aligned}\mathbb{E}[Q_i] =& \frac{n^2(2-\epsilon_{k,n}(\delta))}{2\epsilon_{k,n}^2(\delta)} + \frac{n\mu_{\tilde{X}}}{\epsilon_{k,n}(\delta)} + \frac{n(2-\epsilon_{k,n}(\delta))\mathbb{E}[Z]}{\epsilon_{k,n}^2(\delta)} \\ &+ \frac{\mu_{\tilde{X}}\mathbb{E}[Z]}{\epsilon_{k,n}(\delta)} + \frac{1}{2}\frac{\mathbb{E}[Z^2]}{\epsilon_{k,n}(\delta)} + \frac{(1-\epsilon_{k,n}(\delta))\mathbb{E}[Z]^2}{\epsilon_{k,n}^2(\delta)}\end{aligned} \tag{6.18}$$

where $\mathbb{E}[Z]$ and $\mathbb{E}[Z^2]$ can be calculated using (6.6) and $\mu_{\tilde{X}}$ can be calculated using (6.10). Hence, the average AoI Δ_{MDS-ST} in (6.11) can be found by substituting with the expressions in (6.17) and (6.18).

6.3.2 Best-Effort Policy

We now consider the case when the transmitter does not wait at the beginning in order to save energy, instead it begins transmission immediately. The error events in

this case can be either an erasure in the communication channel or an energy outage at the transmitter. These two events may occur for each transmitted symbol. Hence, for the symbol to be received without an error, there should be no energy outage and no channel erasure; this forms a Bernoulli random variable with probability of success equal to $q \triangleq p(1-\delta)$. The evolution of AoI is similar to Fig. 6.3 but in this case, Z_{ij} is equal to zero as the transmitter does not wait to save energy.

Using analysis similar to the previous scheme, but with having the probability of success equal to q, the average AoI in this case can be written as:

$$\Delta_{MDS-BE} = \frac{n}{\epsilon_n} - \frac{n}{2} + \frac{k\epsilon_{k+1,n+1}(q)}{q\epsilon_{k,n}(q)} \tag{6.19}$$

This can also be obtained using the same analysis as in [60], but with probability of success equal to q,

6.4 AoI Under Rateless Channel Coding

6.4.1 Best-Effort Policy

We consider here the case when the transmitter begins to transmit immediately. In each slot, the transmitter suffers two possible error events. The first is channel erasure and the second is energy outage. Hence, a symbol will be received successfully if neither error occurs, which happens with probability equal to q. The channel is now equivalent to an erasure channel, similar to the one considered in [60], but with probability of success equal to q. Following analysis similar to the one in [60], but

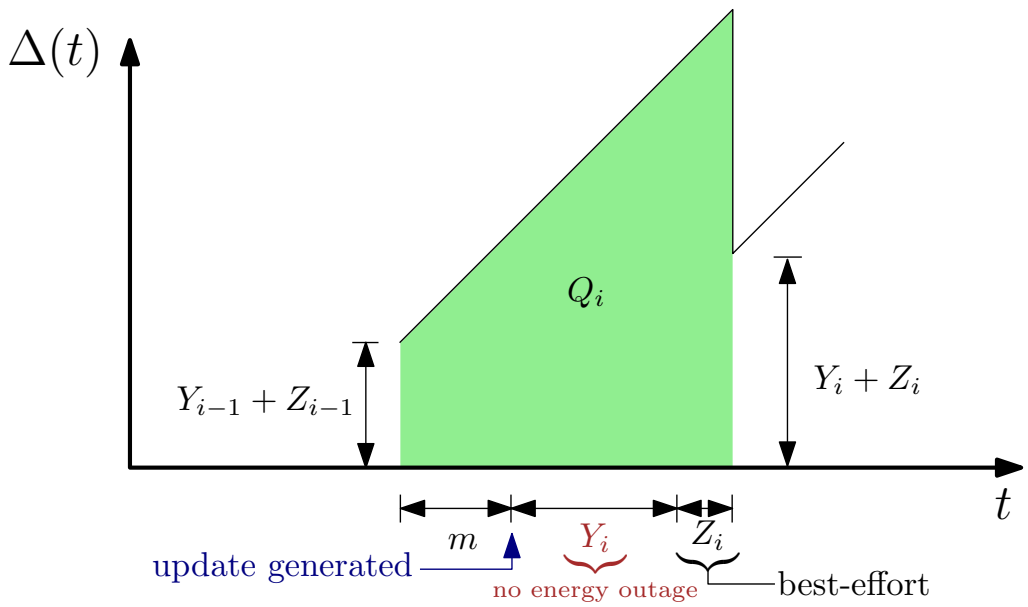

Figure 6.4: An example for the evolution of the age of information under the save-and-transmit scheme for the rateless channel coding case.

with probability of success equal to q, the average AoI in this case is equal to:

$$\Delta_{RC-BE} = \frac{k}{q}\left(\frac{3}{2} + \frac{1-q}{k}\right) \tag{6.20}$$

6.4.2 Save-and-Transmit Policy

In this policy, we consider the case when the transmitter does not generate a new update immediately once the transmission of the previous update is successful, but it waits for a deterministic time of m slots. Here, m is a deterministic number which both the transmitter and the receiver know in advance; this m should then be optimized to minimize the average AoI and will be a function of δ, p and k.

The transmission in this policy proceeds as follows: once the previous update is successful, the transmitter begins a saving phase of duration m slots. Then,

the transmitter generates a new update and begins transmitting it to the receiver. While transmitting the update, the transmitter may receive more energy arrivals; however, the amount of energy in the battery will always be non-increasing as the transmitter transmits a symbol in each slot while the energy may not arrive at every slot. The transmitter keeps transmitting the update until its battery state hits zero; this declares the end of the *no-outage* phase. We denote the number of symbols sent successfully in this phase by k_i. If $k_i \geq k$, then no more transmission is required and the update is successful. Otherwise, the transmitter transmits the remaining $k - k_i$ using the best-effort scheme described in Subsection 6.4.1.

We denote the duration the transmitter transmits with no outage by Y_i and we denote the duration we transmit using the best-effort scheme by Z_i. An example for the evolution of the AoI in this case is shown in Fig. 6.4. The average AoI can be calculate as follows,

$$\Delta_{RC-ST} = \frac{\mathbb{E}[Q_i]}{m + \mathbb{E}[Y_i + Z_i]} \tag{6.21}$$

$$= \frac{\mathbb{E}\left[(m + Y_i + Z_i)^2 + 2\,(m + Y_i + Z_i)\,(Y_{i-1} + Z_{i-1})\right]}{2m + 2\mathbb{E}[Y_i + Z_i]} \tag{6.22}$$

This AoI can be calculated explicitly once $\mathbb{E}[Y_i]$, $\mathbb{E}[Y_i^2]$, $\mathbb{E}[Z_i]$, $\mathbb{E}[Z_i^2]$ and $\mathbb{E}[Y_i Z_i]$ are calculated. We note that Y_i and Z_i are dependent on each other while Y_i and Y_{i-1} are independent due to using a renewal policy.

We now define the random variables $\{E_i\}_{i=1}^{\infty}$; the random variable E_1 represents the amount of energy harvested in the first m slots. For $i \geq 2$, the random variable E_i represents the amount of energy harvested during the previous E_{i-1}

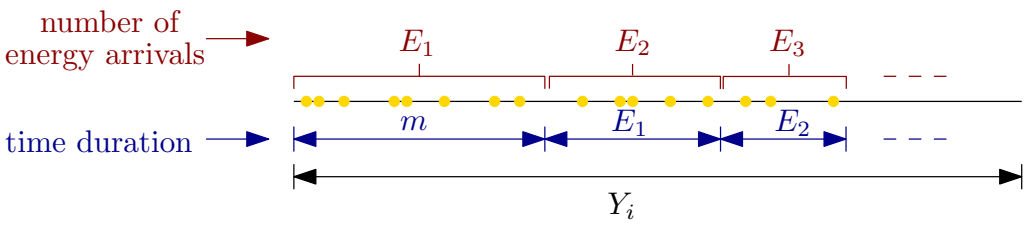

Figure 6.5: An example to illustrate the random variable Y_i.

slots. Hence, we have $E_i \leq E_{i-1}$.

We now characterize the random variable Y_i,

$$Y_i = \sum_{i=1}^{\infty} E_i \tag{6.23}$$

where E_1 is Bin(m, p), and for $i \geq 2$, E_i given $E_{i-1} = e_{i-1}$ is Bin(e_{i-1}, p); Bin(.) denotes binomial distribution. An example for the evolution of Y_i is shown in Fig. 6.5.

We can obtain the marginal pmf for the random variables E_i, $i \geq 2$, by applying [106, Theorem 6.12] and using [106, Table 6.1]. Each E_i consists of a sum of i.i.d. Bernoulli random variables and the number of these random variables is distributed according to a binomial distribution of E_{i-1} which is independent of the Bernoulli random variables. Hence, the marginal pmf of the random variable E_i is Bin(m,p^i).

We can now calculate $\mathbb{E}[Y_i]$ as,

$$\mathbb{E}[Y_i] = \sum_{i=1}^{\infty} \mathbb{E}\left[E_i\right] = \frac{mp}{1-p} \tag{6.24}$$

Next, we want to calculate $\mathbb{E}[Y_i^2]$ which we calculate as $\mathbb{E}[Y_i^2] = \text{var}(Y_i) + \mathbb{E}[Y_i]^2$.

The term $\text{var}(Y_i)$ can be calculated as follows

$$\text{var}(Y_i) = \sum_{i=1}^{\infty} \text{var}(E_i) + 2\sum_{i<j}^{\infty} \text{cov}(E_i, E_j) \tag{6.25}$$

$$= \frac{mp}{1-p^2} + 2\sum_{i<j} \text{cov}(E_i, E_j) \tag{6.26}$$

This requires the calculation of $\text{cov}(E_i, E_j)$, $\forall i > j$. To calculate the covariance, we first calculate the conditional probability $\mathbb{P}(E_{j+1}|E_i)$. For $j > i$, we have that $\mathbb{P}(E_j|E_i)$ is distributed as $\text{Bin}(E_i, p^{j-i})$. This again follows by applying [106, Theorem 6.12] and using [106, Table 6.1].

We now calculate for $j > i$ $\text{cov}(E_j, E_i)$ as follows:

$$\text{cov}(E_j, E_i) = \mathbb{E}[E_j E_i] - \mathbb{E}[E_j]\mathbb{E}[E_i] = mp^j(1-p^i) \tag{6.27}$$

Next, we calculate $\sum_{i<j} \text{cov}(E_i, E_j)$ as follows:

$$\sum_{i<j} \text{cov}(E_i, E_j) = \sum_{i=1}^{\infty}\sum_{j=i+1}^{\infty} mp^j(1-p^i) \tag{6.28}$$

$$= \frac{mp^2}{(1-p)(1-p^2)} \tag{6.29}$$

Therefore, $\text{var}(Y_i)$ is equal to

$$\text{var}(Y_i) = \frac{mp}{1-p^2} + 2\frac{mp^2}{(1-p)(1-p^2)} = \frac{mp(1+p)}{(1-p)(1-p^2)} \tag{6.30}$$

Hence, $\mathbb{E}[Y_i^2]$ can be calculated as follows:

$$\mathbb{E}[Y_i^2] = \frac{mp(1+p)}{(1-p)(1-p^2)} + \frac{m^2p^2}{(1-p)^2} \tag{6.31}$$

Next, we calculate $\mathbb{E}[Z_i]$, $\mathbb{E}[Z_i^2]$ and $\mathbb{E}[Y_iZ_i]$. The pmf of $Z_i|Y_i = k_1$ is negative binomial distribution as in (6.5) but with number of successes equal to $\max(k-k_1, 0)$ and with success probability equal to q. The value of $\mathbb{E}[Z_i|Y_i = y_i]$ can then be calculated using conditional expectation as follows:

$$\mathbb{E}[Z_i|Y_i = y_i] = \sum_{w=0}^{y_i} \binom{y_i}{w} \delta^{y_i-w}(1-\delta)^w \frac{g(w)}{q} \tag{6.32}$$

and the value of $\mathbb{E}[Z_i^2|Y_i = y_i]$ can be calculated as follows

$$\mathbb{E}[Z_i^2|Y_i = y_i] = \sum_{w=0}^{y_i} \binom{y_i}{w} \delta^{y_i-w}(1-\delta)^w \frac{g(w)(g(w)+(1-q))}{q^2} \tag{6.33}$$

where $g(w) \triangleq \max(k-w, 0)$. Similarly, we can obtain $\mathbb{E}[Y_iZ_i|Y_i = y_i]$. Now, it remains to calculate the expectation over the pmf of Y_i. Due to the dependency between the terms E_i and their infinite sum, there is no closed form for the pmf of Y_i and it can be found numerically.

6.5 Numerical Results

In this section, we compare the performances of the proposed schemes. When there is no energy harvesting, i.e., energy arrives with probability $p = 1$ at every slot,

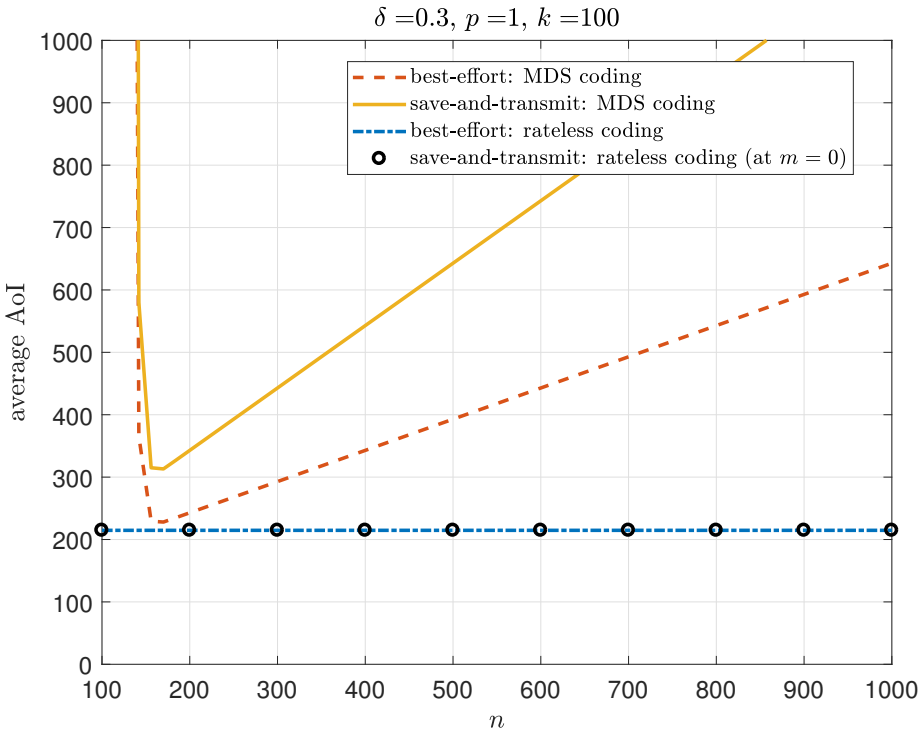

Figure 6.6: Comparison of average AoI, $p = 1$.

rateless coding has the best AoI (this mimics the result obtained in [60]) and save-and-transmit with MDS coding has the worst performance. The reason that the save-and-transmit with MDS coding has the worst performance is that it requires a saving phase of at least n slots, which is not necessary as the energy arrives at all slots. When the probability of energy arrivals decreases to $p = 0.7$, save-and-transmit with MDS coding performs the same as the best-effort rateless coding case, as shown in Fig. 6.7. Rateless coding with save-and-transmit performs slightly better than all the other policies. As the probability of energy arrival decreases further, save-and-transmit with MDS coding outperforms all the best-effort policies as shown in Fig. 6.8 and Fig. 6.9. As shown in Fig. 6.9, the gain becomes significant for low values of p. The reason for this is that save-and-transmit eliminates the errors

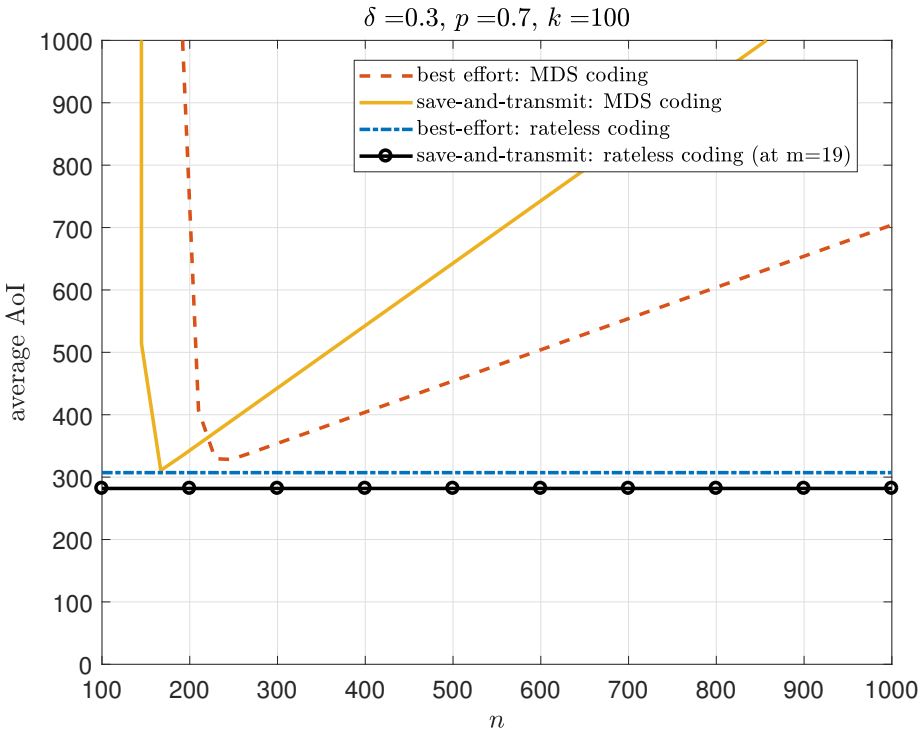

Figure 6.7: Comparison of average AoI, $p = 0.7$.

due to energy outage by saving sufficient energy before attempting to transmit. For example, in Fig. 6.9, for the best-effort scheme, the probability of success in transmitting a symbol is equal to $q = 0.2 \times 0.7 = 0.14$, while if we eliminate the energy outage due to energy harvesting as in save-and-transmit scheme, the success probability for reach symbol will be 0.7, which is much higher than the best-effort scheme. Rateless coding with save-and-transmit is better than MDS coding with save-and-transmit, because rateless coding with save-and-transmit gives more flexibility for the transmitter to choose just the right saving duration, while in MDS coding case, the transmitter is forced to save for a multiple of n slots.

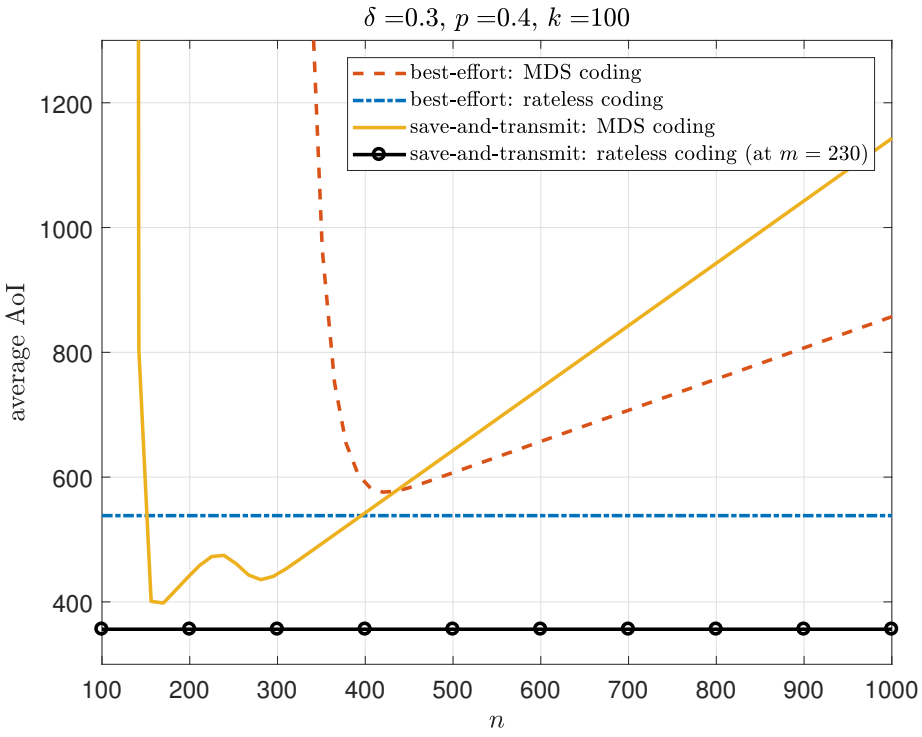

Figure 6.8: Comparison of average AoI, $p = 0.4$.

6.6 Conclusion

In this chapter, we studied a single-user energy harvesting setting in which the transmitter sends status updates to the receiver through an erasure channel. We studied MDS and rateless coding in conjunction with two different policies: best-effort and save-and-transmit. For each of these schemes, we derived the long term average AoI. We showed through numerical results that the rateless coding with save-and-transmit always out performs the others. The reason for this is that rateless coding with save-and-transmit saves energy for just the right duration. For low values of average energy arrival, MDS coding with save-and-transmit performs the worst. The reason for this is that the transmitter saves for some slots which is

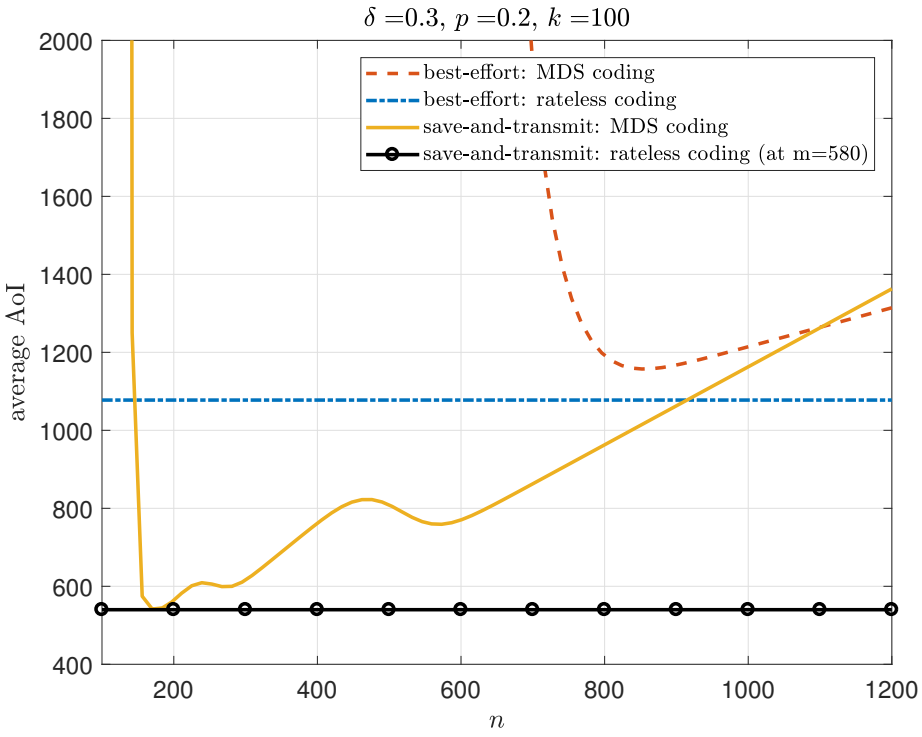

Figure 6.9: Comparison of average AoI, $p = 0.2$.

unnecessary.

CHAPTER 7

Sending Information Through Status Updates

7.1 Introduction

We consider an energy harvesting transmitter sending status updates to a receiver via status update packets; see Fig. 7.1. Each status update packet requires a unit of energy; and the transmitter harvests energy stochastically over time, one unit at a time, at random times.[1] The timings of the status updates also carry a message independent of the status updates. We study the trade-off between the achievable AoI and the achievable message rate.

7.2 System Model

We consider a noiseless binary energy harvesting channel where the transmitter sends status updates and an independent message simultaneously as in Fig. 7.1. The transmitter has a unit size battery, i.e., $B = 1$. Energy arrivals are known causally at the transmitter and are distributed according to an i.i.d. Bernoulli distribution with parameter q, i.e., $\mathbb{P}[E_i = 1] = 1 - \mathbb{P}[E_i = 0] = q$. Hence, the inter-arrival

[1] Energy requirements and energy harvests are normalized.

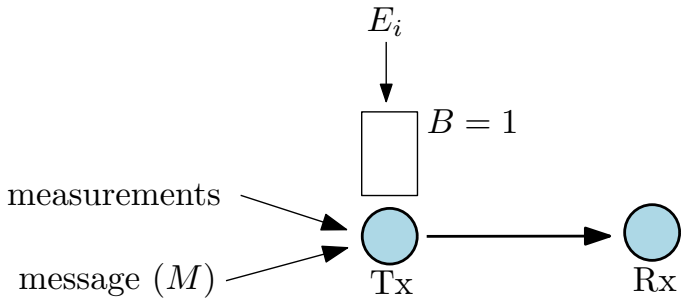

Figure 7.1: An energy harvesting transmitter with a finite-sized battery, that sends status updates and independent information to a receiver.

times between the energy arrivals, denoted as $\tau_i \in \{1, 2, \cdots\}$, are geometric with parameter q. Each transmission costs unit energy; thus, when the transmitter sends an update, its battery is depleted. The timings of the transmitted updates determine the average AoI and the message rate.

The instantaneous AoI is given by

$$\Delta(t) = t - u(t) \tag{7.1}$$

where $u(t)$ is the time stamp of the latest received status update packet and t is the current time. An example evolution of the AoI is shown in Fig. 7.2. The average long-term AoI is

$$\Delta = \limsup_{n\to\infty} \mathbb{E}\left[\frac{\sum_{j=1}^{n} Q_j}{\sum_{j=1}^{n} T_j}\right] \tag{7.2}$$

$$= \limsup_{n\to\infty} \mathbb{E}\left[\frac{\sum_{j=1}^{n} T_j^2}{2\sum_{j=1}^{n} T_j}\right] \tag{7.3}$$

where T_i is the duration between two updates, $Q_j = T_j^2/2$ is the total accumulated age between two updates represented by the area (see Fig. 7.2), and the expectation

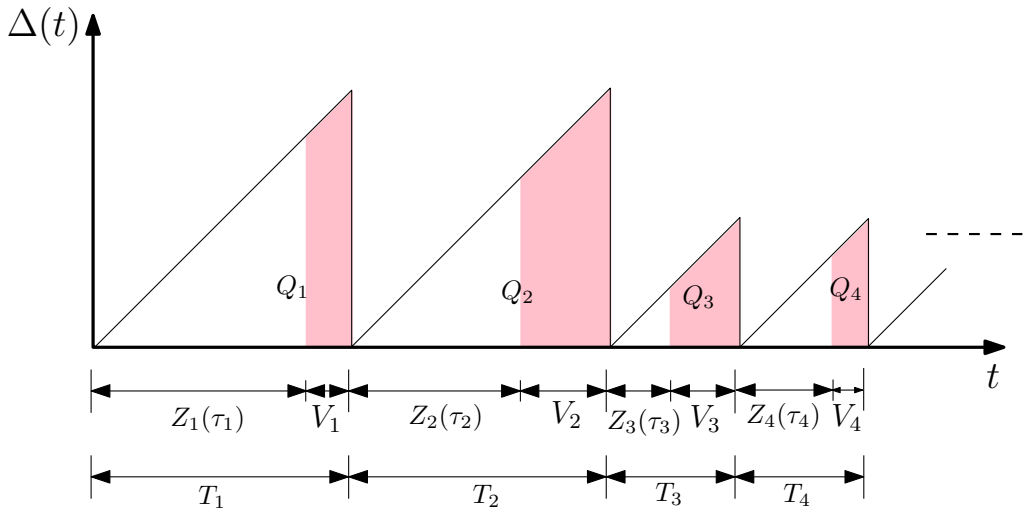

Figure 7.2: An example evolution of instantaneous AoI.

is over the energy arrivals and possible randomness in the transmission decisions. Then, the minimum AoI is given by

$$\Delta^* = \inf_{\pi \in \Pi} \Delta = \inf_{\pi \in \Pi} \limsup_{n \to \infty} \mathbb{E}\left[\frac{\sum_{j=1}^{n} T_j^2}{2\sum_{j=1}^{n} T_j}\right] \tag{7.4}$$

where Π is the set of all feasible policies. Since the transmitter is equipped with a unit-sized battery and due to energy causality [1], we have $T_i \geq \tau_i$. Note that due to the memoryless property of the geometric distribution, we assume without loss of generality, that τ_i is the time from the instant of the previous update and not the time from the instant of the previous energy arrival.

To send information through the timings of the status updates, we consider the model studied in [74, Section V.A]. Thus, here, we assume the knowledge of the energy arrival instants causally at the transmitter and the receiver. The information in the time duration T_i is carried by the random variable $V_i \in \{0, 1, \cdots\}$ where we

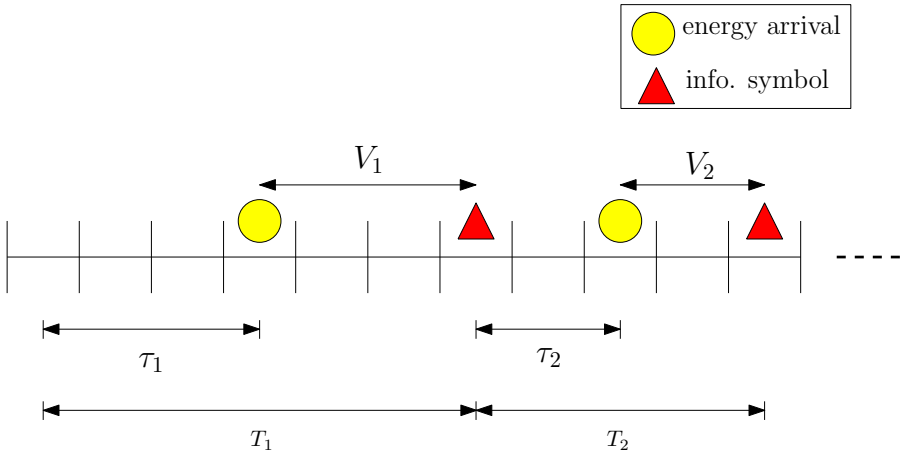

Figure 7.3: Sending information through a timing channel.

have here $T_i = \tau_i + V_i$, see Fig. 7.3. The achievable rate of this timing channel is [74],

$$R = \liminf_{n} \sup_{p(V^n|\tau^n)} \frac{I(T^n; V^n|\tau^n)}{\sum_{i=1}^{n} \mathbb{E}[V_i] + \mathbb{E}[\tau_i]} \tag{7.5}$$

$$= \liminf_{n} \sup_{p(V^n|\tau^n)} \frac{H(V^n|\tau^n)}{\sum_{i=1}^{n} \mathbb{E}[V_i] + \mathbb{E}[\tau_i]} \tag{7.6}$$

where the second equality follows since $H(V^n|\tau^n, T^n) = 0$.

We denote the AoI-rate trade-off region by the tuple $(\text{AoI}(r), r)$, where r is the achievable rate and $\text{AoI}(r)$ is the minimum achievable AoI given that a message rate of at least r is achievable,

$$\text{AoI}(r) = \inf_{\mathcal{M}} \limsup_{n\to\infty} \mathbb{E}\left[\frac{\sum_{j=1}^{n} T_j^2}{2\sum_{j=1}^{n} T_j}\right] \tag{7.7}$$

where $\mathcal{M}$ is defined as

$$\mathcal{M} = \left\{ \{T_i\}_{i=1}^{\infty} \middle| T_i \geq \tau_i, \liminf_{n} \sup_{p(V^n|\tau^n)} \frac{H(V^n|\tau^n)}{\sum_{i=1}^{n} \mathbb{E}[V_i] + \mathbb{E}[\tau_i]} \geq r \right\} \tag{7.8}$$

where V^n denotes $(V_1, \cdots, V_n)$ and similarly for τ^n. An alternate characterization for the trade-off region can also be done using the tuple $(\alpha, R(\alpha))$ where the achievable AoI is equal to α and $R(\alpha)$ is the maximum achievable information rate given that the AoI is no more than α.

7.3 Achievable Trade-off Regions

In this section, we consider several achievable schemes. All considered achievable schemes belong to the class of renewal policies. A renewal policy is a policy in which the action T_i at time i is a function of only the current energy arrival instant τ_i. The long-term average AoI under renewal policies is,

$$\Delta = \limsup_{n\to\infty} \mathbb{E}\left[\frac{\sum_{j=1}^{n} T_j^2}{2\sum_{j=1}^{n} T_j}\right] = \frac{\mathbb{E}[T_i^2]}{2\mathbb{E}[T_i]} \tag{7.9}$$

which results from renewal reward theory [88, Theorem 3.6.1]. Since we use renewal policies and τ_i is i.i.d., hereafter, we drop the subscript i in the random variables. Then, the maximum achievable information rate in (7.6) reduces to,

$$R = \max_{p(v|\tau)} \frac{H(V|\tau)}{\mathbb{E}[V] + \mathbb{E}[\tau]} \tag{7.10}$$

and the AoI in (7.9) reduces to

$$\Delta = \frac{\mathbb{E}[T^2]}{2\mathbb{E}[T]} = \frac{\mathbb{E}[(V+\tau)^2]}{2\mathbb{E}[V+\tau]} \tag{7.11}$$

Next, we present our achievable schemes. In the first scheme, information transmission is adapted to the timing of energy arrivals: If it takes a long time for energy to arrive, the transmitter tends to transmit less information and if energy arrives early, the transmitter tends to transmit more information. This scheme fully adapts to the timings of the energy arrivals, but this comes at the cost of high computational complexity. We then relax the adaptation into just two regions, divided by a threshold c: If energy arrives in less than c slots, we transmit the information using a geometric distribution with parameter p_b, and if energy arrives in more than c slots, we transmit the information using another geometric random variable with parameter p_a. The choice of a geometric random variable for V here and hereafter is motivated by the fact that it maximizes the information rate when the energy arrival timings are known at the receiver; see [74, Section V.A].

In the previous schemes, the instantaneous information rate depends on the timings of energy arrivals. We next relax this assumption and assume that the instantaneous information rate is fixed and independent of timings of energy arrivals. We call such policies *separable* policies. In these policies, the transmitter has two separate decision blocks: The first block is for the status update which takes the decision depending on the timing of the energy arrival, and the second block is for encoding the desired message on top of the timings of these updates. This is similar in spirit to super-position coding. In the first separable policy, the update decision is a threshold based function inspired by [75]: if the energy arrives before a threshold τ_0, the update block decides to update at τ_0 and if the energy arrives after τ_0, the update block decides to update immediately. The information block

does not generate the update immediately, but adds a geometric random variable to carry the information in the timing on top of the timing decided by the update block. In the second separable policy, which we call zero-wait policy, the update block decides to update in the channel use immediately after an energy arrival.

7.3.1 Energy Timing Adaptive Transmission Policy (ETATP)

In this policy, the information which is carried in V is a (random) function of the energy arrival realization τ. This is the most general case under renewal policies. The optimal trade-off can be obtained by solving the following problem

$$\begin{aligned} \min_{p(v|\tau)} \quad & \frac{\mathbb{E}[(V+\tau)^2]}{2\mathbb{E}[V+\tau]} \\ \text{s.t.} \quad & \frac{H(V|\tau)}{\mathbb{E}[V]+\mathbb{E}[\tau]} \geq r \end{aligned} \tag{7.12}$$

The maximum possible value for r is equal to $r^* = \max_{p(v|\tau)} \frac{H(V|\tau)}{\mathbb{E}[V]+\mathbb{E}[\tau]}$. The solution of this problem can be found by considering the following alternative problem which gives the same trade-off region

$$\begin{aligned} \max_{p(v|\tau),m} \quad & \frac{H(V|\tau)}{m} \\ \text{s.t.} \quad & \mathbb{E}[(V+\tau)^2] \leq 2\alpha\mathbb{E}[V+\tau] \\ & \mathbb{E}[V+\tau] = m \end{aligned} \tag{7.13}$$

For a fixed m, problem (7.13) is concave in $p(v|\tau)$ and can be solved efficiently. Then, to obtain the entire trade-off region, we sweep over all possible values of the

parameter α (which are all possible values of the AoI). The solution for (7.13) is found numerically by optimizing over all possible conditional pmfs $p(v|\tau)$ for each value of m. Then, we use line search to search for the optimal m. All this, has to be repeated for all possible values of the AoI α. Finding the optimal solution for (7.13) has a high complexity, hence, we propose the following policy which reduces this complexity significantly, and at the same time adapts to the timing of the energy arrivals to the extent possible within this set of policies.

7.3.2 Simplified ETATP

In this policy, we simplify the form of the dependence of the transmission on the timings of energy arrivals significantly. The transmitter waits until an energy arrives, if the energy takes more than c slots since the last update, we transmit the information using a geometric random variable with probability of success p_b, otherwise the transmitter transmits the information using a geometric random variable with probability of success p_a, i.e., the transmitter chooses $p(v|\tau)$ as follows

$$p(v|\tau) = \begin{cases} p_b(1-p_b)^{v-1}, & \tau < c \\ p_a(1-p_a)^{v-1}, & \tau \geq c \end{cases}, \; v = 1, 2, \cdots \tag{7.14}$$

In this case, p_a, p_b and c are the variables over which the optimization is performed. The average achieved information rate as a function of p_a, p_b and c can be obtained

as,

$$R = \frac{\frac{H_2(p_b)}{p_b}(1-(1-q)^c) + \frac{H_2(p_a)}{p_a}(1-q)^c}{\mathbb{E}[\tau] + \mathbb{E}[V]} \tag{7.15}$$

where $\mathbb{E}[V]$ is equal to

$$\mathbb{E}[V] = \frac{(1-p_b)}{p_b}(1-(1-q)^c) + \frac{(1-p_a)}{p_a}(1-q)^c \tag{7.16}$$

Now, we can calculate the average AoI with this policy as,

$$\Delta = \frac{\mathbb{E}[(\tau+V)^2]}{2\mathbb{E}[\tau+V]} = \frac{\frac{2-q}{q^2} + \mathbb{E}[V^2] + 2\mathbb{E}[\tau V]}{2\mathbb{E}[\tau] + 2\mathbb{E}[V]} \tag{7.17}$$

where we have $\mathbb{E}[V^2]$ as

$$\mathbb{E}[V^2] = \left(\frac{2+p_b^2-3p_b}{p_b^2}\right)(1-(1-q)^c) + \left(\frac{2+p_a^2-3p_a}{p_a^2}\right)(1-q)^c \tag{7.18}$$

and $\mathbb{E}[\tau V]$ as

$$\begin{aligned}\mathbb{E}[\tau V] =& \frac{(1-p_b)}{p_b}\left(\frac{1}{q}(1-(1-q)^{c+1}) - (c+1)(1-q)^c\right) \\ &+ \frac{(1-p_a)}{p_a}\left(\frac{(1-q)^{c+1}}{q} + c(1-q)^{c-1}\right)\end{aligned} \tag{7.19}$$

This schemes is simpler than the general class of ETATP; still, we need to search for the optimal p_a, p_b and c. We reduce this complexity further in the next policy.

7.3.3 Threshold Based Transmission Policy

We now present the first separable policy. In this policy, we assume that $T = Z(\tau) + V$, where the information is still carried only in V; see Fig. 7.2. $Z(\tau)$ is the duration the transmitter decides to wait in order to minimize the AoI, while V is the duration the transmitter decides to wait to add information in the timing of the update. $Z(\tau)$ and V are independent which implies that $H(V|Z(\tau)) = H(V|\tau) = H(V)$. The duration $Z(\tau)$ is determined according to a threshold policy as follows,

$$Z(\tau) = \tau U(\tau - \tau_0) + \tau_0 U(\tau_0 - \tau - 1) \tag{7.20}$$

The optimal value of τ_0 is yet to be determined and is an optimization variable. The optimal value of τ_0 is to be calculated and, thus, known both at the transmitter and the receiver; hence, this threshold policy is a deterministic policy. This ensures that we still have $H(V^n|\tau^n, T^n) = 0$, which is consistent with (7.6). We then choose V to be a geometric random variable with parameter p. The trade-off region can then be written as,

$$\begin{aligned} \min_{T(\tau),p} \quad & \frac{\mathbb{E}[(Z(\tau)+V)^2]}{2\mathbb{E}[Z(\tau)+V]} \\ \text{s.t.} \quad & Z(\tau) \geq \tau \\ & r \leq \frac{H_2(p)/p}{(1-p)/p + \mathbb{E}[Z(\tau)]} \end{aligned} \tag{7.21}$$

where r is a fixed positive number. The feasible values of r are in $[0, r*]$ where

r^* is equal to $r^* = \max_{p\in[0,1]} \frac{H_2(p)/p}{(1-p)/p+\mathbb{E}[\tau]}$. This follows because the smallest value that $Z(\tau)$ can take is equal to τ. The optimization problem in this case becomes a function of only τ_0 and p.

We now need to calculate $\mathbb{E}[Z(\tau)]$ and $\mathbb{E}[Z^2(\tau)]$. We calculate $\mathbb{E}[Z(\tau)]$ as follows,

$$\mathbb{E}[Z(\tau)] =(1-q)^{\tau_0} + \frac{(1-q)^{\tau_0+1}}{q} + \tau_0 \tag{7.22}$$

and we calculate $\mathbb{E}[Z^2(\tau)]$ as follows,

$$\mathbb{E}[Z^2(\tau)] = \left(\frac{2-3q}{q^2}\right)(1-q)^{\tau_0}+2(\tau_0+1)(1-q)^{\tau_0}+2(\tau_0+1)\frac{(1-q)^{\tau_0+1}}{q}+\tau_0^2 \tag{7.23}$$

Finally, we note that in this case $\mathbb{E}[V^2]$ is equal to,

$$\mathbb{E}[V^2] = \frac{2+p^2-3p}{p^2} \tag{7.24}$$

Substituting these quantities in the above optimization problem and solving for p and τ_0 jointly gives the solution.

7.3.4 Zero-Wait Transmission Policy

This policy is similar to the threshold based policy, with one difference: The update block does not wait after an energy arrives, instead, it decides to update right away,

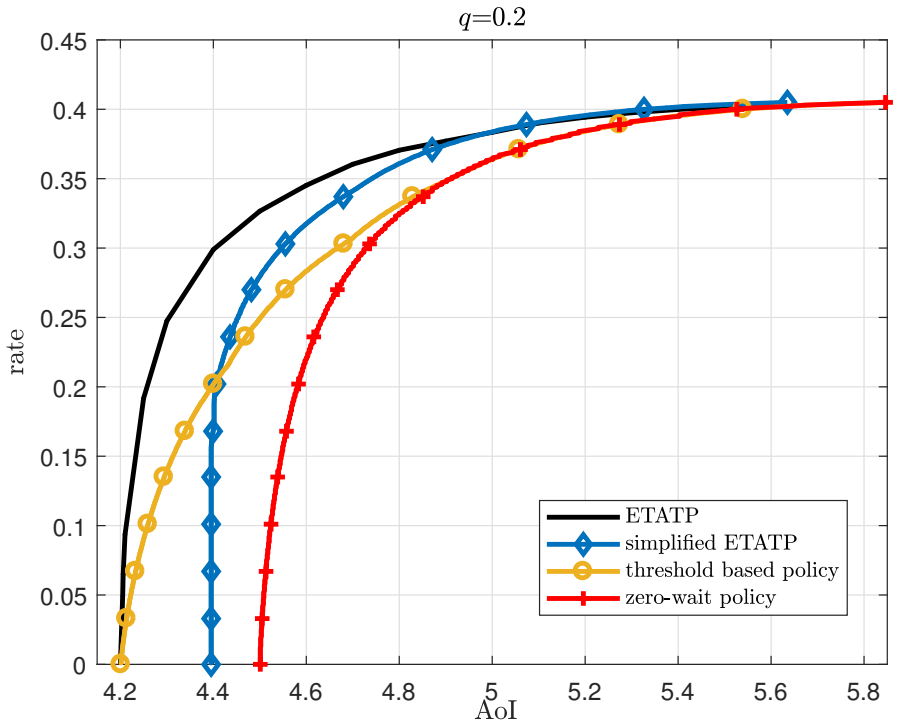

Figure 7.4: The rate-AoI trade-off region for $q = 0.2$.

i.e., $Z(\tau) = \tau$. Hence, the trade-off region can be obtained by solving,

$$\begin{aligned} \min_{p} \quad & \frac{\mathbb{E}[(\tau+V)^2]}{2\mathbb{E}[\tau+V]} \\ \text{s.t.} \quad & r \leq \frac{H_2(p)/p}{(1-p)/p + \mathbb{E}[\tau]} \end{aligned} \tag{7.25}$$

We can then calculate $\mathbb{E}[(\tau+V)^2] = \mathbb{E}[\tau^2+V^2+2V\tau]$, where V and τ are independent as the message is independent of the energy arrivals. Since τ is geometric $\mathbb{E}[\tau^2] = \frac{2-q}{q^2}$. This optimization problem is a function of only a single variable p. This problem is solved by line search over $p \in [0, 1]$.

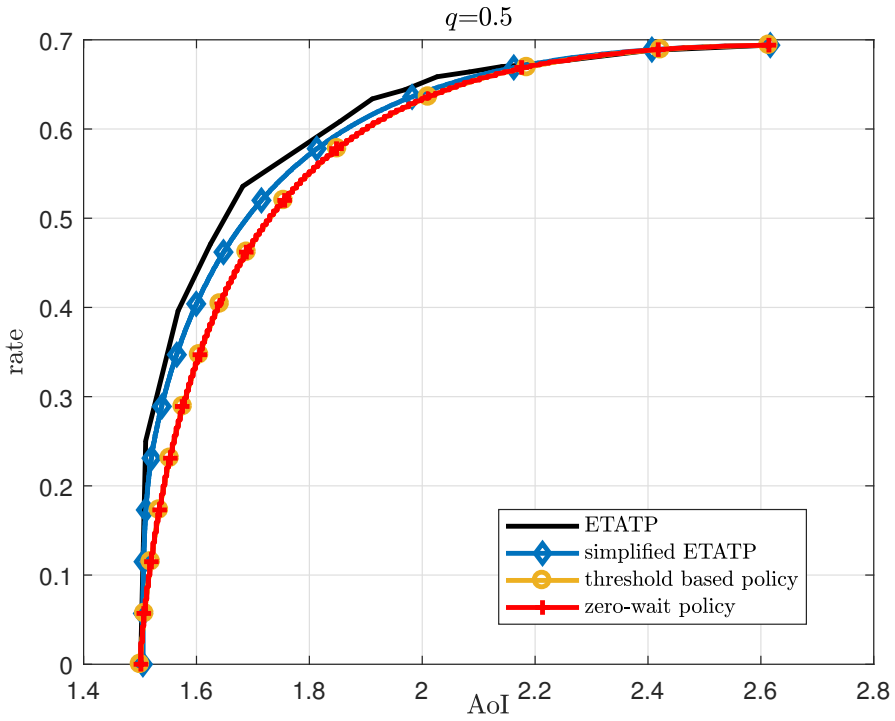

Figure 7.5: The rate-AoI trade-off region for $q = 0.5$.

7.4 Numerical Results

Here, we compare the trade-off regions resulting from the proposed schemes. We plot these regions in Figs. 7.4-7.6 for different values of average energy arrivals, namely, $q = 0.2$, $q = 0.5$ and $q = 0.7$. For low values of q, as for $q = 0.2$ in Fig. 7.4, there is a significant gap between the performance of ETATP and the simplified schemes. For this value of q, in most of the region, simplified ETATP performs better than the threshold and zero-wait policies. As the value of q increases as shown in Fig. 7.5 and Fig. 7.6, the gap between the performance of the different policies decreases significantly. In Fig. 7.5, the threshold and zero-wait policies overlap. In Fig. 7.6, simplified ETATP, threshold and zero-wait policies overlap. In all cases, zero-wait

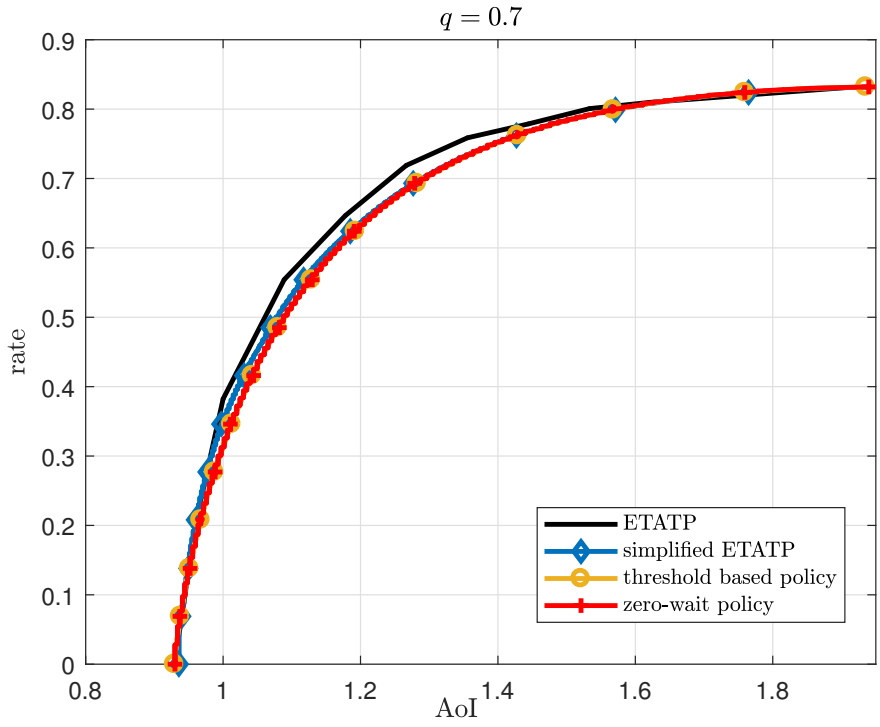

Figure 7.6: The rate-AoI trade-off region for $q = 0.7$.

policy performs the worst. This is consistent with early results e.g., [51], early results in the context of energy harvesting e.g., [61,62], and recent results [66,67,75], where updating as soon as one can is not optimum.

7.5 Conclusion

In this chapter, we considered a single-user energy harvesting setting with a unit battery. The transmitter harvests energy and uses it to send status updates to the receiver along with an independent message encoded in the timings of these status updates. We studied the trade-off between the minimum AoI and the maximum information rate of the message. We first presented the general setting and then restricted our attention to renewal policies. Under renewal policies, we proposed

four achievable schemes. These schemes differ in the complexity and the achievable AoI-rate region; low complexity schemes come at the cost of smaller AoI-rate region.

CHAPTER 8

Energy Harvesting Communications Under Temperature Constraints

8.1 Introduction

We consider several effects of the temperature on the offline power allocation problem. We first study the effect of temperature dependent energy leakage. As the temperature of the transmitter increases due to information transmission, the energy leakage increases. Next, we consider the problem of processing costs. We tackle this problem by allowing the transmitter to divide the transmission duration into two consecutive transmission and silence periods, and identify the optimal policy in this case. Then, we study temperature increases caused by the energy harvesting process itself. As the transmitter admits the incoming energy arrivals, its temperature may increase.

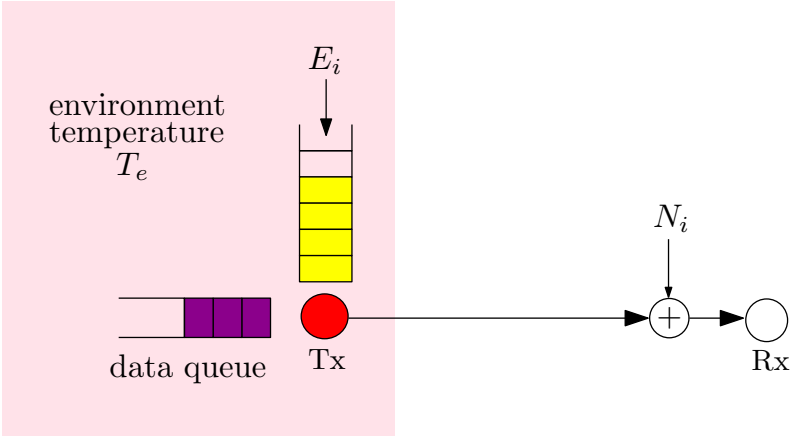

Figure 8.1: System model representing an energy harvesting transmitter in an environment with temperature T_e.

8.2 Model and Problem Formulation

We consider a single-user energy harvesting channel, Fig. 8.1, subject to temperature constraints. The physical layer is an additive Gaussian noise channel where the noise variance is unity for convenience. We use a continuous time model: In an infinitesimal time duration dt in $[t, t+dt]$, the transmitter decides a feasible transmit power level $p(t)$, and $\frac{1}{2}\log(1+p(t))\,dt$ units of data is sent to the receiver.

The battery at the transmitter has unlimited size and the initial energy available in the battery at time zero is E_0. Energy arrivals occur at times $\{s_1, s_2, \ldots\}$ in amounts $\{E_1, E_2, \ldots\}$. We call the time interval between two consecutive energy arrivals an *epoch*. D is the deadline. E_i and s_i are known offline. Let $h(t) = \max\{k : s_k < t\}$. Power policy $p(t)$ is subject to energy causality constraints as [1]:

$$\int_0^t p(\tau)d\tau \leq \sum_{i=0}^{h(t)} E_i, \qquad \forall t \in [0, D] \tag{8.1}$$

We adopt the following first order thermal model:

$$\frac{dT(t)}{dt} = ap(t) - b(T(t) - T_e) + c(t) \tag{8.2}$$

where T_e is the environment temperature, $T(t)$ is the temperature at time t, $c(t)$ represents additional heat sources, and a, b are non-negative constants. With the initial temperature $T(0) = T_e$, the solution of (8.2) is [107]:

$$T(t) = e^{-bt} \int_0^t e^{b\tau} \left(ap(\tau) + c(\tau)\right) d\tau + T_e \tag{8.3}$$

First, we consider the throughput maximization problem with temperature dependent energy leakage:

$$\begin{aligned} \max_{p(t)} \quad & \frac{1}{2} \int_0^D \log(1 + p(\tau)) d\tau \\ \text{s.t.} \quad & \int_0^t p(\tau) d\tau + \int_0^t \epsilon_l (T(t) - T_e) d\tau \leq \sum_{i=0}^{h(t)} E_i \\ & p(t) \geq 0, \ \forall t \in [0, D] \end{aligned} \tag{8.4}$$

where ϵ_l is the energy leakage coefficient. Energy leakage happens even when the transmitter is not transmitting. In particular, $\epsilon_l T_e D$ is the nominal energy leakage, which is the amount of energy that leaks when the transmitter is not transmitting and the temperature is T_e. We assume that $\tilde{E}_i \geq \epsilon_l T_e (s_{i+1} - s_i)$ is the actual harvested energy at $t = s_i$ and that E_i in the formulation in (8.4) is $E_i = \tilde{E}_i - \epsilon_l T_e (s_{i+1} - s_i)$.

Next, we consider the throughput maximization problem under temperature constraints in the presence of processing costs due to power spent for the transmitter to be on:

$$\begin{aligned}
\max_{p(t),\{\theta_i\}} \quad & \int_{\theta_1}^{\theta_2} \frac{1}{2}\log(1+p(\tau))d\tau + \int_{\theta_3}^{\theta_4} \frac{1}{2}\log(1+p(\tau))d\tau \\
\text{s.t.} \quad & \int_{\theta_1}^{\theta_2} (\epsilon_p + p(\tau))d\tau + \int_{\theta_3}^{\theta_4} (\epsilon_p + p(\tau))d\tau \leq E \\
& T(t) \leq T_c \\
& 0 \leq \theta_1 \leq \theta_2 \leq \theta_3 \leq \theta_4 \leq D \\
& p(t) \geq 0, \ \forall t \in [0, D]
\end{aligned} \tag{8.5}$$

where ϵ_p is the processing cost, E is the available energy at the transmitter. This problem is motivated by the approach in [32]. It is well-known that, when there is processing cost, the transmission becomes *bursty*. Under temperature constraints, in general, there may be many intervals of being on and off for the transmitter. In the formulation in (8.5), we allow the transmitter to divide the transmission session into two parts only and to *cool-down* in between transmissions. Here, in the single epoch formulation in (8.5), the transmitter is active in the intervals $[\theta_1,\ \theta_2]$ and $[\theta_3, \theta_4]$ and silent in the rest.

Finally, we consider the temperature increase due to energy harvesting. In this case, $c(t) = \sum_{i=1}^{N} \epsilon_h \alpha_i E_i \delta(t - s_i)$ where E_i is the available energy and $\alpha_i E_i$ is the amount of *harvested* energy (i.e., energy intake) with $\alpha_i \in [0, 1]$. Note that α_i is controlled by the transmitter. Here, ϵ_h is the coefficient that determines the temper-

ature increase due to energy harvesting. In particular, at time $t = s_i$, temperature increases with amount $\epsilon_h \alpha_i E_i$. We impose a hard temperature constraint $T(t) \leq T_c$ for all $t \in [0, D]$. This constraint is equivalent to:

$$\int_0^t a e^{b\tau} p(\tau) d\tau + \sum_{i=1}^{h(t)} \epsilon_h \alpha_i E_i e^{b s_i} u(t - s_i) \leq T_\delta e^{bt}, \ \forall t \tag{8.6}$$

where $u(\cdot)$ is the unit step function. We consider the following problem:

$$\begin{aligned} \max_{p(t), \{\alpha_i\}} \quad & \frac{1}{2} \int_0^D \log(1 + p(\tau)) d\tau \\ \text{s.t.} \quad & \int_0^t p(\tau) d\tau \leq \sum_{i=0}^{h(t)} \alpha_i E_i \\ & \int_0^t a e^{b\tau} p(\tau) d\tau + \sum_{i=1}^{h(t)} \epsilon_h \alpha_i E_i e^{b s_i} u(t - s_i) \leq T_\delta e^{bt} \\ & p(t) \geq 0, \ \forall t \in [0, D] \end{aligned} \tag{8.7}$$

In the following sections, we specialize in the problems stated in (8.4), (8.5), and (8.7).

8.3 Temperature Dependent Energy Leakage: Problem in (8.4)

In this section, we focus on the throughput maximization problem in (8.4) with temperature dependent energy leakage. The problem is convex and the Lagrangian is:

$$\mathcal{L} = - \int_0^D \log(1 + p(\tau)) d\tau + \int_0^D \lambda(t) \left(\int_0^t p(\tau) d\tau \right) dt$$

$$+\int_0^D \lambda(t)\left(\int_0^t \epsilon_l(T(\tau)-T_e)d\tau-\sum_{i=0}^{h(t)}E_i\right)dt \tag{8.8}$$

The KKT optimality conditions are:

$$-\frac{1}{1+p(t)}+\int_t^D \lambda(\tau)d\tau+\epsilon_l a e^{bt}\int_t^D\int_t^x \lambda(x)e^{-b\tau}dxd\tau=0 \tag{8.9}$$

In the following sub-sections, we first investigate the solution for a single energy arrival, then for multiple energy arrivals, and then provide the general form of the solution.

8.3.1 Single Energy Arrival

In this case, (8.9) reduces to the following:

$$p(t)=\left(\frac{1}{\lambda\left(1+\frac{\epsilon_l a}{b}(1-e^{b(t-D)})\right)}-1\right)^+ \tag{8.10}$$

Lemma 8.1 *The optimal power, $p(t)$, is monotone increasing and convex.*

Proof: Since $1+\frac{\epsilon_l a}{b}(1-e^{b(t-D)})$ is a monotone decreasing, concave and positive function, its reciprocal is a monotone increasing and convex function. Hence, from (8.10), the optimum power is monotone increasing and convex. ■

Lemma 8.1 suggests that in the optimal policy, energy utilization is deferred to the future to the extent possible. This enables a controlled increase in the temperature and the energy loss due to leakage. Note that the linear dependence of the energy leakage on the temperature forms a positive feedback loop in that more

energy is lost as the temperature increases.

Lemma 8.2 *The temperature, $T(t)$, resulting from the optimal power policy is monotone increasing.*

Proof: First, we need to calculate the temperature based on the optimal power policy (8.10). It suffices to consider only the term with the integration in the temperature expression in (8.3) since T_e is constant and will not affect the analysis. Since the power is increasing, there exists $t = t_0$ such that $p(t) > 0$ for all $t \in [t_0, D]$. Hence, using (8.10) we have,

$$T(t) - T_e = \frac{e^{-b(t-D)}}{\lambda \epsilon_l} \log \left(\frac{\lambda + \frac{\epsilon_l \lambda a}{b} \left(1 - e^{-b(D-t_0)}\right)}{\lambda + \frac{\epsilon_l \lambda a}{b} \left(1 - e^{-b(D-t)}\right)} \right) - \frac{a}{b} \left(1 - e^{b(t_0-t)}\right) \tag{8.11}$$

Next, we need to show that this $T(t)$ is increasing. To check this, we evaluate the derivative of $T(t)$ as follows,

$$\begin{aligned}
\frac{dT}{dt} =& - \frac{be^{-b(t-D)}}{\lambda \epsilon_l} \log \left(\frac{1 + \frac{\epsilon_l a}{b} \left(1 - e^{-b(D-t_0)}\right)}{1 + \frac{\epsilon_l a}{b} \left(1 - e^{-b(D-t)}\right)} \right) \\
&+ \frac{a}{\lambda + \frac{\epsilon_l \lambda a}{b} \left(1 - \lambda e^{-b(D-t)}\right)} - a e^{b(t_0-t)} \qquad (8.12) \\
=& - \frac{be^{-b(t-D)}}{\lambda \epsilon_l} \log \left(\frac{\frac{\epsilon_l a}{b} \left(e^{-b(D-t)} - e^{-b(D-t_0)}\right)}{1 + \frac{\epsilon_l a}{b} \left(1 - e^{-b(D-t)}\right)} + 1 \right) \\
&+ \frac{a}{\lambda + \frac{\epsilon_l \lambda a}{b} \left(1 - \lambda e^{-b(D-t)}\right)} - a e^{b(t_0-t)} \qquad (8.13) \\
\geq& - \frac{be^{-b(t-D)}}{\lambda \epsilon_l} \left(\frac{\frac{\epsilon_l a}{b} \left(e^{-b(D-t)} - e^{-b(D-t_0)}\right)}{1 + \frac{\epsilon_l a}{b} \left(1 - e^{-b(D-t)}\right)} \right) \\
&+ \frac{a}{\lambda + \frac{\epsilon_l \lambda a}{b} \left(1 - e^{-b(D-t)}\right)} - a e^{b(t_0-t)} \qquad (8.14)
\end{aligned}$$

$$= a e^{b(t_0 - t)} p^*(t) > 0 \tag{8.15}$$

where the inequality follows since $\log(1+x) \leq x$. Hence, the temperature is strictly increasing whenever the optimum power is non-zero. ■

Lemma 8.3 *Optimum Lagrange multiplier satisfies* $\lambda \in (0, 1)$.

Proof: From (8.10), we know that the optimum power is increasing, and if it is non-zero, then, it is non-zero specifically at $t = D$. Hence, we have,

$$\lambda \left(1 + \frac{\epsilon_l a}{b}(1 - e^{b(t-D)})\right)\Big|_{t=D} < 1 \tag{8.16}$$

which in turn implies that $\lambda < 1$. In addition, the Lagrange multiplier cannot be zero, as this would imply the power to be infinity. Combining this with the non-negativity of the Lagrange multiplier gives the desired result. ■

Note that the only variable in the expression in (8.10) is λ. The optimal power can be obtained by one-dimensional search on $\lambda \in (0, 1)$. The next lemmas will be useful in providing the optimal algorithm for the multiple energy arrival case. They state the monotonicity of the power with the harvested energy.

Lemma 8.4 *In the optimal power policy, the energy constraint is satisfied with equality.*

Proof: The proof follows by contradiction. If the optimal power does not satisfy the energy constraint with equality, then we can increase the power which strictly

increases the objective function, and this violates the optimality. ■

Lemma 8.5 *$p(t)$ is monotonically increasing with E.*

Proof: Assume we have energy arrival E, and corresponding power $p(t)$. We know that the constraint will be satisfied with equality. Then, if we increase the energy to $E+\epsilon$ for any $\epsilon > 0$, the constraint is not satisfied. Hence, there exists $\delta > 0$ such that when λ is replaced with $\lambda - \delta$, equality is achieved. Decreasing λ increases $p(t)$ for all $t \in [0, D]$. ■

8.3.2 Multiple Energy Arrivals

Lemma 8.6 *$p(t)$ is monotonically increasing throughout the transmission duration.*

Proof: Using (8.9) we have

$$p^*(t) = \left(\frac{1}{\int_t^D \lambda(\tau) d\tau + \epsilon_l a e^{bt} \int_t^D \int_t^x \lambda(x) e^{-b\tau} d\tau dx} - 1 \right)^+ \tag{8.17}$$

which when the inner integral is evaluated becomes,

$$p^*(t) = \left(\frac{1}{\int_t^D \lambda(\tau) d\tau + \frac{\epsilon_l a}{b} \int_t^D \lambda(x)[1 - e^{-b(x-t)}] dx} - 1 \right)^+ \tag{8.18}$$

Since the denominator is a decreasing function of t, $p(t)$ is increasing in t. ■

Lemma 8.7 *The battery can be empty only at the energy arrival instants. It is certainly empty at the end.*

Proof: This follows since the optimal power is monotonically increasing throughout the transmission duration, hence, there does not exist a duration of non-zero measure with zero power. Hence, the battery can never be empty for a non-zero measure interval. Therefore, the battery cannot be empty except a duration of measure zero, which can only happen at energy arrival instants or at the end of the deadline. If the battery is not empty at the end, then we can always increase the power without violating the constraint, which violates optimality. ■

Lemma 8.8 *The transmission power may have possible positive jumps only at the energy arrival instants.*

Proof: From Lemma 8.7, we have that the energy can be consumed fully only at the energy arrivals or the deadline, hence, the energy constraint can be tight only at these instants. Therefore, from the complementary slackness, we have,

$$\lambda(t) = \sum_{i=1}^{N} \lambda_i \delta(t - s_i) \tag{8.19}$$

Then, substituting this in (8.18), we have,

$$p^*(t) = \left(\frac{1}{\sum_{i=1}^{N} \lambda_i u(s_i - t) \left(1 + \frac{\epsilon_l a}{b}[1 - e^{-b(s_i - t)}]\right)} - 1 \right)^+ \tag{8.20}$$

which may have positive jumps at the instants s_i due to the presence of the unit step function. ■

Lemma 8.9 *The temperature is monotone increasing throughout the communica-*

tion session.

Proof: We show this for a two epoch system, however, the proof for N epochs follows identical steps. It is clear that for the second slot temperature is increasing since the power in the second epoch has the form,

$$p^*(t) = \frac{1}{\lambda_2 \left(1 + \frac{\epsilon_l a}{b}[1 - e^{-b(s_2 - t)}]\right)} - 1 \tag{8.21}$$

which is the same form as in the case of a single epoch, hence we can proceed as in the proof of Lemma 8.2. Thus, it remains to show the same for the first epoch. The optimal power in the first epoch can be written as,

$$p^*(t) = \frac{1}{\sum_{i=1}^{2} \lambda_i \left(1 + \frac{\epsilon_l a}{b}[1 - e^{-b(s_i - t)}]\right)} - 1 \tag{8.22}$$

$$= \frac{1}{\tilde{\lambda} + \tilde{\lambda}\frac{\epsilon_l a}{b} - \frac{\epsilon_l a}{b}\left(e^{-bs_1}\lambda_1 + e^{-bs_2}\lambda_2\right)e^{bt}} - 1 \tag{8.23}$$

$$= \frac{1}{\tilde{\lambda}\left(1 + \frac{\epsilon_l a}{b}[1 - e^{-b(\tilde{D} - t)}]\right)} - 1 \tag{8.24}$$

where $\tilde{\lambda} = \lambda_1 + \lambda_2$ and $\tilde{D}$ is some number between s_1, s_2. The existence of $\tilde{D}$ is guaranteed since we have,

$$\tilde{\lambda} \min\{e^{-bs_1}, e^{-bs_2}\} \leq \lambda_1 e^{-bs_1} + \lambda_2 e^{-bs_2} \tag{8.25}$$

$$\leq \tilde{\lambda} \max\{e^{-bs_1}, e^{-bs_2}\} \tag{8.26}$$

and the exponential function is continuous. We can now apply again the proof in

Lemma 8.2. Hence, the temperature is strictly increasing within each slot, and therefore, throughout the communication session. It also follows that the temperature can be constant only when the power is zero, which can happen only at the beginning of the transmission duration. ■

8.3.3 Optimal Policy

We provide the optimal policy first for the case of a single arrival and then for the case of multiple arrivals.

8.3.3.1 Single Energy Arrival

For the single energy arrival case, we showed that the optimal solution depends only on λ. We also showed in Lemma 8.3 that λ lies in the interval $(0, 1)$. Also, using the fact that the energy constraint is always satisfied with equality, λ satisfies the following equation:

$$\int_{p(t)\geq 0} (p(\tau) + \epsilon_l(T(\tau) - T_e))d\tau = E \tag{8.27}$$

where $p(t)$ is given in (8.10). Hence, the optimal λ is found by a one-dimensional search on $(0, 1)$. Note also that since $p(t)$ is monotone in λ and (8.27) is linear in $p(t)$, (8.27) is monotone in λ. Hence, we can search for λ using the bisection method in the range $(0, 1)$ until this equation is satisfied with equality.

8.3.3.2 Multiple Energy Arrivals

We know from (8.19) that the optimal multiple epoch problem reduces to finding $\{\lambda_i\}_{i=1}^{N}$. The algorithm begins by solving each slot individually using the single epoch solution. However, the epochs are not completely independent of each other, due to the temperature accumulation throughout the transmission duration.

We begin by assuming an initial energy allocation, where we use only the energy that arrived in each epoch with no energy transfer between the epochs. We first solve for epoch 1 power allocation. In the first epoch, there is no temperature accumulation which should be taken into account. Next, we solve for epoch 2 power allocation, but with setting the temperature as follows,

$$T(t) = e^{-bt} \int_0^t e^{b\tau} ap(\tau) d\tau + T(s_1) \tag{8.28}$$

where $T(s_1)$ is the temperature of the system at the end of the epoch 1, i.e., the system starts at the second slot from temperature $T(s_1)$ instead of T_e. Note that this can be calculated using the optimal λ, t_0 from (8.11). In effect, this is equivalent to subtracting from the available energy in the second epoch an amount equal to $(s_2 - s_1)\epsilon_l(T(s_1) - T_e)$, where $s_2 - s_1$ is the duration of the second epoch. Similarly, we proceed to solve for power allocation in all epochs with setting the temperature at epoch i as,

$$T(t) = e^{-bt} \int_0^t e^{b\tau} ap(\tau) d\tau + T(s_{i-1}) \tag{8.29}$$

Until this point, the obtained solution may not be optimal. We need to check if the solution satisfies the optimality conditions. If the power allocations between the slots is increasing, then indeed this is the optimal solution, according to Lemma 8.6, since we can find the corresponding Lagrange multipliers.

Next, if the solution for the power is not increasing, then this is not the optimal solution, and it needs to be modified. If slots i and $i-1$ do not satisfy this, then we transfer energy from slot $i-1$ to slot i, and re-solve the problem until we equate the powers at time s_i. According to Lemma 8.5, transferring energy from one slot to another decreases the power in slot $i-1$ while increases the power in slot i, which guarantees the existence of an increasing solution by transferring energy. In this case, we have $\lambda_i = 0$. We repeat this procedure between every two consecutive slots which have non-increasing power until the power is increasing throughout the transmission duration.

8.4 Non-zero Processing Power: Problem in (8.5)

In this section, we focus on the throughput maximization problem in (8.5) with processing cost. First, we discuss the interpretation of the possible solutions of problem (8.5). If $\theta_1^* = 0$, $\theta_2^* = \theta_3^*$ and $\theta_4^* = D$, then this corresponds to the case that the transmitter is on for the whole duration. This usually happens when the transmitter has sufficient energy. If $\theta_1^* = 0$, $\theta_1^* < \theta_2^* < \theta_3^*$ and $\theta_3^* = \theta_4^* = D$, then the problem reduces to a problem similar to the one proposed at [32]. If $\theta_1^* < \theta_2^* < \theta_3^* < \theta_4^*$, then there is a cooling down phase for the duration $[\theta_2, \theta_3]$.

We now argue that without loss of generality we can set $\theta_1^* = 0$ and $\theta_4^* = D$. The intuition behind this is that we want to separate the two transmissions as much as we can to give the system the longest time to cool down, and hence may achieve a better rate. The problem in this case is:

$$\begin{aligned}
\max_{p(t),\{\theta_i\}} \quad & \int_0^{\theta_1} \frac{1}{2}\log(1+p(\tau))d\tau + \int_{\theta_2}^{D} \frac{1}{2}\log(1+p(\tau))d\tau \\
\text{s.t.} \quad & \int_0^{\theta_1} (\epsilon_p + p(\tau))d\tau + \int_{\theta_2}^{D} (\epsilon_p + p(\tau))d\tau \leq E \\
& T(t) \leq T_c \\
& 0 \leq \theta_1 \leq \theta_2 \leq D \\
& p(t) \geq 0, \ \forall t \in [0, D]
\end{aligned} \tag{8.30}$$

Lemma 8.10 *Problems (8.5) and (8.30) are equivalent.*

Proof: To prove this, we need to show that the optimal solution of each problem is feasible in the other problem with optimal value no less than the other.

It is clear that the optimal solution for (8.30) is always feasible in (8.5) with the same optimal value. Now, for (8.5), assume that the optimal solution is $\theta_1^* > 0$ and $\theta_4^* < D$. We now need to check the feasibility of it in (8.30). The feasibility is easy to check for the energy constraint, since it only depends on the duration and not the position. The temperature constraint is also feasible, since the heat generated for (8.5) in the duration $[\theta_1^*, \theta_2^*]$ is the same as when translated to $[0, \theta_2^* - \theta_1^*]$. Thus, we have now verified that the problem is feasible for $t \in [0, \theta_3^*]$. Similarly the heat generated $[\theta_3^*, \theta_4^*]$ will be the same as when translated to $[D - (\theta_4^* - \theta_3^*), D]$ and

also the temperature at $D-(\theta_4^*-\theta_3^*)$ is lower that the original problem since we allowed more time for it to cool down. Hence, the temperature constraint is also feasible. Additionally, the objective function is the same. Hence, the two problems are equivalent. ■

The advantage of considering problem (8.30) is that we have eliminated two variables from the original problem (8.5). Hereafter, we will only consider problem (8.30).

8.4.1 Characterization of the Optimal Solution

In this section, we provide the properties of the optimal of (8.30). This problem is not convex due to the presence of the variables $\{\theta_i\}$ in the integration limits. The main challenge besides the non-convexity of this problem is the non-uniqueness of the global optimal solution. In some cases, we can show that there exists an infinite number of global optimal solutions. A simple example is the case when the temperature constraint is never tight. Hence, in what follows we provide sufficient conditions for the optimality of the solution.

First, we assume that the optimal value for $\{\theta_i^*\}$s are known. Fixing the $\{\theta_i^*\}$s yields a convex optimization problem in $p(t)$. Hence, KKT conditions are now necessary and sufficient. The Lagrangian of the problem is:

$$\begin{aligned}\mathcal{L} = &-\int_0^{\theta_1^*}\frac{1}{2}\log(1+p(\tau))d\tau-\int_{\theta_2^*}^{D}\frac{1}{2}\log(1+p(\tau))d\tau\\&+\lambda\left(\int_0^{\theta_1^*}(\epsilon_p+p(\tau))d\tau+\int_{\theta_2^*}^{D}(\epsilon_p+p(\tau))d\tau-E\right)\end{aligned}$$

$$+\int_0^D \beta(t)\left[\int_0^t ae^{b\tau}p(\tau)d\tau - T_\delta e^{bt}\right]dt \tag{8.31}$$

which yields KKT optimality conditions:

$$p(t) = \left[\frac{1}{\lambda + e^{bt}\int_t^D \beta(\tau)d\tau} - 1\right]^+, \forall t \in [0,\theta_1^*] \cup [\theta_2^*, D] \tag{8.32}$$

Next, we study the properties of the optimal solution. We first state the lemma indicating the non-increasing property of the power. The proof follows as [107, Lemma 2].

Lemma 8.11 *The optimal power allocations is monotonically non-increasing in the durations* $(0,\theta_1^*)$ *and* (θ_2^*, D).

Next, we show that if the temperature constraint is *never tight*, or equivalently, the temperature constraint is removed, then we get back to the formulation proposed in [32] which yields constant transmission power. We also highlight the fact that the number of solutions can be infinite.

Lemma 8.12 *If there is no temperature constraint (or equivalently, the temperature constraint is never tight), then the optimal power,* $p^*(t)$*, is constant and* $\theta_2 = D$ *achieves the optimal solution. However, the solution is not unique.*

Proof: When the temperature constraint is never tight, from slackness we have $\lambda(t) = 0,\ \forall t$. Hence, using this along with (8.31) we have:

$$p^*(t) = \frac{1}{\lambda} - 1, \quad \forall t \in [0,\theta_1^*] \cup [\theta_2^*, D] \tag{8.33}$$

which proves that the power is constant. Then, if $\theta_2^* < D$, we can define a new policy,

$$\tilde{p}(t) = \begin{cases} p^*(t), \ \forall t \in [0, \theta_1^*] \\ \\ p^*(t + \theta_2^* - \theta_1^*), \quad \forall t \in [\theta_1^*, D - (\theta_2^* - \theta_1^*)] \end{cases} \tag{8.34}$$

This new policy is then feasible since the temperature constraint is not active. Hence, $\theta_2^* = D$ is feasible and gives the optimal solution.

Now, for the non-uniqueness, note that if we have an optimal solution which is $p^*(t) = c$ for $t \in [0, \theta_1^*]$, then for any $\delta \in [0, \theta_1^*]$, $p^*(t) = c$ for $t \in [0, \theta_1^* - \delta] \cup [D - \delta, D]$ is also an optimal solution. This follows since, for all these values of δ, we still have the same value for the objective function. ■

Lemma 8.13 *Assume that we fix θ_2 to a value and solve for the optimal value of $\theta_1 < \theta_2$. Then, if the resultant optimal power is constant, then: 1) the power level in both slots is equal, 2) the energy constraint will be satisfied with equality, and 3) if this obtained transmission duration $(\theta_1 + D - \theta_2)$ is equal to the optimal duration with no temperature constraint, then the obtained $(\theta_1, \theta_2, p(t))$ is the optimal solution for this problem.*

Proof: Since the power is constant, this means that the temperature constraint can be tight at most on an interval of zero measure, i.e., only at θ_1, D. Hence, we have $\beta(t) = \beta(\theta_1)\delta(t - \theta_1) + \beta(D)\delta(t - D)$. Since the power is constant, from (8.32), this implies that $\beta(\theta_1) = \beta(D) = 0$. Hence, the power in both slots are equal, and equal

to

$$p(t) = \frac{1}{\lambda} - 1, \forall t \in [0, \theta_1] \cup [\theta_2, D] \tag{8.35}$$

Since $p(t)$ should be finite, we must have $\lambda \neq 0$. Hence, from complementary slackness, the energy constraint must be satisfied with equality. Since the energy constraint is satisfied with equality, power is constant and the duration $\theta_1 + D - \theta_2$ is the same as with no temperature constraint, we obtain a solution equal to the unconstrained solution. Since the unconstrained problem forms an upper bound to our temperature constrained problem, this is the optimal solution. ■

Hence, if we restrict $\theta_2 = D$ and solve problem (8.30), if the solution results in an inactive temperature constraint, then solving the original problem (8.30) optimally without this restriction gives the same value and the power is constant in both cases.

The next lemma states that if we restricted our solution to $\theta_2 = D$, to obtain the optimal θ_1^*, if the temperature constraint is tight for a non-zero measure, then the obtained solution in this case is strictly sub-optimal than allowing $\theta_2 < D$.

Lemma 8.14 *It cannot happen that the temperature constraint is active for an interval of non-zero measure and $\theta_2^* = D$, while $\theta_1^* < D$.*

Proof: Define $t' = \arg\min\{t \in [0, \theta_1^*] : T(t) = T_c\}$, which is the first instant at which the temperature touches T_c. From [107, Lemma 6], we have that $p^*(t) = \frac{T_\delta b}{a}, \forall t \in [t', \theta_1^*]$. This also implies that the power was monotone decreasing before

t', since if it was constant and equal to $\frac{T_\delta b}{a}$, it would not have touched T_c. We then proceed to the proof by contradiction. Assume the statement is not true, then consider a modified policy as follows:

$$\tilde{p}_\delta(t) = \begin{cases} p^*(t), & \forall t \in [0, \delta] \\ p^*(t + \theta_1^* - D), & \forall t \in [D - \theta_1^* + \delta, D] \\ 0, & \text{otherwise} \end{cases} \tag{8.36}$$

In this policy, we transfer all but δ part of the power to the end of the duration. This policy will give the same optimal value. However, since the temperature constraint was originally tight for an interval, the power would have been monotone decreasing for at least an interval. Then, we can take a small enough interval $[0, \delta]$ in $\tilde{p}(t)$ and replace it by its average, i.e.,

$$\hat{p}_\delta(t) = \begin{cases} \frac{\int_0^\delta \tilde{p}_\delta(t)}{\delta}, & \forall t \in [0, \delta] \\ \tilde{p}_\delta(t), & \text{otherwise} \end{cases} \tag{8.37}$$

For small enough δ, this will result in a feasible policy with a strictly higher objective function, since we strictly decreased the temperature at the point $D - \theta_1^* + \delta$, so we had room to equalize the power more. This contradicts the optimality of the original policy. ■

8.4.2 Solving the Problem for Fixed $\{\theta_i\}$

We will discuss how to obtain the optimal solution for $\{\theta_i\}$ and $p(t)$. In general, we may need to perform line search over all the possible values of θ_1, θ_2. However, with the aid of the previously derived lemmas, we may be able to reduce this search significantly. In the following, we first state how to solve the problem for a fixed $\{\theta_i\}$, then discuss how to search for these optimal $\{\theta_i\}$.

8.4.2.1 Case: $\theta_1 = \theta_2$

In this case, we have the transmitter is on throughout the interval $[0, D]$. In this case, the optimization problem can be rewritten as:

$$\begin{aligned} \max_{p(t),\{\theta_i\}} \quad & \int_0^D \frac{1}{2}\log(1+p(\tau))d\tau \\ \text{s.t.} \quad & \int_0^D p(\tau)d\tau \leq E - \epsilon_p D \\ & T(t) \leq T_c \end{aligned} \tag{8.38}$$

This is the same problem as the single energy arrival case in [107] but with a modified energy arrival equal to $E - \epsilon_p D$. Hence, the solution can be obtained as in [107]. Note that this case will happen only if the energy is large enough to overcome the power needed for processing cost.

8.4.2.2 $0 < \theta_1$ and $\theta_2 = D$

Obtaining the solution for this case is similar to the previous case, however, here the deadline will be θ_1 instead, and the modified energy is equal to $E - \theta_1 \epsilon_p$.

8.4.2.3 $0 < \theta_1 < \theta_2 < D$

In this case, the problem in (8.30) can be equivalently written as:

$$\begin{aligned} \max_{p(t),\alpha} \quad & \int_0^{\theta_1} \frac{1}{2}\log(1+p(\tau))d\tau + \int_{\theta_2}^{D} \frac{1}{2}\log(1+p(\tau))d\tau \\ \text{s.t.} \quad & \int_0^{\theta_1} (\epsilon_p + p(\tau))d\tau \leq \alpha E \\ & \int_{\theta_2}^{D} (\epsilon_p + p(\tau))d\tau \leq (1-\alpha)E \\ & T(t) \leq T_c, \quad p(t) \geq 0, \quad \alpha \in [0,1] \end{aligned} \tag{8.39}$$

For each fixed value of α, the above problem breaks down into two single epoch temperature constrained problem as in [107]. However, the rise in temperature in the first epoch due to $[0, \theta_1]$ should be taken into consideration while solving $[\theta_2, D]$. Hence, finding the optimal $\alpha \in [0, 1]$ solves the problem.

8.4.3 Solving for the Optimal $\{\theta_i\}$

We note that the problem is not jointly convex, hence using the KKTs may lead to a local optimal solution. Thus, one optimal way for determining the solution is to search over θ_1, θ_2; however, due to the previously derived properties, we can limit

the computation complexity significantly. We assume without loss of generality that there always exists an optimal policy for which $\theta_1^* > 0$. This follows since we can always shift the transmission to the beginning without violating the constraints, and with the same objective function.

We now present our approach to determine the optimal $\{\theta_i\}$. First, we begin by assuming $\theta_2 = D$ and solve for the optimal $\theta_1 \in [0, D)$, which can be done using line search on $[0, \theta_2]$. If for the optimal θ_1, the optimal power policy is constant, then we terminate the algorithm and this is the optimal solution. Otherwise, if the power is decreasing or if the temperature constraint is tight for an interval of non-zero measure, then according to Lemma 8.14, this implies that there has to be another phase of transmission, i.e., $\theta_2 = D$ cannot be optimal. Hence, we can decrease θ_2 gradually and obtain the corresponding optimal θ_1. If it happens that we get to a constant power allocation of a duration equal to the unconstrained problem, then by Lemma 8.13, this is an optimal solution, and the search is terminated. Otherwise, we will have to continue searching and then take the highest optimal value recorded and its corresponding $\{\theta_i\}$.

8.5 Temperature Increase Due to Energy Harvesting: Problem in (8.7)

In this section, we focus on the throughput maximization problem in (8.7) with temperature increase due to the energy harvesting process. Note that this problem is a direct generalization of the problem considered in [107]. In particular, the

transmitter is allowed to determine the amount of harvested energy by determining α_i while this is not allowed in [107].

The problem in (8.7) is convex and the Lagrangian is:

$$\begin{aligned}\mathcal{L} = &\int_0^D \frac{1}{2}\log\left(1+p(t)\right)dt \\ &- \int_0^D \beta(t)\left(\int_0^t ae^{b\tau}p(\tau)d\tau + \sum_{i=0}^{h(t)} e^{bs_i}\epsilon_h\alpha_i E_i u(t-s_i) - T_\delta e^{bt}\right)dt \\ &- \int_0^D \lambda(t)\left(\int_0^t p(\tau)d\tau - \sum_{i=0}^{h(t)}\alpha_i E_i\right)dt \end{aligned} \tag{8.40}$$

The KKT optimality conditions are:

$$\frac{1}{1+p(t)} - e^{bt}\int_t^D \beta(\tau)d\tau - \int_t^D \lambda(\tau)d\tau = 0 \tag{8.41}$$

which gives

$$p(t) = \left[\frac{1}{\int_t^D \lambda(\tau)d\tau + e^{bt}\int_t^D \beta(\tau)d\tau} - 1\right]^+ \tag{8.42}$$

We also have the following condition due to the derivative with respect to α_i:

$$\sum_{k=i}^{N} E_k\left(-\int_0^D \beta(t)e^{bs_k}\epsilon_h u(t-s_k)dt + \int_0^D \lambda(t)dt\right) = 0 \tag{8.43}$$

whenever $0 < \alpha_i^* < 1$. If $\alpha_i^* = 1$, then the left hand side in (8.43) is non-negative and if $\alpha_i^* = 0$, it is non-positive.

We first note that the transmitter has to harvest the energy that will be utilized

and energy is never wasted.

Lemma 8.15 *At $t = D$, we have $\int_0^D p(\tau)d\tau = \sum_{i=0}^{N} \alpha_i E_i$.*

Proof: Assume $\int_0^D p(\tau)d\tau < \sum_{i=0}^{N} \alpha_i E_i$ and let $i^* = \max\{i : \alpha_i > 0\}$. Then, α_{i^*} can be replaced with $\tilde{\alpha}_{i^*} < \alpha_{i^*}$ so that $\int_0^D p(\tau)d\tau = \sum_{i=0}^{i^*-1} \alpha_i E_i + \tilde{\alpha}_{i^*} E_{i^*}$. This replacement yields a lower temperature increase and a larger set for feasible power policies $p(t)$ and, therefore, yields larger throughput. ■

We note that despite no energy waste property, the temperature constraint may or may not be tight at $t = D$. Next, we specialize in the solution for the single energy arrival case.

8.5.1 Single Energy Arrival

In the single energy arrival case, since non-zero energy is needed to perform transmission, $\alpha^* > 0$. Therefore, the constraint in (8.43) reduces to the following:

$$-\int_0^D \beta(t)\epsilon_h dt + \int_0^D \lambda(t)dt \geq 0 \tag{8.44}$$

with equality whenever $\alpha^* < 1$. For fixed α_i, the problem is identical to that in [107] with an arbitrary initial temperature. Therefore, the properties identified in [107] for the single energy arrival case hold here as well in the current setting. Still, there are additional properties that arise due to the fact that the transmitter is allowed to determine the amount of harvested energy. We first note the following:

Lemma 8.16 *If $\epsilon_h \geq \frac{a}{bD}$ or $E \leq \frac{T_\delta bD}{a}$, then $p(t) = \frac{\alpha^* E}{D}$.*

Proof: If $E \leq \frac{T_\delta bD}{a}$, then $\alpha E \leq \frac{T_\delta bD}{a}$. This follows immediately irrespective of α and we select $\alpha^* = \min\left\{\frac{T_\delta}{\epsilon_h E}, 1\right\}$ so that $\epsilon_h \alpha E \leq T_\delta$. By [107, Lemma 5], $T(t) \leq T_c$ if $p(t) \leq \frac{T_\delta b}{a}$ for all $t \in [0, D]$. Therefore, $p(t) = \frac{\alpha E}{D}$ yields $T(t) \leq T_c$ and hence is optimal. Now, assume $\epsilon_h \geq \frac{a}{bD}$. Since the temperature increase due to harvested energy at $t = 0$ is $\epsilon_h \alpha E \leq T_\delta$, we have $\frac{\alpha^* E}{D} \leq \frac{T_\delta b}{a}$. By [107, Lemma 5], $T(t) \leq T_c$ and therefore, $p(t) = \frac{\alpha^* E}{D}$ is optimal. ■

We note that for $E \leq E_{critical} = \frac{bT_\delta D e^{bD}}{a(e^{bD}-1)}$, optimal power policy is the constant power policy for $\epsilon_h = 0$, see [107]. Next, we extend this property.

Lemma 8.17 *If $E \leq E_{critical}$ and $\epsilon_h \leq \frac{T_\delta}{E} - \frac{a}{bD}\left(1 - e^{-bD}\right)$ then $p(t) = \frac{E}{D}$ is optimal.*

Proof: We first note that $T(t)$ expression under the constant power policy $p(t) = \frac{\alpha E}{D}$ is:

$$T(t) = T_e + \frac{a}{b}\frac{\alpha E}{D} + \alpha E\left(\epsilon_h - \frac{a}{bD}\right)e^{-bt} \tag{8.45}$$

Note that when $0 \leq \epsilon_h < \frac{a}{bD}$, $T(t)$ in (8.45) is monotone increasing. Therefore, in this case, it suffices to guarantee that $T(t) \leq T_c$ at $t = D$. If $E \leq E_{critical}$ and $\epsilon_h \leq \frac{T_\delta}{E} - \frac{a}{bD}\left(1 - e^{-bD}\right) \leq \frac{a}{bD}$ then $T(D) \leq T_c$ when $p(t) = \frac{E}{D}$. If $\alpha = 1$ yields $T(D) \leq T_c$, then for $\lambda(t) = \tilde{\lambda}\delta(t - D)$ and $\beta(t) = 0$, (8.44) holds and hence $\alpha^* = 1$ and $p(t) = \frac{E}{D}$ is optimal. If $\epsilon_h > \frac{a}{bD}$, then $T(t)$ in (8.45) is monotone decreasing and hence it suffices to guarantee $T(0) = T_e + \epsilon_h E \leq T_c$. For $\epsilon_h \leq \frac{T_\delta}{E} - \frac{a}{bD}\left(1 - e^{-bD}\right)$, we have $\epsilon_h E \leq T_\delta$, and therefore, $\alpha^* = 1$ and $p(t) = \frac{E}{D}$ is optimal. ■

Lemma 8.18 *For $\frac{T_\delta bD}{a} \leq E \leq E_{critical}$ and $\frac{T_\delta}{E} - \frac{a}{bD}\left(1 - e^{-bD}\right) < \epsilon_h < \frac{a}{bD}$, optimal*

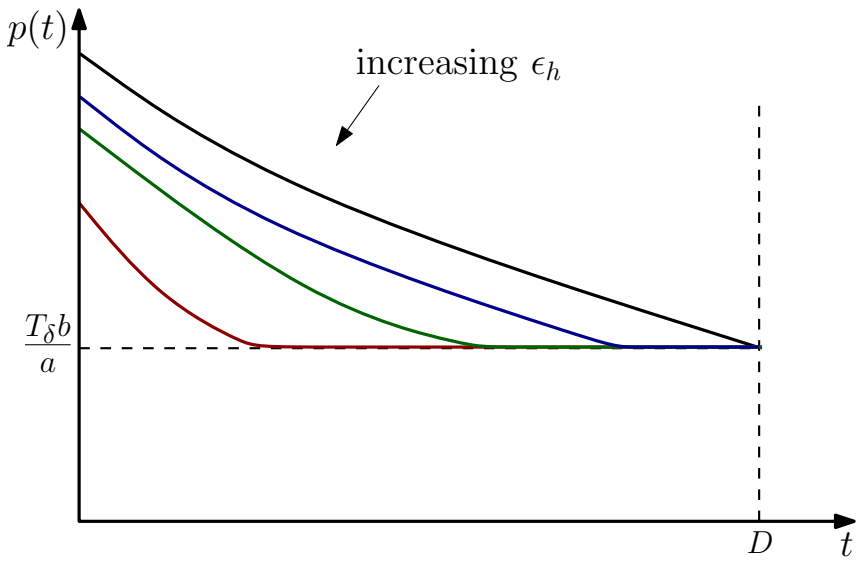

Figure 8.2: Optimal power policy with increasing ϵ_h when $E > E_{critical}$.

$p(t)$ cannot be constant.

Proof: For $\frac{T_\delta bD}{a} \leq E \leq E_{critical}$ and $\frac{T_\delta}{E} - \frac{a}{bD}\left(1 - e^{-bD}\right) < \epsilon_h < \frac{a}{bD}$, $T(t)$ is monotone increasing and $T(D) > T_c$ if $p(t) = \frac{E}{D}$. Hence, if $p(t) = \frac{\alpha E}{D}$, then $\alpha < 1$ is necessary for $T(D) \leq T_c$, and therefore, (8.44) has to be satisfied with equality if optimal $p(t)$ is constant. This, in turn, means $\int_0^D \beta(\tau)d\tau > 0$. However, the only possible solution is $\beta(t) = \tilde{\beta}\delta(t - D)$ with $\tilde{\beta} > 0$, and from (8.42), $p(t)$ cannot be constant in this case. ■

We observe that if $E > E_{critical}$, then constant power policy $p(t) = \frac{\alpha^* E}{D}$ is optimal only for $\epsilon_h \geq \frac{a}{bD}$. In this case, as ϵ_h increases from 0 to $\frac{a}{bD}$, the length of the time interval in which the optimal power policy remains constant also increases. We illustrate the variation of the optimal policy with the coefficient ϵ_h when $E > E_{criticial}$ in Fig. 8.2.

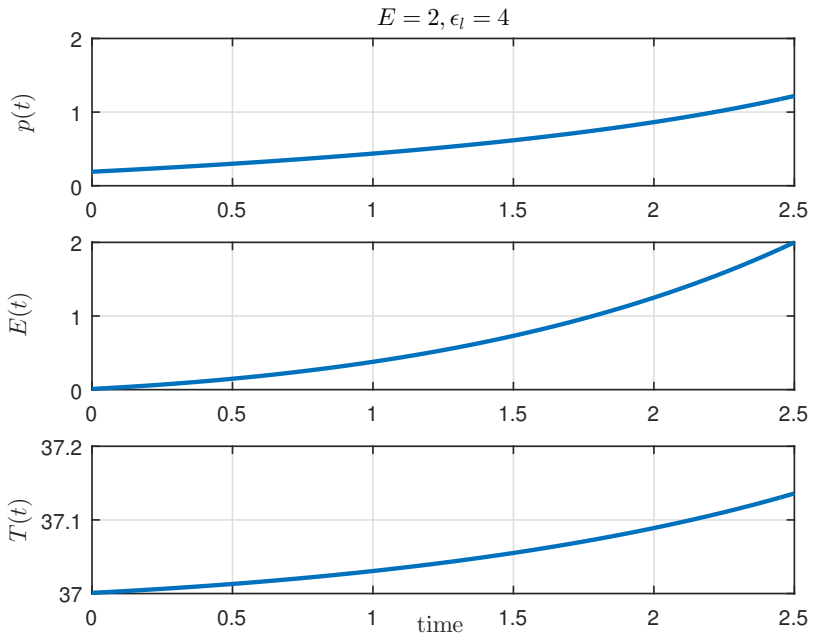

Figure 8.3: Optimal policy for the single energy arrival with temperature dependent energy leakage.

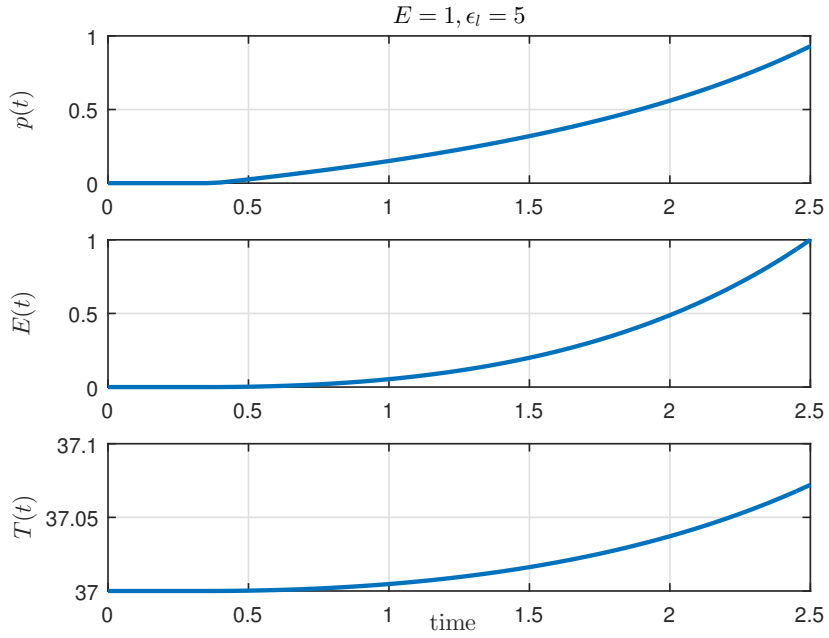

Figure 8.4: Illustration of the impact of a large leakage coefficient on the optimal policy in the single epoch case.

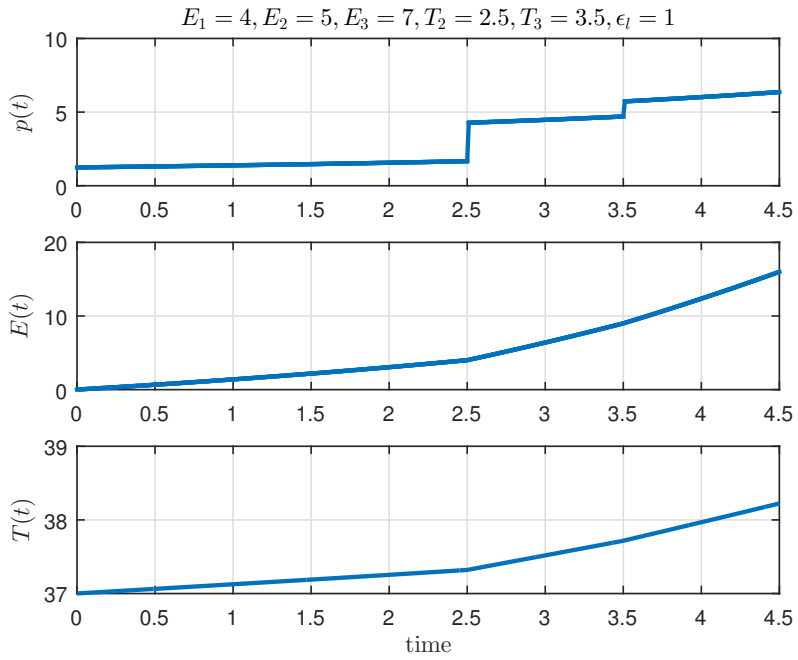

Figure 8.5: Optimal policy for three energy arrivals with temperature dependent energy leakage.

8.6 Numerical Results

In this section, we present numerical examples to illustrate our results. We take the environment temperature as $T_e = 37$.

8.6.1 Temperature Dependent Energy Leakage

In this section, we present numerical results for the problem in (8.4). We set $a = b = 0.1$. We first study the single energy arrival case. In this case, as proved in Lemma 8.1, the transmit power is strictly increasing as shown in Figs. 8.3 and 8.4. However, in Fig. 8.4, we note that since the energy is small and leakage cost is high, the transmitter remains silent at the beginning of the transmission, and begins transmission only at $t = 0.5$. The temperature is increasing as shown in Lemma 8.2.

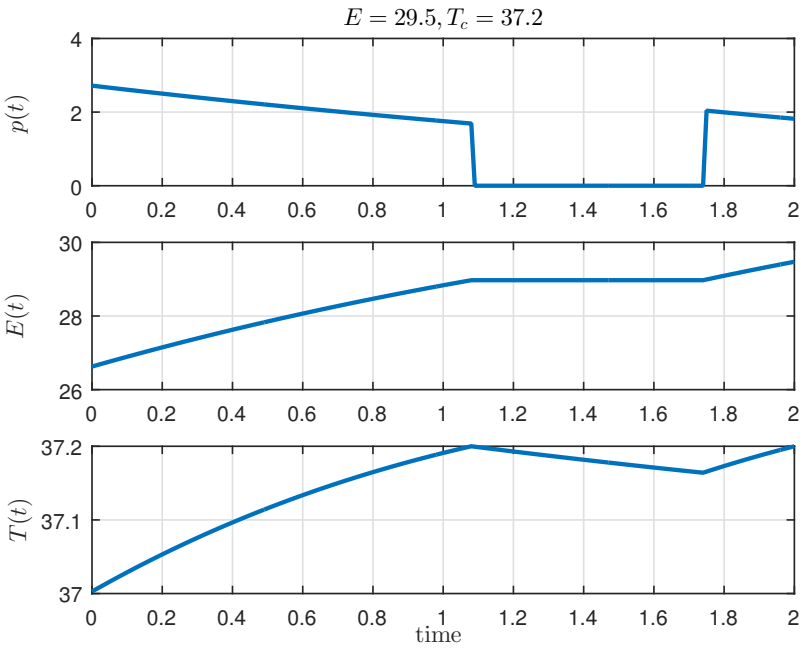

Figure 8.6: Considering both θ_1 and θ_2 with processing cost.

The battery is empty only at the end.

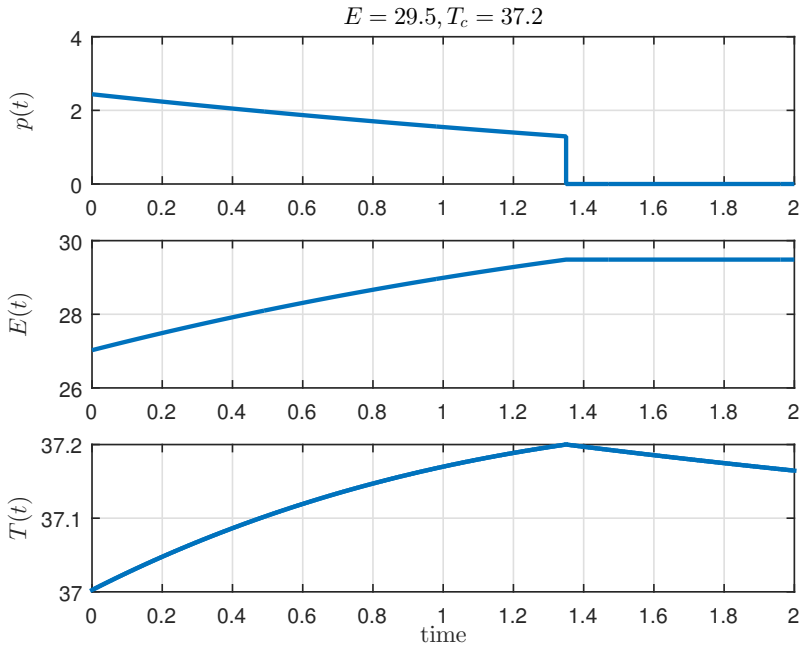

Figure 8.7: Considering only θ_1 and setting $\theta_2 = D$ with processing cost.

Then, we study the multiple energy arrival case. Fig. 8.5 shows that the power

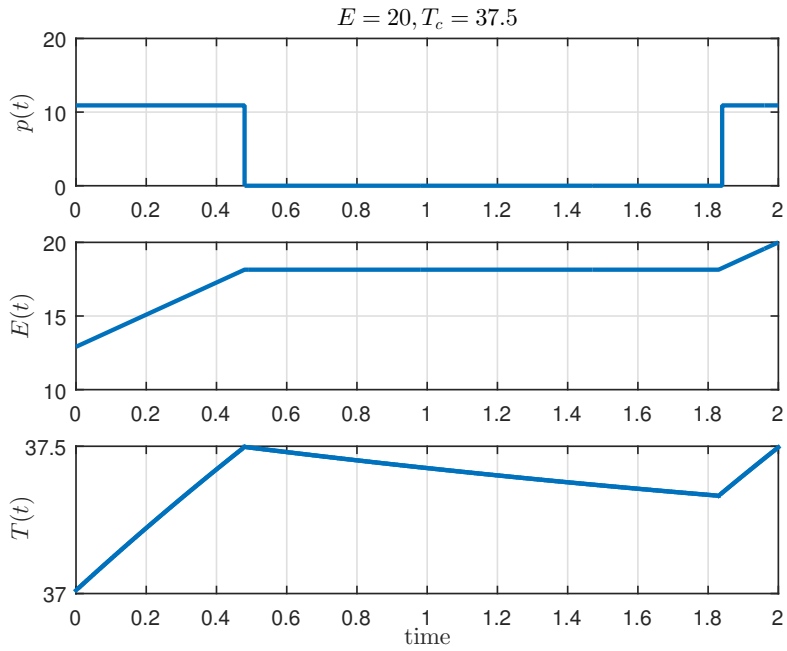

Figure 8.8: Considering both θ_1 and θ_2 with processing cost.

and temperature are strictly increasing. In Fig. 8.5, there are two positive jumps, each at an energy arrival instant. Hence, energy of each slot is used individually, and no energy is transferred between epochs.

8.6.2 Non-zero Processing Power

In this section, we present numerical results for the problem in (8.5). We set $a = 0.1$, $b = 0.3$, $\epsilon_p = 20$ and $D = 2$. We first study the setting in Fig. 8.6. The optimal value in this setting is equal to 0.77. As shown in the figure, the temperature constraint is tight at the end of transmission in each duration, hence power is decreasing in both epochs. In the middle, when the transmitter is silent, the temperature drops to create a margin for the second transmission epoch. If we do not allow splitting the transmission into two epochs, i.e., $\theta_2 = D$, then Fig. 8.7 shows the optimal solution.

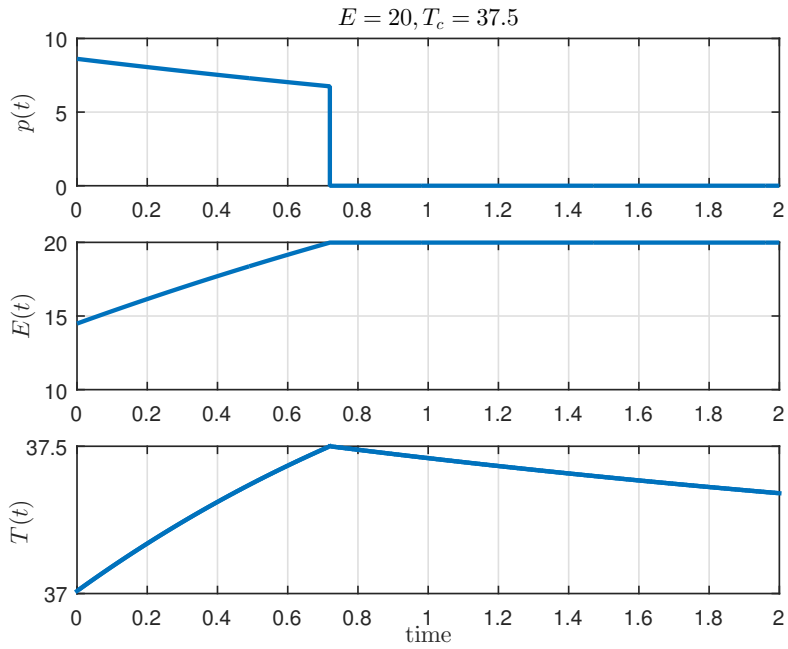

Figure 8.9: Considering only θ_1 and setting $\theta_2 = D$ with processing cost.

The optimal value in this case is 0.7 which is strictly less than the two epoch case.

Then, we study another case in Fig. 8.8. In this case, the optimal transmission power is constant. The optimal value in this case is equal to 0.82. Also, it is equal to the solution when the temperature constraint is removed. If we restrict the system to only one epoch as in Fig. 8.9, then we obtain strictly less optimal value which is 0.78, as this forces the temperature constraint to be tight and the power to be decreasing, and hence, giving less throughput.

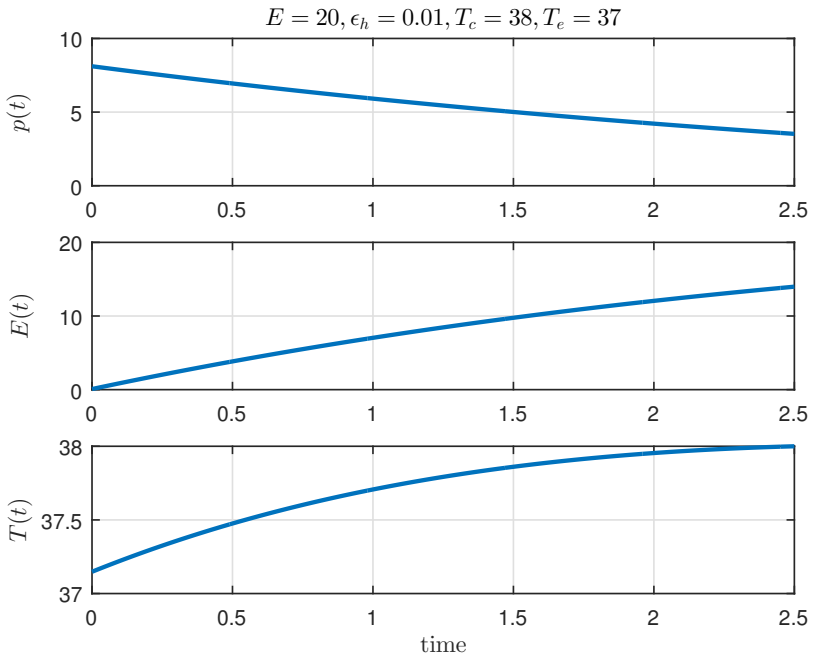

Figure 8.10: Temperature increase due to energy harvesting: single epoch.

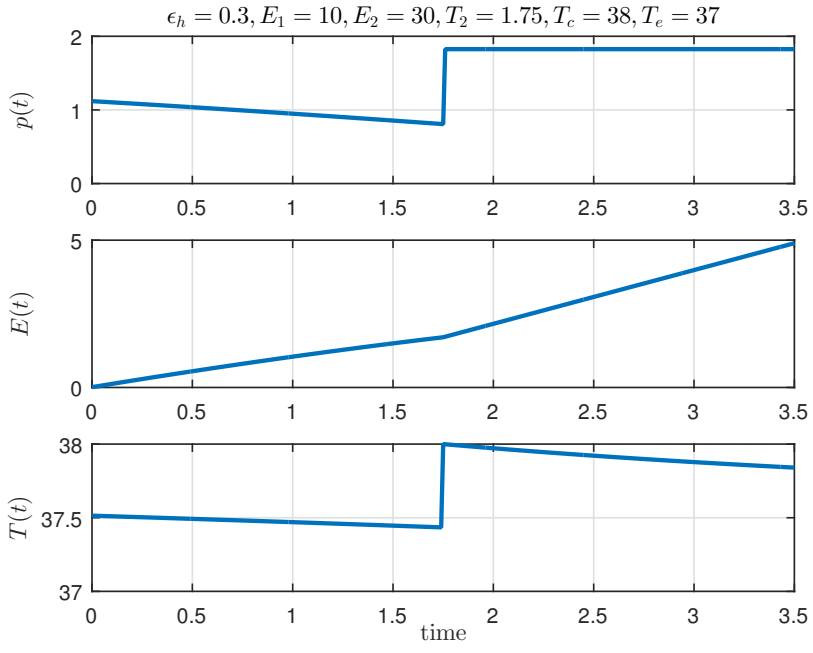

Figure 8.11: Temperature increase due to energy harvesting: multiple epochs.

8.6.3 Temperature Increase Due to Energy Harvesting

In this section, we present numerical results for the problem in (8.7). We set $a = 0.1$ and $b = 0.3$. In Fig. 8.10, we show the optimal power in the single energy arrival case. The power is monotonically decreasing, and all the admitted energy is consumed by the end of the deadline. In Fig. 8.11, we show the multiple energy arrival case, where the power is decreasing in the first epoch and the temperature is also decreasing in order to give more temperature room for the second epoch.

In both single and multiple energy arrival cases, we note that there is a positive temperature jump at the instants of the energy arrivals. This is due to the immediate heat generated by the admitted energy at these instants due to the energy harvesting process.

8.7 Conclusion

In this chapter, we studied three effects of the temperature on the power allocation of a single-user energy harvesting system. We first studied a temperature dependent energy leakage setting. In this setting, we showed that the optimal power allocation is non-decreasing, i.e, the transmitter increases the transmission rate gradually as it gets closer to the deadline. Next, we studied the effect of processing costs at the receiver with a peak temperature constraint on the policy. We restricted our attention to the case when there is only one silence (cooling) duration throughout the communication session. We showed that the cooling period needs to be in the middle of the total communication session and the optimal power allocation is non-

increasing before and after the cooling period. We studied temperature increase due to the energy harvesting process itself. We showed that it is optimal to admit energy which will be totally used.

CHAPTER 9

Energy Harvesting Communications under Explicit and Implicit Temperature Constraints

9.1 Introduction

We study the optimal power allocation policies for single-user energy harvesting communication setting, see Fig. 9.1, under temperature constraints. We consider two discrete temperature models. Each model captures a different aspect of the temperature effect on the energy harvesting communication system. The first model we study, which we coin explicit temperature constraint model, the maximum peak temperature is constrained by a fixed value. This constraint makes sure that the device does not overheat beyond a certain temperature. Next, we study another model which we coin implicit temperature constraint case. In this model, the temperature affects the channel quality. This happens as the increase in temperature is proportional to an increase in the variance of the thermal noise. We characterize the optimal power allocation for both models.

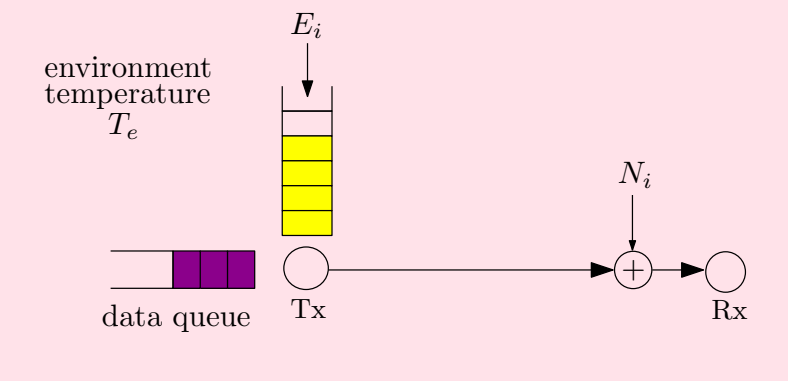

Figure 9.1: System model: the system heats up due to data transmission.

9.2 System Model

We consider an energy harvesting communication system in which the transmitter harvests energy $\tilde{E}_i$ in the ith slot, see Fig. 9.1. We consider the temperature model considered in [30,93]. In this model, the temperature, $T(t)$, evolves according to the following differential equation,

$$\frac{dT(t)}{dt} = ap(t) - b(T(t) - T_e) \tag{9.1}$$

where T_e is the environment temperature, $T(t)$ is the temperature at time t, $p(t)$ is the power, and a, b are non-negative constants. With the initial temperature $T(0) = T_e$, the solution of (9.1) is:

$$T(t) = e^{-bt} \int_0^t e^{b\tau} ap(\tau) d\tau + T_e \tag{9.2}$$

In what follows we assume that the duration of each slot is equal to Δ, which can take any positive value. Let us define $T_i \triangleq T(i\Delta)$ as the temperature level by

the end of the ith slot, $P_i \triangleq P(i\Delta)$ as the power level used in the ith slot. Using (9.2), T_i can be expressed as:

$$\begin{aligned} T_i =& e^{-bi\Delta} \int_0^{i\Delta} e^{b\tau} ap(\tau) d\tau + T_e & (9.3)\\ =& e^{-b\Delta} e^{-b(i-1)\Delta} \int_0^{(i-1)\Delta} e^{b\tau} ap(\tau) d\tau + e^{-bi\Delta} \int_{(i-1)\Delta}^{i\Delta} e^{b\tau} aP_i d\tau + T_e & (9.4)\\ =& e^{-b\Delta}(T_{i-1} - T_e) + \frac{aP_i}{b}\left[1 - e^{-b\Delta}\right] + T_e & (9.5)\\ =& \alpha T_{i-1} + \beta P_i + \gamma & (9.6) \end{aligned}$$

where $\alpha = e^{-b\Delta}$, $\beta = \frac{a}{b}\left[1-\alpha\right]$ and $\gamma = T_e\left[1-\alpha\right]$.

The effect of Δ in (9.6) appears through the constants α, β, γ. As the slot duration increases, the values of β, γ increase while the value of α decreases; as the slot duration increases, the temperature at the end of the slot becomes more dependent on the power transmitted within this slot and less dependent on the initial temperature at the beginning of the slot.

We now eliminate the previous temperature readings in T_i making the temperature a function of the powers only. We can do this by recursively substituting T_{i-1} in T_i in (9.6) to have

$$T_k = \beta \sum_{i=1}^{k} \alpha^{k-i} P_i + T_e \tag{9.7}$$

This formula shows that the temperature at the end of each slot depends on the power transmitted in this slot and all previous slots through an exponentially decaying *temperature filter*. We note that this is the same formula that was developed

in [79] in which the slot duration was assumed to be unity; here we assume a general slot duration which is equal to Δ. In what follows, we denote the vector of elements by the bold letter without a subscript, i.e., for example, the vector of powers is defined as $\mathbf{P} \triangleq [P_1, \ldots, P_D]$.

9.3 Explicit Peak Temperature Constraint

We now consider the model in which we have an energy harvesting transmitter with a peak temperature constraint. The noise variance is the same throughout the communication session and is set to σ^2. We consider a slotted system with a constant power per slot. There are D slots. It follows from (9.4) (and also [30, equation (47)]), that the temperature is monotone within the slot duration. Hence, for the peak temperature constrained case, it suffices to constrain the temperature only at the end of each slot; we begin the communication with the system having temperature T_e. In this case, the problem can be written as

$$\begin{aligned} \max_{\mathbf{P}\geq\mathbf{0}} \quad & \sum_{i=1}^{D} \frac{\Delta}{2} \log\left(1+\frac{P_i}{\sigma^2}\right) \\ \text{s.t.} \quad & T_k \leq T_c \\ & \sum_{i=1}^{k} \Delta P_i \leq \sum_{i=1}^{k} \tilde{E}_i, \ \forall k \end{aligned} \tag{9.8}$$

where Δ in the objective function and the energy constraint is to account for the slot duration. In what follows, without loss of generality, we drop Δ since it is just a constant multiplied in the objective function and by defining $E_i = \frac{\tilde{E}_i}{\Delta}$.

We rewrite problem (9.8) making use of (9.7) as

$$\begin{aligned} \max_{\mathbf{P}\geq\mathbf{0}} \quad & \sum_{i=1}^{D} \frac{1}{2}\log\left(1+\frac{P_i}{\sigma^2}\right) \\ \text{s.t.} \quad & \sum_{i=1}^{k} \alpha^{k-i} P_i \leq \frac{T_c - T_e}{\beta} \\ & \sum_{i=1}^{k} P_i \leq \sum_{i=1}^{k} E_i, \ \forall k \end{aligned} \tag{9.9}$$

In the last slot, either the temperature or the energy constraint has to be satisfied with equality. Otherwise, we can increase one of the powers until one of the constraints is met with equality and this strictly increases the objective function.

This problem is a convex problem, which can be solved optimally using the KKT conditions. The Lagrangian function for (9.9) is:

$$\begin{aligned} \mathcal{L} = & -\sum_{i=1}^{D} \log\left(1+\frac{P_i}{\sigma^2}\right) + \sum_{k=1}^{D} \lambda_k \left(\sum_{i=1}^{k} \alpha^{k-i} P_i - \frac{T_c - T_e}{\beta}\right) \\ & + \sum_{k=1}^{D} \mu_k \left(\sum_{i=1}^{k} P_i - \sum_{i=1}^{k} E_i\right) \end{aligned} \tag{9.10}$$

where λ_k and μ_k represent the Lagrange multipliers corresponding to the first set and the second set of constraints in (9.9), respectively. Differentiating with respect to P_i and equating to zero we get,

$$P_i = \frac{1}{\alpha^{-i}\sum_{k=i}^{D} \lambda_k \alpha^k + \sum_{k=i}^{D} \mu_k} - \sigma^2 \tag{9.11}$$

Additionally, the corresponding complementary slackness conditions are

$$\lambda_k \left(\sum_{i=1}^{k} \alpha^{k-i} P_i - \frac{T_c - T_e}{\beta} \right) = 0 \tag{9.12}$$

$$\mu_k \left(\sum_{i=1}^{k} P_i - \sum_{i=1}^{k} E_i \right) = 0 \tag{9.13}$$

In the optimal solution, if neither constraint was tight in slot $i < D$, then the power in slot $i+1$ is strictly less than the power in slot i. This follows from complementary slackness in (9.12)-(9.13) since if at slot i, if both constraints were not tight then we have $\lambda_i = \mu_i = 0$ which, using (9.11), implies that $P_i > P_{i+1}$.

In the optimal solution, the optimal Lagrange multipliers are non-negative, i.e., $\mu_i, \lambda_i \geq 0$. Hence, from (9.11), the following two equations are satisfied:

$$\frac{1}{P_i + \sigma^2} - \frac{1}{P_{i+1} + \sigma^2} \geq \alpha^{-i} \sum_{k=i}^{D} \lambda_k \alpha^k - \alpha^{-(i+1)} \sum_{k=i+1}^{D} \lambda_k \alpha^k \tag{9.14}$$

$$\frac{1}{P_i + \sigma^2} - \sum_{k=i}^{D} \mu_k \geq \alpha \left(\frac{1}{P_{i+1} + \sigma^2} - \sum_{k=i+1}^{D} \mu_k \right) \tag{9.15}$$

where, in slot i, (9.14) is with equality when the energy constraint is tight and (9.15) is with equality when the temperature constraint is tight. If (9.14) is not satisfied, then this implies that $\mu_i < 0$. Then, this means that we need to increase P_{i+1} or decrease P_i. The optimal solution can be found by searching over the feasible values of λ_i, μ_i until we find any solution satisfying the KKTs. The feasible values for λ_i and also μ_i is $[0, 1/A_i]$, where $A_i = \left\{ \sum_{k=1}^{i} E_k, \frac{T_c - T_e}{\beta} + \sigma^2 \right\}$. Alternatively, solving this problem can be done numerically by using standard techniques for constrained

convex optimization. In particular, one can use projected gradient descent [102] to determine the optimal Lagrange multipliers and corresponding power allocation.

In the following two subsections, we consider special cases of (9.9) which we call *energy limited case* and *temperature limited case*. In the energy limited case, the temperature budget is sufficiently large so that the problem reduces to that limited by the energy constraints only. In the temperature limited case, energy budget is sufficiently large so that the problem reduces to that limited by temperature constraints only.

9.3.1 Energy Limited Case

In this subsection, we study a sufficient condition under which the system becomes energy limited, i.e., when the temperature budget is sufficiently large so that the temperature constraints are not binding. For all slots j in which the following is satisfied

$$\sum_{i=1}^{j} E_i \leq \frac{T_c - T_e}{\beta} \tag{9.16}$$

the temperature constraint cannot be tight. Intuitively, in this case, the incoming energy is so small that it can never overheat the system. Therefore, the binding constraint here is the availability of energy. In particular, when (9.16) is satisfied for $j = D$, then the temperature constraint can be completely removed from the system. To prove this, we assume for the sake of contradiction that we have at slot

j, $\sum_{i=1}^{j} E_i \leq \frac{T_c - T_e}{\beta}$ while the temperature constraint is tight, which implies:

$$\frac{T_c - T_e}{\beta} = \sum_{i=1}^{j} \alpha^{j-i} P_i < \sum_{i=1}^{j} P_i \leq \sum_{i=1}^{j} E_i \tag{9.17}$$

which contradicts the assumption $\sum_{i=1}^{j} E_i \leq \frac{T_c - T_e}{\beta}$. The strict inequality follows since $\alpha < 1$. The structure of the optimal solution for this case is studied in [1].

9.3.2 Temperature Limited Case

In this subsection, we first study a sufficient condition for problem (9.9) to be temperature limited, i.e., when the energy budget is sufficiently large so that the energy constraints are not binding. The energy constraint is never tight if the following condition is satisfied:

$$\frac{T_c - T_e}{\beta} < \frac{\sum_{i=1}^{k} E_i}{k}, \ \forall k \in \{1, \ldots, D\} \tag{9.18}$$

Intuitively, the incoming energy is so large that there will never be a shortage of energy. Therefore, the binding constraint here is overheating the system. For the temperature limited case, an upper bound on the transmission powers is equal to $\frac{T_c - T_e}{\beta}$. This follows because for any slot k we have $\sum_{i=1}^{k-1} \alpha^{k-i} P_i + P_k \leq \frac{T_c - T_e}{\beta}$, thus P_k can be at most equal to $\frac{T_c - T_e}{\beta}$. Hence, (9.18) is sufficient to satisfy $\sum_{i=1}^{k} P_i < \sum_{i=1}^{k} E_i$.

In what follows, we study the structure of the optimal policy for the temperature limited case. In the last slot, the temperature constraint is satisfied with equal-

ity. The optimal powers are monotonically decreasing in time. The proof follows by contradiction. Assume for some index j that we have $P_j^* < P_{j+1}^*$. We now form another policy, denoted as $\{\bar{P}_i\}$, which has $\bar{P}_i = P_i^*$ for all slots $i \neq j, j+1$, while we change the powers of slots $j, j+1$ to be $\bar{P}_j = P_j^* + \delta$ and $\bar{P}_{j+1} = P_{j+1}^* - \delta$ for small enough $\delta > 0$. This δ always exists as $P_j^* < P_{j+1}^*$ implies that $\sum_{k=1}^{j} \alpha^{j-k} P_k^* < \frac{T_c - T_e}{\beta}$. Since the objective function is strictly concave, this new policy yields a strictly higher objective function, which contradicts the optimality of $P_j^* < P_{j+1}^*$. Now it remains to check that with this new policy, the temperature constraint is still feasible for any slot $k \geq j+1$ which follows from:

$$\sum_{i=1,\neq j,j+1}^{k} \alpha^{k-i} \bar{P}_i + \alpha^{k-j} \bar{P}_j + \alpha^{k-j-1} \bar{P}_{j+1} = \sum_{i=1,\neq j,j+1}^{k} \alpha^{k-i} P_i^* + \alpha^{k-j} \bar{P}_j + \alpha^{k-j-1} \bar{P}_{j+1} \tag{9.19}$$

$$< \sum_{i=1,\neq j,j+1}^{k} \alpha^{k-i} P_i^* + \alpha^{k-j} P_j^* + \alpha^{k-j-1} P_{j+1}^* \tag{9.20}$$

$$= \sum_{i=1}^{k} \alpha^{k-i} P_i^* \tag{9.21}$$

$$< \frac{T_c - T_e}{\beta} \tag{9.22}$$

Since this is valid for any $k \geq j+1$, we can take in particular $k = D$. Now we can increase any of the powers to satisfy the last inequality by equality which strictly improves the objective function. Hence, this violates the optimality of any policy which has $P_i^* < P_{i+1}^*$ for any $i \in \{1, \ldots, D\}$.

Moreover, the optimal temperature levels are non-decreasing in time. To prove this, using (9.7), it suffices to show that:

$$\sum_{i=1}^{k} \alpha^{k-i} P_i^* \leq \sum_{i=1}^{k+1} \alpha^{k+1-i} P_i^*, \quad \forall k = \{1, \ldots, D-1\} \tag{9.23}$$

We rewrite (9.23) as follows,

$$(1-\alpha) \sum_{i=1}^{k} \alpha^{k-i} P_i^* \leq P_{k+1}^*, \quad \forall k = \{1, \ldots, D-1\} \tag{9.24}$$

Since, we know that the last slot has to be satisfied with equality then we know $\sum_{i=1}^{D} \alpha^{D-i} P_i^* = \frac{T_c - T_e}{\beta}$. Hence, for the constraint at $k = D-1$ we have:

$$\sum_{i=1}^{D-1} \alpha^{D-1-i} P_i^* \leq \frac{T_c - T_e}{\beta} = \sum_{i=1}^{D} \alpha^{D-i} P_i^* \tag{9.25}$$

which can be written as follows

$$(1-\alpha) \sum_{i=1}^{D-1} \alpha^{D-1-i} P_i^* \leq P_D^* \tag{9.26}$$

which proves (9.24) for $k = D-1$. Now assume for the sake of contradiction that (9.24) is false for $k = D-2$, i.e.:

$$P_{D-1}^* < (1-\alpha) \sum_{i=1}^{D-2} \alpha^{D-2-i} P_i^* \tag{9.27}$$

Substituting this in (9.26), we get:

$$P^*_{D-1} = \alpha P^*_{D-1} + (1-\alpha)P^*_{D-1} \tag{9.28}$$

$$< \alpha(1-\alpha)\sum_{i=1}^{D-2} \alpha^{D-2-i} P^*_i + (1-\alpha)P^*_{D-1} \tag{9.29}$$

$$= (1-\alpha)\sum_{i=1}^{D-1} \alpha^{D-1-i} P^*_i \leq P^*_D \tag{9.30}$$

But since we know that in the optimal policy the power sequence is monotone decreasing, this is a contradiction and (9.24) holds for $k = D-2$. The same argument follows for any $k < D-2$.

In the optimal solution, if the constraint is satisfied with equality for two consecutive slots then the power in the second slot must be equal to $(1-\alpha)\frac{T_c - T_e}{\beta}$. To obtain this, the two consecutive constraints which are satisfied with equality are solved simultaneously for the power in the second slot. In addition, when the temperature hits the critical temperature for the first time, the transmission power in that slots will be *strictly higher* than $(1-\alpha)\frac{T_c - T_e}{\beta}$. To show this we denote the time slot at which the temperature hits T_c for the first time as i^*. Hence, we have:

$$\sum_{i=1}^{i^*-1} \alpha^{i^*-1-i} P_i < \frac{T_c - T_e}{\beta}, \quad \sum_{i=1}^{i^*} \alpha^{i^*-i} P_i = \frac{T_c - T_e}{\beta} \tag{9.31}$$

Using both equations in (9.31) simultaneously we have:

$$(1-\alpha)\frac{T_c - T_e}{\beta} < P_{i^*} \tag{9.32}$$

which is the power of the slot at which temperature hits the critical temperature for the first time.

Hence, when the temperature hits the critical temperature, the optimal transmission power in all the subsequent slots becomes constant and equal to $(1-\alpha)\frac{T_c-T_e}{\beta}$. This follows since the temperature is increasing, thus whenever the constraint becomes tight, it remains tight for all subsequent slots. We now conclude that the transmission power at all slots are bounded as follows

$$(1-\alpha)\frac{T_c-T_e}{\beta} \leq P_i \leq \frac{T_c-T_e}{\beta}, \quad \forall i = \{1,\ldots,D\} \tag{9.33}$$

The lower bound follows from the discussion above while the upper bound follows from the feasibility of the constraints.

We now proceed to find the optimal power allocation. Since the problem is convex, a necessary and sufficient condition is to find a solution satisfying the KKTs. The optimal power is given by setting $\boldsymbol{\mu} = \mathbf{0}$ in (9.11), which gives:

$$P_i = \frac{\alpha^i}{\sum_{k=i}^{D} \lambda_k \alpha^k} - \sigma^2 \tag{9.34}$$

It follows from the complementary slackness that if at slot i the temperature constraint is satisfied with strict inequality then $P_{i+1} < P_i$.

To this end we present an approach to obtain the optimal powers. We use line search to search for the time slot at which the temperature constraint becomes tight, which we denote as i^*. Then, slots $i = \{i^*+1,\ldots,D\}$ have power allocation

equal to $(1-\alpha)\frac{T_c-T_e}{\beta}$, while the power allocations for slots $i = \{1, \ldots, i^*\}$ are strictly decreasing and strictly higher than $(1-\alpha)\frac{T_c-T_e}{\beta}$. Hence, we initialize $i^* = D$ and search for a solution for the powers satisfying the KKTs. If we obtain a solution then we stop and this is the optimal solution. Otherwise, we decrease i^* by one and repeat the search.

9.4 Implicit Temperature Constraint

We now consider the case when the dynamic range of the temperature increases. In this case, we need to consider the change in the thermal noise of the system due to temperature changes. The thermal noise is linearly proportional to the temperature [108, Chapter 11]. The problem can be written as:

$$\begin{aligned} \max_{\mathbf{P}\geq\mathbf{0}} \quad & \sum_{i=1}^{D} \frac{1}{2}\log\left(1+\frac{P_i}{cT_{i-1}+\sigma^2}\right) \\ \text{s.t.} \quad & \sum_{i=1}^{k} P_i \leq \sum_{i=1}^{k} E_i, \ \forall k \end{aligned} \tag{9.35}$$

where c is the proportionality constant between the thermal noise and the temperature. In this setting, the noise variance in each slot is determined by the value of the temperature at the beginning of the slot. Using (9.7) in (9.35), the problem can now be written in terms of only transmission powers as follows:

$$\max_{\mathbf{P}\geq\mathbf{0}} \quad \sum_{i=1}^{D} \frac{1}{2}\log\left(1+\frac{P_i}{c\left(\beta\sum_{k=1}^{i-1}\alpha^{i-1-k}P_k+T_e\right)+\sigma^2}\right)$$

$$\text{s.t.} \quad \sum_{i=1}^{k} P_i \leq \sum_{i=1}^{k} E_i, \ \forall k \tag{9.36}$$

where we define $\text{SINR}_i \triangleq \frac{P_i}{c\beta \sum_{k=1}^{i-1} \alpha^{i-1-k} P_k + cT_e + \sigma^2}$. In what follows, in order to simplify the notation, we assume without loss of generality that $c\beta = 1$ and we define $\Gamma_j \triangleq \frac{cT_e+\sigma^2}{\alpha^j}$. Therefore, SINR_i inside the log in (9.36) becomes $\text{SINR}_i = \frac{P_i}{\sum_{k=1}^{i-1} \alpha^{i-1-k} P_k + \Gamma_0}$.

The problem in this form highlights the effect of previous transmissions on subsequent slots. The transmission power at time i appears as an *interfering term* at slot indices greater than i with an exponentially decaying weight due to the *filtering* in the temperature. Using (9.7), the maximum temperature the system can reach is equal to $T_{max} \triangleq \beta \sum_{i=1}^{D} E_i + T_e$. This occurs when the transmitter transmits all its energy arrivals in the last slot. The value of T_{max} is useful in determining the maximum possible temperature for the system. As we show, in the low SINR case in Section 9.4.1, the optimal power allocation results in system temperature equal to T_{max}.

The problem in (9.36) is non-convex and determining the global optimal solution is generally a difficult task. Next, we adapt the signomial programming based iterative algorithm in [83] for the energy harvesting case. This algorithm provably converges to a local optimum point. The problem in (9.36) can be written in the following equivalent signomial minimization problem

$$\begin{aligned} \min_{\mathbf{P} \geq \mathbf{0}} \quad & \prod_{i=1}^{D} \left(\frac{\sum_{k=1}^{i-1} \alpha^{i-1-k} P_k + \Gamma_0}{\sum_{k=1}^{i-1} \alpha^{i-1-k} P_k + \Gamma_0 + P_i} \right) \\ \text{s.t.} \quad & \sum_{i=1}^{k} P_i \leq \sum_{i=1}^{k} E_i, \ \forall k \end{aligned} \tag{9.37}$$

The objective function in (9.37) is a signomial function which is a ratio between two posynomials. Note also that the energy harvesting constraints in (9.37) are posynomials in P_i.

In each iteration we approximate the objective by a posynomial. We do this by approximating the posynomial in the denominator by a monomoial. Appropriate choice of an approximation which satisfies the conditions in [109] guarantees convergence to a local optimal solution. Let us denote the posynomial in the ith denominator evaluated using a power vector $\mathbf{P}$ by $u_i(\mathbf{P})$, i.e., we have

$$u_i(\mathbf{P}) \triangleq \sum_{k=1}^{i+1} v_k^i(\mathbf{P}) = \sum_{k=1}^{i-1} \alpha^{i-1-k} P_k + P_i + \Gamma_0 \tag{9.38}$$

where for $k = \{1, \ldots, i-1\}$ we have $v_k^i(\mathbf{P}) = \alpha^{i-1-k} P_k$, $v_i^i(\mathbf{P}) = P_i$ and $v_{i+1}^i(\mathbf{P}) = \Gamma_0$.

Using the arithmetic-geometric mean inequality, we approximate each posynomial by a monomial as follows:

$$u_i(\mathbf{P}) \geq \left(\prod_{k=1}^{i-1} \left(\frac{\alpha^{i-1-k} P_k}{\theta_k^i} \right)^{\theta_k^i} \right) \left(\frac{P_i}{\theta_i^i} \right)^{\theta_i^i} \left(\frac{\Gamma_0}{\theta_{i+1}^i} \right)^{\theta_{i+1}^i} \tag{9.39}$$

where $\sum_{k=1}^{i+1} \theta_k^i = 1$ for all $i = \{1, \ldots, D\}$.

We now solve the problem in (9.37) iteratively. First, we initialize the power allocation to any feasible power allocation $\mathbf{P}^0$. Then, we approximate the posynomials $u_i(\mathbf{P}^0)$ using the arithmetic-geometric mean inequality shown above. In each iteration j, where the power allocation is $\mathbf{P}^j$, we choose θ_k^i as a function of the

Algorithm 1 Single-condensation method

1: Initialize $P_i = E_i$
2: **repeat**
3: For $k = \{1, \ldots, i-1\}$, calculate $v_k^i(\mathbf{P}) = \alpha^{i-1-k} P_k$
4: Set $v_{i+1}^i(\mathbf{P}) = \Gamma_0$ and $v_i^i(\mathbf{P}) = P_i$
5: Calculate $u_i(\mathbf{P})$ using (9.38)
6: Calculate $\theta_k^i(\mathbf{P}^j)$ according to (9.40)
7: Approximate $u_i(\mathbf{P})$ using (9.39)
8: Solve problem (9.37) using the approximate objective function calculated in Step 7
9: **until** Convergence to a local optimal solution

posynomials and the current power allocation as follows:

$$\theta_k^i(\mathbf{P}^j) = \frac{v_k^i(\mathbf{P}^j)}{u_i(\mathbf{P}^j)} \tag{9.40}$$

which satisfies $\sum_{k=1}^{i+1} \theta_k^i(\mathbf{P}^j) = 1$. This choice of $\theta_k^i(\mathbf{P}^j)$ guarantees that the iterations converge to a KKT point of the original problem [109]. In particular, for each iteration this is a geometric program and as required by [109], this can be transformed into a convex problem; see also [83]. A pseudo code for this procedure is provided in Algorithm 1. In each iteration, the computation complexity of finding the solution of the convex problem is polynomial in the number of constraints and the number of variables, see [110].

The above iterative approach converges to a local optimal solution. Achieving the global optimal solution is of exponential complexity. Alternatively, to get to the optimal solution, an approach introduced in [111] can be used. This approach solves

the following problem iteratively:

$$\begin{aligned} \min_{\mathbf{P}\geq\mathbf{0},t} \quad & t \\ \text{s.t.} \quad & O(\mathbf{P}) \leq t \\ & t \leq \frac{t_0}{\alpha} \\ & \sum_{i=1}^{k} P_i \leq \sum_{i=1}^{k} E_i, \ \forall k \end{aligned} \tag{9.41}$$

where $O(\mathbf{P})$ is the objective function of (9.37) and α is chosen to be a number which is slightly more than 1 and t_0 can be initialized to be the solution of problem (9.37) and then updated as the optimal solutions resulting from (9.41).

This completes our treatment of the general problem for the case of implicit temperature constraints. In the following two subsections, we consider the two special cases of low and high SINR, where we are able to provide more structural solutions.

9.4.1 Low SINR Case

The low SINR case occurs when the incoming energies are small with respect to the noise variance. In this case, an approximation to the logarithm function in the objective function is the linear function, i.e., $\log(1+x) \approx x$. Hence, the objective function of (9.36) can be written as follows, c.f. [112, equation (14)]:

$$\sum_{i=1}^{D} \frac{P_i}{\sum_{k=1}^{i-1} \alpha^{i-1-k} P_k + \Gamma_0} \tag{9.42}$$

We next show that the optimal power allocation dictates that the energy is saved till the last slot and transmitted then, i.e.,

$$P_i^* = 0, \quad i \leq D-1, \quad \text{and} \quad P_D^* = \sum_{i=1}^{D} E_i \tag{9.43}$$

This can be proved by developing an upper bound as follows:

$$\sum_{i=1}^{D} \frac{P_i}{\sum_{k=1}^{i-1} \alpha^{i-1-k} P_k + \Gamma_0} \leq \sum_{i=1}^{D} \frac{P_i}{\Gamma_0} \tag{9.44}$$

$$\leq \frac{\sum_{i=1}^{D} E_i}{\Gamma_0} \tag{9.45}$$

and noting that this bound is achieved by the claimed power allocation.

A sufficient condition to have a low SINR regime is $\sum_{i=1}^{D} E_i \ll \Gamma_0$. The temperature at the end of the communication session is equal to $T_{max} = \beta \sum_{i=1}^{D} E_i + T_e$. Also, the optimal power allocation does not need the non-causal knowledge of the energy arrival process, as all the harvested energy is used in the last slot.

9.4.2 High SINR Case

When the values of c and σ are small, SINR is high and we approximate the objective function by ignoring 1 inside the logarithm, i.e., $\log(1+x) \approx \log(x)$. Hence, the problem in (9.36) can be written as:

$$\max_{\mathbf{P} \geq \mathbf{0}} \quad \sum_{i=1}^{D} \frac{1}{2} \log \left(\frac{P_i}{\sum_{k=1}^{i-1} \alpha^{i-1-k} P_k + \Gamma_0} \right)$$

$$\text{s.t.} \quad \sum_{i=1}^{k} P_i \leq \sum_{i=1}^{k} E_i, \ \forall k \tag{9.46}$$

The problem in (9.46) has the Lagrangian:

$$\mathcal{L} = -\sum_{i=1}^{D} \log\left(\frac{P_i}{\sum_{k=1}^{i-1} \alpha^{i-1-k} P_k + \Gamma_0}\right) + \sum_{k=1}^{D} \mu_k \left(\sum_{i=1}^{k} P_i - \sum_{i=1}^{k} E_i\right) \tag{9.47}$$

Taking the derivative with respect to P_i gives,

$$\frac{\partial \mathcal{L}}{\partial P_i} = -\frac{1}{P_i} + \sum_{j=i+1}^{D} \frac{\alpha^{j-1-i}}{\sum_{k=1}^{j-1} \alpha^{j-1-k} P_k + \Gamma_0} + \sum_{k=i}^{D} \mu_k \tag{9.48}$$

and then equating to zero gives:

$$\frac{1}{P_i} - \sum_{j=i+1}^{D} \frac{\alpha^{j-1-i}}{\sum_{k=1}^{j-1} \alpha^{j-1-k} P_k + \Gamma_0} = \sum_{k=i}^{D} \mu_k \tag{9.49}$$

Although the problem in (9.46) is non-convex, it is a geometric program and we show next that any local optimal solution for this problem is globally optimal. To show this, we consider the following equivalent problem:

$$\begin{aligned} \min_{\mathbf{x} \in \mathbb{R}^D} \quad & \sum_{i=1}^{D} \frac{1}{2} \log\left(\frac{\sum_{k=1}^{i-1} \alpha^{i-1-k} e^{x_k} + \Gamma_0}{e^{x_i}}\right) \\ \text{s.t.} \quad & \sum_{i=1}^{k} e^{x_i} \leq \sum_{i=1}^{k} E_i, \ \forall k \end{aligned} \tag{9.50}$$

This equivalent problem is obtained by substituting $P_i = e^{x_i}$ and letting $x_i \in \mathbb{R}$. The equivalent problem in (9.50) is a convex optimization problem since the objective

is a convex function in the form of a log-sum-exponent and the constraint set is a convex set [102]. Hence, the KKTs are necessary and sufficient for global optimality. We show this as follows.

We first write the Lagrangian of problem (9.50) as:

$$\mathcal{L} = -\sum_{i=1}^{D} \log\left(\frac{e^{x_i}}{\sum_{k=1}^{i-1} \alpha^{i-1-k} e^{x_k} + \Gamma_0}\right) + \sum_{k=1}^{D} \nu_k \left(\sum_{i=1}^{k} e^{x_i} - \sum_{i=1}^{k} E_i\right) \tag{9.51}$$

Taking the derivative with respect to x_i gives,

$$\frac{\partial \mathcal{L}}{\partial x_i} = -1 + \sum_{j=i+1}^{D} \frac{\alpha^{j-1-i} e^{x_i}}{\sum_{k=1}^{j-1} \alpha^{j-1-k} e^{x_k} + \Gamma_0} + e^{x_i} \sum_{k=i}^{D} \nu_k \tag{9.52}$$

which provides the following necessary condition:

$$e^{-x_i} - \sum_{j=i+1}^{D} \frac{\alpha^{j-1-i}}{\sum_{k=1}^{j-1} \alpha^{j-1-k} e^{x_k} + \Gamma_0} = \sum_{k=i}^{D} \nu_k \tag{9.53}$$

Using the transformation $x_i = \log(P_i)$ and setting $\nu_i = \mu_i$, we observe that any solution of (9.49) satisfies (9.53). Also, complementary slackness corresponding to (9.47) is satisfied if and only if it is satisfied by those for (9.51). Since the equivalent problem in (9.50) is convex, any solution satisfying the KKTs is global optimal and through the transformation $x_i = \log(P_i)$, $\mu_i = \nu_i$ is also global optimal in the original problem in (9.46).

The equivalent problem in (9.50) can be solved using any convex optimization toolbox. We further note that the equivalent problem and the original problem both have unique solutions. More generally, for any fixed multipliers $\boldsymbol{\mu}$, the primal

problem of minimizing the Lagrangian function in (9.47) has a unique solution. This follows because the Lagrangian function in (9.51) is strictly convex as it is formed with strictly convex constraint functions and a convex objective function; for fixed Lagrange multipliers the Lagrangian function in (9.51) is strictly convex.

We now focus on the KKT conditions of the original problem (9.46). Our ultimate goal in the following discussion is to show that the optimal solution of (9.46) has a power allocation which is monotone increasing in time index i, that is, $P_i \leq P_{i+1}$. We prove this by showing that the solution of the corresponding KKTs in (9.49) with an arbitrary $\boldsymbol{\mu} \geq 0$ is monotone increasing in time index i, hence, this also follows for the optimal $\boldsymbol{\mu}^*$. We provide the proof for this fact in Appendix 9.8.1. The proof is enabled by developing an algorithm with an update rule which satisfies the properties of *standard interference functions* introduced in [113]. Hence, from [113, Theorem 2], the algorithm converges to a unique fixed point. We then show that the power allocation at this unique fixed point is monotone increasing in time. Then, from strict convexity of this problem, we know that KKTs in (9.49) have a unique solution. Hence, our algorithm converges to the unique solution of the KKTs in (9.49) and this solution has monotone increasing power allocations. When compared to its predecessors in [1–5, 8], our method yields a more general class of problems in which optimal power allocation is monotone increasing under energy harvesting constraints. We also note that due to [30, Lemma 3] and since the powers are monotone increasing, the temperature sequence T_i^* resulting from the optimal power allocation P_i^* is also monotone increasing.

In order to obtain the optimal solution, one has to determine the optimal

Lagrange multipliers $\boldsymbol{\mu}^*$ and the power allocation $\mathbf{P}$. This can be done numerically by using standard techniques for constrained convex optimization. In particular, one can use projected gradient descent [102] in the equivalent convex problem in (9.50) to determine $\boldsymbol{\mu}^*$ and corresponding power allocation.

9.5 Explicit and Implicit Temperature Constraints

In this section, we consider the case when both implicit and explicit temperature constraints are active. In this case, the temperature controls the channel quality and is also constrained by a critical level. This problem is in the following form:

$$\begin{aligned} \max_{\mathbf{P}\geq\mathbf{0}} \quad & \sum_{i=1}^{D} \frac{1}{2} \log\left(1 + \frac{P_i}{\sum_{k=1}^{i-1} \alpha^{i-1-k} P_k + \Gamma_0}\right) \\ \text{s.t.} \quad & \sum_{i=1}^{k} \alpha^{k-i} P_i \leq \frac{T_c - T_e}{\beta} \\ & \sum_{i=1}^{k} P_i \leq \sum_{i=1}^{k} E_i, \ \forall k \end{aligned} \tag{9.54}$$

which is a non-convex optimization problem. We can tackle the challenge due to non-convexity here as we did in Section 9.4. In particular, in the general SINR case, one can reach a local optimal solution for problem (9.54) using the signomial programming approach described there. On the other hand, in the low SINR case, the objective function in (9.54) is approximated by $\sum_{i=1}^{D} \frac{P_i}{\sum_{k=1}^{i-1} \alpha^{i-1-k} P_k + \Gamma_0}$ and it is a fractional program which can in general be mapped to a linear program.

The problem in (9.54) possesses some of the properties of the problem with explicit temperature constraints only studied in Section 9.3. In particular, if the

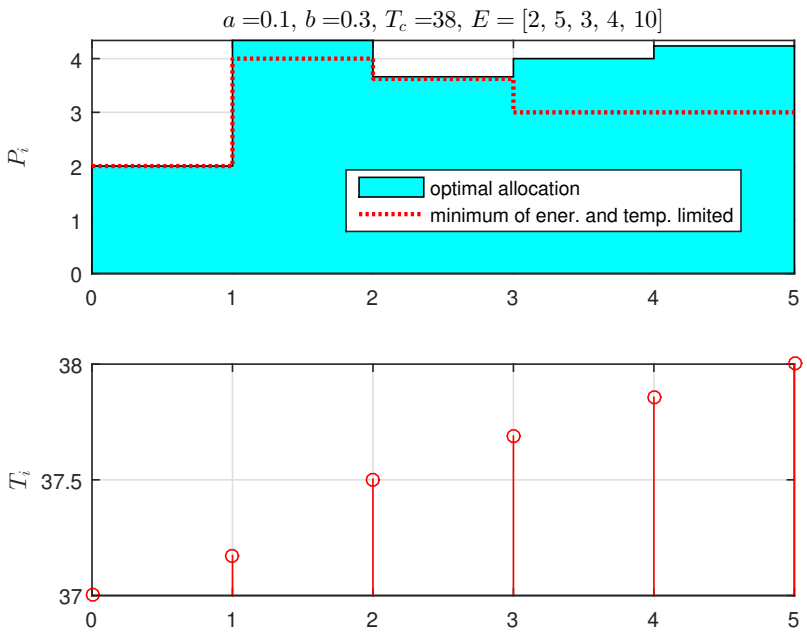

Figure 9.2: Simulation for explicit temperature constraint: general case.

temperature constraint is tight for two consecutive slots in the optimal solution, then the power level in the second slot must be equal to $\frac{T_c-T_e}{\beta}(1-\alpha)$. Additionally, when the temperature at the end of a slot hits T_c for the first time, then the power in that slot must be strictly higher than $\frac{T_c-T_e}{\beta}(1-\alpha)$. We also note that the problem reduces to the case of implicit temperature constraint when the energy arrivals satisfy $\sum_{i=1}^{D} E_i \leq \frac{T_c-T_e}{\beta}$ as the explicit temperature constraint is never tight in this case.

In the high SINR case, we have $\log(1+x) \approx \log(x)$ and the problem (9.54) is a geometric program which can be transformed to an equivalent convex problem. In general, the optimal power sequence does not have a monotonic structure in this case. When harvested energies are sufficiently large and the energy constraints are not binding, and if $\alpha \leq \frac{\beta\Gamma_0}{T_c-T_e+\beta\Gamma_0}$, then the optimal power sequence P_i is mono-

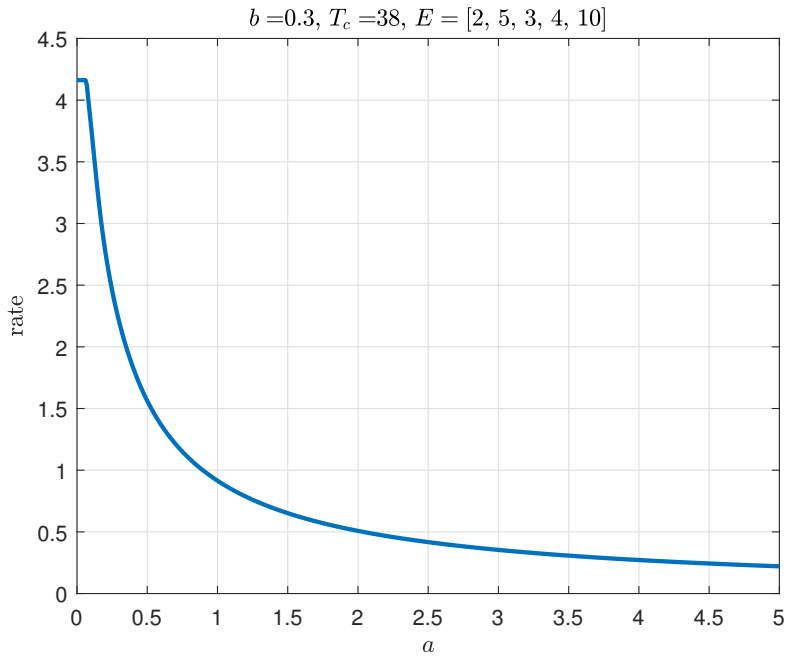

Figure 9.3: Simulation for explicit temperature constraint, general case: optimal achieved rate versus a.

tone decreasing and when the temperature hits T_c, the power becomes constant and is equal to $\frac{(T_c - T_e)(1-\alpha)}{\beta}$. Furthermore, under this condition the temperature is monotone increasing. We provide the proof for these facts in Appendix 9.8.2.

9.6 Numerical Results

In this section we present some numerical results. Unless stated otherwise, we assume σ^2 to be equal to unity throughout this section. We first consider the explicit peak temperature constrained model considered in Section 9.3. As shown in Fig. 9.2, in general the power allocation does not possess any monotonicity. The optimal power allocation is close to the minimum of the power allocation of the energy and temperature limited cases. We also show in Fig. 9.3 the optimal rate versus different

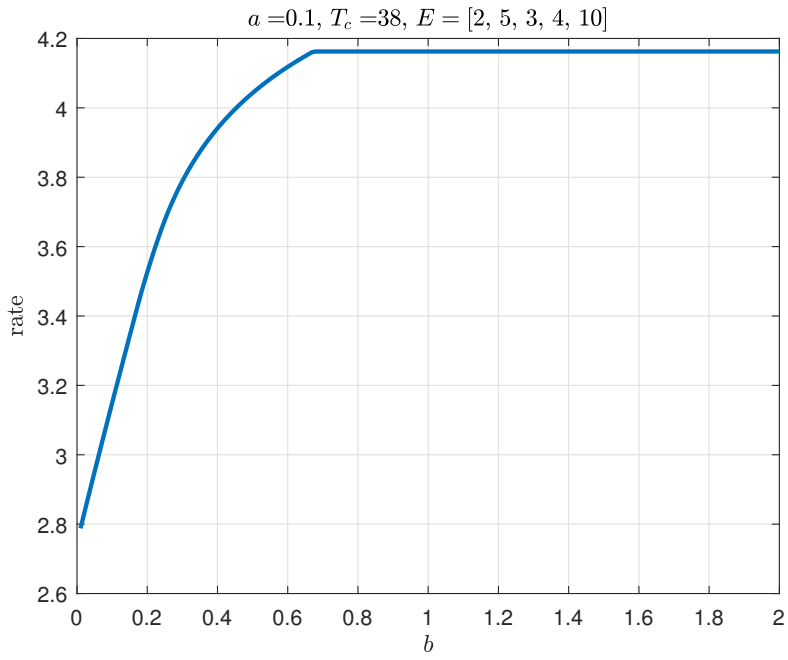

Figure 9.4: Simulation for explicit temperature constraint, general case: optimal rate versus b.

values of a. As the value of a increases, the value fo β increases and hence the effect of the explicit temperature constraint becomes more evident and the rate decreases. The opposite behavior is observed for b. As the value of b increases, the value of β decreases and the effect of the explicit temperature constraint becomes less evident. We study the temperature limited case considered in Section 9.3.2 in Fig. 9.5. When the temperature is strictly increasing, the power is strictly decreasing. When the temperature reaches the critical level, the power remains constant.

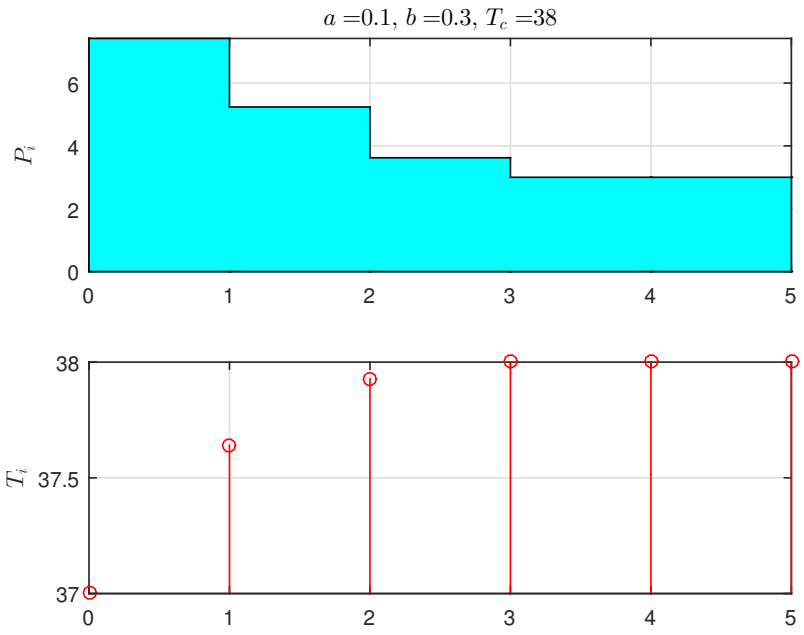

Figure 9.5: Simulation for explicit temperature constraint: temperature limited case.

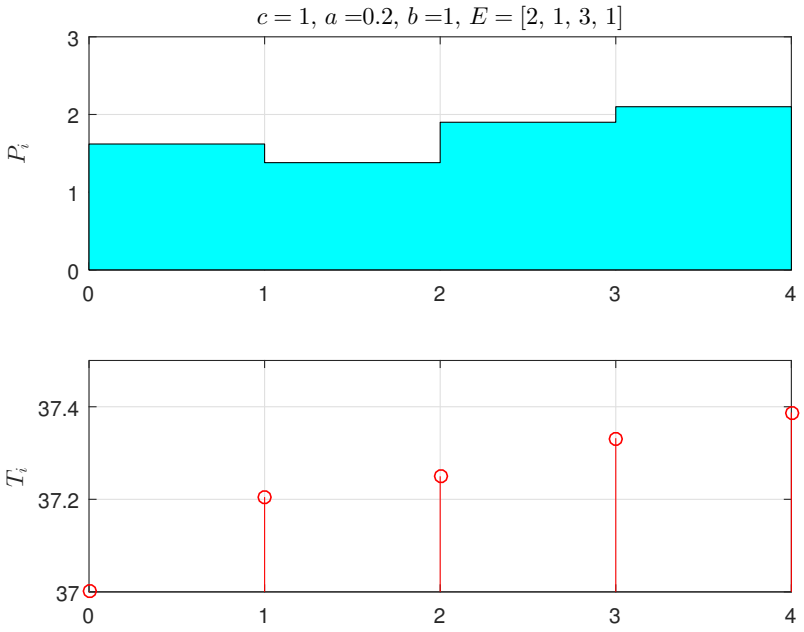

Figure 9.6: Simulation for implicit temperature constraint: general case.

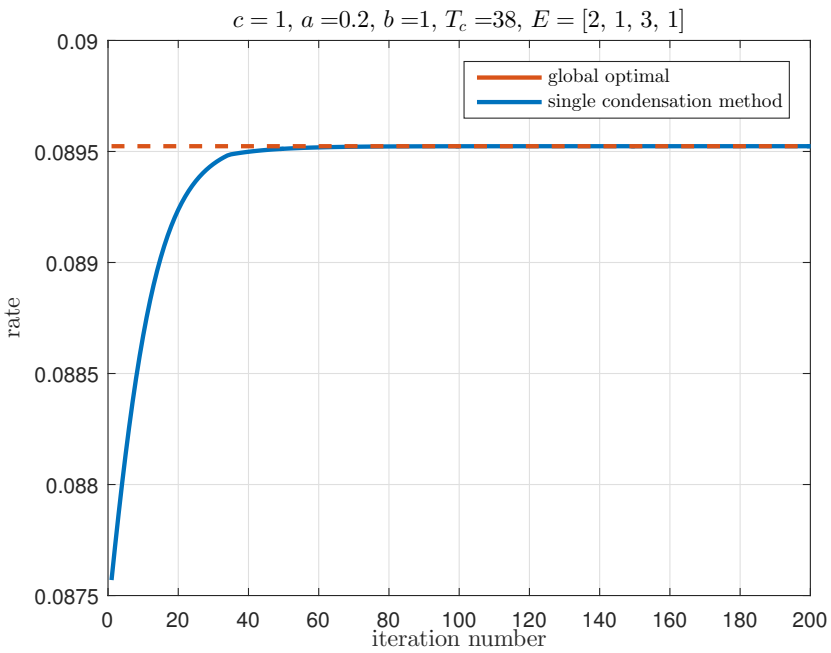

Figure 9.7: Simulation for the implicit temperature constraint, general case: convergence of the achieved rate for the single condensation method.

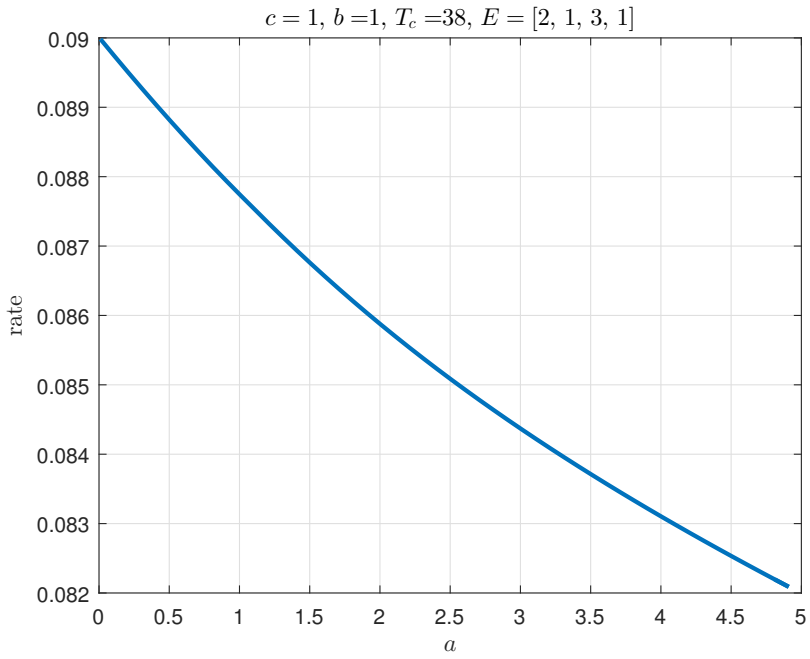

Figure 9.8: Simulation for implicit temperature constraint, general case: achievable rate using single condensation method versus a.

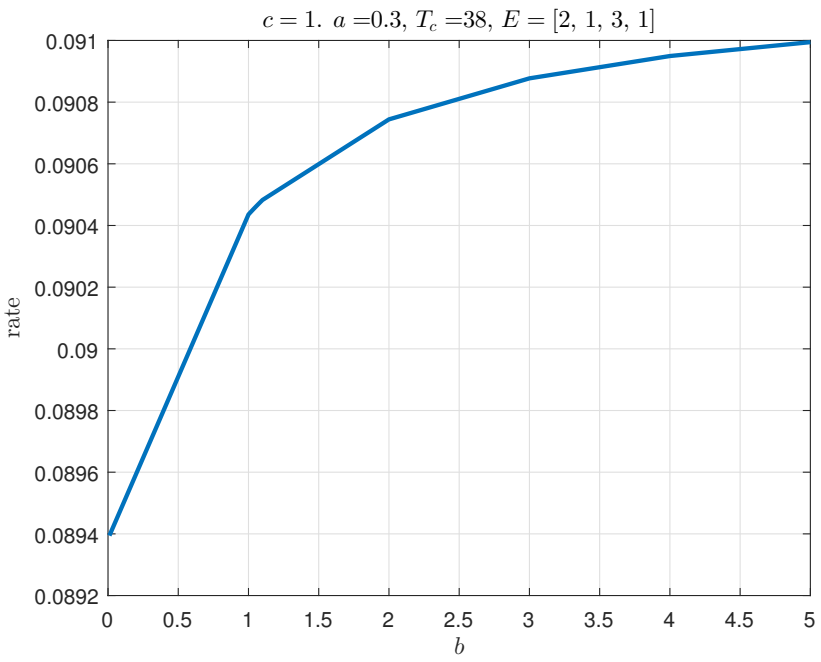

Figure 9.9: Simulation for implicit temperature constraint, general case: achievable rate using single condensation method versus b.

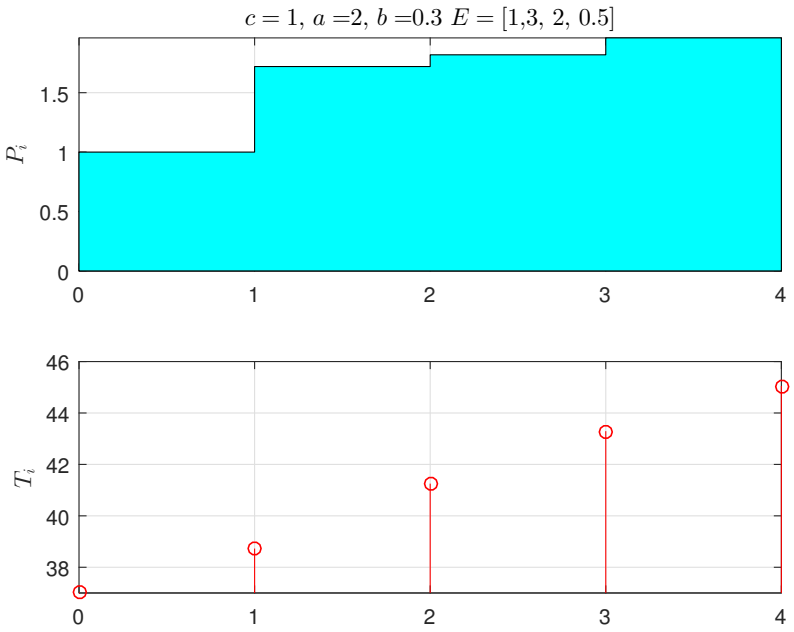

Figure 9.10: Simulation for implicit temperature constraint: high SINR case.

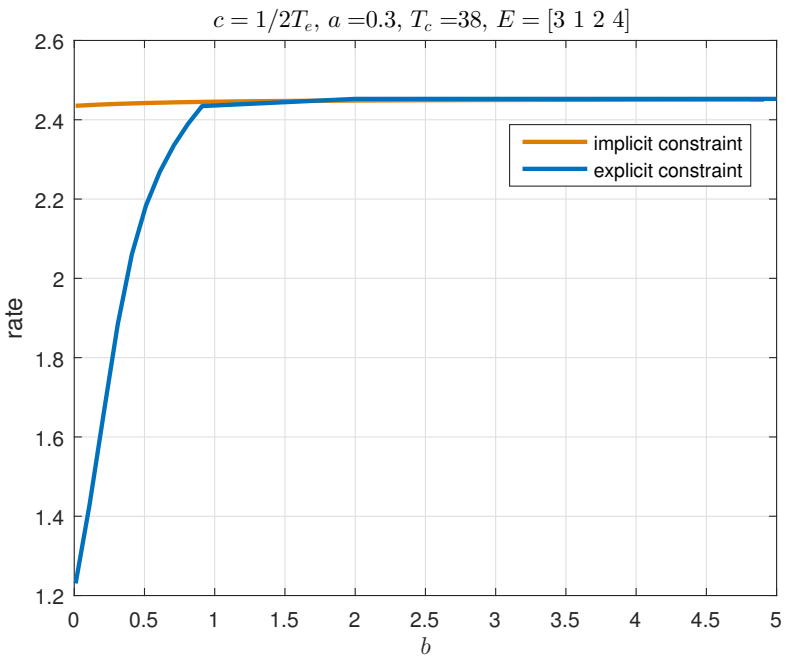

Figure 9.11: Simulation for comparing the explicit and the implicit temperature constraints versus b. We set the noise variance for the explicit constraint case to unity and set the noise variance for the implicit constraint case to 0.5.

We then consider implicit temperature constrained model considered in Section 9.4. For the general SINR case, we initialize the signomial programming problem using a feasible power allocation of $P_i = \min_i E_i$ in all slots. For the case shown in Fig. 9.6, we show the convergence of the single condensation method in Fig. 9.7. In this case, the single condensation method yields a value which is numerically indistinguishable from the global optimal value in approximately 80 iterations. We obtain the global optimal value by exhaustive search over the feasible set. In general, we observe numerically that the single condensation method gives solutions very close to the global optimal solution, however, there is no analytic guarantee for this. For this case, the naive greedy policy yields an objective function equal to 0.0892, which is less than the optimal rate. We then compare the achieved rate

versus the values of a and b in Fig. 9.8 and Fig. 9.9, respectively. As in the explicit temperature case, the rate decreases with a and increases with b. As the value of a increases, the denominator inside the logarithmic function of the objective function in (9.36) increases, until the objective function converges to zero. As b increases the denominator decreases until it converges to a constant which is equal to $cT_e + \sigma^2$. We then present the high SINR case considered in Section 9.4.2 in Fig. 9.10. We observe that the optimal power allocation is monotone increasing as proved. We then compare the performance of the explicit and the implicit temperature constraint cases in Fig. 9.11 when we set $c = 1/2T_e$, set the noise variance for the explicit constraint case to unity and set the noise variance for the implicit constraint case to 0.5. As the value of b increases, the two systems converge to the same rate. This is because as b increases, the explicit temperature constraint becomes loose and the interference in the denominator of the implicit temperature constraint objective function becomes unity. We also notice that in the implicit constraint case, the rate gets near to its maximum value for small values of b, unlike the explicit constraint case which gets to its maximum value approximately when $b = 1$.

Next, we study the case when implicit and explicit temperature constraints are simultaneously active as considered in Section 9.5. For the high SINR case, unlike the implicit temperature constrained case, we observe in Fig. 9.12 that the power sequence does not possess a monotonic structure. We then study the high SINR case when the system is temperature limited in Fig. 9.13. The optimal power allocation is monotone decreasing, corresponding temperature is monotone increasing and the power is constant when the temperature reaches the critical level.

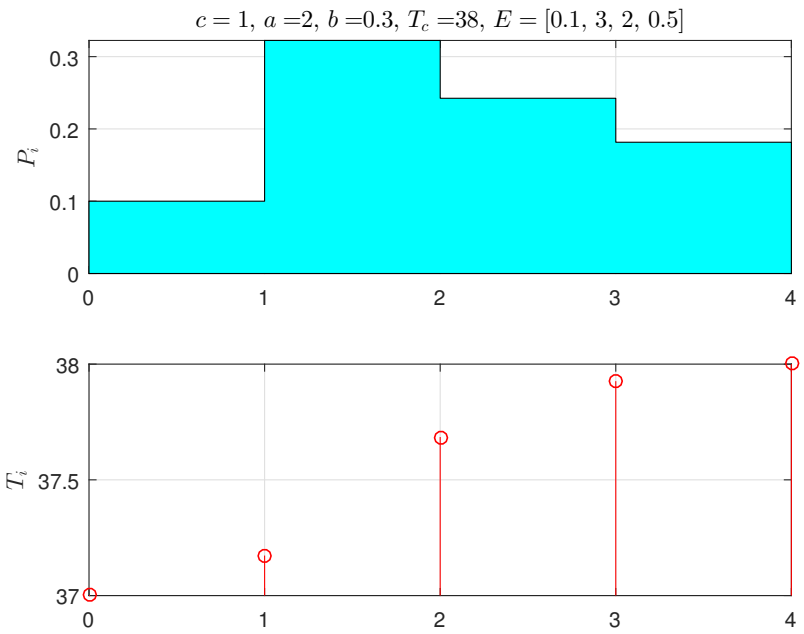

Figure 9.12: Simulation for implicit and explicit temperature constraint: high SINR case.

9.7 Conclusion

We considered explicit and implicit temperature constraints in a single-user energy harvesting communication system in discrete time. Under explicit temperature constraints, the temperature is imposed to be less than a critical level. In this case, we studied optimal power allocation for multiple energy arrivals. For the temperature limited regime, we showed that the optimal power sequence is monotone decreasing while the temperature of the system is monotone increasing. Next, we considered an implicit temperature constraint where the temperature level affects channel quality. We studied the general case as well as the high and low SINR cases. In the low SINR case, we showed that the optimal allocation dictates the transmitter to save its harvested energy till the last slot and transmit all the harvested energy then. In

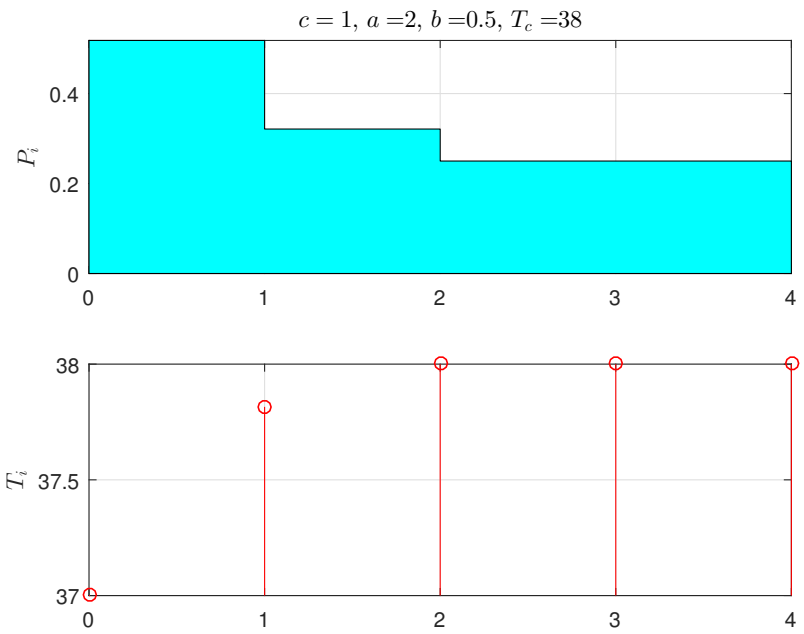

Figure 9.13: Simulation for implicit and explicit temperature constraint: temperature limited high SINR case.

the high SINR case, we observed that the problem is a geometric program and we expanded upon its equivalent convex version to show that optimal power allocation is monotone increasing in time. Finally, we considered the case in which implicit and explicit temperature constraints are simultaneously active. We identified a sufficient condition on the system parameters that results in a monotone decreasing optimal power allocation. Our current investigation leaves several directions to purse in future research, such as, optimal power allocation for the finite battery case; online power allocation under explicit and implicit temperature constraints; explicit and implicit temperature constraints in multi-user settings such as broadcast and multiple access channels.

9.8 Appendix

9.8.1 Proof of the monotonicity of optimal power allocation of Problem (9.46)

In this appendix, we present the proof for the monotonicity of the optimal power allocation for the problem in (9.46). We rewrite its KKTs in (9.49) as follows:

$$\frac{1}{P_i} = \sum_{k=i}^{D} \mu_k + \sum_{j=i+1}^{D} \frac{\alpha^{j-1-i}}{\sum_{k=1}^{j-1} \alpha^{j-1-k} P_k + \Gamma_0} \tag{9.55}$$

Based on this equation, for a fixed $\boldsymbol{\mu}$, we now define an update rule to solve for the power allocation P_i iteratively as follows:

$$P_i(\mathbf{P}) \triangleq \frac{1}{\sum_{k=i}^{D} \mu_k + \sum_{j=i+1}^{D} \frac{\alpha^{j-1-i}}{\sum_{k=1}^{j-1} \alpha^{j-1-k} P_k + \Gamma_0}} \tag{9.56}$$

where the function $P_i(\mathbf{P})$ calculates the updated power P_i when the powers are equal to $\mathbf{P}$. The algorithm proceeds as follows: We first initialize the power allocation with any arbitrary non-negative power allocation $\mathbf{P}^0$, where the superscript denotes the iteration index. We then substitute with $\mathbf{P}^0$ in (9.56) to obtain the new power allocation $\mathbf{P}^1$, where $\mathbf{P}^1 \triangleq (P_1(\mathbf{P}^0), \ldots, P_D(\mathbf{P}^0))$. Similarly, we use the powers $\mathbf{P}^1$ to obtain the updated powers $\mathbf{P}^2$, and repeat this process. We show next that this algorithm converges to a unique fixed point.

To show that these updates converge to a unique fixed point, we first present the following definition of a *standard interference function* [113]:

Definition 9.1 *Interference function $I(\mathbf{P})$ is standard if for all $\mathbf{P} \geq 0$ the following properties are satisfied:*

- *Positivity $I(\mathbf{P}) > 0$.*
- *Monotonicity: If $\mathbf{P} \geq \mathbf{P}'$, then $I(\mathbf{P}) \geq I(\mathbf{P}')$.*
- *Scalability: For all $\theta > 1$, $\theta I(\mathbf{P}) \geq I(\theta \mathbf{P})$.*

Now, we want to show that the update rule $I(\mathbf{P}) = (P_1(\mathbf{P}), P_2(\mathbf{P}), \ldots, P_D(\mathbf{P}))$ is a standard function, i.e., it satisfies the three properties above.

The positivity property follows from,

$$P_i(\mathbf{P}) \geq \frac{1}{\sum_{j=i}^{D} \mu_j} \geq \frac{1}{\mu_D} > 0 \tag{9.57}$$

where $\mu_D > 0$ follows from (9.49) with $i = D$ and since the power P_D is finite due to the finite energy constraint.

The monotonicity property follows since the denominator of $P_i(\mathbf{P})$ is a decreasing function of the powers, and hence, $P_i(\mathbf{P})$ is an increasing function of the powers.

The scalability property follows from the following for $\theta > 1$,

$$P_i(\theta \mathbf{P}) = \frac{1}{\sum_{k=i}^{D} \mu_k + \sum_{j=i+1}^{D} \frac{\alpha^{j-1-i}}{\sum_{k=1}^{j-1} \alpha^{j-1-k} \theta P_k + \Gamma_0}} \tag{9.58}$$

$$= \frac{\theta}{\theta \sum_{k=i}^{D} \mu_k + \sum_{j=i+1}^{D} \frac{\alpha^{j-1-i}}{\sum_{k=1}^{j-1} \alpha^{j-1-k} P_k + \frac{\Gamma_0}{\theta}}} \tag{9.59}$$

$$< \frac{\theta}{\sum_{k=i}^{D} \mu_k + \sum_{j=i+1}^{D} \frac{\alpha^{j-1-i}}{\sum_{k=1}^{j-1} \alpha^{j-1-k} P_k + \Gamma_0}} \tag{9.60}$$

$$= \theta P_i(\mathbf{P}) \tag{9.61}$$

This completes the proof that $I(\mathbf{P}) = (P_1(\mathbf{P}), P_2(\mathbf{P}), \ldots, P_D(\mathbf{P}))$ in (9.56) is a standard interference function.

From [113, Theorem 2], we now conclude that the algorithm in (9.56) converges to a *unique* fixed point. From the equivalence of (9.46) to the strictly convex problem in (9.50), we know that there is only one unique solution to the equations in (9.49), and hence, the algorithm in (9.56) converges to the unique power allocation which solves the KKTs in (9.49).

It now remains to show that at this unique fixed point, the power allocation is monotone increasing in time. We prove this by showing that if we begin with any arbitrary monotone increasing power allocation, the update algorithm retains this ordering for the power allocation in each iteration, and hence, in the limit. To show this, let us assume that we have an arbitrary power vector $\mathbf{P}$ which satisfies $P_i \leq P_{i+1}$ for all $i = \{1, \ldots, D-1\}$. We want to show that $P_i(\mathbf{P}) \leq P_{i+1}(\mathbf{P})$. This follows from:

$$P_{i+1}(\mathbf{P}) = \frac{1}{\sum_{k=i+1}^{D} \mu_k + \sum_{j=i+2}^{D} \frac{\alpha^{j-2-i}}{\sum_{k=1}^{j-1} \alpha^{j-1-k} P_k + \Gamma_0}} \tag{9.62}$$

$$\geq \frac{1}{\sum_{k=i}^{D} \mu_k + \sum_{j=i+2}^{D} \frac{\alpha^{j-2-i}}{\sum_{k=1}^{j-1} \alpha^{j-1-k} P_k + \Gamma_0}} \tag{9.63}$$

$$\geq \frac{1}{\sum_{k=i}^{D} \mu_k + \sum_{j=i+2}^{D} \frac{\alpha^{j-2-i}}{\sum_{k=2}^{j-1} \alpha^{j-1-k} P_k + \Gamma_0}} \tag{9.64}$$

$$= \frac{1}{\sum_{k=i}^{D} \mu_k + \sum_{j=i+2}^{D} \frac{\alpha^{j-2-i}}{\sum_{k=1}^{j-2} \alpha^{j-2-k} P_{k+1} + \Gamma_0}} \tag{9.65}$$

$$\geq \frac{1}{\sum_{k=i}^{D} \mu_k + \sum_{j=i+2}^{D} \frac{\alpha^{j-2-i}}{\sum_{k=1}^{j-2} \alpha^{j-2-k} P_k + \Gamma_0}} \tag{9.66}$$

$$\geq \frac{1}{\sum_{k=i}^{D} \mu_k + \sum_{j=i+1}^{D-1} \frac{\alpha^{j-1-i}}{\sum_{k=1}^{j-1} \alpha^{j-1-k} P_k + \Gamma_0}} \tag{9.67}$$

$$\geq \frac{1}{\sum_{k=i}^{D} \mu_k + \sum_{j=i+1}^{D} \frac{\alpha^{j-1-i}}{\sum_{k=1}^{j-1} \alpha^{j-1-k} P_k + \Gamma_0}} \tag{9.68}$$

$$= P_i(\mathbf{P}) \tag{9.69}$$

where (9.63) follows by adding the non-negative Lagrange multiplier μ_i in the denominator, (9.64) follows by neglecting positive terms in the denominator in the second term of the denominator, (9.65) follows by replacing $\sum_{k=2}^{j-1}$ by $\sum_{k=1}^{j-2}$ and changing the indices inside the summation accordingly, (9.66) follows since we have $P_k \leq P_{k+1}$, (9.67) follows by replacing $\sum_{j=i+2}^{D}$ by $\sum_{j=i+1}^{D-1}$ and changing the indices inside the summation accordingly, and (9.68) follows by adding a positive term in the denominator. Since in each iteration the power is monotone increasing, the power allocation will also be monotone increasing at the fixed point.

9.8.2 Proof of the monotonicity of the optimal power allocation of problem (9.54) when $\alpha \leq \frac{\beta\Gamma_0}{T_c - T_e + \beta\Gamma_0}$

We start the proof by noting that the KKT conditions and the complementary slackness conditions for the problem in (9.54) are necessary and sufficient for optimality.

Let us now define i_1^* as the first slot at which the temperature hits T_c. Since $\mu_k = 0$ for $k = 1, \ldots, i_1^* - 1$, KKT conditions in the integer interval $[1 : i_1^*]$ are in

the following form:

$$\frac{1}{P_i} - \sum_{j=i+1}^{D} \frac{1}{\sum_{k=1}^{j-1} \alpha^{i-k} P_k + \Gamma_{j-1-i}} = \alpha^{-i} W, \quad i = 1, \ldots, i_1^* \tag{9.70}$$

where $W \triangleq \sum_{k=i_1^*}^{D} \alpha^k \mu_k$. By comparing (9.70) for i and $i+1 \leq i_1^*$, we have:

$$\frac{1}{P_i} - \frac{1}{\sum_{k=1}^{i} \alpha^{i-k} P_k + \Gamma_0} = \frac{\alpha}{P_{i+1}} \tag{9.71}$$

We now rewrite (9.71) as follows:

$$P_{i+1} = \alpha \frac{\sum_{k=1}^{i-1} \alpha^{i-k} P_k + P_i + \Gamma_0}{\sum_{k=1}^{i-1} \alpha^{i-k} P_k + \Gamma_0} P_i \tag{9.72}$$

$$= \alpha \left(1 + \frac{P_i}{\sum_{k=1}^{i-1} \alpha^{i-k} P_k + \Gamma_0} \right) P_i \tag{9.73}$$

Now, due to the temperature constraints, we have $P_i \leq \frac{T_c - T_e}{\beta}$ for all i and $\frac{P_i}{\sum_{k=1}^{i-1} \alpha^{i-k} P_k + \Gamma_0} \leq \frac{T_c - T_e}{\beta \Gamma_0}$. Hence, under the assumed condition on α, we have

$$\alpha \left(1 + \frac{P_i}{\sum_{k=1}^{i-1} \alpha^{i-k} P_k + \Gamma_0} \right) \leq 1 \tag{9.74}$$

This proves that $P_{i+1} \leq P_i$ for all $i \in [1 : i_1^* - 1]$, i.e., the optimal power allocation is non-increasing in the slots $\{1, \ldots, i_1^*\}$.

Now, if the temperature drops below T_c after slot i_1^*, say at slot i_2^*, the KKT conditions will have the form identical to (9.70) in the interval $[i_1^* + 1 : i_2^*]$. Following the steps, we have that $P_{i+1} \leq P_i$ for $[i_1^* + 1 : i_2^*]$, i.e., the optimal power allocation is non-increasing in the slots $\{i_1^* + 1, \ldots, i_2^*\}$. It remains to show that the power

allocation is also non-increasing between slots i_1^* and $i_1^* + 1$. Note that it follows that the power in slot i_1^* is strictly higher than $\frac{(T_c - T_e)(1-\alpha)}{\beta}$, while in slot $i_1^* + 1$ the power can be no larger than $\frac{(T_c - T_e)(1-\alpha)}{\beta}$ as otherwise this violates the temperature constraint. Hence, the power allocation between slots i_1^* and $i_1^* + 1$ is non-increasing also. This concludes the proof of the first part. The proof of the monotonicity of the resulting temperature follows similar to (9.23)-(9.30).

CHAPTER 10

Energy Harvesting Multiple Access Channel with Peak Temperature Constraints

10.1 Introduction

We study the optimal power allocation problem for a two-user energy harvesting multiple access channel where the temperatures at the transmitters and the receiver are constrained by a peak value; see Fig. 10.1. The temperature constraint ensures that the nodes do not overheat as a result of data transmission. We first study the optimal power allocation when the nodes are manufactured from different materials, i.e., react differently to the incident transmission power, and have different peak temperature constraints. Then, we derive sufficient conditions under which the multiple access rate region collapses to a single pentagon.

10.2 System model

We consider the temperature model considered at [30, 93, 114, 115]. In the two-user multiple access channel shown in Fig. 10.1, we assume that each node is placed in

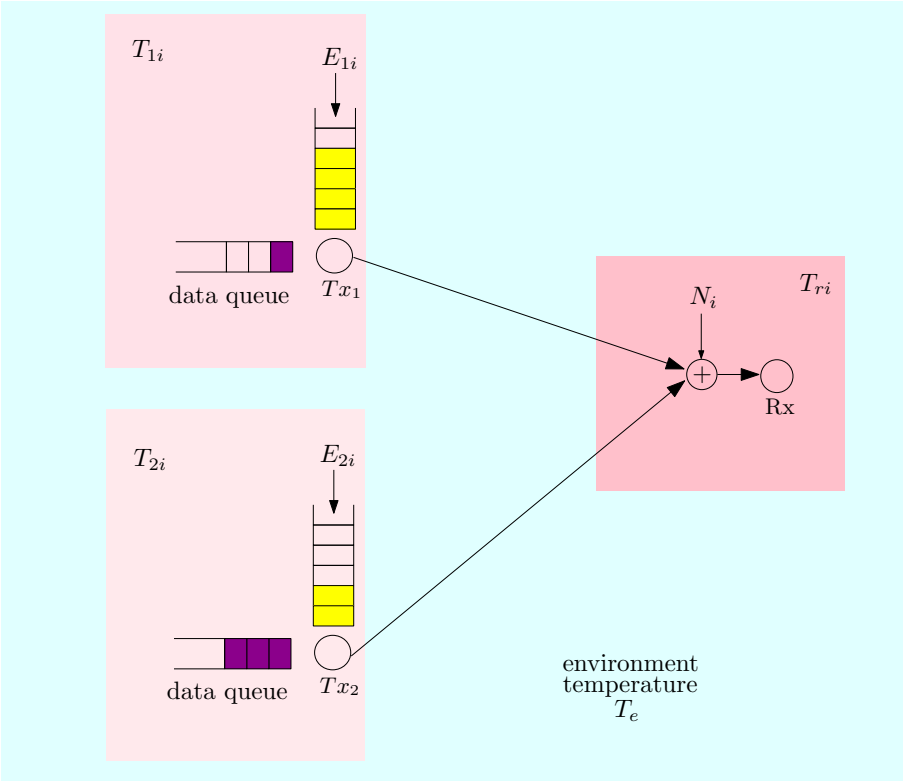

Figure 10.1: An energy harvesting multiple access channel with peak temperature constraints. In general, the critical temperatures at the nodes are different.

a different physical environment with different heat characteristics in the presence of electromagnetic radiation. The temperature at node $j \in \{1, 2, r\}$, $T_j(t)$, is given by the following differential equation

$$\frac{dT_j(t)}{dt} = a_j p_j(t) - b_j(T_j(t) - T_e) \tag{10.1}$$

where T_e is the environment temperature, $p_j(t)$ is the power at user j, and a_j, b_j are non-negative constant parameters in the device temperature evolution model. These parameters determine the speed of heating up and cooling down in the presence of applied electromagnetic radiation. For example, if a_j is small, the device temperature will not change much by the electromagnetic radiations while if

b_i is small, the device will cool down quickly. Incident power at the receiver is $p_r(t) = h_1 p_1(t) + h_2 p_2(t)$. For simplicity, we let $h_1 = h_2 = 1$.

With initial temperature $T_j(0) = T_e$, the solution of (10.1) is:

$$T_j(t) = e^{-b_j t} \int_0^t e^{b_j \tau} a_j p_j(\tau) d\tau + T_e \tag{10.2}$$

Similar to [114, 115], we consider temperature levels at discrete time instants $i\Delta$ where i is the slot index and Δ is the slot length. We define $T_{ji} \triangleq T_j(i\Delta)$ as the temperature level at the end of the ith slot, and $P_{ji} \triangleq p_j(i\Delta)$ as the power level used in the ith slot. Using (10.2), T_{ji} is expressed as:

$$T_{ji} = e^{-b_j i\Delta} \int_0^{i\Delta} e^{b_j \tau} a_j p_j(\tau) d\tau + T_e \tag{10.3}$$

$$= \alpha_j T_{j(i-1)} + \beta_j P_{ji} + \gamma_j \tag{10.4}$$

where $\alpha_j = e^{-b_j \Delta}$, $\beta_j = \frac{a_j}{b_j}\left[1 - \alpha_j\right]$ and $\gamma_j = T_e\left[1 - \alpha_j\right]$.

The goal of this chapter is to determine the optimal power allocation policy which achieves the largest departure region for the Gaussian multiple access channel under temperature and energy constraints. Assuming a unit variance for the Gaussian noise, the achievable rates for the multiple access channel are given by:

$$\begin{aligned} \mathcal{C}(P_{1i}, P_{2i}) = \Big\{ (r_{1i}, r_{2i}) : & r_{1i} \leq \frac{1}{2} \log\left(1 + P_{1i}\right) \\ & r_{2i} \leq \frac{1}{2} \log\left(1 + P_{2i}\right) \\ & r_{1i} + r_{2i} \leq \frac{1}{2} \log\left(1 + P_{1i} + P_{2i}\right) \Big\} \end{aligned} \tag{10.5}$$

The aim is to maximize the cumulative achievable rate region, departure region, i.e., subject to a deadline D.

The maximum allowable peak temperature at node $j \in \{1, 2, r\}$ is T_{cj}. The peak temperature constraint can then be written as follows:

$$\mathcal{T}_k(\{a_j, b_j, T_{cj}\}, j = 1, 2, r) = \Big\{(T_{1i}, T_{2i}, T_{ri})_{i=1}^{k} : T_{1k} \leq T_{c1} \\ T_{2k} \leq T_{c2} \\ T_{rk} \leq T_{cr}\Big\} \tag{10.6}$$

Using (10.4), these temperature constraints can be written in terms of only the transmission powers as follows:

$$\mathcal{T}_k(\{a_j, b_j, T_{cj}\}, j = 1, 2, r) = \Big\{(P_{1i}, P_{2i})_{i=1}^{k} : \sum_{i=1}^{k} \alpha_1^{k-i} P_{1i} \leq \frac{T_{c1} - T_e}{\beta_1} \\ \sum_{i=1}^{k} \alpha_2^{k-i} P_{2i} \leq \frac{T_{c2} - T_e}{\beta_2} \\ \sum_{i=1}^{k} \alpha_r^{k-i} (P_{1i} + P_{2i}) \leq \frac{T_{cr} - T_e}{\beta_r}\Big\} \tag{10.7}$$

Moreover, power allocations P_{1i} and P_{2i} must satisfy the following energy causality constraints:

$$\mathcal{E}_k(\mathbf{E}_1, \mathbf{E}_2) = \Big\{(P_{1i}, P_{2i})_{i=1}^{k} : \sum_{i=1}^{k} P_{1i} \leq \sum_{i=1}^{k} E_{1i}, \sum_{i=1}^{k} P_{2i} \leq \sum_{i=1}^{k} E_{2i}\Big\} \tag{10.8}$$

In this chapter, we characterize the maximum achievable multiple access rate region under the constraints (10.5), (10.7) and (10.8). We first establish the con-

vexity of the region resulting from these constraints in the following lemma:

Lemma 10.1 *The optimal rate region formed by (10.5), (10.7) and (10.8) is a convex region.*

Proof: Let us consider two feasible power policies $(\bar{\mathbf{P}}_1, \bar{\mathbf{P}}_2)$ and $(\tilde{\mathbf{P}}_1, \tilde{\mathbf{P}}_2)$. Let us also consider a new policy which is a convex combination of the previous two feasible policies $(\mathbf{P}_1, \mathbf{P}_2) = \eta(\bar{\mathbf{P}}_1, \bar{\mathbf{P}}_2)+(1-\eta)(\tilde{\mathbf{P}}_1, \tilde{\mathbf{P}}_2)$, where $\eta \in [0, 1]$. Since the constraints (10.7) and (10.8) are linear, this new policy is also feasible in the constraints.

Now assume that policies $(\mathbf{P}_1, \mathbf{P}_2)$, $(\bar{\mathbf{P}}_1, \bar{\mathbf{P}}_2)$ and $(\tilde{\mathbf{P}}_1, \tilde{\mathbf{P}}_2)$ achieve pentagons $\mathcal{C}$, $\bar{\mathcal{C}}$ and $\tilde{\mathcal{C}}$, respectively. Now, choose two points $\bar{q}$ and $\tilde{q}$ such that $\bar{q} \in \bar{\mathcal{C}}$ and $\tilde{q} \in \tilde{\mathcal{C}}$. Then for any $\eta \in [0, 1]$ we define $q = \eta\bar{q} + (1 - \eta)\tilde{q}$. We need to show that q is in $\mathcal{C}$. We show this as follows:

$$q_1 = \eta\bar{q}_1 + (1 - \eta)\tilde{q}_1 \tag{10.9}$$

$$= \eta \sum_{i=1}^{D} \frac{1}{2} \log(1+\bar{P}_{1i})+(1-\eta) \sum_{i=1}^{D} \frac{1}{2} \log(1+\tilde{P}_{1i}) \tag{10.10}$$

$$\leq \sum_{i=1}^{D} \frac{1}{2} \log(1 + \eta\bar{P}_{1i} + (1 - \eta)\tilde{P}_{1i}) \tag{10.11}$$

$$= \sum_{i=1}^{D} \frac{1}{2} \log(1 + P_{1i}) \tag{10.12}$$

which is feasible in $\mathcal{C}$. Similarly, we can show this for q_2 and $q_1 + q_2$. This concludes the proof. ■

Since the region is a convex region, we can characterize it by considering its tangent lines. The tangent lines can be expressed as $\mu_1 r_{1i}+\mu_2 r_{2i}$. Changing the ratio

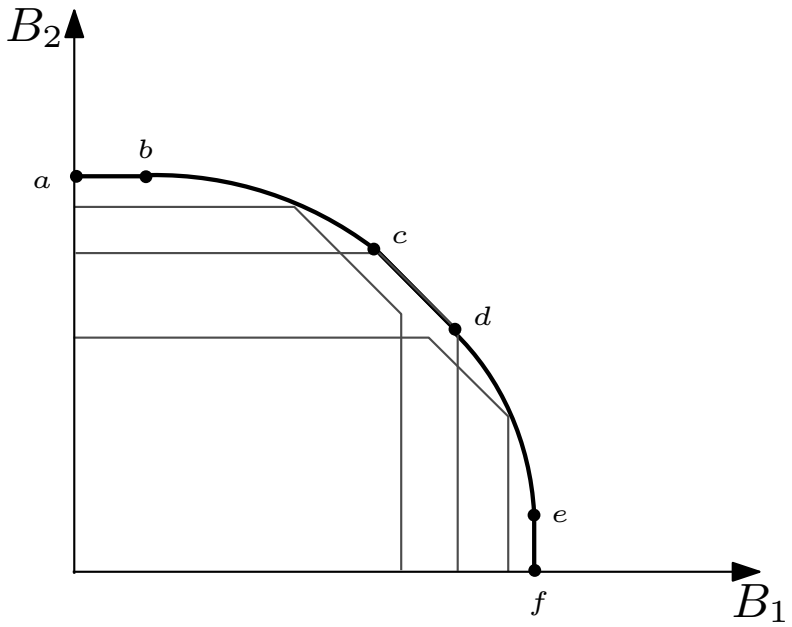

Figure 10.2: The rate region for the multiple access channel.

between μ_1 and μ_2 will change the slope of the tangent line. Hence, we formulate the problem as follows:

$$\begin{aligned} \max_{\{r_i,P_i\}} \quad & \sum_{i=1}^{D} \mu_1 r_{1i} + \mu_2 r_{2i} \\ \text{s.t.} \quad & (P_{1i}, P_{2i})_{i=1}^{k} \in \mathcal{T}_k(\{a_j, b_j, T_{cj}\}, j = 1, 2, r) \\ & (r_{1k}, r_{2k}) \in \mathcal{C}(P_{1k}, P_{2k}) \\ & (P_{1i}, P_{2i})_{i=1}^{k} \in \mathcal{E}_k(\mathbf{E}_1, \mathbf{E}_2), \ \forall k \in \{1, \ldots, D\} \end{aligned} \tag{10.13}$$

for $\mu_1, \mu_2 \in [0, 1]$. For each different value of $\frac{\mu_1}{\mu_2}$ we get a point on the boundary of the optimal achievable rate region, the region is shown in Fig. 10.2, where $B_j = \sum_{i=1}^{D} r_{ji}$.

In what follows, we first study the general case. We show that for the single slot scenario, i.e., when $D = 1$, that the rate region is a single pentagon generated by the intersection of regions generated by the temperature and energy constraints.

We then study the multiple slot setting and show that the optimal power allocation can be obtained by using generalized water-filling algorithms. We then study the temperature limited case and derive sufficient conditions under which the capacity region collapses to a single pentagon.

10.3 General Case

In this section, we first study the single energy arrival. Then we study the multiple energy arrival case.

10.3.1 Single Slot Analysis

In this subsection, we study the case when there is only one energy arrival and one slot to use this incoming energy. The problem in this case is,

$$\begin{aligned} \max_{r_1,r_2,P_1,P_2} \quad & \mu_1 r_1 + \mu_2 r_2 \\ \text{s.t.} \quad & (P_1, P_2) \in \mathcal{T}(\{a_j, b_j, T_{cj}\}, j = 1, 2, r) \\ & (P_1, P_2) \in \mathcal{E}(E_1, E_2), (r_1, r_2) \in \mathcal{C}(P_1, P_2) \end{aligned} \tag{10.14}$$

For this case, the optimal rate region is a single pentagon which we characterize in the next lemma which is also illustrated in Fig. 10.3.

Lemma 10.2 *The optimal rate region for problem (10.14) is a single pentagon and*

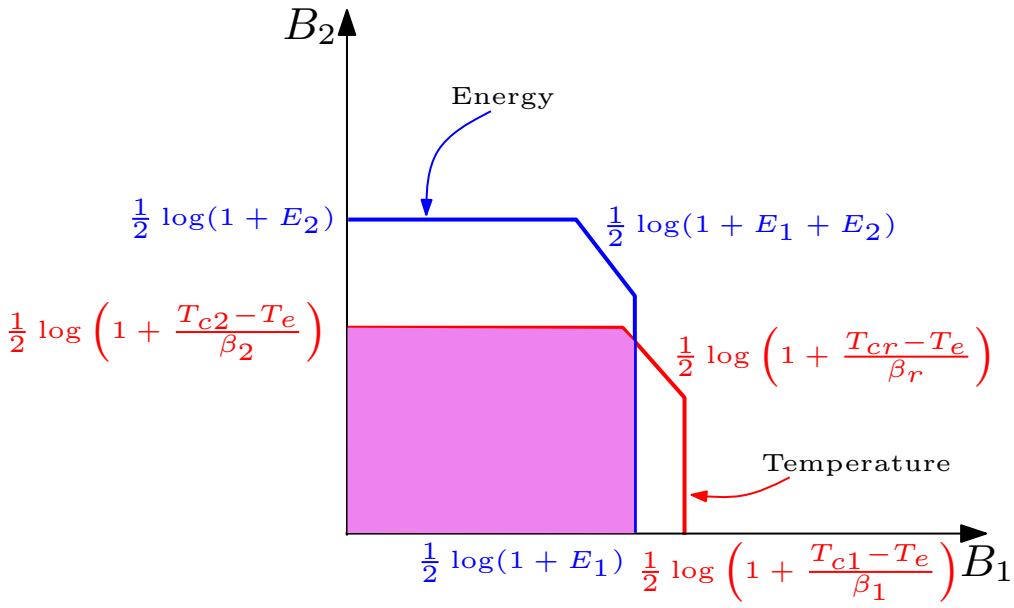

Figure 10.3: The rate region for the multiple access channel with a single energy arrival.

is given by:

$$\mathcal{C}_s(E_1,E_2)=\Bigg\{(r_1,r_2):r_1\leq\frac{1}{2}\log\left(1+\min\left\{E_1,\frac{T_{c1}-T_e}{\beta_1}\right\}\right)$$
$$r_2\leq\frac{1}{2}\log\left(1+\min\left\{E_2,\frac{T_{c2}-T_e}{\beta_2}\right\}\right)$$
$$r_1+r_2\leq\frac{1}{2}\log\left(1+\min\left\{E_1+E_2,\frac{T_{cr}-T_e}{\beta_r}\right\}\right)\Bigg\} \quad (10.15)$$

The proof of Lemma 10.2 follows from the intersection of (10.7) and (10.8) for a single slot setting, i.e., when $D=1$. The rate region is a single pentagon as there is only one transmission policy, which is to use the maximum allowable power in a way to make sure that both energy and temperature constraints are satisfied.

10.3.2 Multiple Slot Analysis

Now, we study the multiple energy arrival case and characterize the optimal solution for different parts of the rate region in Fig. 10.2.

10.3.2.1 Point a

Achieving points a (and similarly f) is similar to the single-user case in [115], however, here there is an extra constraint due to the difference between the transmitter and receiver's material. The problem can be written as follows:

$$\begin{aligned}
\max_{\{P_{2i}\}} \quad & \sum_{i=1}^{D} \frac{1}{2}\log(1+P_{2i}) \\
\text{s.t.} \quad & \sum_{i=1}^{k} \alpha_2^{k-i} P_{2i} \leq \frac{T_{c2}-T_e}{\beta_2} \\
& \sum_{i=1}^{k} \alpha_r^{k-i} P_{2i} \leq \frac{T_{cr}-T_e}{\beta_r} \\
& \sum_{i=1}^{k} P_{2i} \leq \sum_{i=1}^{k} E_{2i}, \ \forall k \in \{1,\ldots,D\}
\end{aligned} \tag{10.16}$$

This problem is a convex optimization problem and the KKTs are necessary and sufficient. The Lagrangian of this problem can be written as follows:

$$\begin{aligned}
\mathcal{L} = & -\sum_{i=1}^{D} \frac{1}{2}\log(1+P_{2i}) + \sum_{k=1}^{D} \lambda_{2k} \left(\sum_{i=1}^{k} \alpha_2^{k-i} P_{2i} - \frac{T_{c2}-T_e}{\beta_2} \right) \\
& + \sum_{k=1}^{D} \lambda_{rk} \left(\sum_{i=1}^{k} \alpha_r^{k-i} P_{2i} - \frac{T_{cr}-T_e}{\beta_r} \right) + \sum_{k=1}^{D} \nu_{2k} \left(\sum_{i=1}^{k} P_{2i} - \sum_{i=1}^{k} E_{2i} \right)
\end{aligned} \tag{10.17}$$

Differentiating with respect to P_{2i} gives the optimal power as:

$$P_{2i} = \left(\frac{1}{\sum_{k=i}^{D} \lambda_{2k} \alpha_2^{k-i} + \lambda_{rk} \alpha_r^{k-i} + \sum_{k=i}^{D} \nu_{2k}} - 1 \right)^+ \tag{10.18}$$

which can be solved by directional generalized water-filling. We next specify a special case in the following lemma.

Lemma 10.3 *When either* $\alpha_r < \alpha_2$ *and* $\frac{T_{c2}-T_e}{\beta_2} \leq \frac{T_{cr}-T_e}{\beta_r}$ *or* $\alpha_r \leq \alpha_2$ *and* $\frac{T_{c2}-T_e}{\beta_2} < \frac{T_{cr}-T_e}{\beta_r}$ *is satisfied, we have* $\lambda_{rk} = 0$ *and the problem reduces to the single-user problem in [115].*

Proof: Let us consider the case when $\alpha_r < \alpha_2$ and $\frac{T_{c2}-T_e}{\beta_2} \leq \frac{T_{cr}-T_e}{\beta_r}$ are satisfied. This implies the following:

$$\sum_{i=1}^{k} \alpha_r^{k-i} P_{2i} < \sum_{i=1}^{k} \alpha_2^{k-i} P_{2i} \leq \frac{T_{c2} - T_e}{\beta_2} \leq \frac{T_{cr} - T_e}{\beta_r} \tag{10.19}$$

From complementary slackness, this implies that $\lambda_{rk} = 0$. The proof follows similarly for the other case. ■

The problem reduces to a single-user problem when either $\alpha_2 < \alpha_r$ and $\frac{T_{cr}-T_e}{\beta_r} \leq \frac{T_{c2}-T_e}{\beta_2}$ or $\alpha_2 \leq \alpha_r$ and $\frac{T_{cr}-T_e}{\beta_r} < \frac{T_{c2}-T_e}{\beta_2}$.

10.3.2.2 Point b

We then study point b (or similarly point e). Point b represents the maximum rate the first user can achieve while user 2 is achieving its single-user rate. Hence, to

achieve point b, we need to fix the second user's power allocation to be the optimal single-user power allocation P_{2i}^s and then solve for the maximum rate for user 1. This can be done by solving the following optimization problem:

$$\begin{aligned}
\max_{\{P_{1i}\}} \quad & \sum_{i=1}^{D} \frac{1}{2} \log\left(1+\frac{P_{1i}}{1+P_{2i}^s}\right) \\
\text{s.t.} \quad & \sum_{i=1}^{k} \alpha_1^{k-i} P_{1i} \leq \frac{T_{c1}-T_e}{\beta_1} \\
& \sum_{i=1}^{k} \alpha_r^{k-i} \left(P_{1i}+P_{2i}^s\right) \leq \frac{T_{cr}-T_e}{\beta_r} \\
& \sum_{i=1}^{k} P_{1i} \leq \sum_{i=1}^{k} E_{1i}, \ \forall k
\end{aligned} \tag{10.20}$$

Here, the power suffers from a different fading of $\frac{1}{1+P_{2i}^s}$ in each slot. Moreover, there is a time-varying peak temperature constraint. Using a Lagrange analysis, the optimal power allocation is given by:

$$P_{1i} = \left(\frac{1}{\sum_{k=i}^{D} \lambda_{1k} \alpha_1^{k-i} + \lambda_{rk} \alpha_r^{k-i} + \sum_{k=i}^{D} \mu_k} - 1 - P_{2i}^s\right)^+ \tag{10.21}$$

The optimal solution can be found using generalized water-filling. Similar to Lemma 10.3, we conclude that if either $\alpha_1 < \alpha_r$ and $\frac{T_{cr}-T_e}{\beta_r} \leq \frac{T_{c1}-T_e}{\beta_1}$ or $\alpha_1 \leq \alpha_r$ and $\frac{T_{cr}-T_e}{\beta_r} < \frac{T_{c1}-T_e}{\beta_1}$ we have $\lambda_{1k} = 0$.

Also note that if for any slot m we have $\sum_{i=1}^{m} \alpha_r^{m-i} P_{2i}^s = \frac{T_{cr}-T_e}{\beta_r}$, this implies that in the optimal solution of (10.20) we have $P_{1i} = 0, \forall i \in \{1, \ldots, m\}$.

10.3.2.3 The points between b and c

The points between b and c can be achieved by setting $\mu_2 > \mu_1 > 0$. In this case, we are aiming to characterize the left corner point of the resulting pentagon. The problem in this case is written as:

$$\begin{aligned}
\max_{\{P_{1i}\},\{P_{2i}\}} & \sum_{i=1}^{D}(\mu_2-\mu_1)\frac{1}{2}\log\left(1+P_{2i}\right)+\mu_1\frac{1}{2}\log\left(1+P_{1i}+P_{2i}\right) \\
\text{s.t.} \quad & (P_{1i},P_{2i})_{i=1}^{k}\in\mathcal{T}_k(\{a_j,b_j,T_{cj}\},j=1,2,r) \\
& (P_{1i},P_{2i})_{i=1}^{k}\in\mathcal{E}_k(\mathbf{E}_1,\mathbf{E}_2),\ \forall k\in\{1,\ldots,D\}
\end{aligned} \tag{10.22}$$

Similar to the previous cases, the optimal power allocation can be obtained using generalized water-filling.

10.3.2.4 Sum-rate (the Line Between c and d)

For the sum-rate, we have $\mu_1 = \mu_2 > 0$ and the problem can be written as:

$$\begin{aligned}
\max_{\{P_i\}} \quad & \sum_{i=1}^{D}\frac{1}{2}\log\left(1+P_{1i}+P_{2i}\right) \\
\text{s.t.} \quad & (P_{1i},P_{2i})_{i=1}^{k}\in\mathcal{T}_k(\{a_j,b_j,T_{cj}\},j=1,2,r) \\
& (P_{1i},P_{2i})_{i=1}^{k}\in\mathcal{E}_k(\mathbf{E}_1,\mathbf{E}_2),\ \forall k\in\{1,\ldots,D\}
\end{aligned} \tag{10.23}$$

The solution in general can be found using generalized water-filling. The problem reduces to a single-user problem in terms of of the sum of the power, i.e., $P_{1i}+P_{2i}$, when either $\max\{\alpha_1,\alpha_2\}<\alpha_r$ and $\frac{T_{cr}-T_e}{\beta_r}\leq\min\{\frac{T_{c1}-T_e}{\beta_1},\frac{T_{c2}-T_e}{\beta_2}\}$ or $\max\{\alpha_1,\alpha_2\}\leq\alpha_r$

and $\frac{T_{cr}-T_e}{\beta_r} < \min\{\frac{T_{c1}-T_e}{\beta_1}, \frac{T_{c2}-T_e}{\beta_2}\}$ is satisfied. The proof follows similar to Lemma 10.3.

10.4 Temperature Limited Case

In this section, we study the case when the system is temperature limited, i.e., when the energy constraint is never binding. This occurs when the following is satisfied:

$$\frac{T_{jc}-T_e}{\beta} < \frac{\sum_{i=1}^{k} E_{ji}}{k}, \ \forall k \in \{1,\ldots,D\}, \quad j=1,2 \tag{10.24}$$

The problem in this case can be written as:

$$\begin{aligned} \max_{\{r_i,P_i\}} \quad & \sum_{i=1}^{D} \mu_1 r_{1i} + \mu_2 r_{2i} \\ \text{s.t.} \quad & (P_{1i},P_{2i})_{i=1}^{k} \in \mathcal{T}_k(\{a_j,b_j,T_{cj}\}, j=1,2,r) \\ & (r_{1k},r_{2k}) \in \mathcal{C}(P_{1k},P_{2k}), \ \forall k \end{aligned} \tag{10.25}$$

We first study the case when a_i, b_i, T_{ic} are not equal.

10.4.1 General Case

In this part, we first study a general characteristic of the rate region. We first have the following lemma.

Lemma 10.4 *At any point of the boundary of the optimal achievable rate region, for any two slots, either P_{1i} or P_{2i} is non-increasing or both are non-increasing.*

Furthermore, for the region between points b and e, $P_{1i} + P_{2i}$ is non-increasing throughout.

Proof: To prove this, we need to show it in each part of the rate. We begin with the sum-rate region. In this case, the problem can be written as follows:

$$\begin{aligned} \max_{\{P_i\}} \quad & \sum_{i=1}^{D} \frac{1}{2} \log\left(1 + P_{1i} + P_{2i}\right) \\ \text{s.t.} \quad & (P_{1i}, P_{2i})_{i=1}^{k} \in \mathcal{T}_k(\{a_j, b_j, T_{cj}\}, j = 1, 2, r), \ \forall k \end{aligned} \tag{10.26}$$

Now, assume for the sake of contradiction that the optimal powers for slots $j < k$ satisfy $P_{1j} + P_{2j} < P_{1k} + P_{2k}$. This means that at least one of the powers is also increasing. Assume without loss of generality that it is at user 2, i.e., $P_{2j} < P_{2k}$. We can then decrease P_{2k} by a small enough δ and increase P_{2j} with the same amount. This remains feasible in all the constraints as this makes room for more temperature budget. Moreover, due to concavity of the objective function this strictly increases the objective function. Hence, $P_t \triangleq P_{1i} + P_{2i}$ has to be non-increasing. This also proves that at least one of the powers has to be non-increasing, as otherwise P_t will be equal to the sum of two increasing sequences which has to be increasing also.

We now consider the case when $\mu_1 > \mu_2$. In this case, the problem can be written as:

$$\begin{aligned} \max_{\{r_i, P_i\}} \quad & \sum_{i=1}^{D} (\mu_1 - \mu_2) \frac{1}{2} \log\left(1 + P_{1i}\right) + \mu_2 \frac{1}{2} \log\left(1 + P_{1i} + P_{2i}\right) \\ \text{s.t.} \quad & (P_{1i}, P_{2i})_{i=1}^{k} \in \mathcal{T}_k(\{a_j, b_j, T_{cj}\}, j = 1, 2, r), \ \forall k \end{aligned} \tag{10.27}$$

The proof again follows by contradiction following the same steps as the previous case. This covers the statement for the curve between points b and e

It remains to consider the optimal individual power allocation for the curve between points a and b (or equivalently point e) in Fig. 10.2. At this point, the second user is transmitting with its single-user power allocation, and it follows from [115] that it is non-increasing. ■

10.4.2 Identical Temperature Parameters

In this part, we consider the case when all nodes have identical temperature dynamics parameters, i.e., $a_i = a$, $b_i = b$. We still allow different critical temperature constraints in each node.

In what follows we study sufficient conditions for which the multiple access rate region reduces to a single pentagon.

Lemma 10.5 *The optimal rate region is a single pentagon when the following condition is satisfied:*

$$\max\{T_{c1}, T_{c2}\} - T_e \leq (T_{cr} - T_e)\,(1-\alpha) \leq (1-\alpha)\min\{T_{c1}, T_{c2}\} \tag{10.28}$$

Proof: To prove this, we need to show that point b is the same as point c. To show this we need to first obtain the optimal sum-power allocation achieving the region between c and d. Then, we need to show that the optimal single user power allocation is feasible in the optimal sum-power allocation. This will imply that point

c is at least the same height as point b, which implies that points b and c are the same point.

We first characterize the optimal power allocation for the sum-rate case. When the following condition is satisfied:

$$T_{cr} \leq \min\{T_{c1}, T_{c2}\} \tag{10.29}$$

the sum-rate problem reduces to only one constraint which is at the receiver. This follows because we have the following:

$$\begin{aligned} \sum_{i=1}^{k} \alpha^{k-i} \max\{P_{1i}, P_{2i}\} &\leq \sum_{i=1}^{k} \alpha^{k-i} \left(P_{1i} + P_{2i}\right) \\ &\leq \frac{T_{cr} - T_e}{\beta} \\ &\leq \frac{\min\{T_{c1}, T_{c2}\} - T_e}{\beta} \end{aligned} \tag{10.30}$$

Hence, whenever the temperature constraint is satisfied at the receiver, it will be also satisfied at both transmitters. Hence, this is reduced to the single-user problem studied in [115] with the optimization variable as $P_{1i} + P_{2i}$. From the properties of the single-user power allocations in [115], we have that the optimal powers satisfy:

$$\left(P_{1i} + P_{2i}\right)^* \geq \frac{T_{cr} - T_e}{\beta} \left(1 - \alpha\right) \tag{10.31}$$

Now for the single-user optimal power allocation of user 2, from the feasibility

we have:

$$P_{2i}^{s} \leq \frac{T_{c2} - T_e}{\beta} \tag{10.32}$$

Therefore, we have:

$$(P_{1i} + P_{2i})^{*} - P_{2i}^{s} \geq \frac{T_{cr} - T_e}{\beta}(1-\alpha) - \frac{T_{c2} - T_e}{\beta} \tag{10.33}$$

$$\geq 0 \tag{10.34}$$

where the last inequality follows from our assumption. Similarly, this follows for the points d and e. ■

Note that only one side of the optimal rate region could indeed collapse, i.e., points b and c may coincide while points d and e are always different. We state this fact in the next corollary.

Corollary 10.1 *In the optimal rate region, point b and point c are the same point when the following is satisfied:*

$$T_{c2} - T_e \leq (T_{cr} - T_e)(1-\alpha) \leq (1-\alpha)\min\{T_{c1}, T_{c2}\} \tag{10.35}$$

10.4.3 Temperature Constraint Only at the Receiver

In this section, we study the case when there is a temperature constraint only at the receiver. In this case, the problem can be written as follows:

$$\begin{aligned} \max_{\{r_i,P_i\}} \quad & \sum_{i=1}^{D} \mu_1 r_{1i} + \mu_2 r_{2i} \\ \text{s.t.} \quad & \sum_{i=1}^{k} \alpha^{k-i} \left(P_{1i} + P_{2i}\right) \leq \frac{T_c - T_e}{\beta} \\ & (r_{1k}, r_{2k}) \in \mathcal{C}(P_{1k}, P_{2k}),\ \forall k \end{aligned} \tag{10.36}$$

We now present the following lemma.

Lemma 10.6 *When $\mu_1 > \mu_2$, the optimal sum-power allocation $P_{1i} + P_{2i}$ is non-increasing. Moreover, user 1 power allocation, P_{1i}, is also non-increasing. Similarly, when $\mu_2 > \mu_1$ we have that the second single-user power allocation, P_{2i}, is non-increasing.*

Proof: When $\mu_1 > \mu_2$, the objective function reduced to:

$$\begin{aligned} \max_{\{r_i,P_i\}} \quad & \sum_{i=1}^{D} (\mu_1 - \mu_2) \frac{1}{2} \log\left(1 + P_{1i}\right) + \mu_2 \frac{1}{2} \log\left(1 + P_{1i} + P_{2i}\right) \\ \text{s.t.} \quad & \sum_{i=1}^{k} \alpha^{k-i} \left(P_{1i} + P_{2i}\right) \leq \frac{T_c - T_e}{\beta},\ \forall k \end{aligned} \tag{10.37}$$

The proof for having $P_{1i} + P_{2i}$ is non-increasing follows similar to Lemma 10.4.

Now, assume that for some $j < k$, we have that $P_{1j} < P_{1k}$. Since we have $P_{1j} + P_{2j} > P_{1k} + P_{2k}$ this implies that $P_{2j} > P_{2k}$. Now, we can decrease P_{2j}

by a small enough δ while increasing P_{1j} with the same amount. This leaves the sum powers to be equal, and hence, does not change the constraint feasibility while strictly increasing P_{1j} and hence strictly increasing the objective function. ■

10.5 Numerical results

In this section, we show a numerical result for the general setting in Fig. 10.4. The optimal power allocation does not possess any monotonicity in general. Moreover, even though the temperature is monotonically increasing at both the transmitters, the temperature is not monotonically increasing at the receiver. We observe a main reason for this as the differences among the system parameters defining the temperature dynamics for each node.

10.6 Conclusion

In this chapter, we studied a two-user multiple access channel with a peak temperature constraint at all the nodes. We first studied the general case where the transmitters and the receiver are made from different materials and have different peak temperature constraints. For this case, we showed that the resulting rate region is a convex region and we characterized the different points of the region. We showed that the optimal power allocation can be obtained using generalized water-filling. Then, we studied the temperature limited case and derived sufficient conditions under which the rate region collapses to a single pentagon.

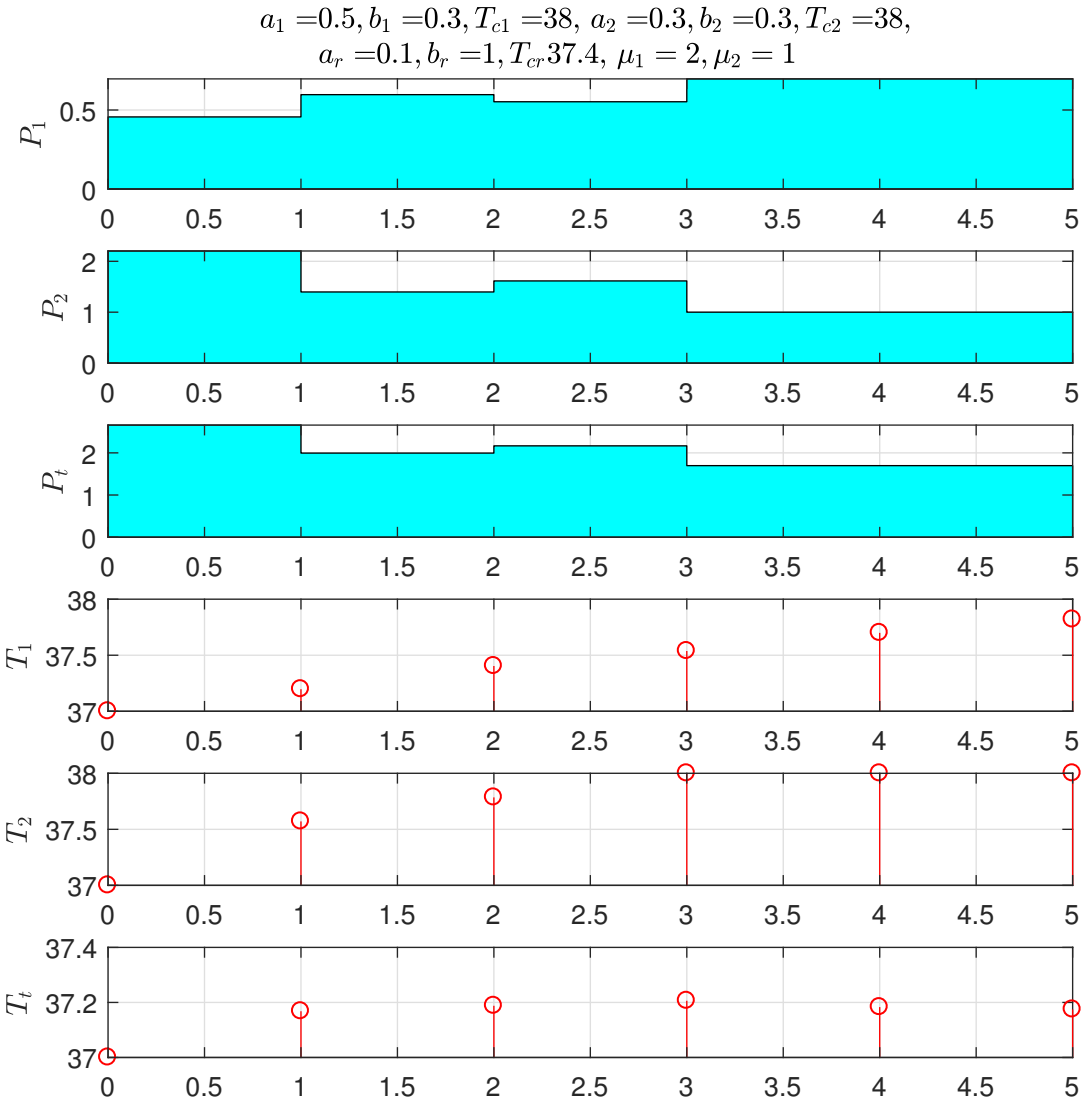

Figure 10.4: Simulation result for the general setting with $\mu_1 > \mu_2$.

CHAPTER 11

Conclusions

In this dissertation, we study online energy management policies for energy harvesting networks under stochastic energy arrivals, Chapters 2-7, and we study offline energy management policies when the network performance is affected by temperature, Chapters 8-10.

In Chapters 2-5, we considered the throughput metric.

In Chapter 2, we considered an energy harvesting broadcast channel in which the energy arrivals are independent and identically distributed (i.i.d.) over time. The transmitter knows the energy arrivals only causally. We studied the optimal power allocation policy for Bernoulli energy arrivals and proposed a near-optimal policy for general energy arrivals. We showed that this policy performs within a constant gap to the optimal for all system parameters.

In Chapter 3, we studied a two-user energy harvesting multiple access channel in which the energy arrivals are i.i.d. over time but arbitrarily correlated between the users. We studied the optimal power allocation for fully-correlated Bernoulli arrivals. Then, for general energy arrivals, we proposed a near-optimal policy which

performs within a constant gap from the optimal policy. The proposed policy is also distributed, i.e., it does need coordination between the users.

In Chapter 4, we studied the impact of processing costs on the online power allocation policies for a single-user channel and a two-way channel. For the single-user channel, we studied the optimal power allocation for Bernoulli energy arrivals and proposed a near-optimal policy for general energy arrivals. Next, for the two-way channel, we restricted our attention to fully correlated energy arrivals between the users. We studied the optimal power allocation for Bernoulli energy arrivals. For general energy arrivals, we proposed a distributed near-optimal policy which performs within a constant gap to the optimal.

In Chapter 5, we considered a single-user energy harvesting channel in which the transmitter has an additional data arrival constraint. We considered the case of fully correlated data and energy arrivals. We characterized the optimal policy for Bernoulli energy arrivals. For general energy arrivals, we proposed a sub-optimal policy. We showed that this policy is within a multiplicative gap to the optimal; it is optimal when the average energy arrival is higher than the energy required to transmit a full data buffer; and it is also within a constant additive gap when the data arrivals are higher than a threshold.

In Chapters 6 and 7, we considered the age of information (AoI) metric.

In Chapter 6, we considered an energy harvesting single-user channel in which the transmitter sends the status updates to the receiver through an erasure channel. The energy arrivals are i.i.d. Bernoulli arrivals. We studied the performance of MDS and rateless coding schemes combined with best-effort and save-and-transmit

schemes. We showed that rateless coding with save-and-transmit performs the best among all the considered schemes.

In Chapter 7, we considered a single-user energy harvesting channel with a transmitter equipped with a unit battery. The transmitter sends status updates to the receiver to minimize the AoI and also sends an independent message through the timings of these updates. We restricted our attention to renewal policies. We studied the optimal renewal policy. Due to the high computational complexity of this policy, we proposed several sub-optimal policies with lower computational complexity. As the average energy arrival rate increases, the gap between the performance of these policies decreases.

In Chapters 8-10, we considered the effects of temperature on the optimal offline power allocation policies. In Chapter 8, we studied a continuous time setting and in Chapters 9 and 10, we considered a discrete time setting.

In Chapter 8, we considered three different models. We studied the effects of temperature dependent energy leakage, processing cost with peak temperature constraint, and temperature increases due to the energy arrival process itself. For each of these models, we studied the optimal power allocation policy.

In Chapter 9, we studied the optimal power allocation for a single-user setting. We considered two temperature models: explicit and implicit temperature constraints. In the explicit temperature constraint model, the peak temperature of the transmitter is constrained by a maximum value. In the implicit temperature constraint model, the peak temperature is not constrained explicitly but it is implicitly constrained as the temperature affects the channel quality. The channel

quality here is captured by the thermal noise which is proportional to the system temperature. For each of these models, we studied the optimal power allocation.

In Chapter 10, we extended the explicit temperature constraint model considered in Chapter 9 to a two-user multiple access energy harvesting channel. We studied the optimal power allocation for the general case. For the temperature limited case, we derived sufficient conditions under which the rate region reduces to a single pentagon.

The contents of Chapter 2 are published in [97, 98], Chapter 3 in [99, 116], Chapter 4 in [104, 105, 117], Chapter 5 in [118], Chapter 6 in [119], Chapter 7 in [120], Chapter 8 in [93], Chapter 9 in [115, 121], and Chapter 10 in [122].

Bibliography

[1] J. Yang and S. Ulukus. Optimal packet scheduling in an energy harvesting communication system. *IEEE Trans. Comm.*, 60(1):220–230, January 2012.

[2] K. Tutuncuoglu and A. Yener. Optimum transmission policies for battery limited energy harvesting nodes. *IEEE Trans. Wireless Comm.*, 11(3):1180–1189, March 2012.

[3] O. Ozel, K. Tutuncuoglu, J. Yang, S. Ulukus, and A. Yener. Transmission with energy harvesting nodes in fading wireless channels: Optimal policies. *IEEE JSAC*, 29(8):1732–1743, September 2011.

[4] C. K. Ho and R. Zhang. Optimal energy allocation for wireless communications with energy harvesting constraints. *IEEE Trans. Signal Proc.*, 60(9):4808–4818, September 2012.

[5] J. Yang, O. Ozel, and S. Ulukus. Broadcasting with an energy harvesting rechargeable transmitter. *IEEE Trans. Wireless Comm.*, 11(2):571–583, February 2012.

[6] M. A. Antepli, E. Uysal-Biyikoglu, and H. Erkal. Optimal packet scheduling on an energy harvesting broadcast link. *IEEE JSAC*, 29(8):1721–1731, September 2011.

[7] O. Ozel, J. Yang, and S. Ulukus. Optimal broadcast scheduling for an energy harvesting rechargeable transmitter with a finite capacity battery. *IEEE Trans. Wireless Comm.*, 11(6):2193–2203, June 2012.

[8] J. Yang and S. Ulukus. Optimal packet scheduling in a multiple access channel with energy harvesting transmitters. *Journal of Comm. and Networks*, 14(2):140–150, April 2012.

[9] Z. Wang, V. Aggarwal, and X. Wang. Iterative dynamic water-filling for fading multiple-access channels with energy harvesting. *IEEE JSAC*, 33(3):382–395, March 2015.

[10] K. Tutuncuoglu and A. Yener. Sum-rate optimal power policies for energy harvesting transmitters in an interference channel. *Journal of Comm. Networks*, 14(2):151–161, April 2012.

[11] C. Huang, R. Zhang, and S. Cui. Throughput maximization for the Gaussian relay channel with energy harvesting constraints. *IEEE JSAC*, 31(8):1469–1479, August 2013.

[12] D. Gunduz and B. Devillers. Two-hop communication with energy harvesting. In *IEEE CAMSAP*, December 2011.

[13] Y. Luo, J. Zhang, and K. Ben Letaief. Optimal scheduling and power allocation for two-hop energy harvesting communication systems. *IEEE Trans. Wireless Comm.*, 12(9):4729–4741, September 2013.

[14] B. Gurakan and S. Ulukus. Energy harvesting diamond channel with energy cooperation. In *IEEE ISIT*, July 2014.

[15] O. Orhan and E. Erkip. Energy harvesting two-hop communication networks. *IEEE JSAC*, 33(12):2658–2670, November 2015.

[16] N. Su, O. Kaya, S. Ulukus, and M. Koca. Cooperative multiple access under energy harvesting constraints. In *IEEE Globecom*, December 2015.

[17] D. Gunduz and B. Devillers. A general ramework for the optimization of energy harvesting communication systems with battery imperfections. *Journal of Comm. Networks*, 14(2):130–139, April 2012.

[18] K. Tutuncuoglu, A. Yener, and S. Ulukus. Optimum policies for an energy harvesting transmitter under energy storage losses. *IEEE JSAC*, 33(3):476–481, March 2015.

[19] J. Xu and R. Zhang. Throughput optimal policies for energy harvesting wireless transmitters with non-ideal circuit power. *IEEE JSAC*, 32(2):322–332, February 2014.

[20] O. Orhan, D. Gunduz, and E. Erkip. Energy harvesting broadband communication systems with processing energy cost. *IEEE Trans. Wireless Comm.*, 13(11):6095–6107, November 2014.

[21] O. Ozel, K. Shahzad, and S. Ulukus. Optimal energy allocation for energy harvesting transmitters with hybrid energy storage and processing cost. *IEEE Trans. Signal Proc.*, 62(12):3232–3245, June 2014.

[22] K. Tutuncuoglu and A. Yener. Communicating with energy harvesting transmitters and receivers. In *UCSD ITA*, February 2012.

[23] H. Mahdavi-Doost and R. Yates. Energy harvesting receivers: Finite battery capacity. In *IEEE ISIT*, July 2013.

[24] R. Yates and H. Mahdavi-Doost. Energy harvesting receivers: Optimal sampling and decoding policies. In *IEEE GlobalSIP*, December 2013.

[25] H. Mahdavi-Doost and R. Yates. Fading channels in energy-harvesting receivers. In *CISS*, March 2014.

[26] J. Rubio, A. Pascual-Iserte, and M. Payaro. Energy-efficient resource allocation techniques for battery management with energy harvesting nodes: a practical approach. In *Euro. Wireless Conf.*, April 2013.

[27] A. Arafa and S. Ulukus. Optimal policies for wireless networks with energy harvesting transmitters and receivers: Effects of decoding costs. *IEEE JSAC*, 33(12):2611–2625, December 2015.

[28] B. Gurakan, O. Ozel, J. Yang, and S. Ulukus. Energy cooperation in energy harvesting communications. *IEEE Trans. Comm.*, 61(12):4884–4898, December 2013.

[29] K. Tutuncuoglu and A. Yener. Energy harvesting networks with energy cooperation: Procrastinating policies. *IEEE Trans. Comm.*, 63(11):4525–4538, November 2015.

[30] O. Ozel, S. Ulukus, and P. Grover. Energy harvesting transmitters that heat up: Throughput maximization under temperature constraints. *IEEE Wireless Comm.*, 15(8):5440–5452, August 2016.

[31] A. Sendonaris, E. Erkip, and B. Aazhang. User cooperation diversity – part I: System description. *IEEE Trans. Comm.*, 51(11):1927–1938, November 2003.

[32] P. Youssef-Massaad, L. Zheng, and M. Medard. Bursty transmission and glue pouring: on wireless channels with overhead costs. *IEEE Trans. Wireless Comm.*, 7(12):5188–6194, December 2008.

[33] A. Sinha and P. Chaporkar. Optimal power allocation for a renewable energy source. In *NCC*, February 2012.

[34] S. Mao, M. Cheung, and V. Wong. An optimal energy allocation algorithm for energy harvesting wireless sensor networks. In *IEEE ICC*, June 2012.

[35] M. Zafer and E. Modiano. Optimal rate control for delay-constrained data transmission over a wireless channel. *IEEE Trans. Info. Theory*, 54(9):4020–4039, August 2008.

[36] V. Sharma, U. Mukherji, V. Joseph, and S. Gupta. Optimal energy management policies for energy harvesting sensor nodes. *IEEE Trans. Wireless Comm.*, 9(4):1326–1336, April 2010.

[37] R. Srivastava and C. E. Koksal. Basic performance limits and tradeoffs in energy-harvesting sensor nodes with finite data and energy storage. *IEEE/ACM Trans. Networking*, 21(4):1049–1062, August 2013.

[38] M. B. Khuzani, H. E. Saffar, E. H. Alian, and P. Mitran. On optimal online power policies for energy harvesting with finite-state Markov channels. In *IEEE ISIT*, July 2013.

[39] Q. Wang and M. Liu. When simplicity meets optimality: Efficient transmission power control with stochastic energy harvesting. In *IEEE INFOCOM*, April 2013.

[40] Y. Dong, F. Farnia, and A. Ozgur. Near optimal energy control and approximate capacity of energy harvesting communication. *IEEE JSAC*, 33(3):540–557, March 2015.

[41] R. Nagda, S. Satpathi, and R. Vaze. Optimal offline and competitive online strategies for transmitter-receiver energy harvesting. In *IEEE ICC*, June 2015. Longer version available: arXiv:1412.2651v2.

[42] C. M. Vigorito, D. Ganesan, and A. G. Barto. Adaptive control of duty cycling in energy-harvesting wireless sensor networks. In *IEEE SECON*, June 2007.

[43] F. Amirnavaei and M. Dong. Online power control strategy for wireless transmission with energy harvesting. In *IEEE SPAWC*, June 2015.

[44] X. Wang, J. Gong, C. Hu, S. Zhou, and Z. Niu. Optimal power allocation on discrete energy harvesting model. *EURASIP Jour. on Wireless Comm. and Networking*, 2015(1):1–14, December 2015.

[45] M. B. Khuzani and P. Mitran. On online energy harvesting in multiple access communication systems. *IEEE Trans. Info. Theory*, 60(3):1883–1898, February 2014.

[46] D. Gunduz P. Blasco and M. Dohler. A learning theoretic approach to energy harvesting communication system optimization. *IEEE Trans. Wireless Comm.*, 12(4):1872–1882, April 2013.

[47] D. Shaviv, P. Nguyen, and A. Ozgur. Capacity of the energy harvesting channel with a finite battery. In *IEEE ISIT 2015*, June 2015.

[48] D. Shaviv and A. Ozgur. Capacity of the AWGN channel with random battery recharges. In *IEEE ISIT*, June 2015.

[49] D. Shaviv and A. Ozgur. Universally near-optimal online power control for energy harvesting nodes. *IEEE JSAC*, 34(12):3620–3631, December 2016.

[50] A. Kazerouni and A. Ozgur. Optimal online strategies for an energy harvesting system with bernoulli energy recharges. In *WiOpt*, May 2015.

[51] S. Kaul, R. Yates, and M. Gruteser. Real-time status: How often should one update? In *IEEE INFOCOM*, March 2012.

[52] S. Kaul, R. Yates, and M. Gruteser. Status updates through queues. In *CISS*, March 2012.

[53] R. Yates and S. Kaul. Real-time status updating: Multiple sources. In *IEEE ISIT*, July 2012.

[54] C. Kam, S. Kompella, and A. Ephremides. Age of information under random updates. In *IEEE ISIT*, July 2013.

[55] M. Costa, M. Codreanu, and A. Ephremides. Age of information with packet management. In *IEEE ISIT*, June 2014.

[56] Y. Sun, E. Uysal-Biyikoglu, R. Yates, C. E. Koksal, and N. B. Shroff. Update or wait: How to keep your data fresh. In *IEEE INFOCOM*, April 2016.

[57] A. Kosta, N. Pappas, and V. Angelakis. Age of information: A new concept, metric, and tool. *Foundations and Trends in Networking*, 12(3):162–259, November 2017.

[58] A. M. Bedewy, Y. Sun, and N. B. Shroff. Age-optimal information updates in multihop networks. *Available at arXiv:1701.05711*, 2017.

[59] P. Parag, A. Taghavi, and J. Chamberland. On real-time status updates over symbol erasure channels. In *IEEE WCNC*, pages 1–6, March 2017.

[60] R. Yates, E. Najm, E. Soljanin, and J. Zhong. Timely updates over an erasure channel. In *IEEE ISIT*, June 2017.

[61] R. Yates. Lazy is timely: Status updates by an energy harvesting source. In *IEEE ISIT*, June 2015.

[62] B. T. Bacinoglu, E. T. Ceran, and E. Uysal-Biyikoglu. Age of information under energy replenishment constraints. In *USCD ITA*, February 2015.

[63] X. Wu, J. Yang, and J. Wu. Optimal status update for age of information minimization with an energy harvesting source. *Available at arXiv:1706.05773*, 2017.

[64] A. Arafa, J. Yang, S. Ulukus, and H. V. Poor. Age-minimal online policies for energy harvesting sensors with incremental battery recharges. In *USCD ITA*, February 2018.

[65] A. Arafa, J. Yang, and S. Ulukus. Age-minimal online policies for energy harvesting sensors with random battery recharges. In *IEEE ICC*, May 2018.

[66] A. Arafa and S. Ulukus. Age minimization in energy harvesting communications: Energy-controlled delays. In *IEEE Asilomar*, October 2017.

[67] A. Arafa and S. Ulukus. Age-minimal transmission in energy harvesting two-hop networks. In *IEEE Globecom*, December 2017.

[68] D. Forte and A. Srivastava. Thermal aware sensor scheduling for distributed estimation. *ACM Trans. on Sensor Networks*, 9(4):53:1–53:31, July 2013.

[69] Q. Tang, N. Tummala, S.K.S Gupta, and L. Schwiebert. Communication scheduling to minimize thermal effects of implanted biosensor networks in homogeneous tissue. *IEEE Trans. on Biomed. Eng.*, 52(7):1285–1294, July 2005.

[70] Y. Liu, R. P. Dick, L. Shang, and H. Yang. Accurate temperature-dependent integrated circuit leakage power estimation is easy. In *Conference on Design, automation and test in Europe*, April 2007.

[71] L. R. Varshney. Transporting information and energy simultaneously. In *IEEE ISIT*, July 2008.

[72] B. Varan and A. Yener. Energy harvesting communications with energy and data storage limitations. In *IEEE Globecom*, December 2014.

[73] O. Ozel and S.Ulukus. Achieving AWGN capacity under stochastic energy harvesting. *IEEE Trans. Info. Theory*, 58(10):6471–6483, October 2012.

[74] K. Tutuncuoglu, O. Ozel, A. Yener, and S. Ulukus. The binary energy harvesting channel with a unit-sized battery. *IEEE Trans. Info. Theory*, 63(7):4240 – 4256, April 2017.

[75] X. Wu, J. Yang, and J. Wu. Optimal status update for age of information minimization with an energy harvesting source. *IEEE Trans. on Green Communications and Networking*, 2(1):193–204, March 2018.

[76] V. Anantharam and S. Verdu. Bits through queues. *IEEE Trans. Info. Theory*, 42(1):4–18, January 1996.

[77] B. Li, L. Peh, and P. Patra. Impact of process and temperature variations on network-on-chip design exploration. In *ACM/IEEE NoC*, April 2008.

[78] N. Kr. Shukla, S. Birla, K. Rathi, R. K. Singh, and M. Pattanaik. Analysis of the effect of temperature and vdd on leakage current in conventional 6 t-sram bit-cell at 90 nm and 65 nm technology. *International Journal of Computer Applications*, 26(10), July 2011.

[79] T. Koch, A. Lapidoth, and P. P. Sotiriadis. Channels that heat up. *IEEE Trans. Info. Theory*, 55(8):3594–3612, July 2009.

[80] D. Ward, N. Martins, and B. M. Sadler. Optimal remote estimation over action dependent switching channels: Managing workload and bias of a human operator. In *ACC*, July 2015.

[81] T. Weissman. Capacity of channels with action-dependent states. *IEEE Trans. on Info. Theory*, 56(11):5396–5411, October 2010.

[82] B. Ahmadi and O. Simeone. On channels with action-dependent states. In *IEEE ISIT*, July 2012.

[83] M. Chiang, C. W. Tan, D. P. Palomar, D. Oneill, and D. Julian. Power control by geometric programming. *IEEE Trans. Wireless Comm.*, 6(7), July 2007.

[84] T. Cover and J. A. Thomas. *Elements of Information Theory*. John Wiley & Sons, 2006.

[85] A. Arapostathis, V. S. Borkar, E. Fernandez-Gaucherand, M. K. Ghosh, and S. I. Marcus. Discrete-time controlled Markov processes with average cost criterion: a survey. *SIAM Journal Control and Opt.*, 31(2):282–344, June 1993.

[86] M. L. Puterman. *Markov Decision Processes: Discrete Stochastic Dynamic Programming*. John Wiley & Sons, 2014.

[87] D. P. Bertsekas. *Dynamic Programming and Optimal Control, 3rd Edition, Volume II*. 2011.

[88] S. M. Ross. *Stochastic Processes*, volume 2. John Wiley & Sons New York, 1996.

[89] D. R. Cox. *Renewal theory*, volume 1. Methuen London, 1962.

[90] D. Gunduz, K. Stamatiou, N. Michelusi, and M. Zorzi. Designing intelligent energy harvesting communication systems. *IEEE Comm. Magazine*, 52(1):210–216, January 2014.

[91] S. Ulukus, A. Yener, E. Erkip, O. Simeone, M. Zorzi, P. Grover, and K. Huang. Energy harvesting wireless communications: A review of recent advances. *IEEE JSAC*, 33(3):360–381, March 2015.

[92] A. Arafa, A. Baknina, and S. Ulukus. Energy harvesting two-way channels with decoding and processing costs. *IEEE Trans. Green Comm. and Networking*, 1(1):3–16, March 2017.

[93] A. Baknina, O. Ozel, and S. Ulukus. Energy harvesting communications under temperature constraints. In *UCSD ITA*, February 2016.

[94] A. Arafa, A. Baknina, and S. Ulukus. Energy harvesting two-way channel with decoding costs. In *IEEE ICC*, May 2016.

[95] B. T. Bacinoglu and E. Uysal-Biyikoglu. Finite horizon online lazy scheduling with energy harvesting transmitters over fading channels. In *IEEE ISIT*, June 2014.

[96] B. T. Bacinoglu, E. Uysal-Biyikoglu, and C. E. Koksal. Finite horizon energy-efficient scheduling with energy harvesting transmitters over fading channels. *arXiv preprint arXiv:1702.06390*, 2017.

[97] A. Baknina and S. Ulukus. Online scheduling for energy harvesting broadcast channels with finite battery. In *IEEE ISIT*, July 2016.

[98] A. Baknina and S. Ulukus. Optimal and near-optimal online strategies for energy harvesting broadcast channels. *IEEE JSAC*, 34(12):3696–3708, December 2016.

[99] A. Baknina and S. Ulukus. Online policies for multiple access channel with common energy harvesting source. In *IEEE ISIT*, July 2016.

[100] H. A. Inan and A. Ozgur. Online power control for the energy harvesting multiple access channel. In *WiOpt*, May 2016.

[101] D. N. C. Tse and S. V. Hanly. Multiaccess fading channels. i. polymatroid structure, optimal resource allocation and throughput capacities. *IEEE Trans. Info. Theory*, 44(7):2796–2815, November 1998.

[102] S. P. Boyd and L. Vandenberghe. *Convex Optimization*. Cambridge University Press, 2004.

[103] I. Olkin and A. W. Marshall. *Inequalities: Theory of Majorization and Its Applications*, volume 143. Academic press, 2016.

[104] A. Baknina and S. Ulukus. Online scheduling for an energy harvesting link with processing costs. In *IEEE Globecom*, December 2016.

[105] A. Baknina and S. Ulukus. Online scheduling for energy harvesting two-way channels with processing costs. In *IEEE Globecom*, December 2016.

[106] R. Yates and D. Goodman. *Probability and Stochastic Processes, 2nd ed.*

[107] O. Ozel, S. Ulukus, and P. Grover. Optimal scheduling for energy harvesting transmitters under temperature constraints. In *IEEE ISIT*, June 2015.

[108] P. R. Gray and R. G. Meyer. *Analysis and Design of Analog Integrated Circuits*. John Wiley & Sons Inc., 1990.

[109] B. R. Marks and G. P. Wright. A general inner approximation algorithm for nonconvex mathematical programs. *Operations Research*, 26(4):681–683, July/August 1978.

[110] Y. Nesterov and A. Nemirovskii. *Interior-Point Polynomial Algorithms in Convex Programming*. SIAM, 1994.

[111] M. Chiang. Geometric programming for communication systems. *Foundations and Trends in Communications and Information Theory*, 2(1–2):1–154, 2005.

[112] S. Ulukus and L. J. Greenstein. Throughput maximization in CDMA uplinks using adaptive spreading and power control. In *IEEE Sixth ISSTA*, September 2000.

[113] R. D. Yates. A framework for uplink power control in cellular radio systems. *IEEE JSAC*, 13(7):1341–1347, September 1995.

[114] A. Baknina, O. Ozel, and S. Ulukus. Explicit and implicit temperature constraints in energy harvesting communications. In *IEEE Globecom*, December 2017.

[115] A. Baknina, O. Ozel, and S. Ulukus. Energy harvesting communications under explicit and implicit temperature constraints. *Available at arXiv:1709.03488*, submitted to Trans. Wirless Comm., September 2017.

[116] A. Baknina and S. Ulukus. Energy harvesting multiple access channels: Optimal and near-optimal online policies. *IEEE Trans. on Comm.* To appear.

[117] A. Baknina and S. Ulukus. Online scheduling for energy harvesting channels with processing costs. *IEEE Trans. on Green Communications and Networking*, 1(3):281–293, September 2017.

[118] A. Baknina and S. Ulukus. Single-user channel with data and energy arrivals: Online policies. In *IEEE ISIT*, June 2017.

[119] A. Baknina and S. Ulukus. Coded status updates in an energy harvesting erasure channel. In *CISS*, March 2018.

[120] A. Baknina, O. Ozel, J. Yang, S. Ulukus, and A. Yener. Sending information through status updates. In *IEEE ISIT*, June 2018.

[121] A. Baknina, O. Ozel, and S. Ulukus. Explicit and implicit temperature constraints in energy harvesting communications. In *IEEE Globecom*, December 2017.

[122] A. Baknina, O. Ozel, and S. Ulukus. Energy harvesting multiple access channel with peak temperature constraints. In *IEEE WCNC*, April 2018.